NEW DESIGNS OF RIGID PINCER COMPLEXES WITH PXP LIGANDS AND LATE TRANSITION METALS AND SP^3 C-F BOND ACTIVATION WITH SILYLIUM AND ALUMENIUM SPECIES

A Dissertation

by

WEIXING GU

Submitted to the Office of Graduate Studies of
Texas A&M University
in partial fulfillment of the requirements for the degree of

DOCTOR OF PHILOSOPHY

December 2011

Major Subject: Chemistry

New Designs of Rigid Pincer Complexes with PXP Ligands and Late Transition Metals

and sp^3 C-F Bond Activation with Silylium and Alumenium Species

NEW DESIGNS OF RIGID PINCER COMPLEXES WITH PXP LIGANDS AND LATE TRANSITION METALS AND SP^3 C-F BOND ACTIVATION WITH SILYLIUM AND ALUMENIUM SPECIES

A Dissertation

by

WEIXING GU

Submitted to the Office of Graduate Studies of
Texas A&M University
in partial fulfillment of the requirements for the degree of

DOCTOR OF PHILOSOPHY

Approved by:

Chair of Committee,	Oleg V. Ozerov
Committee Members,	François P. Gabbaï
	John A. Gladysz
	Perla B. Balbuena
Head of Department,	David H. Russell

December 2011

Major Subject: Chemistry

ABSTRACT

New Designs of Rigid Pincer Complexes with PXP Ligands and Late Transition Metals and sp^3 C-F Bond Activation with Silylium and Alumenium Species.

(December 2011)

Weixing Gu, B.S., Fudan University

M.S., Brandeis University;

Chair of Advisory Committee: Dr. Oleg V. Ozerov

In this dissertation, catalytic C-F bond activation mediated by alumenium and silylium species, improved methods for the synthesis of highly chlorinated carboranes and dodecaborates, new type of P_2Si= pincer silylene Pt complexes and PBP pincer Rh complexes are presented.

In Chapter II, the design and synthesis of P_2Si= and PBP ligand precursors is described. $BrC_6H_4PR_2$ is shown to be a useful building block for PXP type of ligands with *o*-arylene backbone. RLi reagents displayed high chemoselectivity towards electrophiles, such as $Si(OEt)_4$ and BX_3 (X = Hal).

In Chapter III, new chlorination methods to synthesize $[HCB_{11}Cl_{11}]^-$ and $[B_{12}Cl_{12}]^{2-}$ are presented. $[HCB_{11}Cl_{11}]^-$ was obtained via reactions of $Cs[HCB_{11}H_{11}]$ with $SbCl_5$ or via reactions of $Cs[HCB_{11}H_{11}]$ with Cl_2 in acetic acid and triflic acid. Heating

$Cs_2[B_{12}H_{12}]$ in mixtures of SO_2Cl_2 and MeCN led to the isolation of $Cs_2[B_{12}Cl_{12}]$ in high yield.

In Chapter IV, $Et_2Al[HCB_{11}H_5Br_6]$ or $Ph_3C[HCB_{11}H_5Br_6]$ were shown to be robust catalysts for sp^3 C-F bond activation with trialkylaluminum as the stoichiometric reagent. Trialkylaluminum compounds were also shown to be able to be used as "clean-up" reagent for the C-F bond activation reactions, which led to ultra high TON for the catalytic reactions.

In Chapter V, a series of (TPB)M complexes (M = Ni, Pd, Pt) were synthesized and characterized by multinuclear NMR spectroscopy and X-ray crystallography. The resulting metal complexes displayed strong dative M→B interaction and unusual tetrahedral geometry for four-coordinate 16ē species, due to the cage structure of the ligand.

In Chapter VI, $(PSi^HP)PtCl$ was synthesized via the reaction of the ligand precursor and $Pt(COD)Cl_2$, which was used to obtain a series of $(PSi^HP)PtX$ complexes(X= I, OTf, Me, Ph, Mes). After hydride abstraction by $Ph_3C[HCB_{11}Cl_{11}]$, the X ligand (X= I, OTf, Me, Ph) migrated from the Pt center to silicon center to give a cationic pincer silyl species. The migration was not observed when mesityl was used as the X ligand, which resulted in the first known pincer complex with central silylene donor.

Our approaches towards PNP pincer boryl Rh complexes were summarized in Chapter VII. $(PB^{Ph}P)Rh$ pivalate complex underwent C-Ph bond activation to yield the pivalate-bridging Rh borane complex.

ACKNOWLEDGEMENTS

First of all I would like to thank my advisor, Dr. Oleg V. Ozerov, for his education, support, patience and encouragement during my Ph.D. study. He is always encouraging and supportive, giving me confidence and has inspired me in my research.

I would like to thank my committee members, Dr. Balbuena, Dr. Gabbaï and Dr. Gladysz, for their time and efforts throughout the course of this research.

I would like to thank Prof. Didier Bourissou for his guidance in the TPB ligand project. I am also very thankful to Professor Bruce Foxman, Dr. Chun-Hsing Chen and Dr. David Herbert for their work on X-ray crystallography.

I would like to thank all members of the Ozerov group, the present and the past, for their friendship and helpful discussions: Dr. Mason Haneline, Dr. Sylvain Gatard, Dr. Chris Douvris, Dr. Deborha Bacciu, Prof. Anthony Fernandez, Dr. C. M. Nagaraja, Dr. Panida Surawatanawong, Dr. Justin Walensky, Dr. Dan Smith, Dr. David Herbert, Dr. Jia Zhou, Dr. Claudia Fafard, Yanjun Zhu, Alyson Christopher, Baofei Pan, Dan Graham, Mayank Puri, Shoshanna Barnett, Laura Gerber, Lauren Gregor, Emily Pelton, Billy McCulloch, Rafael Huacuja, Rodrigo Ramirez, Jillian Davidson, Sam Timpa, Chun-I Lee, Loren Press, Aaron Hollas, Jessica DeMott, Adam Miller, Chrissy Brammell, Chandra Mouli Palit, Chris Pell, Chan Park and Samantha Yruegas.

Lastly and most importantly, I want to thank my parents for everything they have done for me, for their love and care during my whole life. I want to thank my wife, Mingming, for her love and support, and for the happiness she brings to my life.

TABLE OF CONTENTS

CHAPTER Page

LIST OF FIGURES

Page

Page

Page

LIST OF SCHEMES

Page

Page

Page

Page

LIST OF TABLES

Page

Page

CHAPTER I

INTRODUCTION

1.1 Phosphine Based Pincer Ligands

1.1.1 General Introduction for Phosphine Based Pincer Ligands

The study of pincer ligands and their metal complexes has attracted increasing interest since Shaw's early work on PCP metal complexes in 1970s.[1] The term "pincer" was used in 1989 by van Koten[2] to describe tridentate "NCN" (Figure 1-1) metal complexes. Nowadays, the term "pincer ligands" normally represents tridentate ligand sets which usually favor meridional coordination (Figure 1-2). Neutral flanking arms, such as phosphine, amine or sulfur, as well as neutral or anionic central donors are normally employed to construct pincer ligands.[3] Some of the advantages the pincer ligands feature including high thermostability, high tunability at several key positions, compatibility with both early and late transition metals.[4] Pincer ligands and their metal complexes have been the subject of intense study in recent years, due to their potential to support unusual chemical transformations at the transition metal centers.[5] Pincer metal complexes have been used in strong bond activation, such as C-C,[6] C-O,[7] C-N[8] bonds, as well as small molecule activation, such as NH_3,[9] CO_2,[10] H_2O,[11] CH_4.[12]

This dissertation follows the style of *Journal of American Chemical Society*.

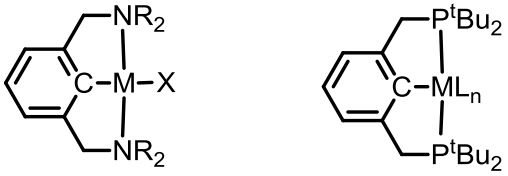

Figure 1-1. Left: NCN pincer metal complexes; Right: Shaw's PCP metal complexes.

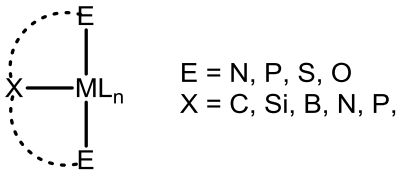

Figure 1-2. General scheme for pincer metal complexes.

Among the various pincer ligands, PXP type of pincer ligands which incorporate two flanking phosphine arms and one central "X" donor have attracted the greatest interest in the past two decades due to their applicability towards various transition metals and many catalytic applications. For example, PNP ligand sets, which feature "soft" phosphine ligands and a "hard" amido donor have been shown to be suitable for both early and late transition metals.[4,5a-c] The incorporation of the phosphine arms also provides a useful ^{31}P NMR spectroscopic probe, which makes it convenient to monitor the transformations of metal complexes by solution or solid state ^{31}P NMR spectroscopy. Besides the original aryl-based PCP frameworks (**A**),[13] other novel backbones have alkyl[14] (**B**), amido[15] (**C**,**D**), boryl[16] (**H**), silyl[17] (**I**), phosphido[18] (**E**) units to provide heterodonor functionality (Figure 1-3). Neutral PXP ligands have also been studied in the past several years, including carbene[19] (**G**)

or pyridine[20] (**F**) based ligand frameworks. Some of the neutral ligands display non-innocent reactivity that involves a reversible tranformation from neutral to monoanionic species.[5d]

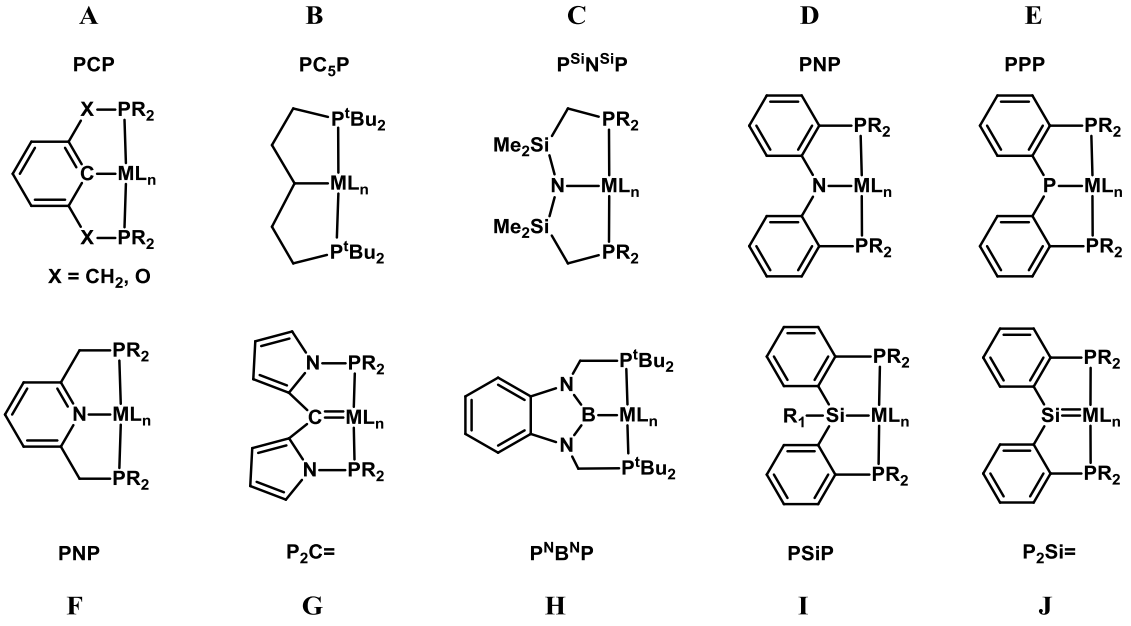

Figure 1-3. Examples of pincer metal complexes.

1.1.2 Synthesis of Cyclometalated Phosphine-Based Pincer Complexes

1.1.2.1 Direct Cyclometalation

Cyclometalation is a type of reaction in which metallacylcle is formed as the product. In order to access pincer ligation, two metallacycles will be formed. Direct cyclometalation is to directly obtain pincer metal complexes from ligand precursors and metal precursors without the change of the oxidation state of the metal center. It is a very attractive method for the formation of pincer metal complexes, since it requires no

prefunctionalization of the pincer ligand to achieve regioselective metalation. Shaw developed the early examples for direct cyclometalation in which C-H bond of PCP ligand precursors was activated to form the PCP metal complexes with Group 9 and Group 10 metals (Scheme 1-1).[1] Recently, direct N-H[21] and Si-H[17a,17c] bond activation have been reported with Ru, Ni, Pd and Pt precursors for the formation of pincer metal complexes in the presence of base (Scheme 1-1). Et_3N or 2,6-lutidine are often used as the base to abstract the HX byproducts which are formed in the activation process.

Scheme 1-1. Synthesis of pincer metal complexes via direct cyclometalation.

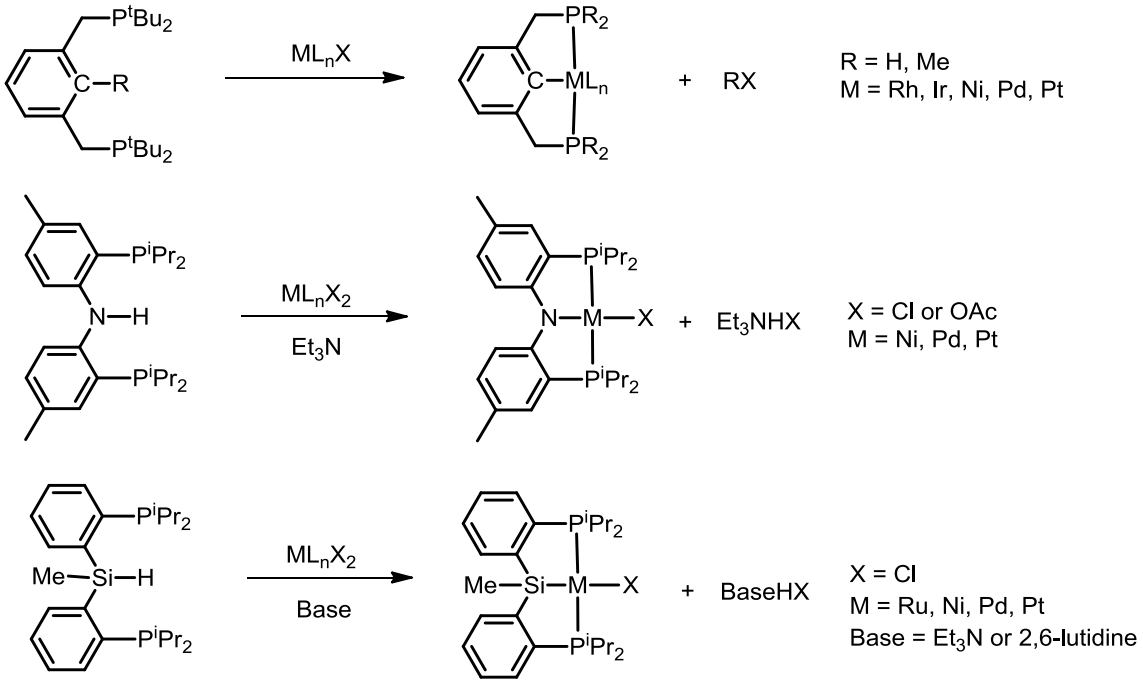

1.1.2.2 Oxidative Addition

Oxidative addition is a type of reaction in which A-B bond is added to the metal center to from an M-A bond and an M-B bond.[22] During the reaction, the oxidation state, electron count and coordination number of the metal all increase by two units. Pincer metal complexes could be synthesized by oxidative addition of X-R (R = Me, H) or X-Hal (X = C, N, B) bonds of ligand precursors to the low valent metal precursors. The flanking phosphine or amine arms may coordinate with the metal center first to facilitate the oxidative addition process (Scheme 1-2). Van Koten and coworkers reported the synthesis of (NCN)Ni complexes via oxidative addition of the C-Br bond to Ni(0) precursors in 1984.[23] Recently, several pincer rhodium and iridium complexes have been reported via corresponding N-H, N-Me or B-H bond oxidative addition.[16,24]

Scheme 1-2. Oxidative addition process of NH bond to metal center.

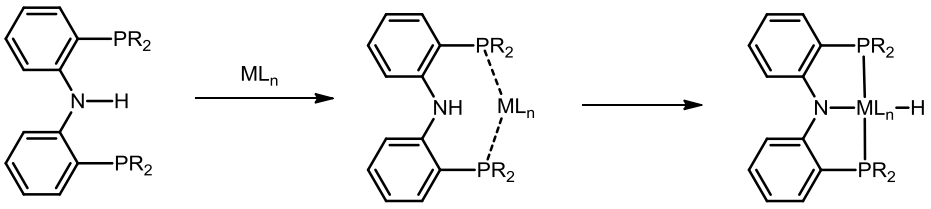

Scheme 1-3. Synthesis of pincer metal complexes via oxidative addition of X-R or X-Hal bonds.

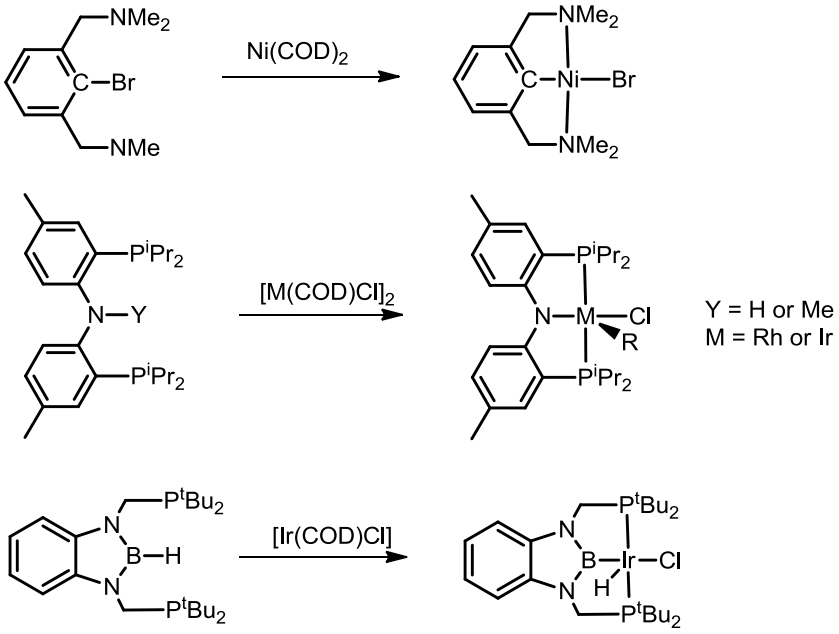

1.1.2.3 Transmetalation

Transmetalation (TM) is a type of reaction in which two metals exchange ligand sets.[22] Pincer metal complexes could be obtained via TM reaction of metal halides or pseudo-halides with lithium or magnesium derivatives of the ligand precursors (Scheme 1-4).[25] However, TM could be problematic for ligands with reactive protons. For example, TM could not be used to obtain (PCP) metal complexes, since lithium reagents tend to attack the more reactive benzylic protons (Scheme 1-5).[26] Ozerov and coworkers reported the synthesis of $[(PNP)Ag]_2$ via the reaction of (PNP)H with Ag_2O or AgOAc/KO^{t}Bu. $[(PNP)Ag]_2$ was stable towards air and moisture (Scheme 1-4).

$[(PNP)Ag]_2$ was shown to be a viable transmetalation reagent for the synthesis of PNP pincer complexes with group 10 metals.[27]

Scheme 1-4. Synthesis of pincer metal complexes via transmetalation.

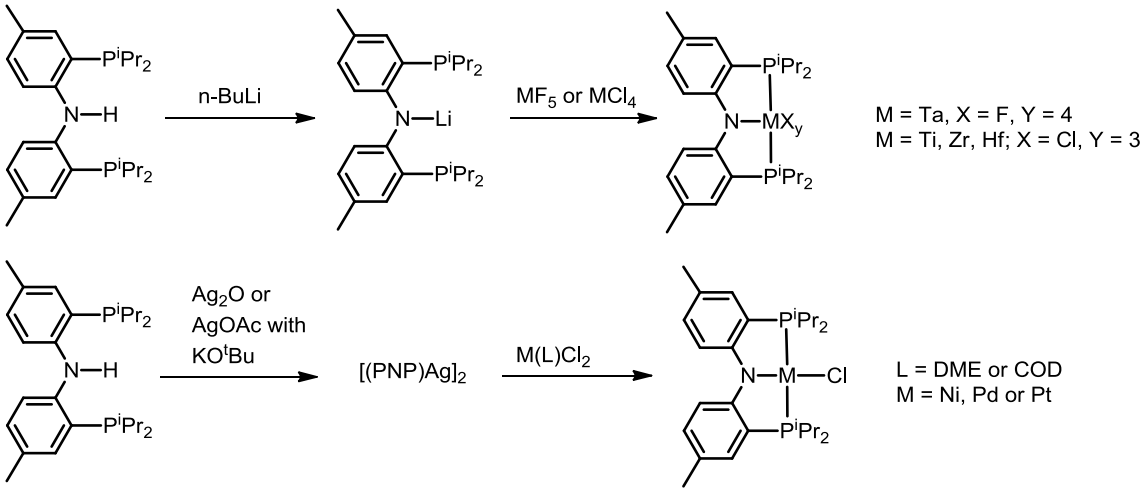

Scheme 1-5. Lithiation of PCP ligand precursor.

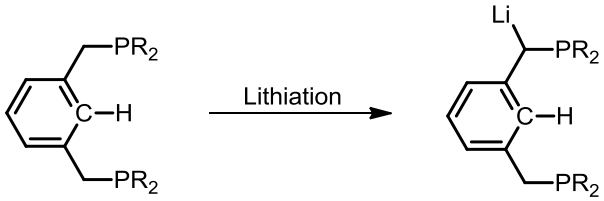

1.1.2.4 Transcyclometalation (TCM)

Transcyclometalation (TCM) is a novel method developed recently for the formation of pincer metal complexes.[28] TCM could be described as the replacement of one cyclometalated ligand with another one without the formation of detectable amount

of purely inorganic salts by dissociation (Scheme 1-6). It was initially investigated with bidentate coordinating ligands.[29] Recently, (PCP)PtCl was successfully obtained via TCM of (NCN)PtCl and (PCP)H. The reaction is likely driven by the formation of stronger phosphine-metal bonds.[30]

Scheme 1-6. General scheme for the transcyclometalation.

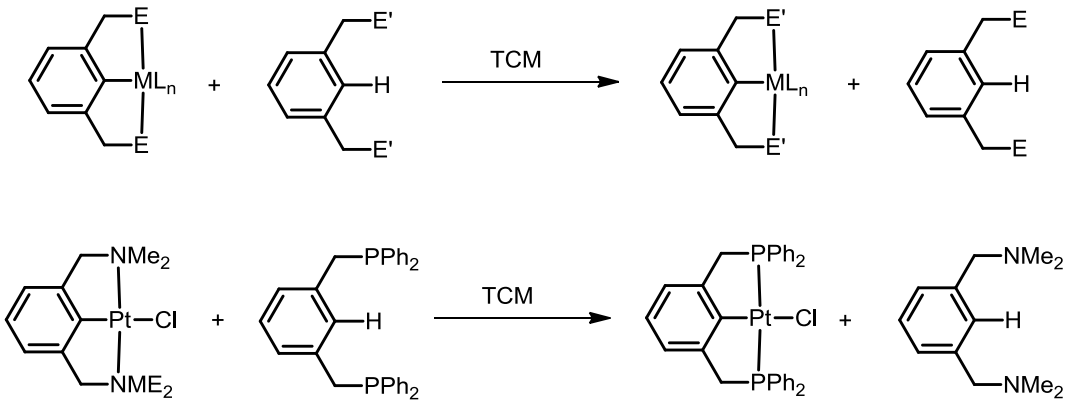

1.1.3 Applications of Phosphine-Based Pincer Complexes

1.1.3.1 High Tunability of Pincer Complexes

One advantage of pincer metal complexes is the high tunability of electronic and steric properties at several key positions, which may alter the reactivity of the resulting metal complexes. In this section, we present several examples illustrating how the variation of the central donor in pincer iridium complexes affected the outcome of the reactions with NH_3.[9]

Ammonia or amine activation by metal complexes via N-H bond oxidative addition is a rare type of reaction in the literature, since amines tend to function as "L" ligands.[31] Meanwhile, utilization of ammonia to produce more complicated molecules would be highly rewarding, as catalytic addition of ammonia to olefin and the coupling of ammonia to arene are considered among the ten greatest current challenges for catalytic transformations.[32] Pincer metal complexes have shown some success in the activation of ammonia recently.[9]

Reaction of (PCP)IrH_2 with norbornene or *tert*-butylethylene generated reactive though unobserved 14ē (PCP)Ir species (**101**).[33] **101** readily performed C-H bond oxidative addition to form corresponding alkyl and aryl hydride species. The Goldman and Hartwig groups found that aniline underwent N-H bond oxidative addition with **101**, to give (PCP)IrH(NHPh) (**102**).[9a] However, the reaction with NH_3 gave only the simple coordination product (PCP)Ir(NH_3) (**104**). Independent synthesis of (PCP)IrH(NH_2) (**103**) revealed that it converted to **104** in 10 min at room temperature (Scheme 1-7), which indicates **103** is less stable compared to **104** at room temperature.[9a]

Scheme 1-7. NH bond activation by (PCP)Ir.

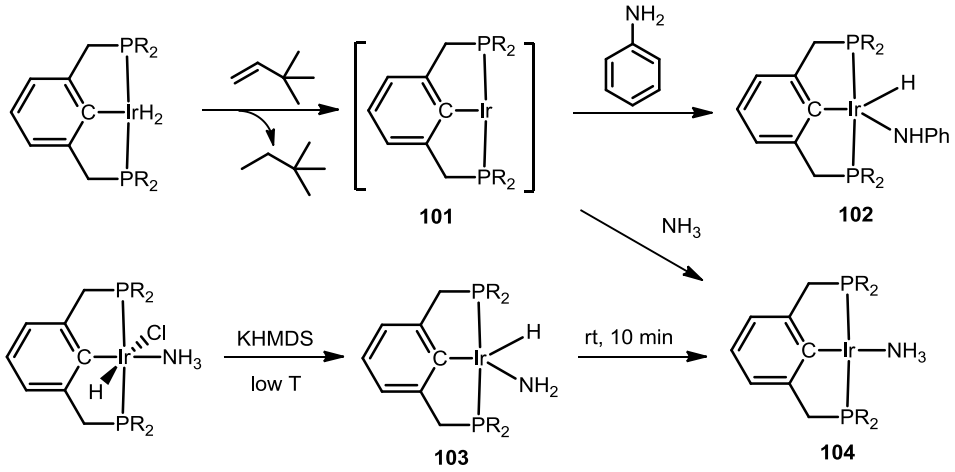

In theory, the thermodynamics of oxidative addition tend to be favored more with electron rich metal centers. Hence, (PC_5P)Ir(propene) (**105**) with a more strongly σ-donating alkyl donor was prepared by the Goldman and Hartwig group (Scheme 1-8). **105** was found to successfully activate NH_3 to give the amido hydride complex (PCP)IrH(NH_2) (**106**), which was the first example of N-H activation of ammonia to form an isolable, terminal, late metal $L_nM(H)(NH_2)$ complex.[9b] Later, Turculet reported that (PSiP)Ir (**107**) with a strongly σ-donating central silyl donor also reacted with ammonia to form (PSiP)IrH(NH_2) (**109**) via N-H bond oxidative addition.[9c] The reactions of NH_3 with **101**, **105** and **107** demonstrate the high tunability of pincer metal complexes. By modifying the electron properties of central donor, the resulting pincer Ir complexes displayed dramatic reactivity difference towards NH_3.

Scheme 1-8. Ammonia activation by (PCP)Ir or (PSiP)Ir complexes.

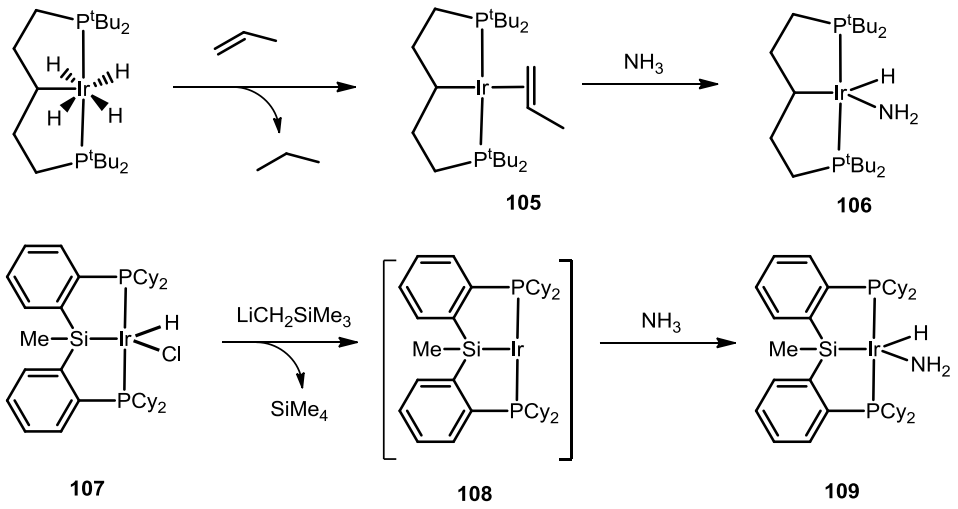

1.1.3.2 High Thermostability of Pincer Complexes

High thermostability is another major advantage of pincer metal complexes which makes them potentially suitable as catalysts for reactions under high temperature. Here, we present one example in which PCP iridium complexes are used as catalyst for alkane dehydrogenation.[34]

Olefins are one of the most versatile and important feedstock for chemical industry. However, their availability in natures is very limited compared to alkanes. Hence, alkane dehydrogenation to produce corresponding alkenes becomes a very important process in chemical industry. Heterogeneous catalysis under high temperature (500-900 ℃) is widely used in industry for alkane dehydrogenation, but their applications have been limited to the production of ethylene and styrene due to low selectivity of the heterogeneous catalysis.[35]

Scheme 1-9. PCP-Ir catalyzed alkane dehydrogenation.

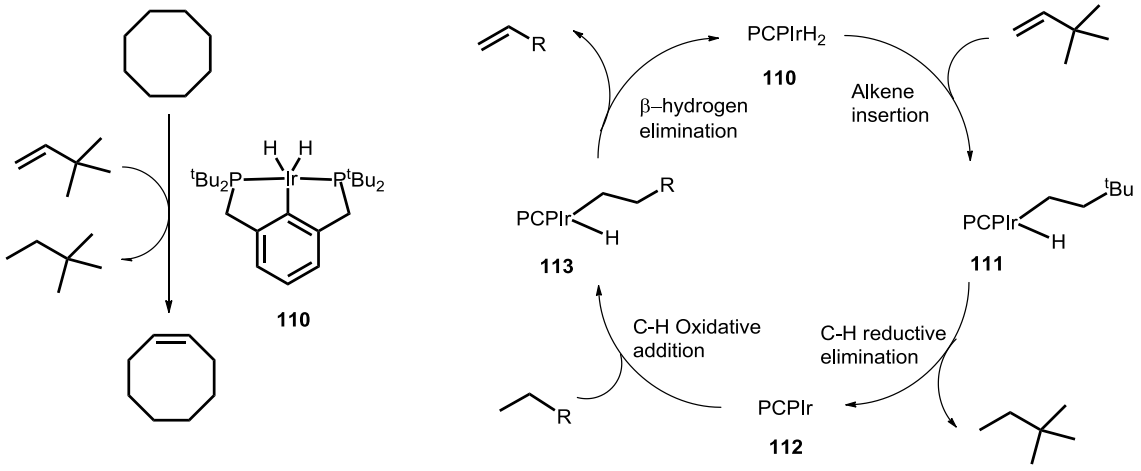

On the other hand, homogeneous catalysts have been shown to perform at relatively mild conditions with higher chemo- and regioselectivity.[36] In 1979, Crabtree reported the first soluble metal complexes $[IrH_2(coe)_2(PPh_3)_2]^+$ which performed stoichiometric alkane dehydrogenation under mild conditions.[37] Many homogeneous catalysts have been developed for alkane dehydrogenation in the past 30 years, by far the performance of (PCP)Ir (**110**) and (P^OC^OP)Ir complexes (Scheme 1-7) are superior in terms of turnover numbers achieved (TON), thermostability and reaction scope.[38] Scheme 1-9 depicts the mechanism of Ir catalyzed alkane dehydrogenation in the presence of an H_2 acceptor.[39] Insertion of *tert*-butyl ethylene (TBE), followed by reductive elimination of alkane gives access to the reactive 14ē (PCP)Ir species (**112**), which undergoes alkane C-H bond OA. Subsequent *β*-hydrogen elimination gives the desired alkene product.

Scheme 1-10. Principles of alkane metathesis.

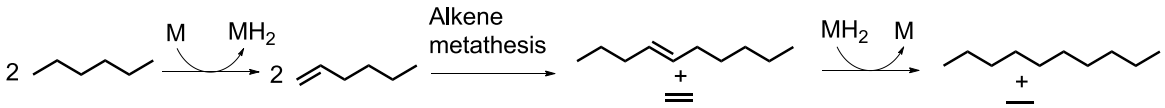

By combining alkane dehydrogenation and alkene metathesis methods, the groups of Goldman and Brookhart developed the so-called "alkane metathesis" process in which longer alkane chains were made from smaller alkanes (Scheme 1-10).[34d] The catalyst tandem was composed of **110** and the Schrock metathesis catalyst[40] (**111**) shown in Figure 1-4. The Ir complex is employed to catalyze the alkane dehydrogenation and alkene hydrogenation process, while the Mo complex is used to catalyze the alkene metathesis reactions. Since longer chain alkenes and ethylene are the intermediates for this reaction, no external H_2 acceptor is used in this tandem catalysis. 125 equivalents of *n*-hexane (relative to Ir) were converted to a range of C_2-C_{15} *n*-alkanes at 125 °C in 24 h. The TON of the reaction was limited by the decomposition of **111** at reaction temperature, normally between 100-150 ℃ .[40] Upon addition of **111**, alkane metathesis was reinitiated which demonstrated the high thermostability of complex **110**.

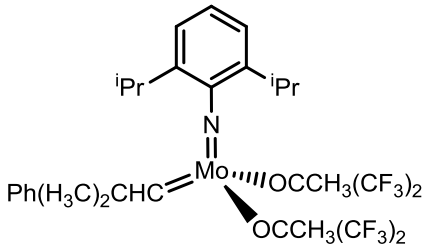

111

Figure 1-4. Left: Mo carbene complexes for alkene metathesis (Schrock catalyst).

1.2 C-F Bond Activation

1.2.1 General Introduction of C-F bond Activation

Fluoroorganic compounds play an integral role in everyday life due to their special chemical, biological and mechanical properties.[41] As present, about 30% of agrochemicals and 20% of pharmaceuticals contain fluorine, including drugs such as Lipitor, Advair and Crestor.[42] Polyfluorinated polymers, such as Teflon, have been widely used in coating and lubricant industry owning to their inertness and "non-stick" properties.[43] Perfluoroalkanes, because of their combined effects of hydrophobicity and oleophobicity, are used as the medium for "fluorous" catalysis.[44] Furthermore, the nonnatural isotope ^{18}F is the most commonly used positron-emitting isotope for molecular positron emission tomography (PET) imaging in oncology.[45]

Despite their great usefulness, there is an increasing environmental concern regarding fluoroorganic compounds.[46] Freons, or chlorofluorocarbons (CFCs), are well known to be destructive towards the ozone layer.[46a-c] Hydrofluorocarbons (HFC), which are commonly used as CFCs replacement as refrigerants are well-documented "super-greenhouse" gases.[46d-e] Perfluoroalkanes (PFC), common byproducts in aluminum and semiconductor industry, are also considered to be "super-greenhouse" gases.

Activation of C-F bond remains a fundamental challenge to chemists, especially with regard to accomplishing it in a catalytic fashion and under mild conditions.[47] The reasons for the challenge of C-F bond activation are the following.[48] 1) Fluorine is the most electronegative element, which forms exceptionally strong C-F bonds. The C-F bond is highly polarized with the electron density substantially on fluorine. Therefore

the strength of C-F bond can be attributed to significant electrostatic attraction between $F^{\delta-}$ and $C^{\delta+}$ rather than the classical electron sharing of a covalent bond. This also explains why C-F bonds in CF_4 are much stronger than C-F bond in monofluorides, since the fluorines in CF_4 are attracted towards a more positive carbon center. 2) The size of fluorine atom is intermediate in size between hydrogen and oxygen but closer to oxygen. Thus, fluorinated alkanes especially perfluoroalkanes are bulkier and their C-F bonds more sterically protected than alkanes and their C-H bonds. 3) Compared to other strong single bonds, such as Si-F bonds in SiF_4, carbon could not increase its coordination number. Whereas, silicon atom in SiF_4 could increase its coordination number from four to five or six which makes it much more reactive. 4) Fluorine is a poor donor as the three lone pairs of fluorine are held tightly to the fluorine center due to its high electronegativity. Moreover, the electrostatic stabilization of C-F bond is sufficiently strong to resist polarization towards free fluoride. Hence fluorides appear as poor leaving groups in organic chemistry.

1.2.2 C-F Bond Activation Mediated by Transition Metal Complexes

The chemical and intellectual challenge of C-F bond activation made it an interesting field that attracted attention from chemists for many years. Most of the previous C-F bond activation process relied on the reductive cleavage of C-F bond, either by oxidative addition to the metal center or by one electron transfer.[48] Most of the transition metal catalyzed C-F activation processes focused on late transition metals, especially platinum group metals,[48e] since early transition metals often formed exceptionally strong bonds with fluorine which make it hard to finish the catalytic cycle.

Fundamental intermolecular C-F bond activation processes mediated by metal complexes could be classified into three categories:[48f] i) Oxidative addition of C-F bonds; ii) nucleophilic attack on the fluorocarbon; iii) defluorination of the fluorocarbon (Scheme 1-11).

Scheme 1-11. C-F bond activation mediated by metal complexes.

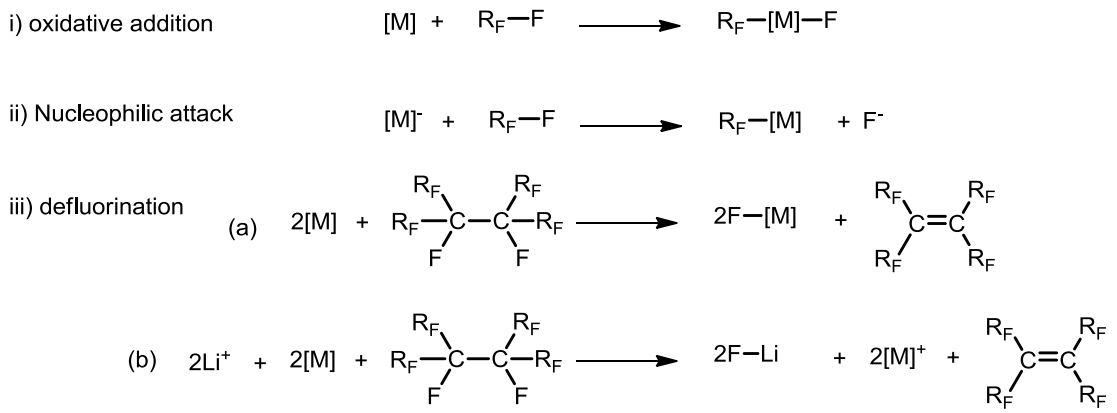

Eisenstein and coworkers carried out theoretical studies with DFT for aryl-H and aryl-F oxidative addition to 16ē Rh(I) species [$CpRh(PH_3)$].[49] It was found that aryl-F oxidative addition was actually thermodynamically preferred. However, the activation energy of C-F bond oxidative addition was considerably higher than that for C-H oxidative addition. Hence, in practice the inertness of C-F bond towards oxidative addition has a kinetic origin. Su and Chu performed theoretical studies on the C-F bond oxidative addition to d^8 14ē $[MX(PH_3)_2]$ (M = Rh, Ir; X = Cl, H, CH_3) species.[50] Several interesting conclusions were drawn from their studies. First, all oxidative addition

reaction were found to be exothermic. Second, it was found that the better π-donor the X ligand was, the smaller the activation energy was. Hence, the activation barrier for C-F bond oxidative addition was calculated to increase in the order $[MCl(PH_3)] < [MH(PH_3)] \sim [MCH_3(PH_3)]$ (M = Rh, Ir). Third, oxidative addition with third row metal was thermodynamically more favorable than that with second row metals. Moreover, the activation barrier of oxidative addition with third row metals was also smaller. Fourth, it was found to be unlikely that radical intermediates were involved in the oxidative addition process.

1.2.2.1 Stoichiometric sp^2 C-F Bond Activation

In practice, stoichiometric sp^2 C-F bond oxidative addition was commonly observed with group 10 metals.[51] The effective metal precursors for C-F bond activation have proven to be different from the typical metal precursors for C-H bond activation. Scheme 1-12 showed two examples in which hexafluorobenzene and pentafluoropyridine were activated by Ni(0) and Pt(0) species, respectively.

Scheme 1-12. Oxidative addition of sp^2 C-F bonds to group 10 metal centers.

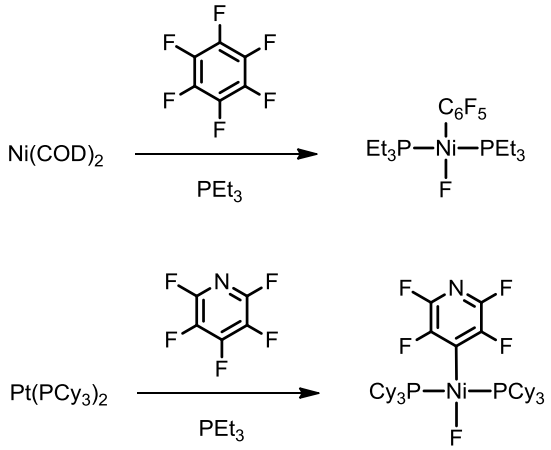

With the formation HF, Si-F, it becomes possible to design potential catalytic system with corresponding H_2 or silanes as stoichiometric reagents. Ru dihydride species were reported to perform activation of C-F bonds from electronically different fluoroarenes (Scheme 1-13).[52] Sp^2 C-F bonds were activated by Rh silyl species with the formation of fluorosilanes.[53]

Scheme 1-13. C-F bond activation with the formation of HF, Si-F or M-F bonds.

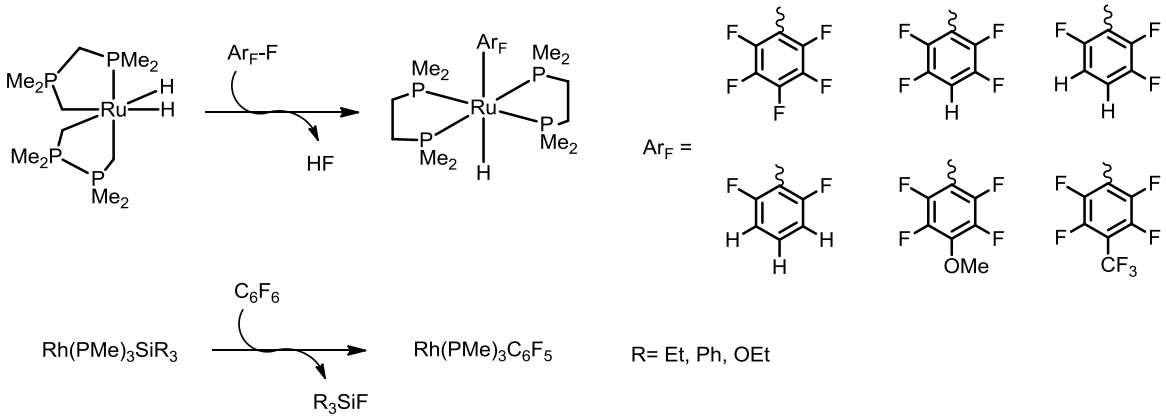

1.2.2.2 Catalytic sp^2 C-F Bond Activation

With the impressive progress on the stoichiometric activation of C-F bond by transition metal complexes, the number of examples of catalytic conversion of C-F bond has been increasing. The most common reaction to catalytically activate C-F bond is hydrodefluorination (HDF) reaction, in which R-F bonds are replace by R-H bonds. In 1994, Milstein and coworkers reported catalytic HDF of aromatic C-F bonds mediated by $C_6F_5Rh(PMe_3)_3$ (Scheme 1-14).[53] High regioselectivity was observed for this

reaction, as in the case of C_6F_5H, only fluorine at the *para* position was activated. Originally, $(EtO)_3SiH$ was employed as the stoichiometric reagent for the HDF process with TON around 30.[53] Later, HDF process was accomplished with H_2 and base as the stoichiometric reagent and TON reached as high as 114. [54]

Scheme 1-14. Catalytic HDF of aromatic fluorides with Rh complexes.

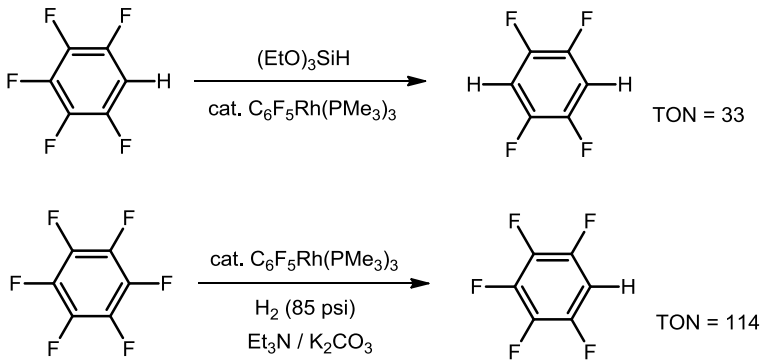

Scheme 1-15 depicted the mechanism for the HDF reactions mediated by Rh complexes. Milstein and coworkers proposed the C-F bond activation step was accomplished via electron transfer from the complex to the substrate and the generation of $C_6F_6^-$, followed by F^- attack on silicon rather than concerted C-F bond oxidative addition to the metal center. The result that HDF of C_6F_6 was much easier than HDF of C_6F_5H is consistent with their proposed mechanism, since C_6F_6 has a greater electron affinity compared with C_6F_5H.[53]

Scheme 1-15. Mechanism for the catalytic HDF of aromatic fluorides with Rh complex.

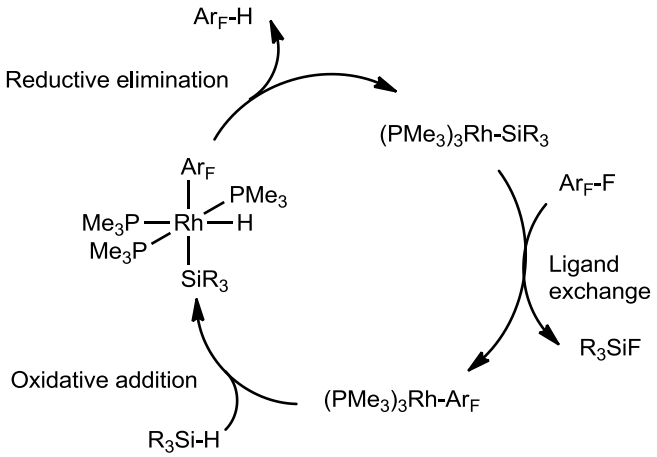

Holland and coworkers reported a Fe complex catalyzed HDF of perfluoroarenes in the presence of Et_3SiH as the reductant (Scheme 1-16).[55] However, the role of the *β*-diketiminate Fe(II) complex as well as the mechanism for this reaction are unclear. There is no evidence of C-F bond activation for the reactions without added silane.

Scheme 1-16. Catalytic HDF of aromatic fluorides with Fe complexes.

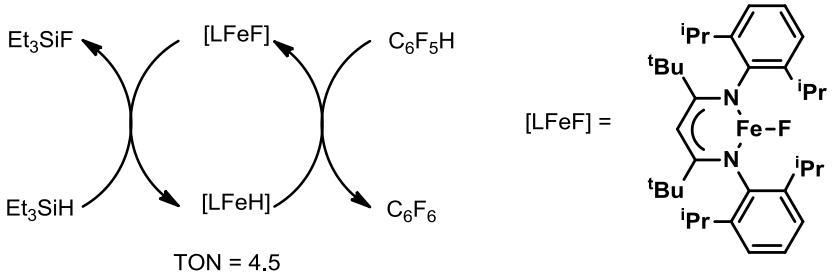

More recently, Whittlesey and coworkers reported a Ru carbene complex catalyzed HDF of perfluorotoluene with Et_3SiH as the reductant (Scheme 1-17).[56] The HDF process showed high chemoselectivity with only sp^2 C-F bonds being activated, though low regioselectivity with C-F bond activation observed at *ortho*, *meta* and *para* positions.

Scheme 1-17. NHC-Ru catalyzed HDF of aromatic fluorides.

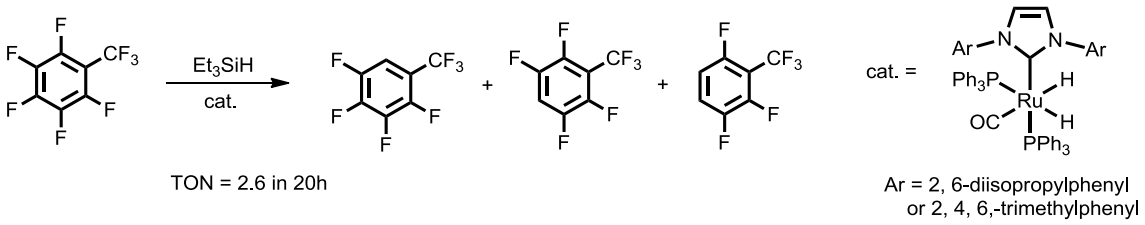

In the absence of Et_3SiH, stoichiometric C-F bond activation was observed to give Ru(II) fluoride as the product (**112**, Scheme 1-18). Hence, the mechanism was proposed in Scheme 1-19 in which C-F bond activation was accomplished via oxidative addition to the metal center.[56] The proposed mechanism is consistent with the observed low regioselectivity. As nucleophilic substitution or electron transfer mechanism would favor activation of the C-F bond which is *para* to an electron-withdrawing group.[48f]

Scheme 1-18. Mechanism for the catalytic HDF of aromatic fluorides with Ru complexes.

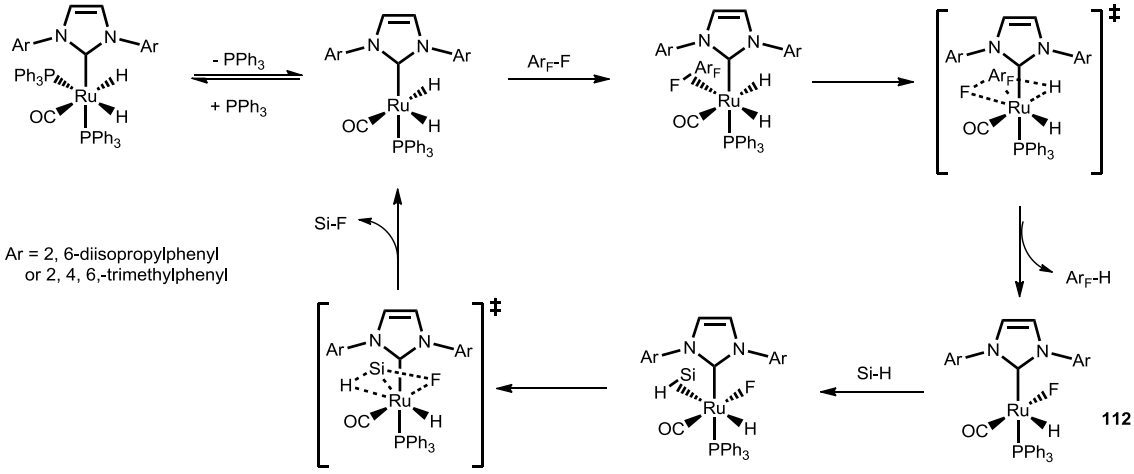

One of the potential uses of metal catalyzed C-F bond activation process is to use fluoroorganic compounds as substrates for cross-coupling reactions.[57] Although aryl iodides and aryl bromides are the most commonly used substrates for cross coupling reactions, there are several recent reports about using aryl fluoride as the coupling substrates.[58] Herrmann and coworkers reported the nickel carbene complex catalyzed Kumada reaction with fluoroarenes as the substrates (Scheme 1-19).[58a] C-F bond oxidative addition to the metal center occurs first, followed by the transmetalation due to the strong affinity of fluorine with magnesium. Finally, reductive elimination gives the desired cross-coupling products. Later, similar chemistry has been accomplished with bidentate phosphine ligands, such as dppe and dppp.[58b]

Scheme 1-19. Kumada coupling reactions with fluoroarene.

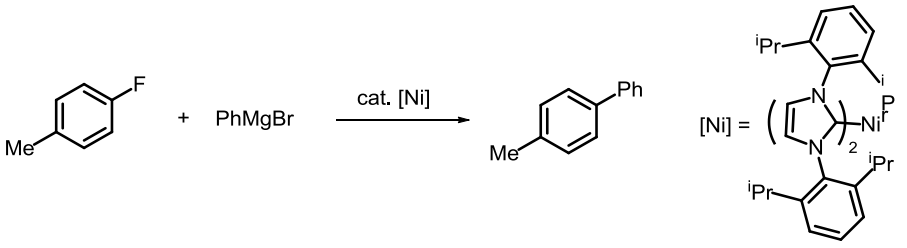

Alkenyl fluorides are employed as the substrates for Pd catalyzed coupling reactions.[58b,58f,58g] Selective activation of C-F bonds was observed in the cross-coupling reaction of *gem*-difluoroalkene to form Z-fluoroalkene as the product (Scheme 1-20).[58b]

Scheme 1-20. Pd catalyzed cross-coupling reaction with alkenyl fluorides.

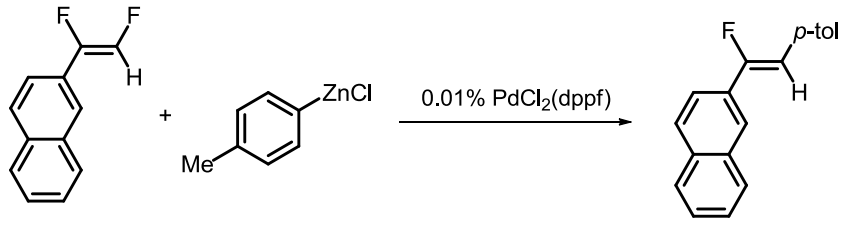

1.2.2.3 Sp^3 C-F Bond Activation

Activation of sp^3 C-F bonds is rare in the literature. One reason is that fluorine prefers to bond to sp^3 rather than sp^2 hybridized carbon atoms, since fluorine could pull electrons from sp^3 carbon to its 2p orbital.[48g] One example of stoichiometric sp^3 C-F bond activation was reported by Jones and coworkers (Scheme 1-21). $(Cp^*)_2ZrH_2$

reacted with primary, secondary or tertiary monofluorides in the presence of H_2.[59] H_2 was employed here to prevent the loss of H_2 from the dihydride and the subsequent formation of the unreactive Zr dimer. Unlike common metal mediated C-F bond activation processes, radical mechanism was proposed here for this Zr mediated transformation (Scheme 1-22).[59] The radical mechanism was confirmed by the reaction with cyclopropylcarbinyl fluoride in which $(Cp^*)_2Zr(n\text{-}Bu)H$ was formed, presumably via a radical ring opening process (Scheme 1-23).

Scheme 1-21. Sp^3 C-F bond activation with zirconocene dihydride.

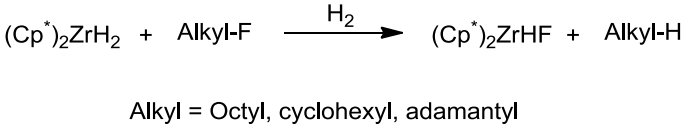

Scheme 1-22. Radical mechanism for the Zr mediated C-F bond activation.

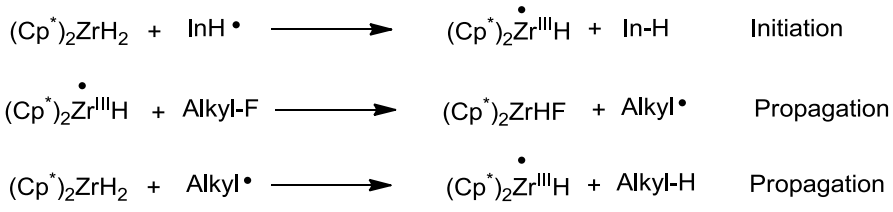

Scheme 1-23. C-F bond activation of cyclopropylcarbinyl fluoride with $(Cp^*)_2ZrH_2$.

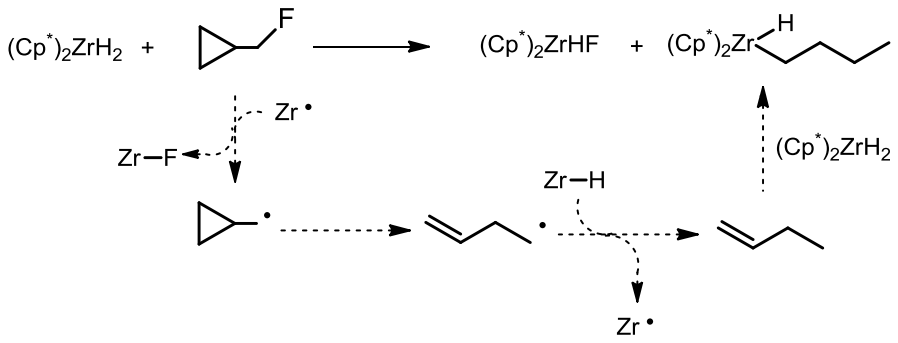

Sp^3 C-F bond activation by (PCP)Ir (**113**) complexes were reported by Goldman and coworkers recently.[60] CH_3F and FCH_2Ar were found to react with **113** to give the C-F bond oxidative addition products at relatively mild conditions (Scheme 1-24). DFT calculation suggests **113** first reacts with CH_3F to give the kinetically favored C-H bond activation product (**114**), then undergoes α-fluorine migration and hydride migration to give the thermodynamically favored C-F bond activation product (**116**) (Scheme 1-25).

Scheme 1-24. Sp^3 C-F bond activation by (PCP)Ir complex.

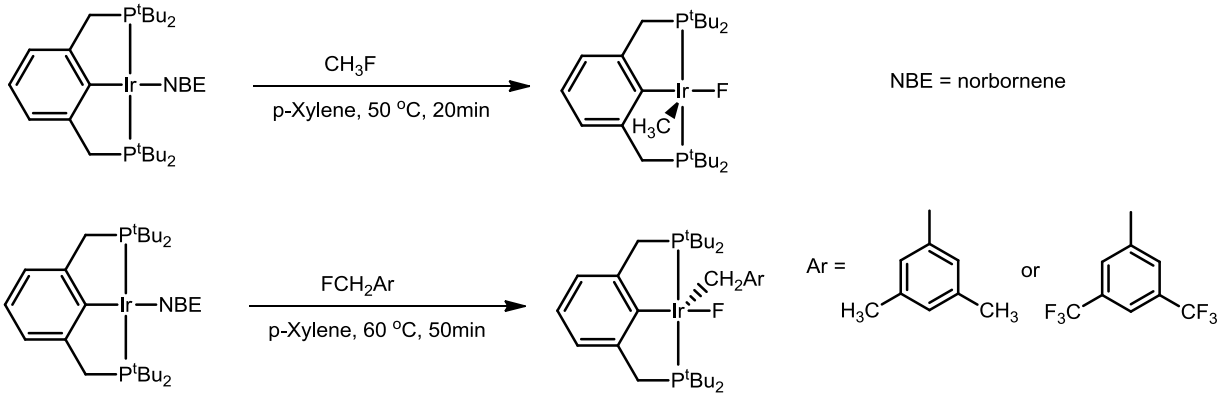

Scheme 1-25. Proposed mechanism for the oxidation addition of CH_3F to (PCP)Ir.

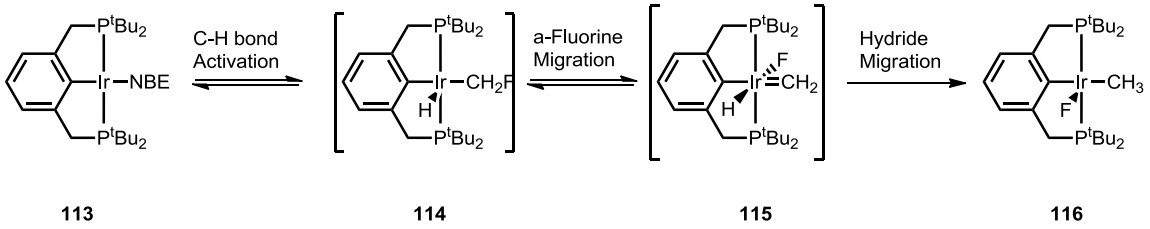

113 **114** **115** **116**

1.3 Weakly Coordinating Anions (WCAs)

1.3.1 General Introduction for WCAs

It is now widely recognized that the once so-called "non-coordinating anions", such as $SO_3CF_3^-$, BF_4^-, ClO_4^-, $[MF_6]^-$ (M = P, As, Sb) are actually capable of coordination with almost all transition metals under many circumstances.[61] Based on structural and spectroscopic data, Rosenthal reported in 1973 "these non coordinating anions are found to be coordinated where water is excluded".[62] Hence, as Strauss stated in his review in 1993, it would be more meaningful as well as more precise to use the relative term "weakly coordinating anion".[61a]

Weakly coordinating anions (WCAs) have attracted increasing attention in the past decade due to their use in both fundamental and applied chemistry.[61,63] They have been widely used in electrochemistry,[64] ionic liquids,[65] lithium-ion batteries,[66] extraction of Ln^{III} anions,[67] photoacid generators[68] and Li^+, Ag^+ catalyzed organic reactions.[69] Highly electrophilic main group and organometallic compounds are often employed as the catalyst for many catalytic transformations, such as group 14 metallocene catalyzed olefin polymerization[70] and silylium catalyzed C-F bond activation.[71] Utilization of

robust and stable WCAs is crucial for the longevity and reactivity for these catalytic transformations.[71d-f]

Several standards should be met for an anion to be considered a WCA.[61a] The anion should have a low overall charge and high charge delocalization. Most of the WCAs in the literature are of -1 charge.[61] The charge should be delocalized over the anion, which means no atom should carry a high concentration of charge. Ideally, WCAs would only have very weakly basic sites on the periphery of the anion. High thermal and kinetic stability would also be crucial properties for WCAs. For example, $[MF_6]^-$ (M = P, As, Sb) are less coordinating than $SO_3CF_3^-$ and ClO_4^-, mainly because $[MF_6]^-$ do not have accessible oxygen groups on their periphery.[72] However the $[MF_6]^-$ type of compounds are less desirable candidates for WCAs, since they were reported to decompose under strong Lewis acidic conditions to release fluorides.[73] Resistance towards oxidation is also required for WCAs, since most electrophilic species are strong oxidants as well.

1.3.2 Tetraphenylborates (BPh_4^-) and Related Anions

Tetraphenylborate anions (BPh_4^-) adopt tetrahedral geometry and the negative charge is delocalized over the four phenyl rings. Although it is prone to chemical and electrochemical oxidation and the phenyl groups are relatively strong coordinating,[74] BPh_4^- has been used as the counterion for soluble Ziegler-Natta catalyst of group 14 metallocene species $M(Cp)_2R^+$ (M = Ti, Hf, Zr).[75]

In order to increase the stability towards oxidation and reduce coordinating ability, the phenyl groups in the borate species are replaced by perfluorinated phenyl groups (C_6F_5) or trifluoromethyl-substituted phenyl groups (3,5-$C_6H_3(CF_3)_2$) to make the so-

called "BARF" anions $[B(C_6F_5)_4]^-$ [76] or $[B(C_6H_3(CF_3)_2)]^-$. [77] The incorporation of fluorine atoms decreases the amount of negative charge on the *ipso* carbon which reduces the tendency of B-C bond cleavage.[61a] Hence, in practice, BARF anions exhibit much better stability compared to BPh_4^- under highly electrophilic conditions. Besides the conventional $[B(C_6F_5)_4]^-$ or $[B(C_6H_3(CF_3)_2)]^-$ anions, other BARF anions have been reported with modification of $-C_6F_5$ groups at *para* position with $-CF_3$,[78] $-Si(^iPr)_3$,[79] $-SiMe_2{}^tBu$[79] or $-C_6F_4\{C(F)(C_6F_5)_2\}$[80] groups. The modified BARF anions show much better solubility in non-polar solvent. The trifluoromethyl groups in $[B(C_6H_3(CF_3)_2)]^-$ anions have been replaced with longer R_f chains, such as n-C_6F_{13},[81] n-C_4F_9[82] or C_3F_7,[82] which makes the corresponding catalysts compatible with fluorous biphasic recycling techniques. Nowadays, BARF anions are arguably the most commonly used WCAs for homogeneous catalysis, as they possess low coordinating ability, good solubility in non-polar solvents and are readily available from commercial suppliers.[63a]

Recently, tetraarylaluminates $[Al(C_6F_5)_4]^-$ and tetraarylgallates $[Ga(C_6F_5)_4]^-$ have been synthesized as the further modification of BARF anions.[83] Although aluminates and gallates are shown to be less stable than their borates analogs, they have already been used as counterions for the cationic species that catalyze polymerization reactions.[84]

1.3.3 Boron Cluster Based Anions ($HCB_{11}H_{11}^-$, $B_{12}H_{12}^{2-}$)

The monocarba-*closo*-dodecaborane anion $[CB_{11}H_{12}]^-$ (Figure 1-5), often referred to as carborane anion, has received growing attention as a promising weakly coordinating anion (WCA) type recently.[63] Carboranes display 3-dimersional

aromaticity which largely contributes to their matchless stability.[85] Differential scanning calorimetry revealed nothing remarkable for carbornae up to 300 ℃ .[86] The 3-dimensional aromaticity of polyhedral boranes was systematically reviewed by King in 2001.[85]

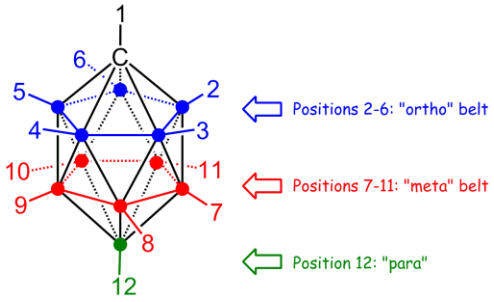

Figure 1-5. Representation of the monocarba-*closo*-dodecaborate(-) $[HCB_{11}H_{11}]^-$ anion, or carborane (dots at vertices 2-12 represent boron atoms; each vertice is capped with a hydrogen atom).

The B-H bonds in carborane are hydridic, therefore similar to aromatics, electrophilic substitution occurs with the B-H bonds, which normally takes place at 12 position first, followed by the substitutions at 7-11 position. Fluorination,[87] chlorination, [88] bromination,[88] iodination,[88] hydroxylation, [89] methylation [90] and trifluoromethylation[91] have been reported with parent carborane.

On the other side of carborane, the C-H bond is somewhat acidic. It was shown to be deprotonated by *n*-BuLi,[92] or even NaOH in some cases.[93] Subsequent addition of electrophiles, such as alkyl iodide, yielded alkyl substituted carboranes [R-$CB_{11}H_{11}$]. [94] The extra electron density donated from alkyl group makes the carborane cage more electron rich which accelerates the electrophilic substitution.[88]

The superior stability, least nucleophilicity and very weak coordinating ability

makes carborane and their deravitives an excellent choice as the counterion for many electrophilic species.[63d] Methyl carborane $Me^+[HCB_{11}Me_5Br_6]$ was isolated and used to methylate benzene to produce toluenium species.[95] The methyl reagents were also shown to abstract hydride from hydrocarbon to form correponding carbocation, which resulted in the isolation of *t*-butyl and vinyl cation species.[96] Trityl species were isolated with various carborane derivatives, which were used to isolate the first "free" silylium compound.[97] $H[HCB_{11}Cl_{11}]$ is the strongest known Brønsted acid which is stable to sublimation at 200 ℃ .[98]

In order to quantify the coordinating ability of WCAs and the acidity of the corresponding "super-acids", Fărcaşiu and Ghenciu developed the method in which strong acid was used to protonated enone.[99] The acidity of the super acid is measured based on the difference of chemical shift ($\Delta\delta$) of C_a and C_b in ^{13}C NMR (Scheme 1-26). The results showed carborane acids to be much stronger than FSO_3H and CF_3SO_3H.[98]

Scheme 1-26. Quantification of acidity of super acids.

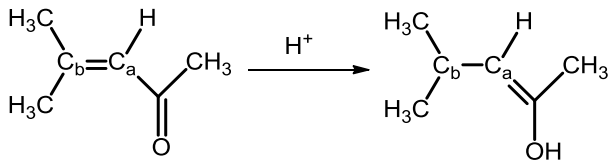

Although BARF anions ($[B(C_6F_5)_4]^-$ or $[B(C_6H_3(CF_3)_2)]^-$) have arguably similar basicity and nucleophilicity compared to halogenated carboranes, their stability is

much worse, especially under highly electrophilic conditions.[63d,97] Dialkylaluminum (R_2Al^+) cation was successfully isolated with halogenated carboranes,[100] on the other hand the degradation of BARF anions was reported to be initaited by R_2Al^+.[83b] In the silylium and alumenium catalyzed C-F bond activation process, it was reported the reactions with halogenated carborane anions could reach turnover number (TON) up to 10000.[71d,f] While the reactions with $[B(C_6F_5)_4]^-$, TON was limited to less than 100 due to the decomposition of the anion.[71a-b, 101]

Despite their great advantages, carborane anions are still in the process of making a transition formulated by Reed in 1998 as being "from exotica to specialty chemicals".[63a] The lengthy and time consuming synthesis of carborane anions as well as their high cost from commercial suppliers prevents their wide applications. In contrast, *closo*-dodecaborates $[B_{12}H_{12}]^{2-}$ (Figure 1-6) and their halogenated derivatives $[B_{12}X_{12}]^{2-}$ (X = Hal) which show similar stability and basicity to carboranes, are relatively easier and cheaper to synthesize.[102] Knapp reported a one step synthesis of $[B_{12}H_{12}]^{2-}$ from $NaBH_4$ in 2009 which make it an easily accessible chemical.[102d] $H_2[B_{12}Cl_{12}]$ showed comparable acidity to carborane acids as $[C_6H_7]_2[B_{12}Cl_{12}]$ and $[C_6H_7][HCB_{11}X_{11}]$ all showed very similar $\nu(CH_2)$ frequencies of the most acidic CH_2 group at the protonated sp^3 carbon atom.[102c] Highly electrophilic species such as Me^+,[102a] $SiEt_3^+$,[102b-c] and Et_2E^+ (E = Al, Ga, In)[103] have been isolated with $[B_{12}Cl_{12}]^{2-}$. We recently reported silylium mediated HDF reactions with $[B_{12}Cl_{12}]^{2-}$ as the couterion which showed comparable reactivity to that with halogenated carboranes as the counterion.[104] Hence, $[B_{12}X_{12}]^{2-}$ anions are a

promising class of WCA despite their relatively low solubility compared to carborane anions.[102,104]

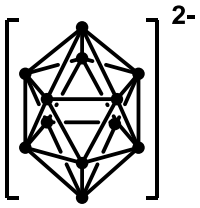

Figure 1-6. Representation of the dodecaborate(2-) $[B_{12}H_{12}]^{2-}$ dianion (dots at vertices 2-12 represent boron atoms; each vertice is capped with a hydrogen atom).

1.3.4 Other Weakly Coordinating Anions ($OTeF_5^-$, anionic aluminoxanes, etc.)

Pentafluoroxotellurate, teflate, has a distorted octehydral structure.[105] One of the notable application of teflate anion is the isolation of $Kr(OTeF_5)_2$ which is one of the few krypton compounds and the first with Kr-O bond.[106] Bound telfate, such as $[B(OTeF_5)_4]^-$ or $[M(OTeF_5)_6]^-$ (M = Sb, As, Bi, Nb) recently became a interesting choice for WCAs.[107] The -1 charge of the bound teflate is delocalized over 20-30 fluorine atoms. It was reported that the borate $[B(OTeF_5)_4]^-$ was less stable than arsenate $[As(OTeF_5)_6]^-$ or antimonate $[Sb(OTeF_5)_6]^-$ species, as the borate species tend to lose $OTeF_5^-$ under high electrophilic conditions.[107a] Nevertheless, the borate, arsenate and antimonate species have all been reported to stablize electrophilic $[AsX_4]^+$, $[SbX_4]^+$ and $[CX_3]^+$ (X = Cl or Br) species.[108]

Methylaluminoxanes (MAO) are commonly used as cocatalyst for Ziegler-Natta polymerization, since MAO is employed to activate Cp_2MX_2 to access the active catalyst $[(Cp)_2MX]^+[X(Al(Me)(\mu\text{-}O))_n]^-$.[70a] Up to now, little is known about the

poorly defined oligomer structure of MAO as well as the anionic $[X(Al(Me)(\mu\text{-}O))_n]^-$ species. However, model studies showed $[(Cp)_2MX]^+[X(Al(Me)(\mu\text{-}O))_n]^-$ to be the active species in Ziegler-Natta polymerization.[75a]

$[Al\{OC(CF_3)\}_4]^-$ is a new stable and weakly coordinating anion. Lithium salt of $[Al\{OC(CF_3)\}_4]^-$ could be easily prepared from commercially available starting materials on a hundred gram scale.[109] While the aluminate anions are generally unstable towards hydrolysis, $[Al\{OC(CF_3)_3\}_4]^-$ is stable in nitric acid due to the shielding effect of the oxygen atoms by the steric bulky $C(CF_3)_3$ groups.[109] Studies of the solid state structure of silver salts of several WCAs suggest that $[Al\{OC(CF_3)_3\}_4]^-$ displays similar weakly coordinating ability as $[HCB_{11}H_5Cl_6]^-$. In practice, $[Al\{OC(CF_3)_3\}_4]^-$ has been used as the counterion for cationic polymerization[61b] and alumenium mediated hydrodefluorination.[101] In both cases $[Al\{OC(CF_3)_3\}_4]^-$ showed similar reactivity to $[B(C_6F_5)_4]^-$ anion. However, $[Al\{OC(CF_3)_3\}_4]^-$ displayed much worse longevity compared to carborane anions in the alumenium mediated hydrodefluorination reactions.[101]

CHAPTER II

DESIGN AND SYNTHESIS OF PINCER PSiP AND PBP LIGAND PRECURSORS

2.1 Introduction

2.1.1 Pincer Ligands with Boron or Silicon as Central Element

Pincer ligands and their metal complexes have been the subject of intense study in recent years,[4,5] due to their potentials to support unusual chemical transformations on the transition metal centers. In contrast to the extensive work on PCP[5a,5b](**A**, **B, C**) and PNP[5c,5d](**D, E, F**) pincer complexes, only a limited amount of work has been reported on pincer ligands using Si or B as the central element (Figure 2-1). We are especially interested in the PXP ligands wherein *o*-arylene units link the central donor and phosphine arms (**E**, **G**, **H, J**), since they have stronger perference for meridional geometry for the resulting metal complexes. Furthermore, the lack of reactive proton or other sensitive functional groups make their metal complexes more stable and resistant towards oxdiation.[110] For example, the benzylic hydrogen in **A** is shown to be deprotonated by lithium reagent,[26] while the silicon backbone of **F** leads

to high sensitivity to OH and other O-containing groups.[111] Stobart and coworkers reported a series of metal complexes with bi-, tri- and tetradentate phosphinosilyl ligands.[112] The PSiP ligand (**G**) was reported by Turculet group in 2007,[9c,17a-e] they also reported the resulting metal complexes in C-H and N-H activation process. Iwasawa[17f-g] and coworkers recently reported the use of (PSiP)PdOTf as the catalyst for dehydrogenative borylation as well as hydrocarboxylation of allenes with CO_2. However, there has been no report of a tridentate P_2Si= ligand (**H**). It is thus appealing to us to obtain the P_2Si= (Silylene) metal complexes to compare with the well-known carbene analogs.[113] The PBP (boryl) ligand (**I**) was first reported by Nozaki group in 2009.[16] Pincer boryl ligands (**L**, SeBSe and SBS) supported by *m*-carborane were recently reported by the Mirkin group (Figure 2-2).[114] Nakamura reported the use of similar pincer boryl complexes **M** as the catalyst for asymmetric reduction of α,β-unsaturated esters and asymmetric reductive aldol reaction of *tert*-butyl acrylate and benzaldehyde.[115]

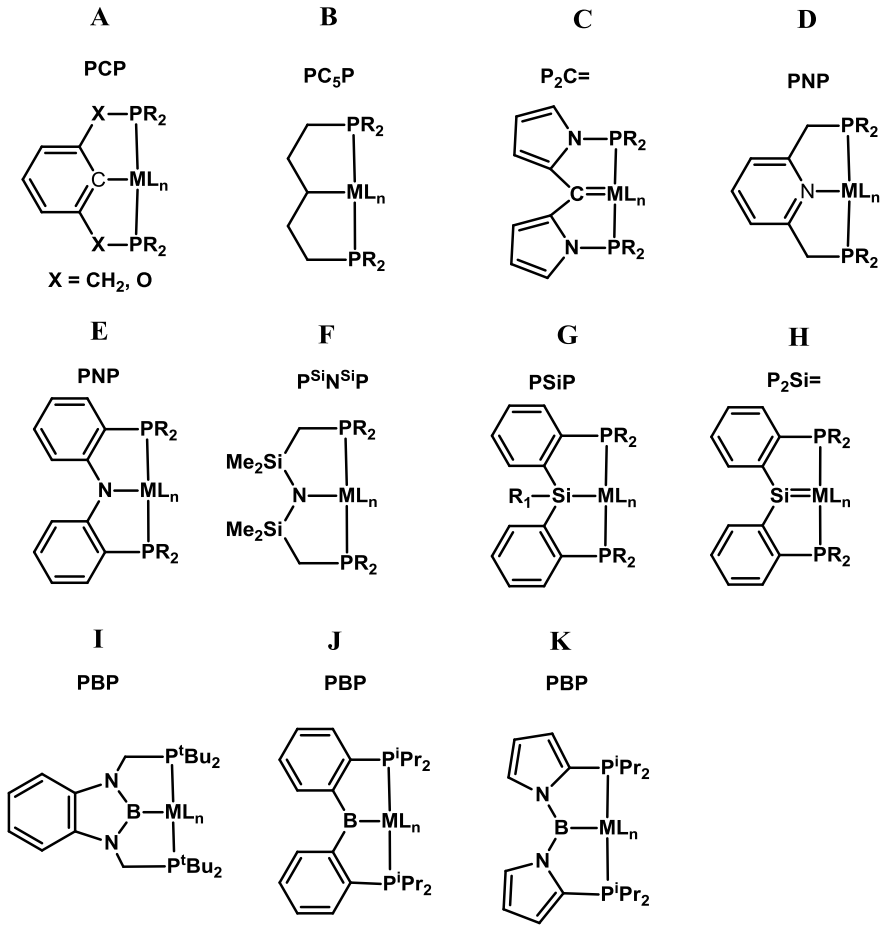

Figure 2-1. Examples of pincer PXP metal complexes.

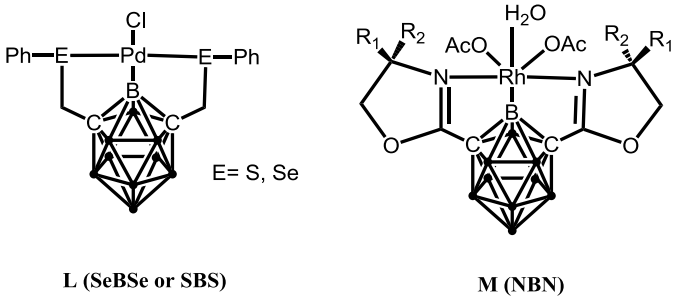

Figure 2-2. Carborane based pincer boryl complexes known in the literature. (Each dot on the cage represnts one BH group)

2.1.2 *Trans* Influence and *Trans* Effect

Trans influence is the ground-state phenomenon of weakening the bond to a *trans*-ligand.[22] Generally, ligands with strong σ-donating characteristics exhibit strong *trans* influence, such as hydride, silyl, alkyl, boryl, etc. Ligands that form strong multiple bonds to metal center also show strong *trans* influence. As shown in Figure 2-3, the two ligands that are *trans* to each other on one metal center are essentially using the same set of s/d hybridized orbital for bonding.[22] Hence, the stronger one ligand is bound to the metal center, the higher energy orbital it will be for the other ligand to bind. *Trans* effect, on the other hand, is a kinetic effect of facilitating substitution *trans* to the ligand.

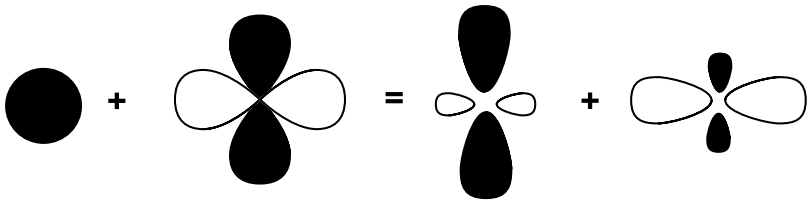

Figure 2-3. s/d hybridized orbital.

One way to elucidate the *trans* influence of a certain ligand is to measure the bond length of the ligand *trans* to it. A series of P_2PtClX (X = B, C, N) complexes are shown in Figure 2-4 as well as their corresponding Pt-Cl bond length.[116] The Pt-Cl bond length is the shortest when it is *trans* to an amido group and the longest when it is *trans* to a boryl group, which is consistent with boryl being the stronger σ-donating group. In the examples we discussed in Section 1.1.3.1, ammonia

underwent oxidative addition with (PC_5P)Ir and (PSiP)Ir complexes which featured strong *trans* influence alkyl or silyl group. On the other hand, (PCP)Ir complex which featured moderate *trans* influence aryl group, reacted with ammonia to form ammonia coordination product. Hence, we expect PBP metal complexes (**J**), which feature a strong *σ*-donor and *trans* labilizing boryl group, will promote the formation of coordinatively unsaturated complexes, which often shows enhanced reactivity.[5]

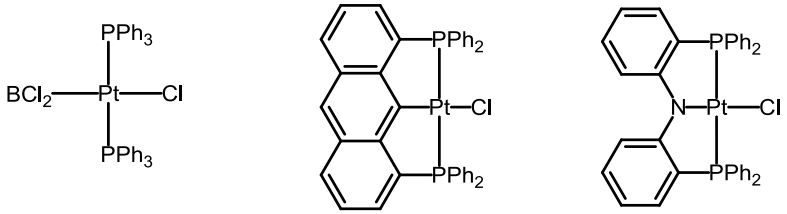

Figure 2-4. Square planar Pt(II) complexes and the Pt-Cl bond length.

2.1.3 Synthesis of $BrC_6H_4PR_2$ and its Use as a Building Block for Polydentate Ligands

We set to obtain pincer complexes **H, J** and **K** (Scheme 2-1). These ligand sets may not only be viewed as a new membe of "pincer toolbox" for organometallic chemist but also bring new reactivity to the resulting boryl and silylene species. Complexes **J** might be synthesized through oxidative addition of B-H or B-Hal bond of ligand precursors **201** and **202** to transition metal center. B-Hal bond oxidative addtion has been intensely studied with group 10 metals, especially platinum,[117] while B-H bond oxidative addition has been reported with Ir.[16] We expect to obtain

complexes **H** via two separate Si-H bond activation process. Complex **203** is expected to obtain via one Si-H bond activation reaction of **204** with metal halides in the presence of base, similar to the reaction reported with the PSi(H)(Me)P ligand.[17a] The second Si-H bond activation is expected to be accomplished via hydride abstraction with trityl salts, which is a well known method to access metal silylene complexes.[118] Similar to the phenyl ring, a pyrrole ring is a rigid, planar aromatic system. The P_2C= ligand (**C**) have been reported with pyrrole as the linkage.[19] Here, we propose to synthesize pincer boryl complex **K** with pyrrole linkers. Here the ligand set is linked through N-pyrrole rather than 2-pyrrole in complex **C**. Complexes **C** could be obtained via B-H bond oxidative addition of **205** to metal center. **205** might be synthesized via N-B bond coupling reaction[16a] of BH_3 and 2-phosphinoprrole, which might be obtained via reaction of lithiated pyrrole ring and ClP^iPr_2. Proposed complexes **J** and **K** not only eliminate the potentially reactive methylene protons in reported PBP complexes **I**, but also mimic the rigid backbone set our group reported before in complexes **C** and **E**, which would be easier in the future to evaluate the electronic effect of boryl central donor in complexes **J** and **K**.

Scheme 2-1. Retrosynthetic analysis of target PSiP and PBP ligand precursors.

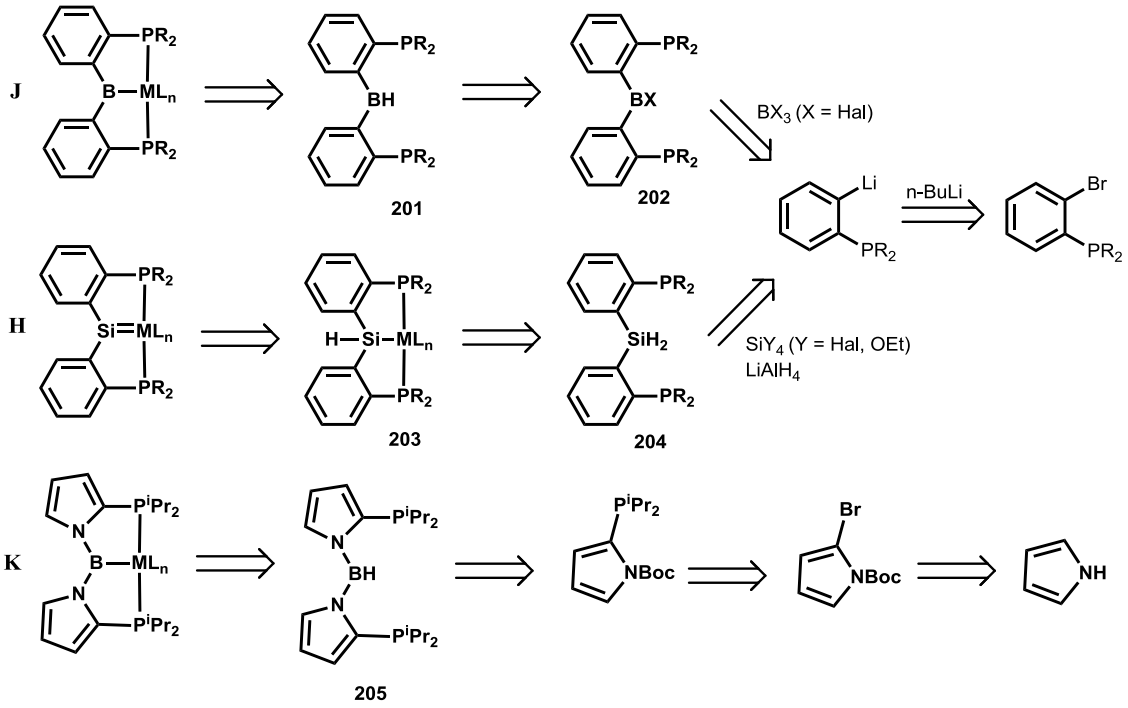

The key to obtain our proposed ligand precursors **202** and **204** is to form the corresponding C-Si and C-B bonds. Conventional benzene based PCP ligand[119] precursors (**A**) or pyridine based PNP ligand[120] precursors (**D)** were synthesized from corresponding resorcinol or 2,6-lutidine. The frameworks of diarylamine based PNP ligands[121] (**E**) or dipyrromethane based PCP ligands[19a] (**C**) were made via C-N Buchwald-Hartwig coupling reactions or Lewis acid catalyzed condensation reactions between formaldehyde and pyrrole, respectively (Scheme 2-2). However, all these methods are not suitable to synthesize our proposed ligand precursor **202** and **204**. On the other hand, the reactions of R-Li with various electrophiles were proven to be a

reliable and versatile method to form C-X bonds (X = B, Si, P).[122] The R-Li reagents could be easily obtained via lithium halogen exchange of R-Br and BuLi. Hence, the retrosynthetic analysis of target PBP and PSiP ligands led to *o*-bromophenylphosphine as the viable starting material (Scheme 2-2).

Scheme 2-2. Conventional methods to synthesize ligand precursors (**A**, **C**, **D, E**).

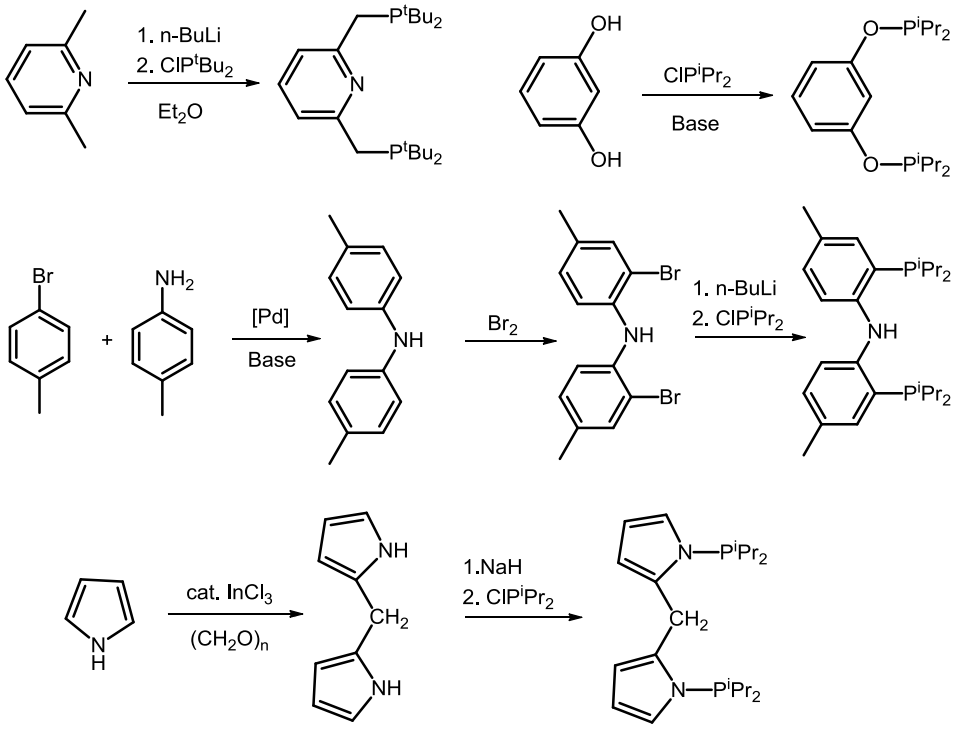

As shown in Scheme 2-3, several methods for the synthesis of $BrC_6H_4PR_2$ have been presented in the literature.[123] In method **I**, *o*-bromophenyl-di-*iso*-propylphosphine was synthesized by mono-lithiation of *o*-dibromobenzene followed by addition of chlorodi-*iso*-propylphosphine.[123b] This is arguably the most efficient and straightforward

way to synthesize $BrC_6H_4PR_2$ type of compounds. However, it suffered from inconsistent reproducibility [124] and small reaction scope. Only the synthesis of $BrC_6H_4PR_2$ has been reported by this method. Bromophenyldiphenylphosphine was obtained through Pd catalyzed C-P coupling reaction from *o*-bromoiodobenzene and diphenylphosphine (Method **II**).[123d] Nevertheless, this method has only been used to synthesize the diaryl-substituted bromophenylphosphine, probably because dialkylphosphines are generally more expensive and more difficult to handle compared to corresponding chlorodialkylphosphine. Method **III** avoided the use of dialkylphosphine reagents, but it was a two step synthesis which normally means longer workup procedure and lesser overall yield.[123a, 123c]

Scheme 2-3. Various procedures for the synthesis of $BrC_6H_4PR_2$.

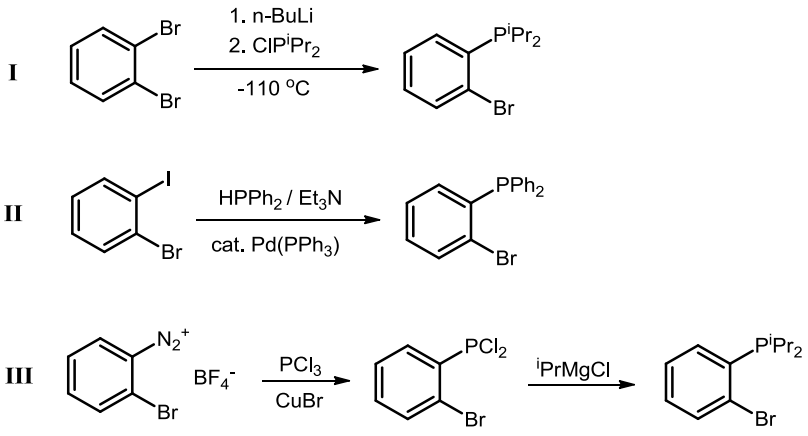

2.2 Results and Discussion

2.2.1 Design and Synthesis of $PSi(H_2)P^{iPr}$

Following the literature procedure shown in Scheme 2-3 method **I**, *o*-bromophenyldi-*iso*-propylphosphine (**206**) was obtained in good yield, normally above 80%.[123b] However, the yield was very low (<20%) in our hands if the temperature was not well controlled to be below -100 °C throughout the reaction time. *o*-Lithiobromobenzene, the key intermediate in this reaction, was shown to decompose to form benzyne at -90 °C with a half-life time around 30 min.[125] The reaction worked best in 1:1 mixture of diethyl ether and THF solution. Low yield (around 10%) was obtained when pure diethyl ether or THF was used as solvent, presumably because diethyl ether (-116 °C) and THF (-108 °C) both have m.p. close to -110 °C, which would possibly decrease the reaction efficiency under the reaction conditions. *o*-Lithiation of dibromobenzene, followed by reaction with di-*tert*-butyl-chlorophosphine did not proceed to yield *o*-bromophenyldi-*tert*-butylphosphine, presumably because chlorodi-*tert*-butylphosphine is a worse electrophile compared to chlorodi-*iso*-propylphosphine. More donating solvents such as DME and TMEDA have been tested for this reaction, however no successful production of bromophenyldi-*tert*-butylphosphine has been accomplished.

As depicted in Scheme 2-5, bis-2-phosphinophenylsilane (**207**) was synthesized from **206** via a multi-step synthetic method without purification of the intermediates. Lithiation of **206**, followed by addition of tetraethoxysilane and, subsequently, lithium aluminum hydride, yielded **207** in 79% yield after workup. Less than 5% mono-2-

phosphinophenylsilane was often observed after the reaction which could be removed by vacuum distillation. Fortunately, **207** freezes at around 5 °C. Therefore, the undesired mono-substituted byproduct could also be removed by recrystallization from n-pentane at -35 °C. **207** displayed a singlet at 2.5 ppm in its $^{31}P\{^{1}H\}$ NMR spectrum and a triplet of triplets at -39.6 ppm in its ^{29}Si NMR spectrum. Its ^{1}H NMR spectrum featured one resonance for the 2 H on the silicon center with coupling to both silicon and phosphorus. All these characteristics of NMR spectra are consistent with our structural assignment for **207**. When lithiated **206** was treated with $SiCl_4$ instead of $Si(OEt)_4$, multiple products, such as mono-, bis- and tris-substituted silanes were observed(Scheme 2-4).[122b]

Scheme 2-4. The synthesis of compound **207** and **208**.

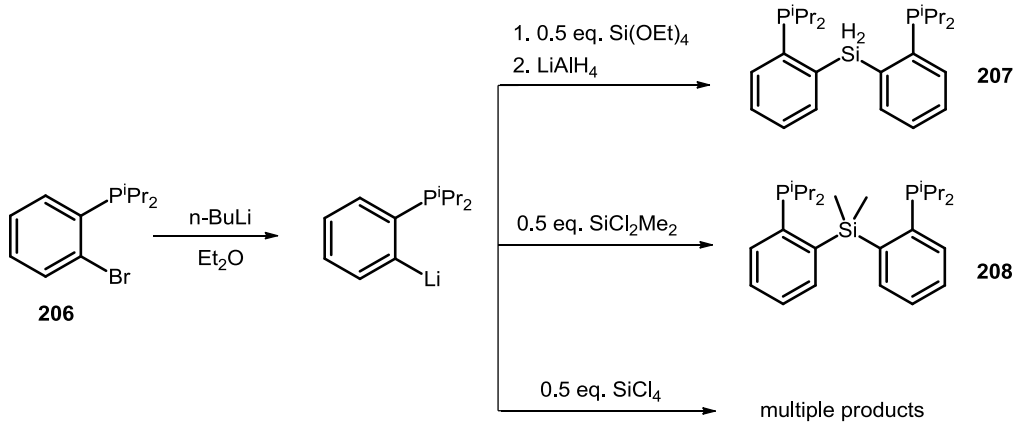

Bis(2-(di-*iso*-propylphosphino)phenyl)-dimethylsilane (**208**) was synthesized via reaction of lithiated **206** and $SiCl_2Me_2$. Since exhaustive arylation of dichlorodimethylsilane was targeted here, the selectivity was not an issue. **208** was

isolated in 98% yield after workup following the procedure described in Scheme 2-4. **208** displayed similar spectroscopic data to **207**, with one singlet at 1.5 ppm in its $^{31}P\{^{1}H\}$ NMR spectrum and one triplet for the Si-*Me* group at 5.4 ppm in the $^{13}C\{^{1}H\}$ NMR spectrum. The details of the chemistry of **207**, **208** and group 10 metals are discussed in Chapter IV.

2.2.2 Efforts towards PBP Ligand

Scheme 2-5. Synthesis of compound **209**.

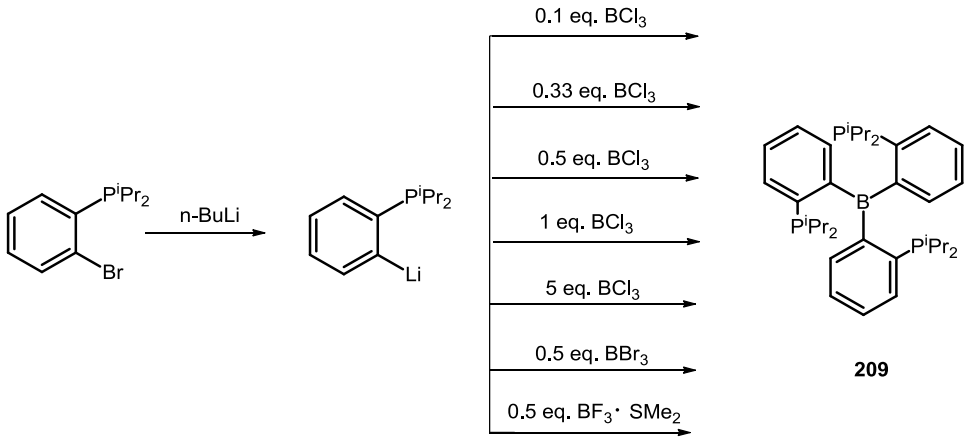

Encouraged by the synthesis of the PSiP ligand precursors, we set to explore the similar chemistry to synthesize the PBP ligand precursors. Chloro-bis-2-phosphino-phenylborane **202** was expected to be obtained via reaction of BX_3 and 2 equivalents of lithiated **206**, similarly to the reaction of SiX_4 and lithiated **206**. Although B-C bond formation was observed for the reaction with B-X and R-Li, we were not able to obtain the desired **202** by controlling the reaction stoichiometry. Indeed, we found the

reactions between the lithium salt of **206** and BX_3 (X = halogen) showed superb selectivity. Tris-2-phosphinophenyl borane **(209)** was isolated as the only product through reactions with lithiated **206** and various BX_3 reagents (Scheme 2-5). The solid state structure[126] of **209** revealed that one phosphorus was bound to the boron center, while the other two were relatively far away (Figure 2-5). Only one resonance at 5.3 ppm was found in solution $^{31}P\{^{1}H\}$ NMR spectrum at room temperature which indicated all three phosphorus were equivalent to each other. During the progress of this project, Bourissou and coworkers communicated the same ligand in 2007.[127] The details of the chemistry of **209** with group 10 metals are discussed in Chapter V.

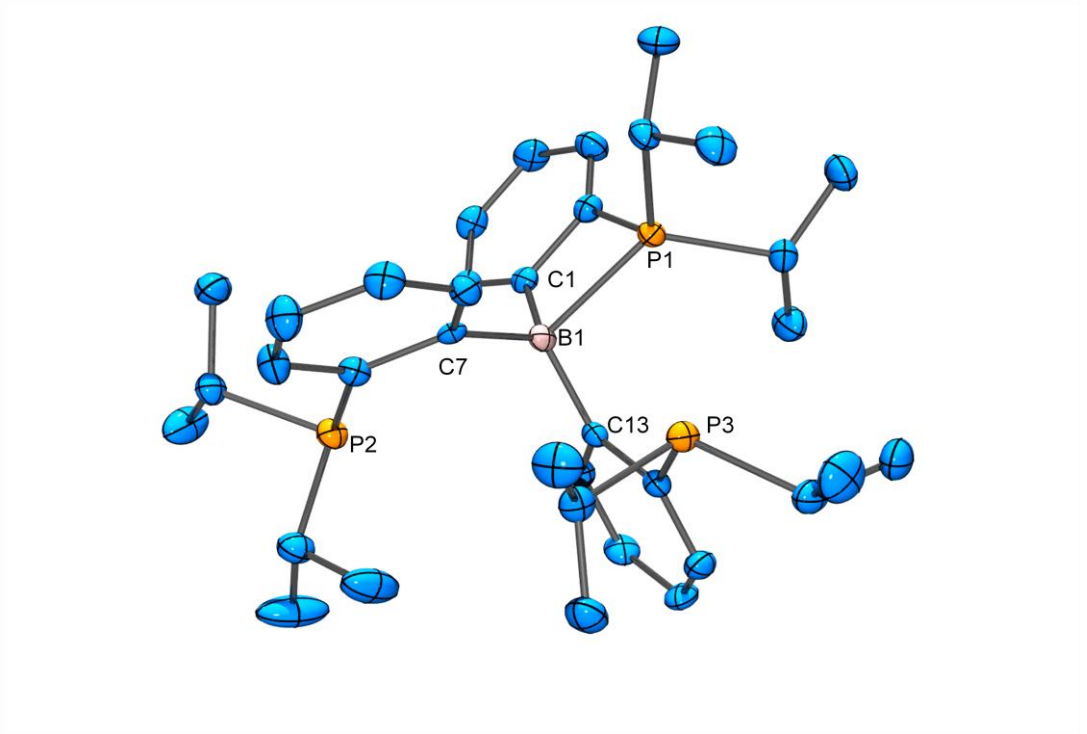

Figure 2-5. ORTEP[128] drawing (50% probability ellipsoids) of **209.** Omitted for clarity: H atoms. Selected distance (Å) and angles (deg) follow: B1-P2, 2.137 (2); B1-C1, 1.621 (3); B1-C7: 1.650 (3); B1-C13, 1.632 (3).

Since the reactions with boron trihalides only yielded tris-2-phosphinophenyl-borane, we decided to synthesize phenyl-bis-2-phosphinophenylborane (**210**) as our ligand presursor to access pincer boryl metal complexes. **210** was previously reported by Bourissou group via reaction of lithiated **206** and $ClBPh_2$ (Scheme 2-6).[129] We expect to obtain our target pincer boryl complexes via oxidative addition of B-Ph bond to the transition metal center. The details of chemistry between **210** and Rh are presented in Chapter VII.

Scheme 2-6. Synthesis of compound **210**.

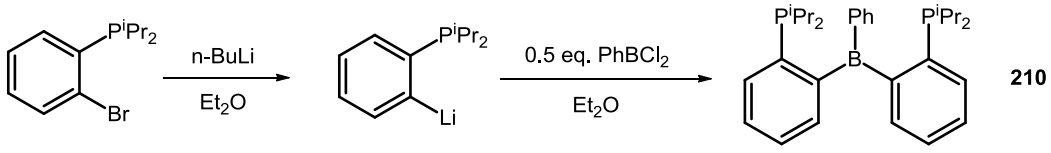

In the PBP ligand synthesized by the Nozaki group,[16] the chelating diamino substitutes were shown to stabilize the electrophilic main-group elements. Hence we set to synthesize pyrrole based PBP ligand **205**. The synthetic route was summarized in Scheme 2-7. Although we were able to selectively brominate pyrrole at the 2-position,[130] 2-bromopyrrole was not stable at room temperature. Subsequent protection of pyrrole by Boc group ($-CO_2{}^tBu$) allowed us to isolate compound **211** in high yield. However, lithiation of compound **211** followed by addition of ClP^iPr_2 only yielded the **212** after protic workup, which indicated that the lithium salt of the Boc-protected pyrrole is not nucleophilic enough to react with ClP^iPr_2 to yield the desired 2-phosphino-

pyrrole product. It might be worth trying more electron-donating protecting group in the future, which might make the lithiated **211** type of compounds more reactive towards ClP^iPr_2.

Scheme 2-7. Attempts to synthesize ligand 2-phosphino-pyrrole**.**

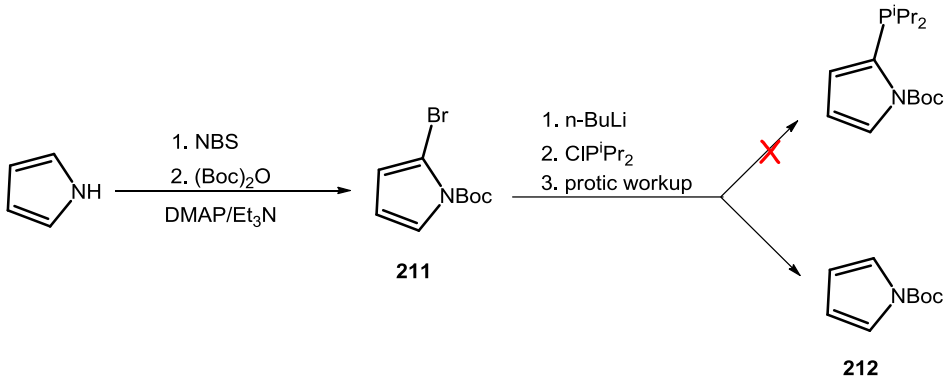

2.3 Conclusion

In conclusion, $BrC_6H_4P^iPr_2$ was synthesized in high yield via a one step procedure from commercial available chemicals, which was later shown to react with various electrophiles after lithiation. Efforts have been made towards the synthesis of $BrC_6H_4P^tBu_2$. However due to the low electrophilicity of ClP^tBu_2, it showed no reaction with *o*-$BrLiC_6H_4$ under tested conditions. Lithiated **206** displayed different chemo selectivity in the reactions with Si-OEt bonds and Si-Cl bonds. Ligand **207** was isolated as a pure product via reaction of lithiated **206** and $SiOEt_4$ by controlling the reaction stoichiometry. On the other hand, no chemo selectivity was observed for the reaction

between Si-Cl and R-Li, as mono-, bis- and tris-substituted silanes were observed as the products. The reaction between B-Cl and R-Li showed great chemo selectivity, as **TPB** compound was obtained as the only product.

2.4 Experimental Details

General considerations. Unless specified otherwise, all reactions and manipulations were carried out under an argon atmosphere using glovebox or Schlenk line techniques. Dry, oxygen–free solvents were employed. Toluene, pentane, diethyl ether, THF and C_6D_6 were dried over NaK / Ph_2CO / 18-crown-6, distilled and stored over molecular sieves in an Ar-filled glove box. Pyrrole, σ-dibromobenzene, phenyldichloroborane, $Si(OEt)_4$ and 2,6-lutidine were fractionally distilled prior to use. Chlorodi-iso-propylphosphine and chlorodi-tert-butylphosphine were purchased from Dalchem and used as received. All other chemicals were used as received from commercial vendors unless otherwise noted.

Physical methods. NMR spectra were recorded on a Varian iNova 300 spectrometer (^{1}H NMR, 299.9 MHz, ^{13}C NMR, 75.4 MHz, ^{31}P NMR, 121.4 MHz), a Varian iNova 400 spectrometer (^{1}H NMR, 400.0 MHz, ^{13}C NMR, 100.5 MHz, ^{31}P NMR, 161.9 MHz ^{29}Si NMR, 79.4 MHz, ^{11}B NMR, 120.4 MHz) and a Varian iNova 500 spectrometer (^{13}C NMR, 125.7 MHz, ^{11}B NMR, 160.5 MHz) in noted solvents. Chemical shifts were given in δ (ppm). ^{29}Si NMR spectra were referenced externally with $SiMe_4$ at δ 0. ^{11}B NMR spectra were referenced externally with BF_3 etherate at δ 0. ^{31}P NMR spectra were referenced externally with 85% phosphoric acid at δ 0. ^{1}H NMR and ^{13}C NMR

spectra were referenced using the solvent signals. Elemental analyses were performed by CALI, Inc. (Parsippany, NJ). The solid state structure of **209** was solved by Prof. Bruce M. Foxman and Dr. Chun-Hsing Chen.

Synthesis of 2-di-*iso*-propylphosphinophenyl bromide (Compound 206). To a solution of dibromobenzene (10.9 g, 46.2 mmol) in diethyl ether (80 mL) and THF (80 mL) was slowly added a solution of *n*-BuLi (18.5 mL, 2.5 M in hexanes, 46.2 mmol) at -110 °C. The mixture was stirred at same temperature for 45 min. White percipitates were observed during the time. Chlorodi-*iso*-propylphosphine (8.3 mL, 43.9 mmol) was then slowly added into the mixtures at -110 °C, which slowly became a deep purple suspension. The mixtures were stirred at same temperture for another 30 min before it was warmed up to room temperature. After removal of all volatiles, the residue was dissolved in 100 mL of pentane and stirred with 10 g of silical gel for 1 h at room temperature. After passed through Celite, all volatiles were removed under vacuum to yield 11.7 g (97%) of clear oil as crude product. The colorless oil is pure by $^{31}P\{^{1}H\}$ NMR and good for further reactions. The crude product could be further purified by vacuum distillation if necessary. $^{31}P\{^{1}H\}$ NMR (121.4 MHz, C_6D_6): δ 8.5 (s). ^{1}H NMR (299.9 MHz, C_6D_6): δ 7.45 (dd, J_{H-H} = 7 Hz, J_{H-H} = 2 Hz, 1H, Ar-*H*), 7.10 (dt, J_{H-H} = 7 Hz, J_{H-H} = 2 Hz,1, Ar-*H*), 6.91 (td, J_{H-H} = 7 Hz, J_{H-H} = 2 Hz, 1H, Ar-*H*), 6.70 (td, J_{H-H} = 7 Hz, J_{P-H} = 2 Hz, 1H, Ar-*H*), 1.88 (m, 2H, C*H*Me$_2$), 1.10 (dd, J_{P-H} = 14 Hz, J_{H-H} = 7 Hz, 6H, CH*Me*$_2$), 0.86 (dd, J_{P-H} = 14 Hz, J_{H-H} = 7 Hz, 6H, CH*Me*$_2$). (Figure 2-6)

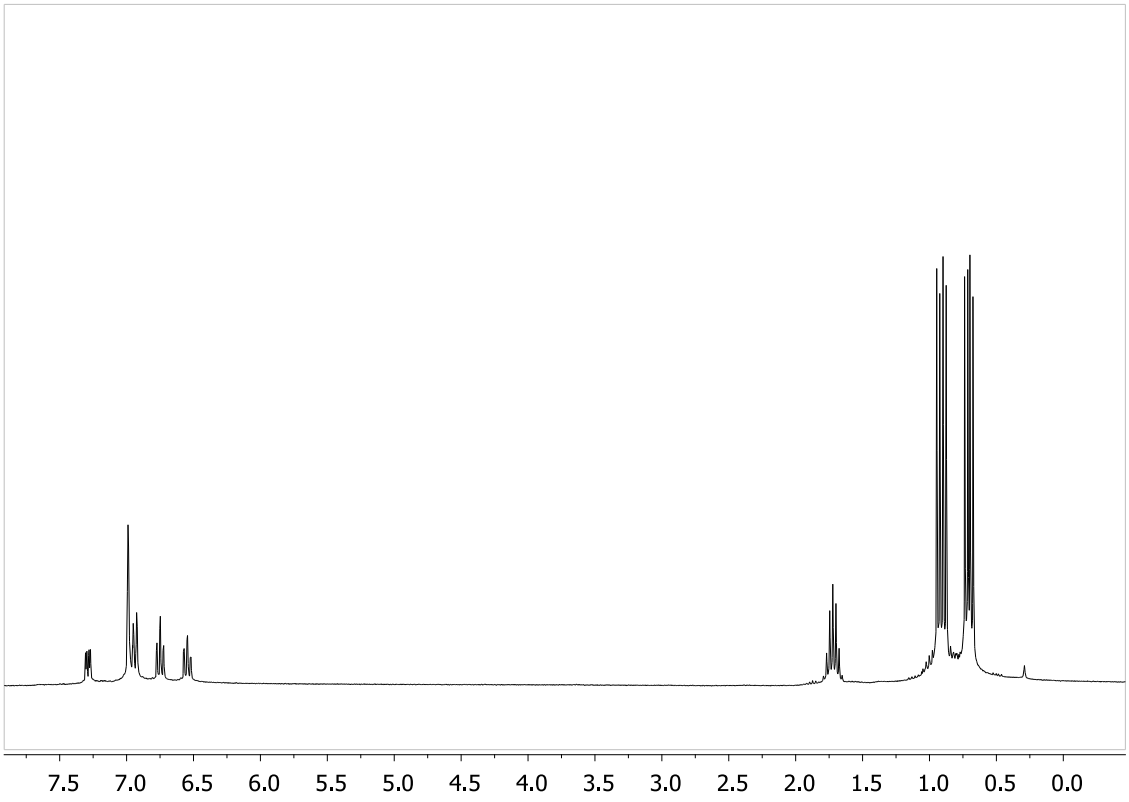

Figure 2-6. ^{1}H NMR spectrum of **206** in C_6D_6 at 23°C measured on a 300 MHz Varian iNova. (Trace amount of silicon grease)

Synthesis of (PSiP)H_2 (Compound 207). To a cold solution of **206** (4.85 g, 17.77 mmol) in diethyl ether (100 mL) was slowly added a solution of *n*-BuLi (7.8 mL, 2.5 M in hexanes, 19.50 mmol). The reaction mixtures were stirred at room temperature for 2 h. Then it was cooleded to -30 °C and slowly added to a cold solution of $Si(OEt)_4$ (1.68 g, 8.01 mmol) in diethyl ether (25 mL). The reaction mixtures were stirred at room temperature for 12 h before a solution of $LiAlH_4$ (14.8 mL, 2.4 M in THF, 35.54 mmol) was slowly added. The resulting pale yellow suspension was

stirred at room temperature for 6 h. After removal of all volatiles, the residue was redisolved in 100 mL pentane and stirred with silica gel for 1 h. The reaction mixtures were passed through a short plug of Celite. (**Caution:** *The solid wastes here were transfered to a Schlenk flask and quenched by acetone under Ar.*) After removal of all volatiles, a pale yellow oil was obtained which was mixed with 1 mL pentane and stayed at -30 °C overnight. 2.6 g of white solid was obtained as final product which was washed with 1 mL of cold pentane three times. (The final product was stored in the freezer) Yield: 2.6 g (79%). $^{31}P\{^{1}H\}$ NMR (121.4 MHz, C_6D_6): δ 2.5 (s). ^{1}H NMR (299.9 MHz, C_6D_6): δ 7.86 (dt, J_{H-H} = 7 Hz, J_{P-H} = 2 Hz, 2H, Ar-*H*), 7.33 (dt, J_{H-H} = 7 Hz, J_{P-H} = 2 Hz, 2H, Ar-*H*), 7.17-7.11 (m, 4H, Ar-*H*), 5.89 (t, J_{P-H} = 9 Hz, J_{Si-H} = 204 Hz, 2H, Si-*H*), 1.92 (m, 4H, C*H*Me_2), 1.06 (dd, J_{P-H} = 14 Hz, J_{H-H} = 7 Hz, 12H, CH*Me*$_2$), 0.85 (dd, J_{P-H} = 14 Hz, J_{H-H} = 7 Hz, 12H, CH*Me*$_2$). (Figure 2-7) $^{13}C\{^{1}H\}$ NMR (125.7 MHz, C_6D_6): δ 144.4 (d, J_{P-C} = 15 Hz), 144.1 (dd, J_{P-C} = 46 Hz, J_{P-C} = 4 Hz), 138.9 (dd, J_{P-C} = 15 Hz, J_{P-C} = 3 Hz), 131.8 (d, J_{P-C} = 3 Hz), 129.3 (s), 128.3 (m), 25.1 (d, J_{P-C} = 14 Hz, *C*HMe_2), 20.3 (d, J_{P-C} = 18 Hz, *C*HMe_2), 20.0 (d, J_{P-C} = 11 Hz, CH*Me*$_2$). ^{29}Si NMR (79.4 MHz, C_6D_6): δ -39.6 (tt, J_{Si-H} = 204 Hz, J_{Si-P} = 22 Hz).

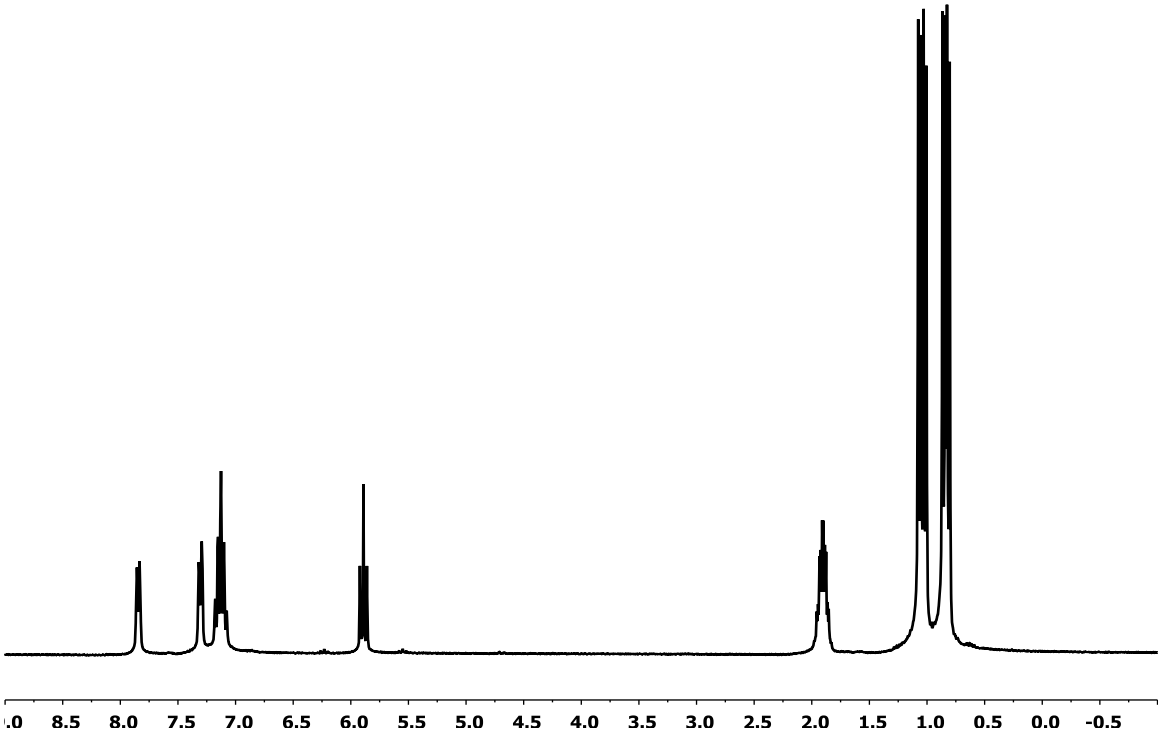

Figure 2-7. ^{1}H NMR spectrum of **207** in C_6D_6 at 23°C measured on a 300 MHz Varian iNova.

Synthesis of (PSiP)Me$_2$ (Compound 208). To a cold solution of **206** (2.17 g, 7.96 mmol) in diethyl ether (50 mL) was slowly added a solution of *n*-BuLi (2.6 mL, 2.5 M in hexanes, 6.5 mmol). The reaction mixtures were stirred at room temperature for 2 h. Then it was cooleded to -30 ℃ and slowly added to a cold solution of $SiCl_2Me_2$ (0.38 mL, 3.18 mmol) in diethyl ether (25 mL). The resulting pale yellow

suspension was stirred at room temperature for 6 h. After removal of all volatiles, the residue was redisolved in 50 mL pentane and passed through a short plug of Celite and silica gel. After removal of all volatiles, the crude products were rerystallized from pentane at -30 ℃ to yield white crystals as final products. Yield: 1.1 g (78%). $^{31}P\{^{1}H\}$ NMR (161.9 MHz, C_6D_6): δ 1.6 (s). ^{1}H NMR (400.0 MHz, C_6D_6): δ 7.85 (br, 2H, Ar-*H*), 7.37 (br, 2H, Ar-*H*), 7.13 (m, 4H, Ar-*H*), 1.81 (m, 4H, C*H*Me_2), 1.10 (m, 6H, Si*Me*$_2$), 1.06 (dd, J_{P-H} = 14 Hz, J_{H-H} = 7 Hz, 12H, CH*Me*$_2$), 0.81 (dd, J_{P-H} = 14 Hz, J_{H-H} = 7 Hz, 12H, CH*Me*$_2$). (Figure 2-8) $^{13}C\{^{1}H\}$ NMR (100.5 MHz, C_6D_6): δ 149.0 (d, J_{P-C} = 44 Hz), 145.0 (d, J_{P-C} = 17 Hz), 137.2 (d, J_{P-C} = 15 Hz), 132.1(s), 128.4 (s), 126.5 (m), 26.1 (d, J_{P-C} = 20 Hz, *C*HMe_2), 21.2 (d, J_{P-C} = 14 Hz, *C*HMe_2), 5.4 (t, J_{P-C} = 12 Hz, Si*Me*$_2$).

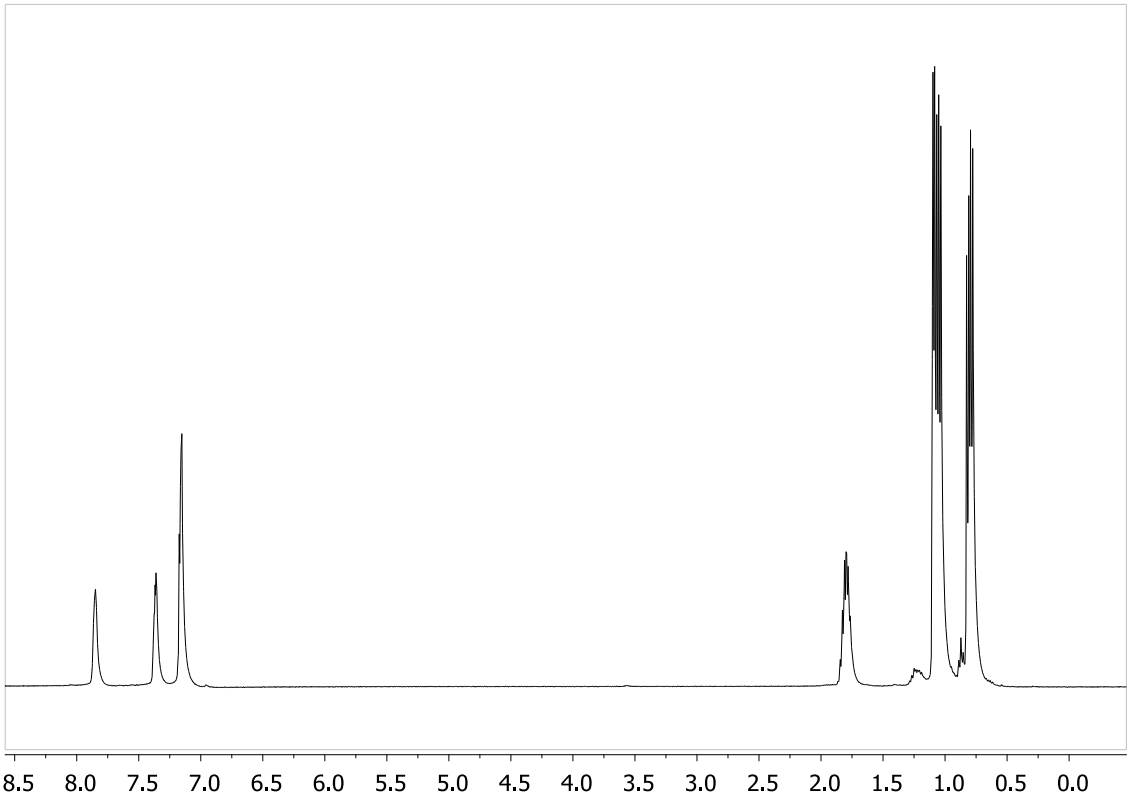

Figure 2-8. ^{1}H NMR spectrum of **208** in C_6D_6 at 23°C measured on a 400 MHz Varian iNova. (Trace amount of n-pentane)

Synthesis of $(C_6H_4P^{iPr2})_3B$ (TPB) (Compound 209). To a cold solution of **206** (0.75 g, 2.74 mmol) in toluene (5 mL) was slowly added a solution of *n*-BuLi (1.2 mL, 2.4 M in hexanes, 2.88 mmol). The reaction mixtures were stirred at room temperature for 2 h. Then it was cooleded to -30 ℃ and BCl_3 (0.91 mL, 1M in heptane, 0.91 mmol) was slowly added in to the mixture. The reaction mixtures were stirred at room temperature for 2 h. The resulting pale yellow suspension was passed through a short plug of Celite. After removal of all volatiles, a pale yellow powder

was recrystallized from toluene at -30 ℃ to yield 0.42 g (79%) of white crystals as the final product. $^{31}P\{^{1}H\}$ NMR (161.9 MHz, C_6D_6): δ 5.3 (s). ^{1}H NMR (400.0 MHz, C_6D_6): δ 8.15 (br, 3H, Ar-*H*), 7.33 (d, J_{H-H} = 7 Hz, 3H, Ar-*H*), 7.22 (t, J_{H-H} = 7 Hz, 3H, Ar-*H*), 7.14(m, 3H, Ar-*H*), 1.97 (m, 6H, C*H*Me_2), 1.06 (m, 18H, CHMe_2), 0.85 (m, 18H, CHMe_2). (Figure 2-9)

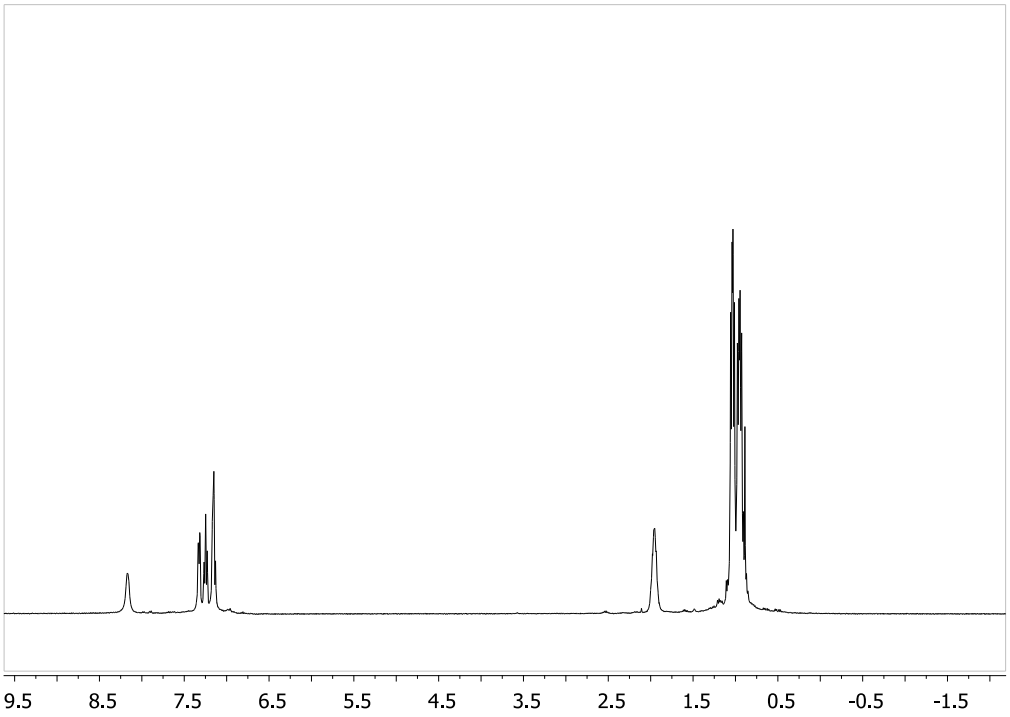

Figure 2-9. ^{1}H NMR spectrum of **209** in C_6D_6 at 23°C measured on a 400 MHz Varian iNova.

Reaction of 206 with 1 eq. BCl_3. To a cold solution of **206** (0.29 g, 1.1 mmol) in toluene (3 mL) was slowly added a solution of *n*-BuLi (0.47 mL, 2.4 M in hexanes, 1.2 mmol). The reaction mixtures were stirred at room temperature for 2 h. Then it was cooleded to -30 ℃ and BCl_3 (1.1 mL, 1M in heptane, 1.1 mmol) was slowly added in to the mixture. The reaction mixtures were stirred at room temperature for 2 h. The resulting pale yellow suspension was passed through a short plug of Celite. After removal of all volatiles, the pale yellow powder was recrystallized from toluene at -30 ℃ to yield 0.15 g (71%) of white crystals as final product. $^{31}P\{^1H\}$ NMR (161.9 MHz, C_6D_6): δ 5.3 (s). ^1H NMR (400.0 MHz, C_6D_6): δ 8.15 (br, 3H, Ar-*H*), 7.33 (d, J_{H-H} = 7 Hz, 3H, Ar-*H*), 7.22 (t, J_{H-H} = 7 Hz, 3H, Ar-*H*), 7.14(m, 3H, Ar-*H*), 1.97 (m, 6H, C*H*Me_2), 1.06 (m, 18H, CH*Me*$_2$), 0.85 (m, 18H, CH*Me*$_2$).

Synthesis of $P^{iPr}B^{Ph}P$ (Compound 210). To a cold solution of **206** (1.27 g, 4.65 mmol) in diethylether (10 mL) was slowly added a solution of *n*-BuLi (1.9 mL, 2.5 M in hexanes, 4.75 mmol). The reaction mixtures were stirred at room temperature for 2 h. Then it was cooleded to -30 ℃ and $PhBCl_2$ (0.30 mL, 2.33 mmol) was slowly added in to the mixture. The reaction mixtures were stirred at room temperature for 2 h. The resulting orange/red suspension was passed through a short plug of Celite. After removal of all volatiles, the pale orange filtrate was concentrated to 10 mL and left at -30 ℃ for recrystallization. Yield 0.85 g (77%). $^{31}P\{^1H\}$ NMR (121.4 MHz, C_6D_6): δ 8.1 (s). ^1H NMR (500.0 MHz, C_6D_6): δ 7.68 (d, J_{H-H} = 7 Hz, 2H, Ar-*H*), 7.44 (t, J_{H-H} = 7 Hz, 2H, Ar-*H*), 7.32 (m, 2H, Ar-*H*), 7.20(t, J_{H-H} = 7 Hz, 2H, Ar-*H*), 7.10-7.14 (m, 5H, Ar-*H*), 1.91 (m, 4H, C*H*Me_2), 0.95 (dd, J_{P-}

$_H$ = 14 Hz, J_{H-H} = 7 Hz, 12H, CH*Me*$_2$), 0.76 (dd, J_{P-H} = 14 Hz, J_{H-H} = 7 Hz, 12H, CH*Me*$_2$) (Figure 2-10). $^{11}B\{^1H\}$ NMR (120.4 MHz, C_6D_6): δ -4.8 (br).

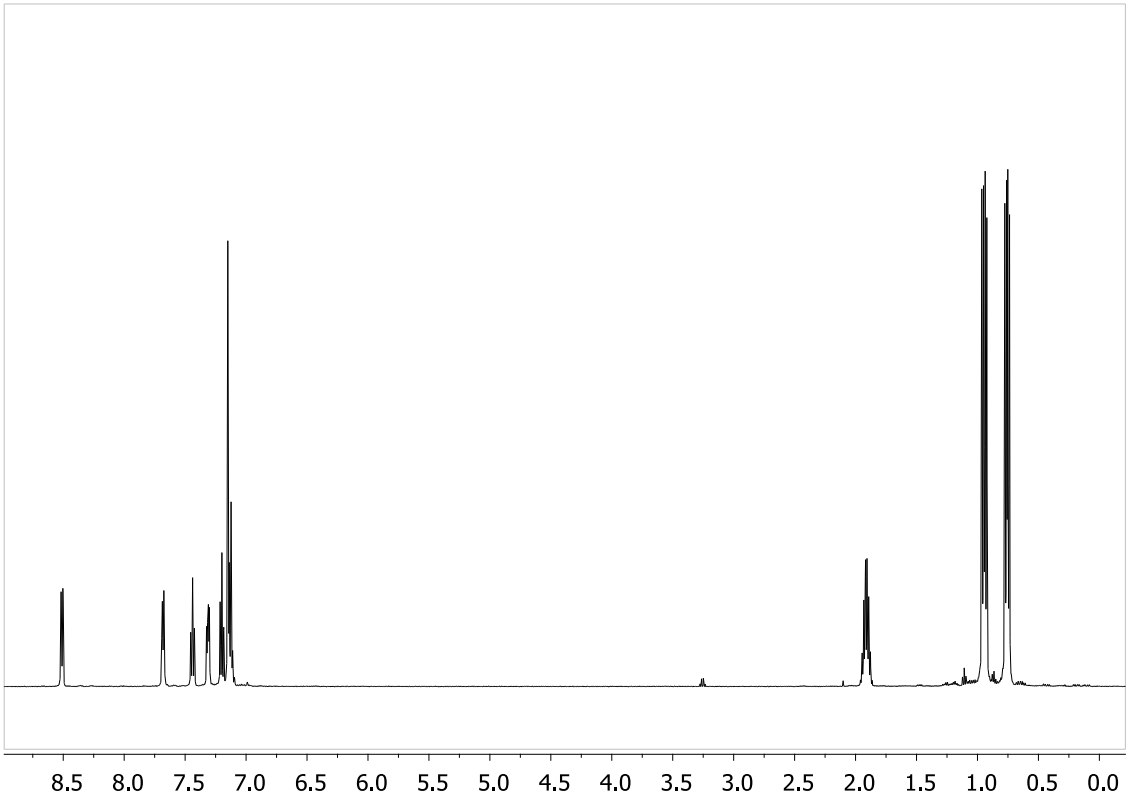

Figure 2-10. ^1H NMR spectrum of **210** in C_6D_6 at 23°C measured on a 500 MHz Varian iNova. (Trace amount of toluene, ether and n-pentane)

Synthesis of N-tert-butyl-carbomate-2-bromo-pyrrole (Compound 211). To a solution of pyrrole (1 mL, 14.4 mmol) in THF (20 mL) was slowly added *N*-Bromosuccinimide (2.56 g, 14.4 mmol) at -78 ℃. The resulting light-green solution

was stirred at same temperature for 2 h. After it was warmed up to room temperature, Et_3N (0.8 mL, 5.8 mmol), 4-dimethylaminopyridine (0.26 g, 0.15 mmol) and di-*tert*-butyl dicarbonate (3.8 g, `17.3 mmol) were added into the light green solution. The mixtures were stirred at room temperature for 2 h. After removal of all volatiles, the crude compound was purified by a column of alumina with hexanes as eluent. After removal of all solvent, white powders were obtained as the final product. Yield: 1.7 g (51%). ^{1}H NMR (299.9 MHz, $CDCl_3$): δ 7.32 (dd, J_{H-H} = 4 Hz, J_{H-H} = 2 Hz, 1H, C_4H_3N), 6.31 (dd, J_{H-H} = 4 Hz, J_{H-H} = 2 Hz, 1H, C_4H_3N), 6.16 (t, J_{H-H} = 4 Hz, 1H, C_4H_3N), CHMe_2), 1.62 (s, 9H, CMe_3). GC/MS: 246.

Attempted reaction to synthesize 2-di-*tert*-butylphosphinophenyl bromide. To a solution of dibromobenzene (0.84 g, 3.6 mmol) in diethyl ether (10 mL) and THF (10 mL) was slowly added a solution of *n*-BuLi (1.4 mL, 2.5 M in hexanes, 3.6 mmol) at -110 ℃ . The mixtures were stirred at same temperature for 45 min. White precipitates were observed during the time. Chlorodi-*tert*-butylphosphine (0.6 mL, 3.2 mmol) was then slowly added into the mixtures at -110 ℃ , which slowly became a deep purple suspension. The mixtures were stirred at same temperature for another 30 min before it was warmed up to room temperature. 50 μL of water was added to quench the reaction. After removal of all volatiles, the residue was dissolved in 20 mL of pentane and passed through Celite and silica gel. After removal of all volatiles, the residue was dissolve in C_6D_6 for ^{1}H and $^{31}P\{^1H\}$ NMR study. No desire product was observed in ^{1}H and $^{31}P\{^1H\}$ NMR spectra. Bromobenzene, chlorodi-*tert*-butylphosphine and bromodi-*tert*-butylphosphine were the major species in these NMR spectra. Other solvent

combinations have been tried with DME, TMEDA, none of them yielded desire products.

Attempted reaction to synthesize N-*tert*-butyl-carbomate-2-phosphino-pyrrole. To a solution of N-tert-butyl-carbomate-2-phosphanyl-pyrrole (1.7 g, 6.9 mmol) in THF (80 mL) was slowly added *n*-BuLi (3.1mL, 2.5 M in hexanes, 7.7 mmol) at -78 ℃ . The resulting yellow solution was stirred at same temperature for 1 h. Chlorodi-*iso*-propylphosphine (1.1 mL, 6.9 mmol) was then slowly added into the mixtures at -78 ℃ . The mixtures were stirred at -78 ℃ for 1 h and then warmed up to room temperature. After removal of all volatiles, the residue was dissolved in 20 mL of pentane and passed through Celite and silica gel. After removal of all volatiles, the residue was redissolved in C_6D_6 for ^1H and $^{31}P\{^1H\}$ NMR study. No desire product was observed in ^1H and $^{31}P\{^1H\}$ NMR spectra. N-*tert*-butyl-carbomate-pyrrole, chlorodi-*iso*-propylphosphine and bromodi-*iso*-propylphosphine were the major species in these NMR spectra.

CHAPTER III

CHLORINATION OF CARBORANES AND DODECABORATES*

3.1 Introduction

3.1.1 Chlorinated Carboranes and Dodecaborates

Since Knoth first prepared carborane anion in 1967,[131] more than 300 carborane derivatives have been reported.[63] Among these, the highly halogenated derivatives are the least nucleophilic and the most robust ones, partly because the delocalized negative charge could be further screened by a layer of halogen substituents.[63a] As a result of decreasing polarizability of the halides, the basicity of halogenated carborane anions decreases in the order I > Br > Cl > F.[63d] However, the synthesis of polyfluorinated carboranes requires the use of F_2, which involves non-trivial setup and training that makes it less accessible to most chemists.[63a]

Hence, highly chlorinated carboranes have become promising candidates for use as counterions for many highly electrophilic species.[63d]

---

* reprinted in part from *Chem. Commun.*, 46, Gu, W.; McCulloch, B. J.; Reibenspies, J. H.; Ozerov, O. V. "Improved Methods for the Halogenation of the $[HCB_{11}H_{11}]^-$ Anion", 2820, reproduced by permission of The Royal Society of Chemistry (RSC) and from *Inorg. Chem.*, 50, Gu, W.; Ozerov, O. V. "Exhaustive Chlorination of $[B_{12}H_{12}]^{2-}$ without Chlorine Gas and the Use of $[B_{12}Cl_{12}]^{2-}$ as Supporting Anion in Catalytic Hydrodefluorination of Aliphatic C-F Bonds", 2726, copyright 2011 American Chemical Society.

$H[HCB_{11}Cl_{11}]$ is the strongest known Bronsted acid which is stable to sublimation at 200 ℃ .[98] Vinyl[132], *t*-butyl,[96] and fullerene[133] cations have all been isolated with chlorinated carboranes. Carborane anions have allowed for the solution chemistry of silylium (R_3Si^+)[134] cations and alumenium (R_2Al^+)[100] cations and even for the isolation of a discrete silylium cation in the solid state.[97,135] On the other hand, although BARF anions ($[B(C_6F_5)_4]^-$ or $[B(C_6H_3(CF_3)_2)]^-$) have arguably similar basicity and nucleophilicity compared to halogenated carboranes,[63d] their stability is much worse, especially under highly electrophilic conditions. The decomposition of perfluorinated tetraphenylborates are reported to be initiated by hard electrophiles, such as alumenium.[83b]

Despite their great advantages, carborane anions are still in the process of making a transition formulated by Reed in 1998 as being "from exotica to specialty chemicals".[63a] In comparison, cesium dodecaborate $Cs_2[B_{12}H_{12}]$ could be easily obtained from commercial available materials.[102d] Recent reports have shown prechlorinated dodecaborate $[B_{12}Cl_{12}]^{2-}$ to be a promising candidate as weakly coordianting anion (WCA) despite its relatively low solubility in common organic solvents.[102] The higher "-2" charge on $[B_{12}Cl_{12}]^{2-}$ dianion makes them an unconventional class of weakly coordinating anions. $Me_2B_{12}Cl_{12}$ was reported by Knapp[102a] and coworkers; it was shown to be a strong methylating agent. The Reed and Knapp groups reported the synthesis of $[Et_3Si]_2[B_{12}Cl_{12}]$ which was used to prepare the diprotic superacid $H_2[B_{12}Cl_{12}]$.[102b,102c] $[B_{12}Cl_{12}]^{2-}$ showed comparable basicity to $[HCB_{11}Cl_{11}]^-$ as $[C_6H_7]_2[B_{12}Cl_{12}]$ and $[C_6H_7][HCB_{11}X_{11}]$ both showed very

similar $\nu(CH_2)$ frequencies of the most acidic CH_2 group at the protonated sp^3 carbon atom.[102c]

3.1.2 Chlorination of Carboranes and Dodecaborates

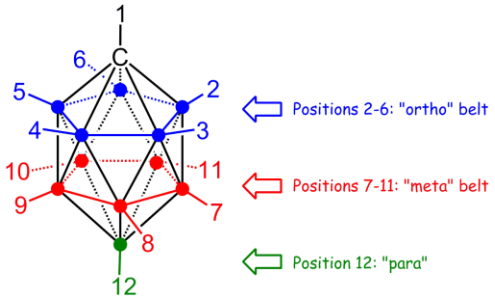

Figure 3-1. Representation of the carborane. (dots at vertices 2-12 represent boron atoms; each vertice is capped with a hydrogen atom).

Chlorination of carboranes has been accomplished using elemental chlorine (or ICl).[63a] Aromaticity of the carborane cage has been studied based on their energies, geometries, magnetic properties and NICS (nucleus-independent chemical shift) method.[136] Therefore, the halogenation of carboranes has been mechanistically likened to classical electrophilic aromatic substitution.[137] All of the examples of halogenation of carboranes in the literature show the substitution proceeds first at the "*para*" position, then at the "*meta*" belt, and finally at the "*ortho*" belt (Figure 3-1). Hexachlorination of carborane can be performed selectively (Scheme 3-1).[138] However, successful execution of the hexachlorination syntheses requires real-time monitoring of the reaction by ^{11}B NMR for hours or days, while deviations from the scale and conditions of the optimized procedure often result in loss of selectivity and

overchlorination. Undecachlorination takes place with ICl in triflic acid after several days at >200 °C (Scheme 3-1).[88,98] This is a consistently reproducible synthesis, but it requires a $3000 pressure- and reagent-resistant reactor for a 2 g batch capacity, and a rather lengthy and complicated workup. $[1\text{-Me-}CB_{11}Cl_{11}]^-$ is synthesized from methylated carborane anion $[1\text{-Me-}CB_{11}H_{11}]^-$ with chlorine gas in glacial acetic acid,[88] but this method requires the presence of the methyl group which limits the further functionalization of vertex-carbon position. We are interested in developing methods for chlorination that ideally a) are reproducible and insensitive to minor variations in conditions, i.e., "foolproof"; b) are scalable; c) do not require monitoring of the course of the reaction; d) do not involve elemental halogens, especially Cl_2 gas; e) proceed under atmospheric pressure and without specialty apparatus; f) use inexpensive reagents.

Scheme 3-1. Methods in the literature to synthesize chlorinated carborane.

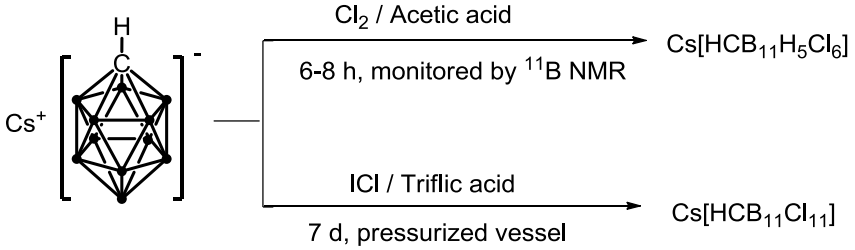

We focused our attention on element chlorides that are known to be oxidizing/chlorinating agents and zero in on SO_2Cl_2 and $SbCl_5$. These reagents are

inexpensive,[139] of relatively low toxicity, and are liquids that possess volatility that allows for a respectable reflux temperature but relative ease of removal of the excess of reagent under vacuum. Although SO_2Cl_2 and $SbCl_5$ are aggressive reagents, they can be handled in the laboratory under standard safety precautions. SO_2Cl_2 has the added advantage of presumably generating only gaseous by-products (SO_2 and HCl). Both SO_2Cl_2[140] and $SbCl_5$[141] have been used for chlorination in organic synthesis, including aromatic chlorination. SbF_5 was also reported to react with *o*-(di)carborane [1,2-$C_2B_{10}H_{12}$] to give partially fluorinated products.[142]

Similarly to the case of carborane, elemental chlorine has normally been used as the chlorinating agent for the syntheses of various polychlorinated dodecaborates (Scheme 3-2). $[B_{12}H_6Cl_6]^{2-}$ was synthesized via reaction of $[H_3O]_2[B_{12}H_{12}]$ with chlorine in water at 0 ℃ .[143] Muetterties reported the synthesis of $[B_{12}Cl_{12}]^{2-}$ by reacting $[B_{12}H_{12}]^{2-}$ with excess chlorine in an autoclave.[144] Knapp later reported an improved method[102d] which avoided the use of the high pressure autoclave by passing chlorine gas through the aqueous solution of $Na_2B_{12}H_{12}$ at 100 ℃ for 40 h. Encouraged by our results with the chlorination of $[HCB_{11}H_{11}]^-$ by SO_2Cl_2, we set to explore the synthesis of $[B_{12}Cl_{12}]^{2-}$ with SO_2Cl_2 as the chlorination reagent.

Scheme 3-2. Methods in the literature to synthesize chlorinated dodecaborate.

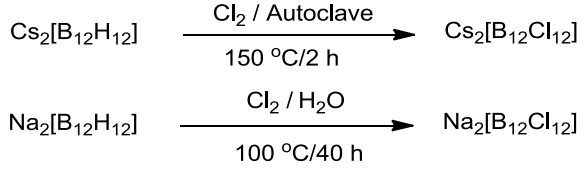

3.2 Results and Discussion

3.2.1 Chlorination of Carborane Anions

3.2.1.1 Chlorination of $Cs[CB_{11}H_{12}]$ with Cl_2

We first examined chlorination of the parent carborane with chlorine gas to obtain one clean partially or fully chlorinated carborane. Based on the previous reports,[63a] chlorination of parent carborane with Cl_2 displayed some chemo-selectivity between chlorinations at 7-12 positions and chlorinations at 2-6 positions. Therefore, it appear reasonable to us to develop chlorination method which would give clean $[HCB_{11}Cl_{11}]^-$ or $[HCB_{11}H_5Cl_6]^-$ products. Chlorination of parent carborane with Cl_2 in acetic acid has been tested by the Xie group for up to one month,[88] which only resulted a mixture of nona-, deca-, and undeca-chlorinatedcarborane anions. Hence, we focused our efforts on the reactions with stronger acid as the solvent, since it is recognized that high acidic conditions would accelerate the halogenation reactions of carborane.[63a] Performing the reaction in triflic acid at 140 °C in the presence of continuous Cl_2 gas flow for 50 h surprisingly yielded a single clean product with monoisotopic mass at 752. We assigned the identity of the product to be $[HCB_{11}Cl_9(CF_3SO_3)_2]^-$ based on the observed isotope pattern which was later confirmed by X-ray crystallography[145] and multinuclear NMR spectroscopy. Triflate groups were only observed at *para* position and *meta* ring based on the solid state structure we obtained (Figure 3-2). Hence, pure $Cs[HCB_{11}Cl_{11}]$ was obtained by performing the chlorination of $Cs[CB_{11}H_{12}]$ with Cl_2 first in acetic acid for 8h and then in triflic acid for 24h. By doing the chlorination in acetic acid first, the 7-12 positions of parent carborane would be chlorinated first which essentially prevent it from

being reacted with triflic acid to give triflyloxylated carboranes. Similar chlorination reactions of $Cs[HCB_{11}H_{11}]$ with Cl_2 were also tested with other acids as the solvent, such as HCl, H_2SO_4, H_3PO_4, CCl_2HCOOH and CCl_3COOH. However, none of these reactions gave the desired $[HCB_{11}Cl_{11}]^-$ or $[HCB_{11}H_5Cl_6]^-$ products (Scheme 3-3).

Scheme 3-3. Chlorination of carborane with Cl_2 in various acids. (*: here the $CsHCB_{11}H_5Cl_6$ is actually a mixture of $CsHCB_{11}H_6Cl_5$, $CsHCB_{11}H_5Cl_6$ and $CsHCB_{11}H_4Cl_7$ which is obtained from the reaction of $CsHCB_{11}H_{11}$ with Cl_2 in acetic acid).

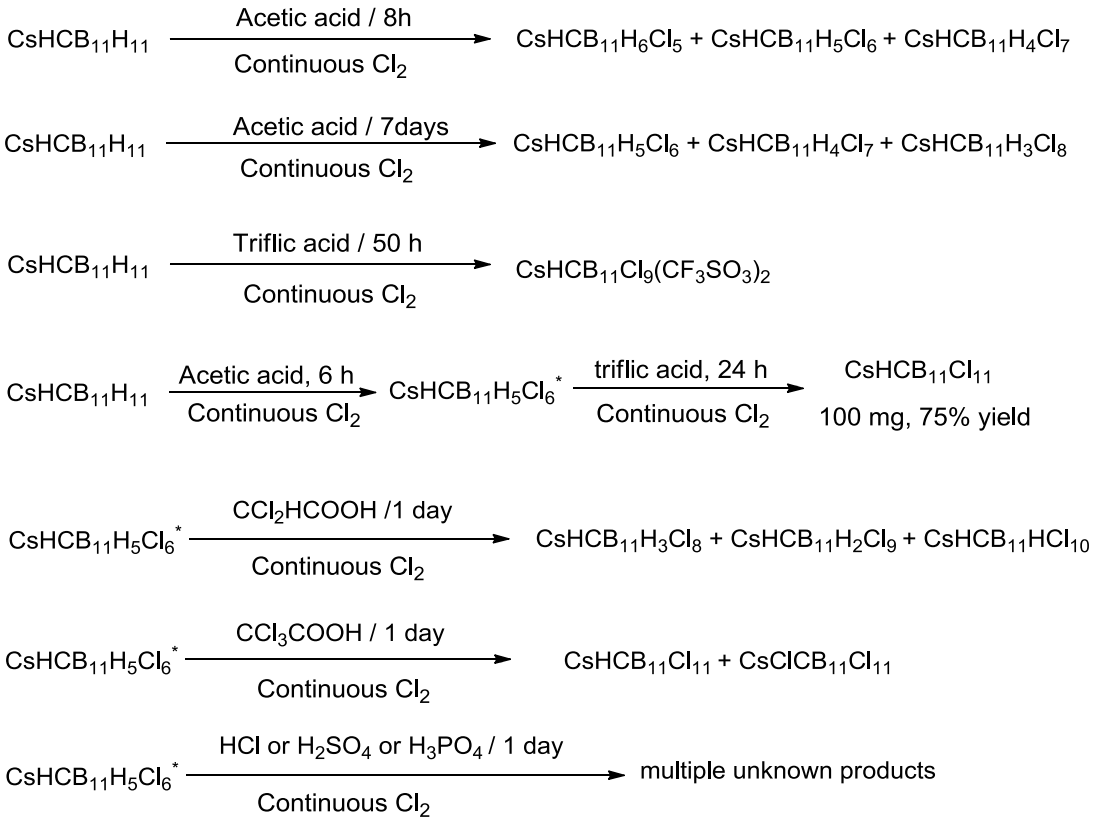

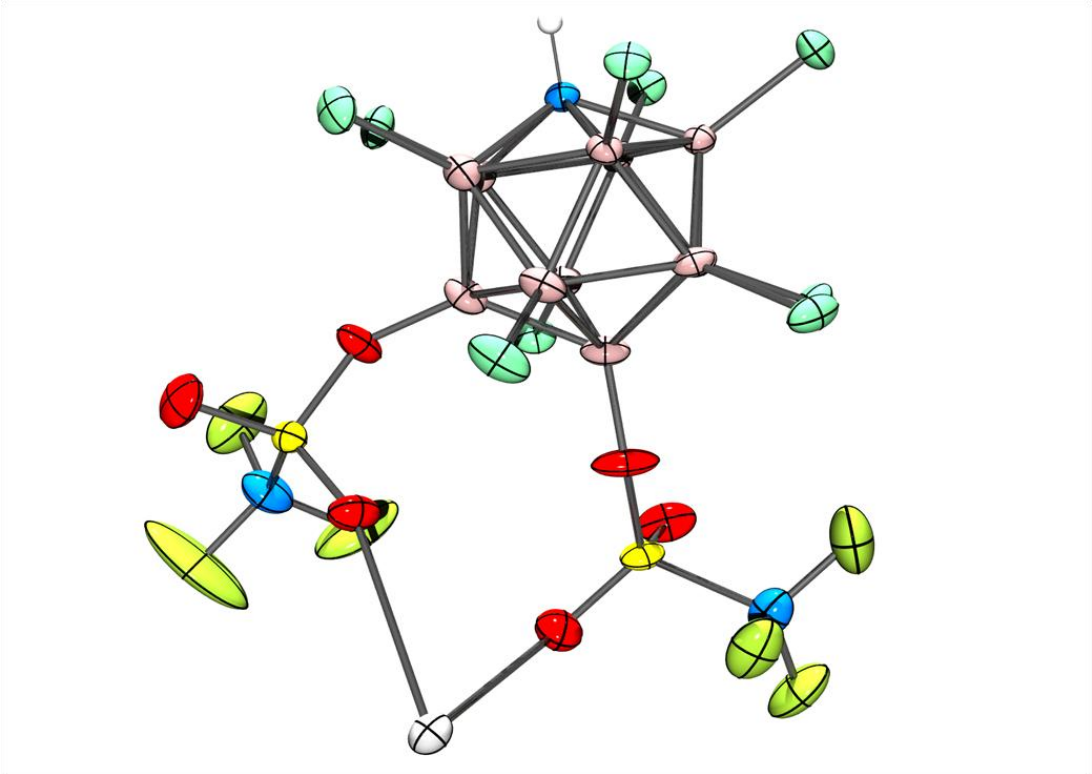

Figure 3-2. ORTEP[128] drawing (50% probability ellipsoids) of $Cs[HCB_{11}Cl_9(CF_3SO_3)_2]$. Disorder of the triflate groups is omitted for clarity.

3.2.1.2 Chlorination of $Cs[CB_{11}H_{12}]$ with SO_2Cl_2

Treatment of $Cs[CB_{11}H_{12}]$ with SO_2Cl_2 at room temperature for 24 h led to a mixture of penta-, hexa-, hepta-, octa- and nonachlorinatedcarborane anions. (Scheme 3-4). Substantial gas evolution was observed as the presumed gaseous byproducts, such as SO_2 and HCl were evolved. Stirring $Cs[CB_{11}H_{12}]$ in refluxing SO_2Cl_2 for 1 d led to a mixture of octa-, nona-, deca-, and undecachlorinated-carborane anions. Unfortunately, there was no significant difference between the mixtures obtained after 1 d and after 5 d, which indicated that $[CB_{11}H_{12}]^-$ might not

be fully converted to $[HCB_{11}Cl_{11}]^-$ in reluxing SO_2Cl_2. Strong Lewis acids, such as $AlCl_3$, have been used to accelerate or catalyze chlorination reactions by SO_2Cl_2 in organic synthesis.[146] However, adding $AlCl_3$ or $TiCl_4$ into the SO_2Cl_2 solution of $Cs[CB_{11}H_{12}]$, followed by reflux for 3 d gave almost the same mixture as that obtained from the reaction in refluxing SO_2Cl_2 without additives. We suspect adventitious water might be the reason for the retardation of the chlorination reactions, since all reactions were performed without Ar protection. Indeed, intentional addition of water (2% equiv. molar vs SO_2Cl_2, 3.4 equiv. molar vs carborane) to the reaction mixture at the start of the reaction severely retarded the chlorination, resulting in no more than quadruple chlorination after 1 d of reflux.

Scheme 3-4. Chlorination of unpurified carborane with SO_2Cl_2 from Aldrich.

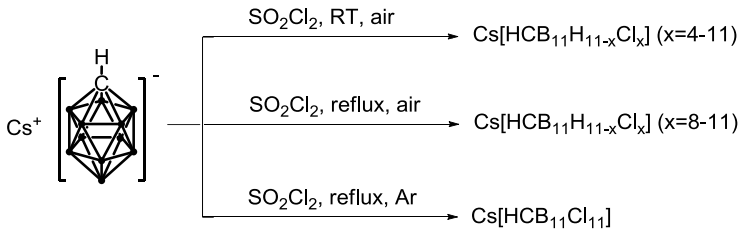

In contrast, reflux $Cs[HCB_{11}H_{11}]$ in SO_2Cl_2 under dry argon for 24 h led to complete conversion to $Cs[HCB_{11}Cl_{11}]$ (MS evidence), which was isolated upon recrystallization from water. We were able to obtain 84-87% yields of $Cs[HCB_{11}Cl_{11}]$ starting with $Cs[HCB_{11}H_{11}]$ and it was characterized by ^1H, ^{11}B, $^{13}C\{^1H\}$ NMR and elemental analysis.

It later came to our notice that the outcome of the reaction of $Cs[HCB_{11}H_{11}]$ with SO_2Cl_2 depended on the batch of $Cs[HCB_{11}H_{11}]$ we used. In our hands, reactions of recrystallized $Cs[HCB_{11}H_{11}]$, partially chlorinated carboranes or recent batch of $Cs[HCB_{11}H_{11}]$ from Katchem with SO_2Cl_2 never gave pure $[HCB_{11}Cl_{11}]^-$ products, suggesting the chlorination reactions might be accelerated or catalyzed by impurities in the unpurified $Cs[HCB_{11}H_{11}]$. Since amines and borane amine adducts are common immpurities in the synthesis of $Cs[HCB_{11}H_{11}]$,[63a] we tested these kinds of compounds as additives for the chlorination reactions with SO_2Cl_2. Although in some of reactions with additives, acceleration of the chlorination reactions was observed, none of these reactions yielded pure $[HCB_{11}Cl_{11}]^-$ products (Table 3-1). It was also noticed that the complete chlorination reactions only occurred when undistilled SO_2Cl_2 from Aldrich (cat. # 320528-1L) was used. Incomplete chlorination was observed when SO_2Cl_2 from Acros (cat. # 169450100) or distilled SO_2Cl_2 was used, suggesting small impurities in the SO_2Cl_2 from Aldrich may accelerate this reaction as well. However, we do not understand the effect of different SO_2Cl_2 batches on the chlorination reactions at this moment. It is unlikely that these reactions are catalyzed by trace amount of transition metals left in the SO_2Cl_2. ICP-MS studies of Fe, Ni, Zn, Cu, Ti, Mn, Co on SO_2Cl_2 from different vendors show no major difference in the content of Ni, Zn, Cu, Ti, Mn, Co, while SO_2Cl_2 from Acros was found to contain more Fe, not less. Light is necessary for the successful chlorination reaction as well, since the chlorination reactions with unpurified carborane and SO_2Cl_2 from Aldrich in the absence of light did not go to

complete chlorination.

Table 3-1. Chlorination reaction of $Cs[HCB_{11}H_{11}]$ by SO_2Cl_2 with various additives. (Here $[HCB_{11}Cl_{11}]^-$ is labelled as Cl11; $[HCB_{11}HCl_{10}]^-$ as Cl10; $[HCB_{11}H_2Cl_9]^-$ as Cl9; $[HCB_{11}H_3Cl_8]^-$ as Cl8; $[HCB_{11}H_4Cl_7]^-$ as Cl7; $[HCB_{11}H_5Cl_6]^-$ as Cl6; $[HCB_{11}H_6Cl_5]^-$ as Cl5; $[HCB_{11}H_7Cl_4]^-$ as Cl4)

Carborane	SO2Cl2	additives	Conditions	Results
Recrystallized	Aldrich undistilled	none	24 h, 80 ℃	Cl6-Cl10, major product Cl8
Recrystallized	Aldrich undistilled	1% Et_3N	24 h, 80 ℃	Cl8-Cl11, major product Cl10
Recrystallized	Aldrich undistilled	1% Et_2NH	24 h, 80 ℃	Cl5-Cl9, major product Cl7
Recrystallized	Aldrich undistilled	1% Ph_2NH	24 h, 80 ℃	Cl4-Cl5, major product Cl4
Recrystallized	Aldrich undistilled	1% iPr_2NH	24 h, 80 ℃	Cl5-Cl9, major product Cl7
Recrystallized	Aldrich undistilled	10% Et_3N	24 h, 80 ℃	Cl5-Cl9, major product Cl7
Recrystallized	Aldrich undistilled	1% BH_3Me_2NH	24 h, 80 ℃	Cl7-Cl11, major product Cl9
Recrystallized	Aldrich undistilled	Saturated with HCl gas	24 h, 80 ℃	Cl8-Cl11, major product Cl10
Recrystallized	Aldrich undistilled	1% $Na[MeCB_{11}Cl_{11}]$	24 h, 80 ℃	Cl6-Cl10, major product Cl8
$Me_3NH[HCB_{11}H_{11}]$	Aldrich undistilled	none	24 h, 80 ℃	Cl4-Cl6, major product Cl5

3.2.1.3 Chlorination of $Cs[CB_{11}H_{12}]$ with $SbCl_5$

Direct reaction (Scheme 3-5) of 1 g $Cs[HCB_{11}H_{11}]$ with refluxing neat $SbCl_5$ led to a clean formation of $[HCB_{11}Cl_{11}]^-$ in 7 d [147] (negative-ion MALDI-MS evidence) [*Caution: violent reaction ensues upon addition of $SbCl_5$ to $Cs[HCB_{11}H_{11}]$*]. After workup, the carborane anion was isolated as a Me_3NH^+ salt in 81% yield. While we have not been able to obtain fully satisfactory elemental analysis data, the NMR data are

consistent with those previously reported. MS analysis also showed essentially only the expected $[HCB_{11}Cl_{11}]^-$ isotope pattern. Notably, using refluxing $SbCl_5$, we are able to convert partially chlorinated carboranes from previous studies to $[HCB_{11}Cl_{11}]^-$ (MS evidence). The workup in this procedure is complicated by the presence of Sb by-products of low volatility (presumably, $SbCl_3$), however, they are successfully removed as elemental analysis of the isolated product showed Sb levels below detection limit of 0.17%. Repeats of this procedure on a 5-10 g scale occasionally led to the detection (by MS) of an impurity. We assign the impurity to be $[HCB_{11}Cl_{10}(OH)]^-$ based on the observed isotope pattern and on that refluxing of a mixture containing this impurity with $(Me_3Si)_2NH$ resulted in the observation of a new MS pattern consistent with $[HCB_{11}Cl_{10}(OSiMe_3)]^-$ (Scheme 3-5). The reason for the formation of the hydroxylation product is most likely adventitious water, as the fraction of this impurity increased dramatically when 5 equivalents of water was added at the beginning of the reaction. $[HCB_{11}Cl_{10}(OH)]^-$ can no longer be detected by MS if an isolated mixture is additionally refluxed with $SbCl_5$ or SO_2Cl_2. Notably, the reaction with purified $SbCl_5$ and purified parent carborane still yielded only $[HCB_{11}Cl_{11}]^-$ product after heating at reflux temperature for 7 d.

Scheme 3-5. Chlorination of carborane with $SbCl_5$.

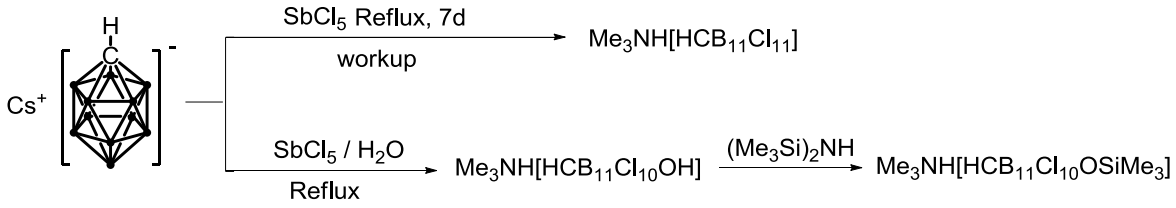

3.2.2 Chlorination of Dodecaborate Dianion

Direct reaction of 100 mg $Cs_2[B_{12}H_{12}]$ with refluxing neat SO_2Cl_2 for 24 h only led to a mixture of various partially chlorinated $[B_{12}H_{12-x}Cl_x]^{2-}$ based on ^{11}B NMR analysis. The incomplete chlorination of $Cs_2[B_{12}H_{12}]$ by neat SO_2Cl_2 is likely owing to the low solubility of $Cs_2[B_{12}H_{12}]$ in neat SO_2Cl_2, since a white suspension was observed throughout the reaction. Converting $Cs_2[B_{12}H_{12}]$ to $(Et_3NH)_2[B_{12}H_{12}]$ did not dramatically improve the solubility in SO_2Cl_2, and the reaction with $[Et_3NH]_2[B_{12}H_{12}]$ in neat SO_2Cl_2 did not lead to complete chlorination either. We noted that acetonitrile, in which $Cs_2[B_{12}H_{12}]$ is more soluble, was successfully used as the solvent for the fluorination of $K_2[B_{12}H_{12}]$ with F_2.[148] Refluxing $Cs_2[B_{12}H_{12}]$ in a 1:1 mixture of SO_2Cl_2 and acetonitrile for 24 h[149] led to complete conversion to $Cs_2[B_{12}Cl_{12}]$ (Scheme 3-6), which was isolated upon recrystallization from water. We are able to obtain 75-82% yields of $Cs_2[B_{12}Cl_{12}]$ starting with 0.1 or 1 and 5 g of $Cs_2[B_{12}H_{12}]$ and it was characterized by ^1H, ^{11}B NMR, ESI-MS, infrared spectroscopy and elemental analysis.

Scheme 3-6. New synthesis of the perchlorinated dodecaborate $[B_{12}Cl_{12}]^{2-}$.

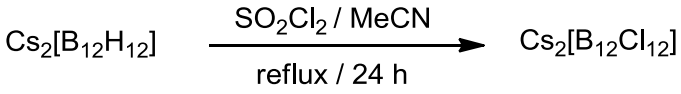

In order to rule out the possibility that the chlorination of $[B_{12}H_{12}]^{2-}$ might also be catalyzed by some impurities in the starting materials, chlorination of $Cs_2[B_{12}H_{12}]$ was performed with recrystallized $Cs_2[B_{12}H_{12}]$, distilled acetonitrile, and distilled SO_2Cl_2 and with protection from light. All of these variations led to complete or almost complete conversion to the $[B_{12}Cl_{12}]^{2-}$ product after 24 h at reflux temperature (Scheme 3-7).

Scheme 3-7. Synthesis of $[B_{12}Cl_{12}]^{2-}$ from purified reagents.

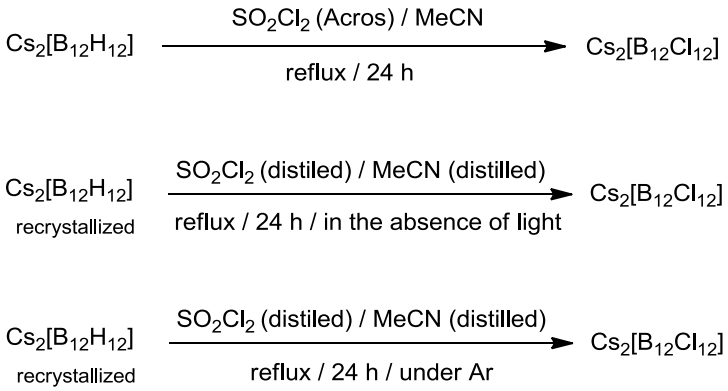

3.3 Conclusion

In conclusion, we report two new, straightforward methods for the synthesis of valuable $[HCB_{11}Cl_{11}]^-$ with either Cl_2 or $SbCl_5$ as chlorination reagents. We obtained $[HCB_{11}Cl_{11}]^-$ product with SO_2Cl_2 as chlorination reagents and an unindentified catalyst. Amines, borane amine adducts and dry HCl have been tested as additives for the chlorination reactions with SO_2Cl_2. Although some of them shifted the reaction towards more chlorinated products, none of them gave pure $[HCB_{11}Cl_{11}]^-$ products. On the other hand, we were able to obtain useful $[B_{12}Cl_{12}]^{2-}$ from $[B_{12}H_{12}]^{2-}$ with SO_2Cl_2 as the chlorination reagent and acetonitrile as cosolvent. While the involved synthesis or the relatively high cost of the requisite parent anion $[HCB_{11}H_{11}]^-$ remain an issue, the syntheses we report here make the subsequent chlorination expedient, economical, and readily available to chemists at large without the need for specialized training or equipment.

3.4 Experimental Details

General considerations. $Cs[HCB_{11}H_{11}]$ was purchased from Katchem spol. s r.o. and used as received unless otherwise noted. $Cs_2[B_{12}H_{12}]$ was purchased from Strem Chemical Inc. (55-1800) and used as received unless otherwise noted. $SbCl_5$ was purchased from Aldrich and fractionally distilled before use. SO_2Cl_2 was purchased from Aldrich (320528-1L) or Acros (169450010) and used as received unless otherwise noted. All other chemicals were purchased from either Aldrich, Alfa Aesar or Acros and used as received unless otherwise noted.

Physical methods. NMR spectra were recorded on a Varian iNova 300 spectrometer (^{1}H NMR, 299.9 MHz) or a Varian iNova 400 spectrometer (^{11}B NMR, 128.2 MHz, ^{19}F NMR, 376.3 MHz) in noted solvents. Chemical shifts are given in δ (ppm). ^{11}B NMR spectra were referenced externally with BF_3 etherate at δ 0. ^{19}F NMR spectra were referenced externally with neat CF_3COOH at δ -78.5. MS characterizations of carborane and dodecaborate dianions were performed either by Texas A&M University Laboratory for Biological Mass Spectrometry (LBMS) or by Brandeis University Mass. Spec. Facility (BUMS). Elemental analyses were performed by CALI, Inc. (Parsippany, NJ). FT-IR spectra were collected using a Bruker ALPHA-P FT-IR Spectrometer with a diamond ATR. The solid state structure of $Cs[HCB_{11}Cl_9(O_3SCF_3)_2]$was solved by Prof. Bruce M. Foxman.

Notes on the labeling on the MS spectra. In our spectra, $[HCB_{11}Cl_{11}]^-$ is labelled as Cl11; $[HCB_{11}HCl_{10}]^-$ as Cl10; $[HCB_{11}H_2Cl_9]^-$ as Cl9; $[HCB_{11}H_3Cl_8]^-$ as Cl8; $[HCB_{11}H_4Cl_7]^-$ as Cl7; $[HCB_{11}H_5Cl_6]^-$ as Cl6; $[HCB_{11}H_6Cl_5]^-$ as Cl5; $[HCB_{11}H_7Cl_4]^-$ as Cl4; $[HCB_{11}H_8Cl_3]^-$ as Cl3; $[HCB_{11}H_9Cl_2]^-$ as Cl2; $[HCB_{11}Cl_{10}OH]^-$ as Cl10OH; $[HCB_{11}Cl_{10}OSiMe_3]^-$ as $Cl10OSiMe_3$; $[HCB_{11}Cl_9(O_3SCF_3)_2]^-$ as $Cl9(O_3SCF_3)_2$; $[ClCB_{11}Cl_{11}]^-$ as Cl12.

Reaction of $Cs[HCB_{11}H_{11}]$ with Cl_2 in triflic acid. To a 50 mL three-neck flask with teflon magnetic stir bar was added $Cs[HCB_{11}H_{11}]$ (0.45 g, 1.63 mmol) and triflic acid (8 mL). The flask was equipped with water-cooled condenser and hose adapter connected via tygon tubing to an inverted filter funnel submerged in a solution of sodium hydroxide and sodium sulfite. Chlorine gas was delivered to the reaction flask from a lecture bottle of chlorine gas with a Monel valve through tygon tubing and a bubbler with concentrated HCl solution. The third neck was equipped with a glass stopper. Chlorine gas was slowly added into the flask and the reaction mixture was heated to 160 °C for 50 h. The flow of chlorine gas was ceased and reaction mixture was allowed to cool down to room temperature after the reaction was finished. All volatiles were removed under vacuum and the resulting white powder was washed with hexanes then dried under vacuum for 3 h. The products were dissolved in CH_3CN for ^{19}F NMR study and MS characterization. The product was confirmed to be $Cs[HCB_{11}Cl_9(CF_3SO_3)_2]$ by ^{19}F NMR spectroscopy (Figure 3-3), X-Ray crystallography (Figure 3-2) and mass spectroscopy (Figure 3-4).

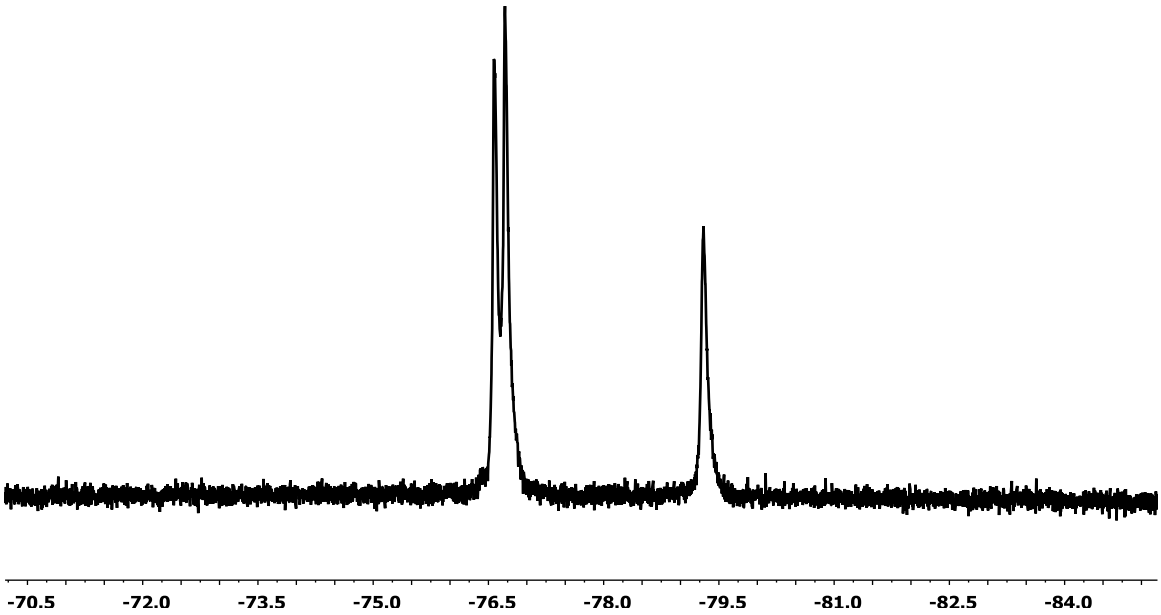

Figure 3-3. ^{19}F NMR spectrum of $Cs[HCB_{11}Cl_9(CF_3SO_3)_2]$ product from the reaction with Cl_2 in triflic acid. (The signal at -79.3 is the residual triflic acid)

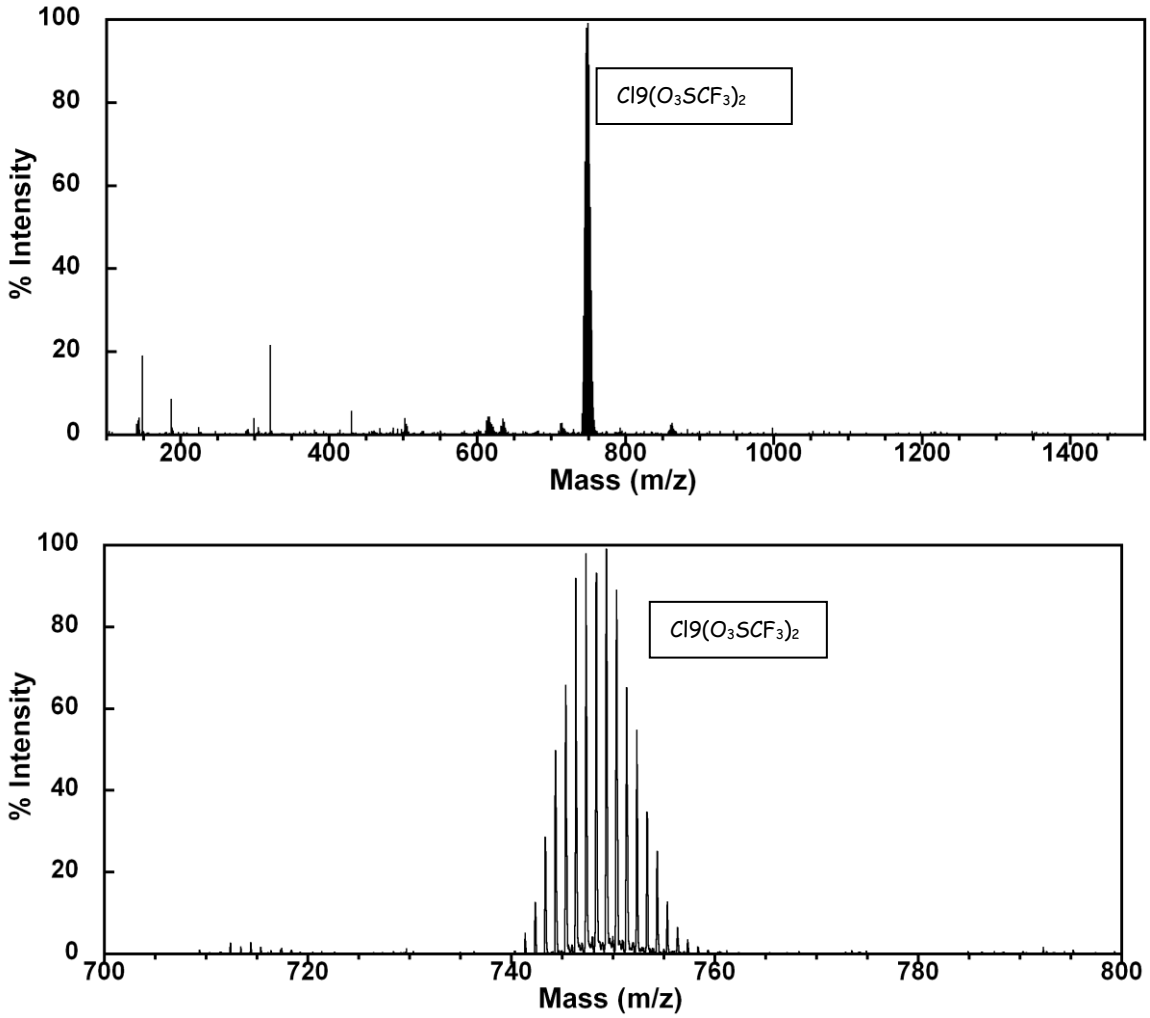

Figure 3-4. MALDI MS spectrum of $Cs[HCB_{11}Cl_9(CF_3SO_3)_2]$. (Top: from 100-1500; Bottom: from 700-800).

Synthesis of $Cs[HCB_{11}Cl_{11}]$ with Cl_2. The reaction setup is the same as the one we use for the reaction of Cs $[HCB_{11}H_{11}]$ with Cl_2 in triflic acid. To a 100 mL three-neck flask with teflon magnetic stir bar was added $Cs[HCB_{11}H_{11}]$ (2.9 g, 10.5 mmol) and acetic acid (30 mL). Chlorine gas was slowly added into the flask and the reaction mixture was heated to reflux for 6 h. After removal of all volatiles, the resulting pale yellow powder

was recrystallized from water with 3.2 g CsCl. The white crystals were dried under vacuum for 4 h at 80 ℃ . Yield: 3.3 g (90%). Mass spectroscopy revealed the product was a mixture of **Cl5** (10%), **Cl6** (80%) and **Cl7** (10%).

To a 25 mL three-neck flask with Teflon magnetic stir bar was added partially chlorination carboranes from the previous reaction (0.27 g, 0.56 mmol) and triflic acid (5 mL). Chlorine gas was slowly added into the flask and the reaction mixture was heated to reflux for 24 h. After removal of all volatiles, the products were recrystallized from hot water. Yield: 243 mg (69%). The product was confirmed to be pure $Cs[HCB_{11}Cl_{11}]$ by ^{1}H NMR, ^{11}B NMR and mass spectroscopy (Figure 3-5).

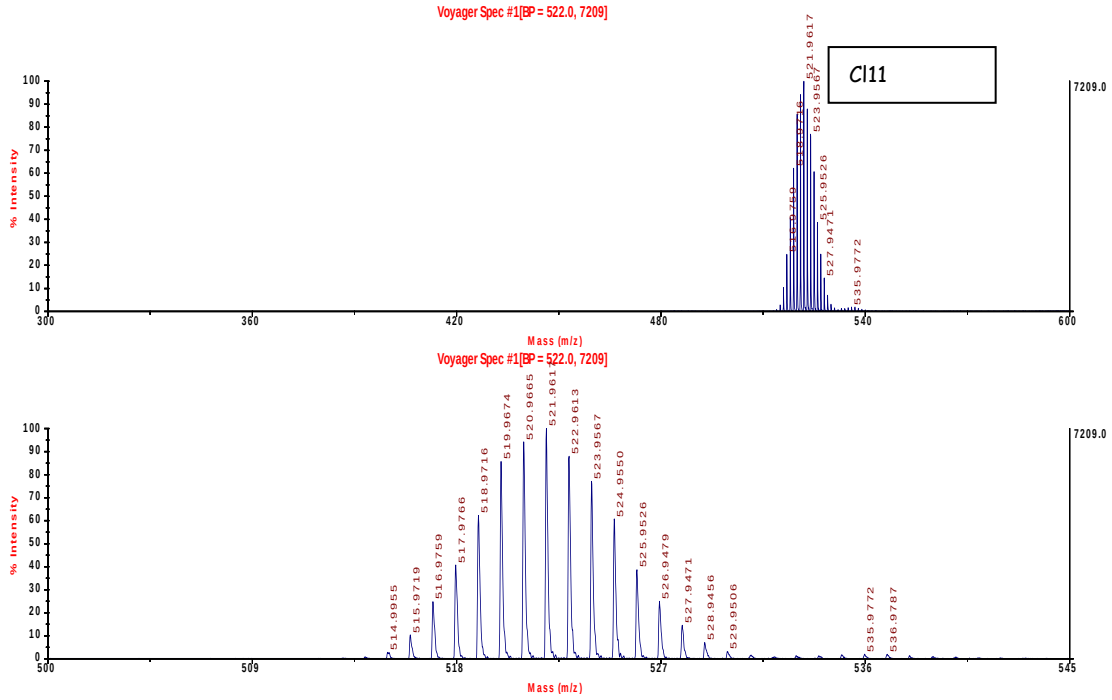

Figure 3-5. MALDI MS spectrum of $Cs[HCB_{11}Cl_{11}]$.

Reaction of $Cs[HCB_{11}H_5Cl_6]^*$ with Cl_2 in CCl_3COOH*: $Cs[HCB_{11}H_5Cl_6]$ used here is from the previous reaction of parent carborane with Cl_2 in acetic acid. It is indeed a mixture of **Cl5**, **Cl6** and **Cl7**. The reaction setup is the same as the one we use for the reaction of Cs $[HCB_{11}H_{11}]$ with Cl_2 in triflic acid. To a 50 mL three-neck flask with teflon magnetic stir bar was added $Cs[HCB_{11}H_5Cl_6]^*$ (0.21 g, 0.44 mmol) and CCl_3COOH (10 g). Chlorine gas was slowly added into the flask and the reaction mixture was heated to 180 ℃ for 24 h. After the reaction, the reactions mixture was dissolved in 5% aq. NaOH. The solution was then concentrated to about 10 mL. After Treatment of the resultant solution with 0.1 g of Me_3NHCl (1.1 mmol) caused formation of a white precipitate. This solid was filtered off, washed with distilled water and dried under vacuum to give 0.30 g of trimethylammonium salts of carborane. MALDI MS (Figure 3-6) revealed the carborane anion here is a mixture of $[HCB_{11}Cl_{11}]^-$ and $[ClCB_{11}Cl_{11}]^-$.

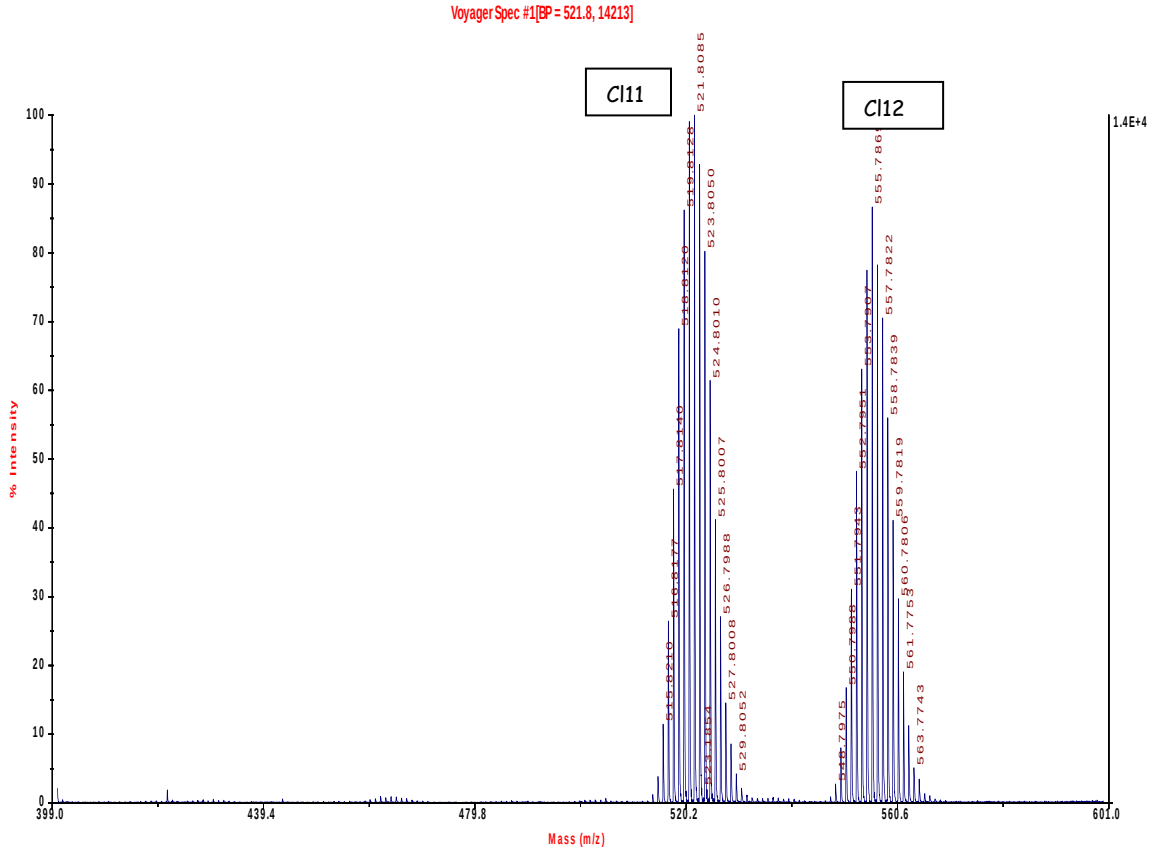

Figure 3-6. MALDI MS spectrum of reaction of $Cs[HCB_{11}H_5Cl_6]^*$ with Cl_2 in CCl_3COOH.

Reaction of $Cs[HCB_{11}H_{11}]$ with SO_2Cl_2 at ambient temperature without Ar protection. A solution of $Cs[HCB_{11}H_{11}]$ (120 mg, 0.43 mmol) in SO_2Cl_2 (8.0 mL, 100 mmol) in a Schlenk flask was stirred at room temperature for 24 h. Aliquot were taken after 1, 2, 3, 4, 5, 6, 8, and 24 h and analyzed by MALDI MS (Figure 3-7) which indicated mixtures of partially chlorinated carboranes up to **Cl10** after 24h with the major products as **Cl6**, **Cl7** and **Cl8**.

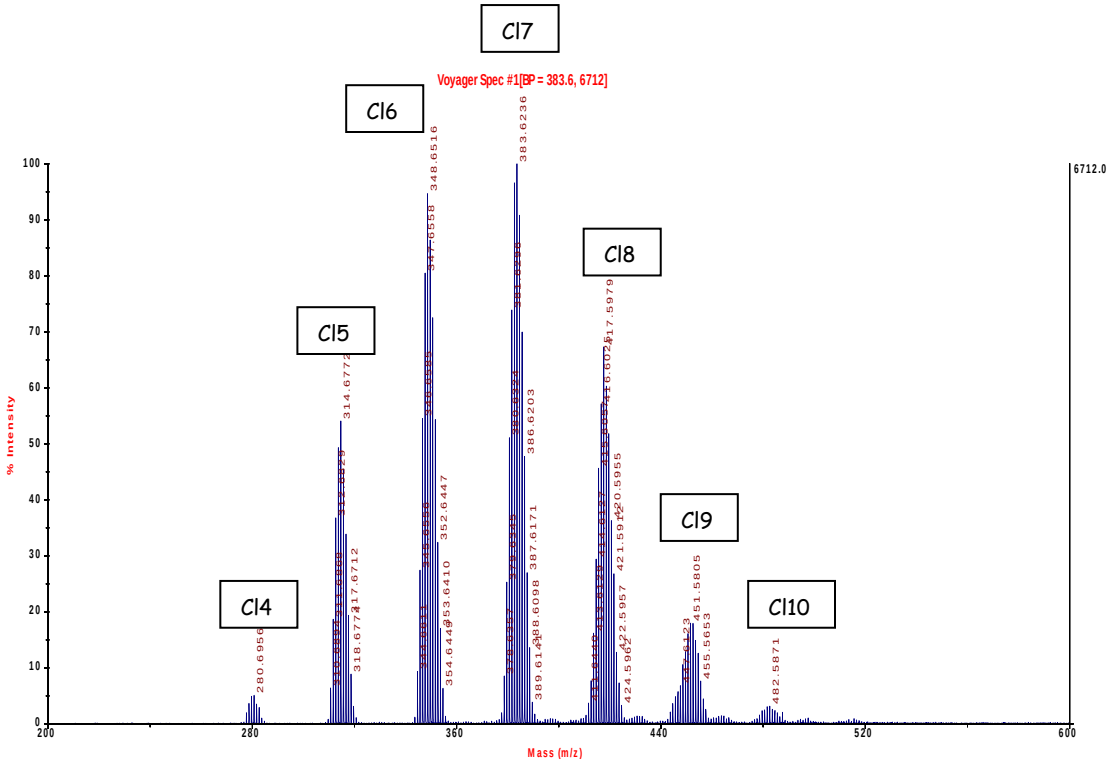

Figure 3-7. MALDI MS spectrum for the reaction with SO_2Cl_2 at ambient temperature without Ar protection for 24 h.

Reaction of $Cs[HCB_{11}H_{11}]$ with SO_2Cl_2 at reflux temperature without Ar protection. A solution of $Cs[HCB_{11}H_{11}]$ (1.03 g, 3.71 mmol) in SO_2Cl_2 (50 mL, 620 mmol) in a Schlenk flask was heated to reflux. After 1 h, formation of white precipitate was observed and an additional 50 mL (620 mmol) of SO_2Cl_2 was added. The mixture was allowed to stir at reflux temperature for 5 d. An aliquot was taken every day and analyzed by MALDI MS (Figure 3-8). After 5 days, removal of the volatiles gave a white solid. MALDI MS analysis indicated that this solid is a mixture of **Cl8**, **Cl9**, **Cl10** and **Cl11**.

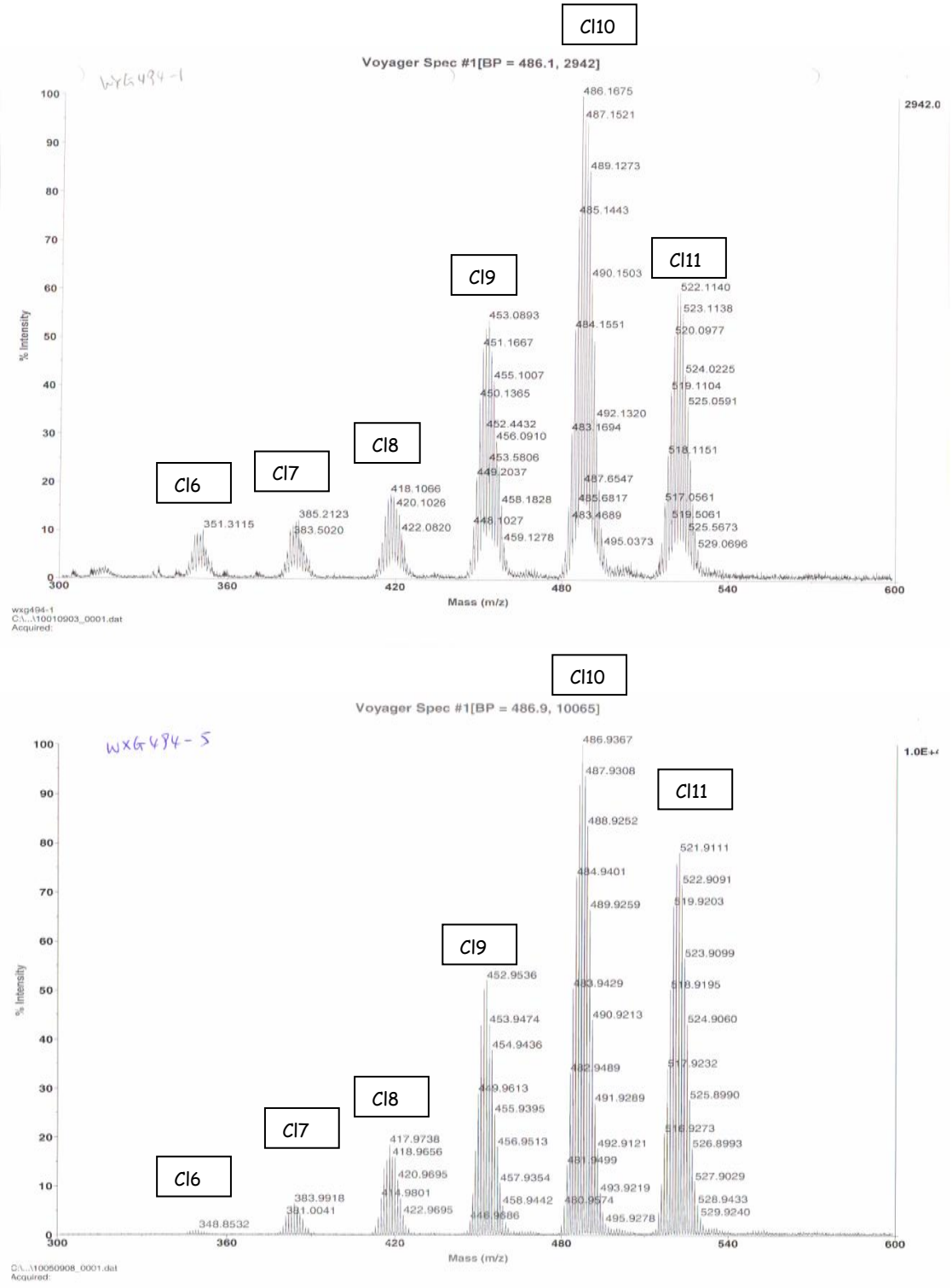

Figure 3-8. MALDI MS spectrum for the reaction with SO_2Cl_2 at reflux temperature without Ar protection for 24 h. (Top: after 1 d; Bottom: after 5d)

Reactions of $Cs[HCB_{11}H_{11}]$ with SO_2Cl_2 and $AlCl_3$ without Ar protection. A solution of $Cs[HCB_{11}H_{11}]$ (90 mg, 0.32 mmol) in SO_2Cl_2 (5.0 mL, 62 mmol) with added $AlCl_3$ (0.60 g, 4.5 mmol) in a Schlenk flask was heated to reflux for 3 d. Removal of the volatiles gave a white solid. MS spectra showed the product is a mixture of predominantly **Cl9** and **Cl10**.

Reactions of $Cs[HCB_{11}H_{11}]$ with SO_2Cl_2 and $TiCl_4$ without Ar protection. A solution of $Cs[HCB_{11}H_{11}]$ (100 mg, 0.36 mmol) in SO_2Cl_2 (5.0 mL, 62 mmol) with added $TiCl_4$ (3.0 mL, 27 mmol) in a Schlenk flask was heated to reflux for 3 d. Removal of the volatiles gave a white solid which was analyzed by MALDI MS which shows no isotope pattern for carborane cages.

Reactions of $Cs[HCB_{11}H_{11}]$ with SO_2Cl_2 with added H_2O versus a control without added H_2O. A pair of reactions were set up in the following way: RX1: 100 mg (0.36 mmol) of $Cs[HCB_{11}H_{11}]$ was mixed with 22 μL (1.22 mmol) of H_2O and 5.0 mL (62 mmol) of SO_2Cl_2 in a Schlenk flask and heated to reflux; RX2: 100 mg (0.36 mmol) of $Cs[HCB_{11}H_{11}]$ was mixed with 5.0 mL (62 mmol) SO_2Cl_2 in a Schlenk flask and heated to reflux. After 1 h, an additional 5.0 mL (62 mmol) of SO_2Cl_2 was added to each reaction. The mixture was allowed to stir at reflux temperature for 24 h. Removal of the volatiles gave in each case a white solid which were analyzed by MALDI MS (Fig. 3-9) which revealed a lower chlorination level in the reaction with added water.

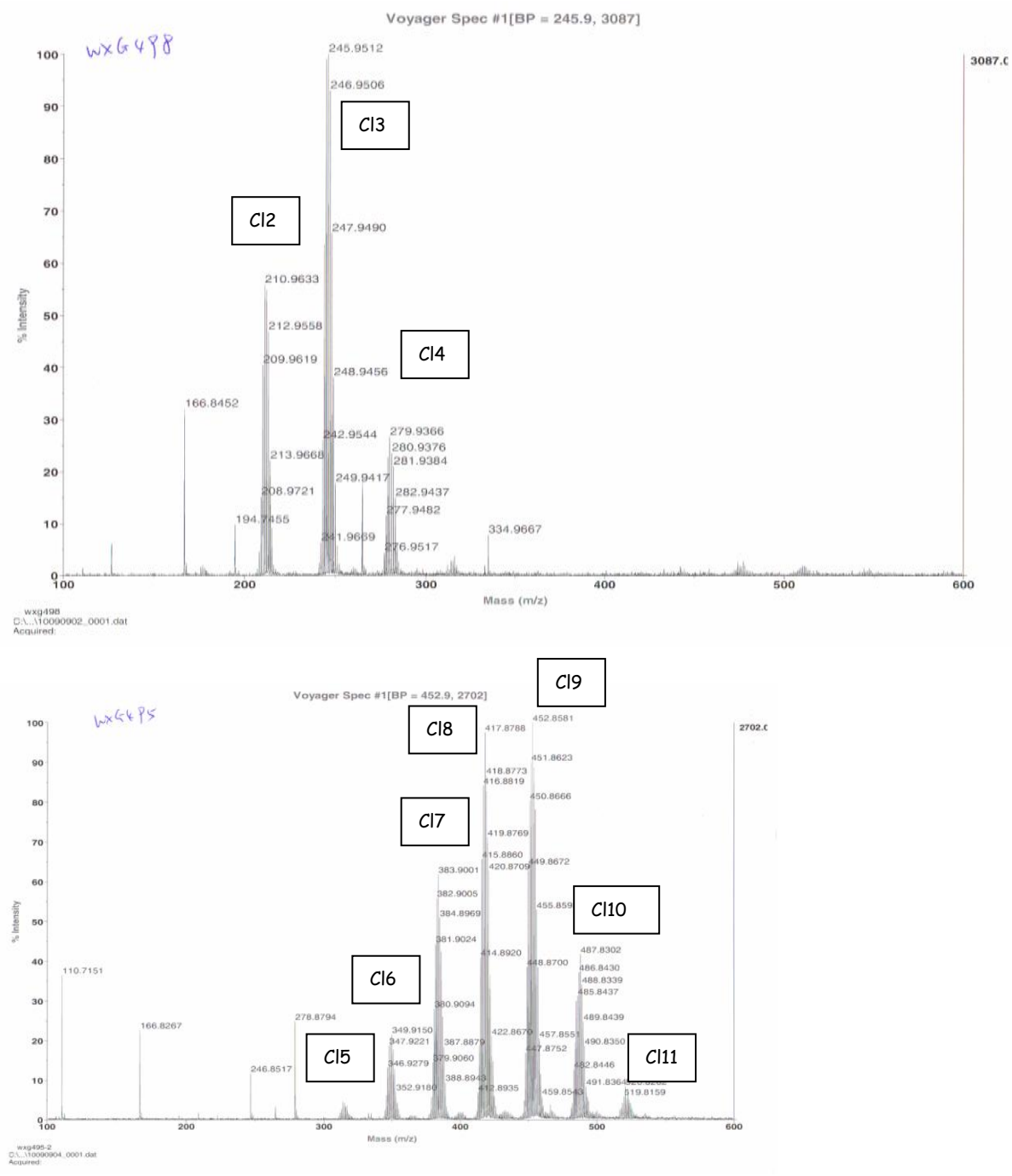

Figure 3-9. MALDI MS spectrum for the reaction with SO_2Cl_2 with 2% H_2O. (Top) MALDI MS spectrum for the reaction with SO_2Cl_2 without H_2O. (Bottom)

Synthesis of $Cs[HCB_{11}Cl_{11}]$ with SO_2Cl_2 under Ar (1 g scale). A solution of $Cs[HCB_{11}H_{11}]$ (1.03 g, 3.71 mmol) in SO_2Cl_2 (50 mL, 620 mmol) in a Schlenk flask was heated to reflux at 80 ℃ under Ar protection. After 1 h, formation of white precipitate was observed and an additional 50 mL (620 mmol) of SO_2Cl_2 was added. The mixture was allowed to stir at reflux temperature for another 24 h. Removal of the volatiles gave a white solid which was recrystallized from water to give pure $Cs[HCB_{11}Cl_{11}]$. Yield: 2.05 g (85%). ^{11}B NMR (128.2 MHz, aceotne): δ -1.7 (s, 1B), -9.0 (s, 5B), -12.1 (s, 5B). ^{1}H NMR (299.9 MHz, acetonitrile-d_3): δ 4.07 (s). Elemental Analysis Calculated (Found) for $CsHCB_{11}Cl_{11}$: H, 0.15% (0.30%); C, 1.83% (1.87%); B, 18.16% (17.97%); Cl, 59.55% (59.39%). Negative-ion MALDI MS, *m/z* (isotopic abundance): calculated for $HCB_{11}Cl_{11}$ 520 (84.7), 521 (96.7), 522 (100), 523 (93.8), 524 (80.3); found 519.7 (80.6), 520.7 (93.2), 521.7 (100), 522.7 (88.2), 523.7 (77.3) (Fig. 3-10).

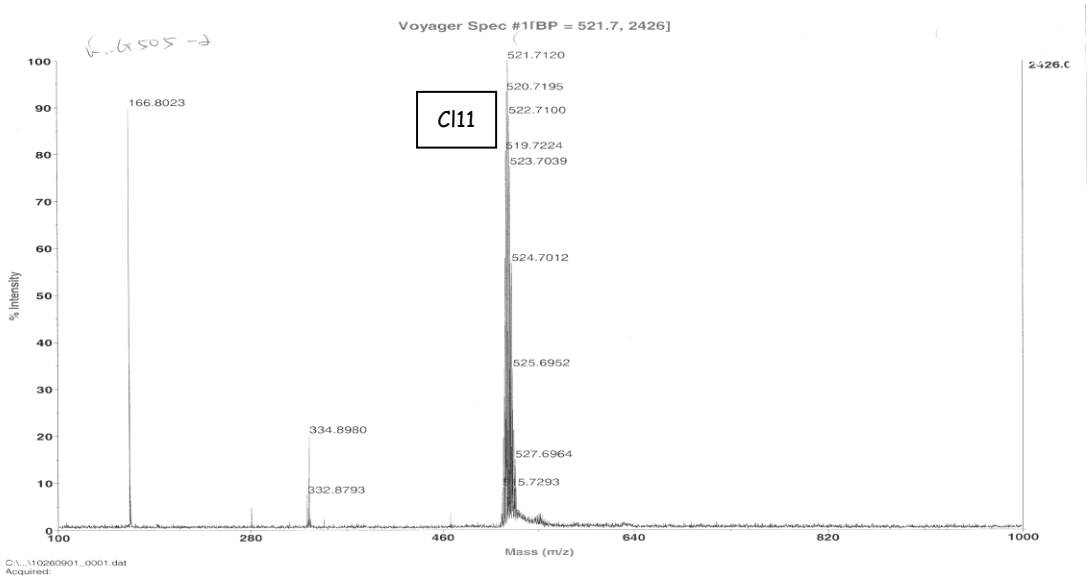

Figure 3-10. MALDI MS spectrum for the reaction with SO_2Cl_2 under Ar protection at 1 g scale.

Reactions of recrystallized Cs[$HCB_{11}H_{11}$] with SO_2Cl_2. The parent carborane used in this reaction was recrystallized from hot water and dried under vacuum at 80 ℃ for 12 h. A solution of Cs[$HCB_{11}H_{11}$] (95 mg, 0.36 mmol) in SO_2Cl_2 (5 mL, 62 mmol) in a Schlenk flask was heated to reflux at 80 ℃ under Ar protection. After 1 h, formation of white precipitate was observed and an additional 5 mL (62 mmol) of SO_2Cl_2 was added. The mixture was allowed to stir at reflux temperature for another 24 h under Ar. Removal of the volatiles gave a white solid. MALDI MS revealed the white powder was a mixture of partially chlorinated carboranes from **Cl6** to **Cl10** with the major products as **Cl8**.

Reactions of recrystallized Cs[$HCB_{11}H_{11}$] with Et_3N in SO_2Cl_2. The parent

carborane used in this reaction was recrystallized from hot water and dried under vacuum at 80 ℃ for 12 h. A solution of $Cs[HCB_{11}H_{11}]$ (100 mg, 0.37 mmol) in SO_2Cl_2 (5 mL, 62 mmol) with 0.5 μL of Et_3N (3.6 μmol) in a Schlenk flask was heated to reflux at 80 ℃ under Ar protection. After 1 h, formation of white precipitate was observed and an additional 5 mL (62 mmol) of SO_2Cl_2 was added. The mixture was allowed to stir at reflux temperature for another 24 h under Ar. Removal of the volatiles gave a white solid. MALDI MS revealed the white powder was a mixture of partially chlorinated carboranes from **Cl8** to **Cl11** with the major products as **Cl10**.

Reactions of recrystallized $Cs[HCB_{11}H_{11}]$ in the presence of dry HCl. The parent carborane used in this reaction was recrystallized from hot water and dried under vacuum at 80 ℃ for 12 h. $Cs[HCB_{11}H_{11}]$ (100 mg, 0.37 mmol) was mixed with SO_2Cl_2 (5 mL, 62 mmol) in a Schlenk flask under Argon. Agron then was removed from the Schlenk flask through "Freeze-Pump-Thaw". Dry HCl was then delivered to the reaction flask from a lecture bottle of chlorine gas with a Monel valve through tygon tubing for 15 min. The reaction mixture was then heated to reflux under Ar. After 1 h, formation of white precipitate was observed and an additional 5 mL (62 mmol) of SO_2Cl_2 was added. The mixture was allowed to stir at reflux temperature for another 24 h under Ar. Removal of the volatiles gave a white solid. MALDI MS revealed the white powder was a mixture of partially chlorinated carboranes from **Cl8** to **Cl11** with the major products as **Cl10**.

Reactions of $Cs[HCB_{11}H_{11}]$ with SO_2Cl_2 in the absence of light. The reaction flask

and condenser were wrapped with Al foil throughout the reaction time. A solution of $Cs[HCB_{11}H_{11}]$ (100 mg, 0.37 mmol) in SO_2Cl_2 (5 mL, 62 mmol) in a Schlenk flask was heated to reflux at 80 ℃ under Ar protection. After 1 h, an additional 5 mL (62 mmol) of SO_2Cl_2 was added. The mixture was allowed to stir at reflux temperature for another 24 h under Ar. Removal of the volatiles gave a white solid. MALDI MS revealed the white powder was a mixture of partially chlorinated carboranes from **Cl7** to **Cl11** with the major products as **Cl9**.

Reactions of recrystallized $Cs[HCB_{11}H_{11}]$ with 1% $Na[MeCB_{11}Cl_{11}]$ in SO_2Cl_2. The parent carborane used in this reaction was recrystallized from hot water and dried under vacuum at 80 ℃ for 12 h. A solution of $Cs[HCB_{11}H_{11}]$ (100 mg, 0.37 mmol) in SO_2Cl_2 (5 mL, 62 mmol) with $Na[MeCB_{11}Cl_{11}]$ (2 mg, 3.6 μmol) in a Schlenk flask was heated to reflux at 80 ℃ under Ar protection. After 1 h, formation of white precipitate was observed and an additional 5 mL (62 mmol) of SO_2Cl_2 was added. The mixture was allowed to stir at reflux temperature for another 24 h under Ar. Removal of the volatiles gave a white solid. MALDI MS revealed the white powder was a mixture of partially chlorinated carboranes from **Cl6** to **Cl10** with the major products as **Cl11**.

Synthesis of $Me_3NH[HCB_{11}H_{11}]$. To a solution of $Cs[HCB_{11}H_{11}]$ (672 mg, 2.43 mmol) in 5 mL H_2O was added 1 mL of 10% HCl aqueous solution at 50 ℃ . The solution was then cooled to room temperature before Me_3NHCl (500 mg, 5.24 mmol) was added. The resulting white suspension was stirred at room temperature for 1 hour. White powder was collected on a "F frit, washed with 1 mL of water three

times and dried under vacuum at 80 ℃ overnight. Yield: 450 mg (91%). ^{11}B NMR (128.2 MHz, aceotne): δ -1.7 (s, 1B), -9.0 (s, 5B), -12.1 (s, 5B). ^{1}H NMR (500.0 MHz, acetonitrile-d_3): δ 2.79 (s, 9H, N*Me*), 2.36 (br s, 1H, C*H*), 1.05-2.08 (br, 11H, B*H*).

Reactions of $Me_3NH[HCB_{11}H_{11}]$ with SO_2Cl_2. The $Me_3NH[HCB_{11}H_{11}]$ used in this reaction was dried under vacuum at 80 ℃ for 12 h before use. A solution of $Cs[HCB_{11}H_{11}]$ (100 mg, 0.37 mmol) in SO_2Cl_2 (5 mL, 62 mmol) in a Schlenk flask was heated to reflux at 80 ℃ under Ar protection. After 1 h, formation of white precipitate was observed and an additional 5 mL (62 mmol) of SO_2Cl_2 was added. The mixture was allowed to stir at reflux temperature for another 24 h under Ar. Removal of the volatiles gave a white solid. MALDI MS revealed the white powder was a mixture of partially chlorinated carboranes from **Cl4** to **Cl6** with the major products as **Cl5**.

Reactions of $Cs[HCB_{11}H_{11}]$ with distilled SO_2Cl_2. SO_2Cl_2 used in this reaction was purchased from Aldrich and fractionally distilled before use. Starting with 100 mL SO_2Cl_2, the middle 50% fraction (50 mL) was collected and used in the reaction. A solution of $Cs[HCB_{11}H_{11}]$ (100 mg, 0.37 mmol) in SO_2Cl_2 (5 mL, 62 mmol) in a Schlenk flask was heated to reflux at 80 ℃ under Ar protection. After 1 h, formation of white precipitate was observed and an additional 5 mL (62 mmol) of SO_2Cl_2 was added. The mixture was allowed to stir at reflux temperature for another 24 h under Ar. Removal of the volatiles gave a white solid. MALDI MS revealed the white powder was a mixture of partially chlorinated carboranes from **Cl7** to **Cl11** with the

major products as **Cl9**.

Synthesis of $Me_3NH[HCB_{11}Cl_{11}]$ with $SbCl_5$ (1 g scale). A solution of $Cs[HCB_{11}H_{11}]$ (1.05 g, 3.8 mmol) in $SbCl_5$ (10 mL, 79 mmol) in a Schlenk flask was heated to reflux at 140 ℃ for 3 d. After removal of most of the volatiles, the residue was dissolved in 10% aq. NaOH, passed through Celite and then neutralized by dilute HCl solution. Treatment of the resultant solution with 0.5 g of Me_3NHCl (5.2 mmol) caused formation of a white precipitate. This solid was filtered off, washed with distilled water and dried under vacuum to give $Me_3NH[HCB_{11}Cl_{11}]$. (Figure 3-11) Yield: 1.8 g (81%). ^{11}B NMR (128.2 MHz, aceotne): δ -1.7 (s, 1B), -9.1 (s, 5B), -12.2 (s, 5B). ^{1}H NMR (299.9 MHz, acetonitrile-d_3): δ 2.71 (s, 9H, Me_3N), 4.07 (s, 1H, cage C-H). $Me_3NH[HCB_{11}Cl_{11}]$ was recrystallized from acetone before it was sent for elemntal analyses. Less than 0.0167% of Sb was detected by elemental analysis.

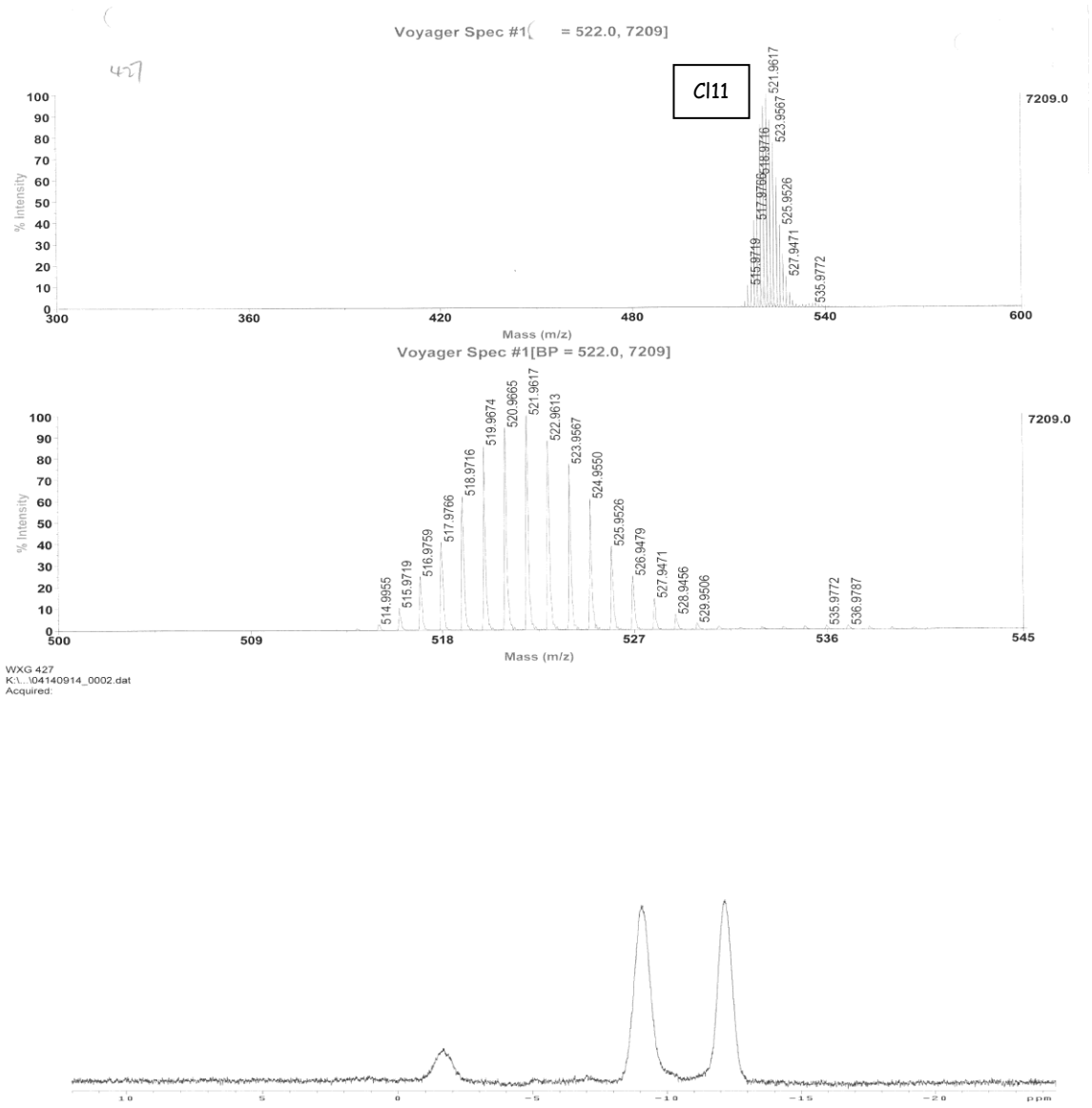

Figure 3-11. $Me_3NH[HCB_{11}Cl_{11}]$ product from the reaction with $SbCl_5$ at 1 g scale. (Top: MALDI-MS; Bottom: ^{11}B NMR in acetone)

Reaction of mixtures of partially chlorinated carborane anions with $SbCl_5$. A solution of $CsHCB_{11}H_xCl_{11-x}$ (130 mg, 0.23 mmol, x= 0~6, avg. ≈ 2.5 by MS; this

material was obtained from a reaction of parent carborane with SO_2Cl_2 without Ar protection) in $SbCl_5$ (0.8 mL, 6.3 mmol) in a Schlenk flask was heated to reflux at 140 ℃ for 1 d. After removal of most of the volatiles, the residue was dissolved in 10% aq. NaOH, passed through Celite and then neutralized by dilute HCl solution. Treatment of the resultant solution with 0.1 g of Me_3NHCl (1.1 mmol) caused formation of a white precipitate. This solid was filtered off, washed with distilled water and dried under vacuum to give 125 mg (86%) of $Me_3NH[HCB_{11}Cl_{11}]$. **Reaction of $Cs[HCB_{11}H_{11}]$ with $SbCl_5$ (5 g scale):** A solution of $Cs[HCB_{11}H_{11}]$ (5.09 g, 18.4 mmol) in $SbCl_5$ (50 mL, 395 mmol) in a Schlenk flask was heated to reflux at 140 ℃ for 1 d. After removal of most of the volatiles, the residue was dissolved in 10% aq. NaOH, passed through Celite and then neutralized by dilute HCl solution. Treatment of the resultant solution with 3 g of Me_3NHCl (31 mmol) caused formation of a white precipitate. This solid was filtered off, washed with distilled water and dried under vacuum to give 8.9 g (82%) of $Me_3NH[HCB_{11}Cl_{11}]$. MALDI MS analysis showed two sets of carborane isotopic patterns (Figure 3-12). One set around 522 corresponds to the $HCB_{11}Cl_{11}$ anion (**Cl11**); another set around 503 corresponds to the $HCB_{11}Cl_{10}OH$ anion (**Cl10OH**).

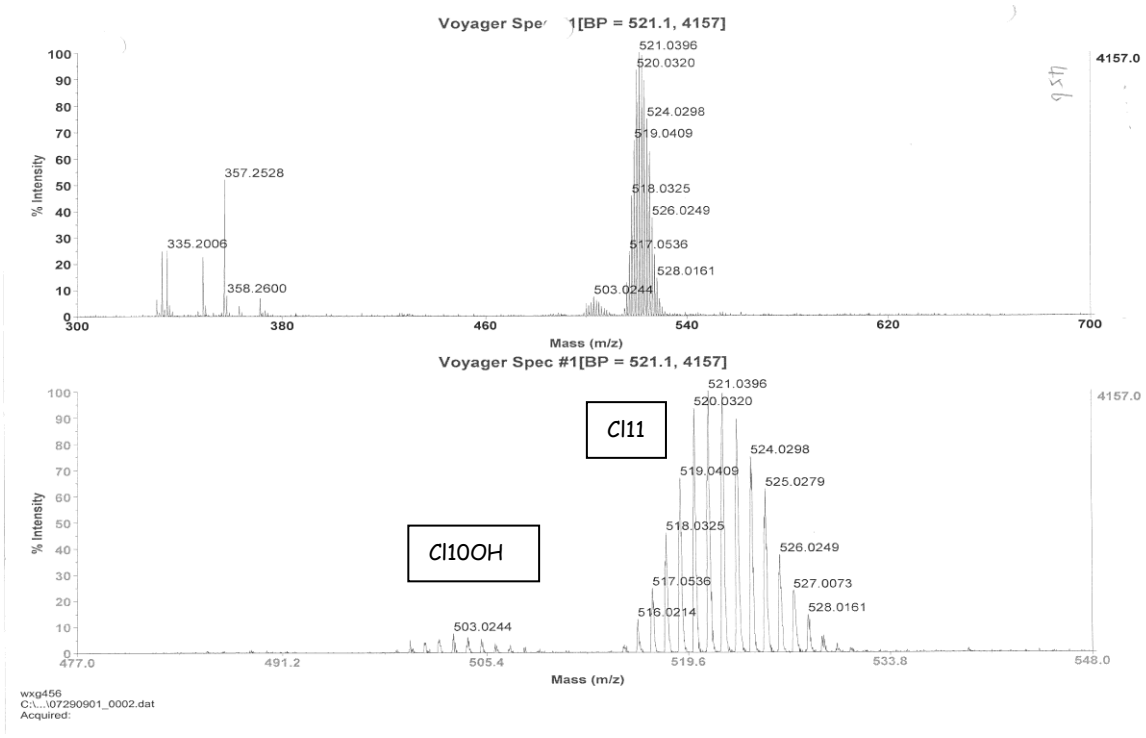

Figure 3-12. MALDI MS spectrum for the reaction with $SbCl_5$ at 5 g scale.

Reaction of a mixture of $Me_3NH[HCB_{11}Cl_{11}]$ and $Me_3NH[HCB_{11}Cl_{10}OH]$ with hexamethyldisilazane. A CH_2Cl_2 solution of a mixture of $Me_3NH[HCB_{11}Cl_{11}]$ and $Me_3NH[HCB_{11}Cl_{10}OH]$ (110 mg, est. 0.22 mmol; obtained from a reaction of $Cs[HCB_{11}H_{11}]$ with $SbCl_5$ as described above) was treated with hexamethyldisilazane (500 µL, 2.4 mmol) and heated to reflux in a Schlenk flask for 24 h. Removal of the volatiles gave a white solid which was analyzed by MALDI MS. MS spectra (Figure 3-13) showed three sets of signals with the carborane isotopic pattern. The set around 522 corresponds to the $HCB_{11}Cl_{11}$ anion (**Cl11**); the set around 487 corresponds to the $HCB_{11}Cl_{10}OH$ anion (**Cl10**); and a new set around 575 corresponds to the $HCB_{11}Cl_{10}OSiMe_3$ anion (**Cl10OSiMe$_3$**).

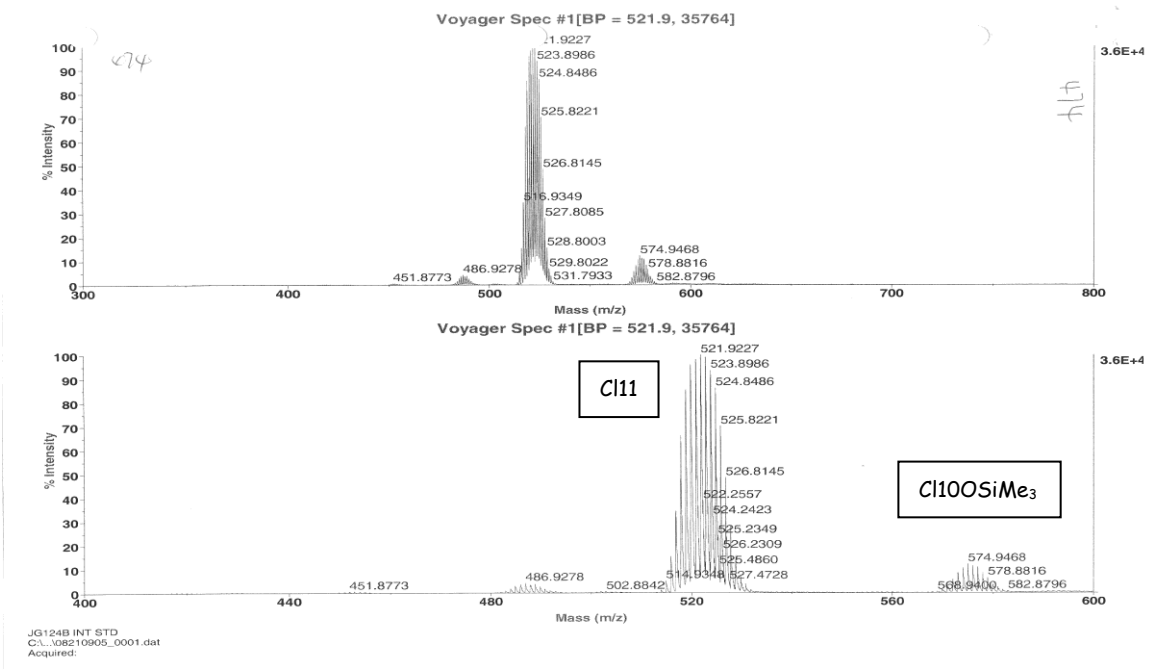

Figure 3-13. MALDI MS spectrum for the reaction mixture of $Me_3NH[HCB_{11}Cl_{11}]$ and $Me_3NH[HCB_{11}Cl_{10}OH]$ with hexamethyldisilazane.

Reaction of $Cs[HCB_{11}H_{11}]$ with $SbCl_5$ with added H_2O. A solution of $Cs[HCB_{11}H_{11}]$ (100 g, 0.36 mmol) in $SbCl_5$ (1 mL, 8 mmol) with added H_2O (30 µL, 1.7 mmol) in a Schlenk flask was heated to reflux at 140 ℃ for 1 d. After removal of the volatiles, the residue was dissolved in 10% aq. NaOH, passed through Celite and then neutralized by dilute HCl solution. Treatment of the resultant solution with 0.1 g of Me_3NHCl (1.1 mmol) caused formation of a white precipitate. This solid was filtered off, washed with distilled water and dried under vacuum to give 150 mg of a solid. MALDI MS (Figure 3-14) analysis showed two sets of carborane isotopic patterns. One set around 522 corresponds to the $HCB_{11}Cl_{11}$ anion (**Cl11**); another set

around 503 corresponds to the $HCB_{11}Cl_{10}OH$ anion (**Cl10OH**).

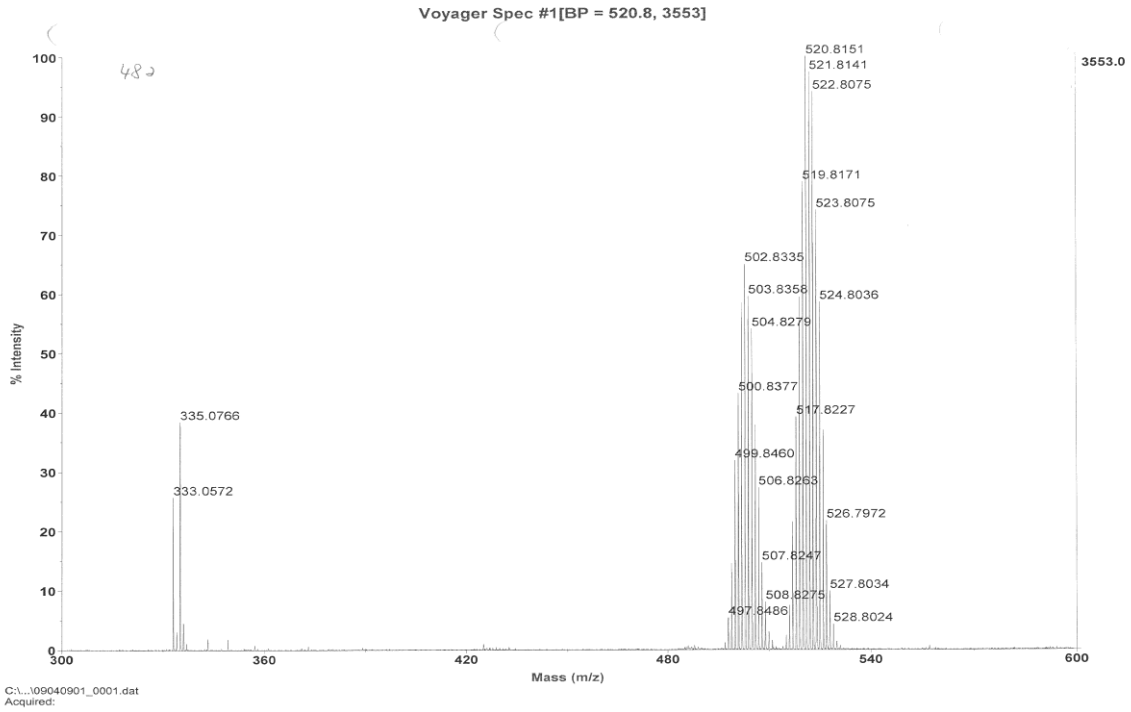

Figure 3-14. MALDI MS spectrum for the reaction with $SbCl_5$ and H_2O.

Reaction of mixture of $Me_3NH[HCB_{11}Cl_{11}]$ and $Me_3NH[HCB_{11}Cl_{10}OH]$ with SO_2Cl_2. A solution of a mixture of $Me_3NH[HCB_{11}Cl_{11}]$ and $Me_3NH[HCB_{11}Cl_{10}OH]$ (220 mg, est. 0.44 mmol; obtained from a reaction of $Cs[HCB_{11}H_{11}]$ with $SbCl_5$ as described above) in SO_2Cl_2 (1.0 mL, 12.4 mmol) was heated to reflux at 80 ℃ in a Schlenk flask for 24 h. Removal of the volatiles gave a white solid (220 mg) which

was analyzed by MALDI MS. MS spectra showed only one set of signals with a carborane pattern around 522 which corresponds to the $HCB_{11}Cl_{11}$ anion (**Cl11**).

Reaction of mixture of $Me_3NH[HCB_{11}Cl_{11}]$ and $Me_3NH[HCB_{11}Cl_{10}OH]$ with $SbCl_5$. A solution of a mixture of $Me_3NH[HCB_{11}Cl_{11}]$ and $Me_3NH[HCB_{11}Cl_{10}OH]$ (207 mg, est. 0.41 mmol; obtained from a reaction of $Cs[HCB_{11}H_{11}]$ with $SbCl_5$ as described above) in $SbCl_5$ (0.5 mL, 4 mmol) was heated to reflux at 140 ℃ in a Schlenk flask for 24 h. After removal of the volatiles, the residue was dissolved in 10% aq. NaOH, passed through Celite and then neutralized by dilute HCl solution. Treatment of the resultant solution with 0.1 g of Me_3NHCl (1.1 mmol) caused formation of a white precipitate. This solid was filtered off, washed with distilled water and dried under vacuum to give 175 mg of a solid. MALDI MS analysis showed only one set of signals with a carborane pattern around 522 which corresponds to the $HCB_{11}Cl_{11}$ anion (**Cl11**).

Reaction of $Cs_2[B_{12}H_{12}]$ with SO_2Cl_2: A suspension of $Cs_2[B_{12}H_{12}]$ (180 mg, 0.44 mmol) in SO_2Cl_2 (10 mL, 124 mmol) in a Schlenk flask was heated to reflux for 24 h. Removal of all volatiles gave a white solid which was redissolved in water for ^{11}B NMR study. ^{11}B NMR (128.2 MHz, aceotne): δ -7.8 (m), -15.2 (d), -17.8 (m). (Figure 3-15) SO_2Cl_2 used in this reaction was purchased from Aldrich and used as received. $Cs_2[B_{12}H_{12}]$ used in this reaction was purchased from Strem and used as received.

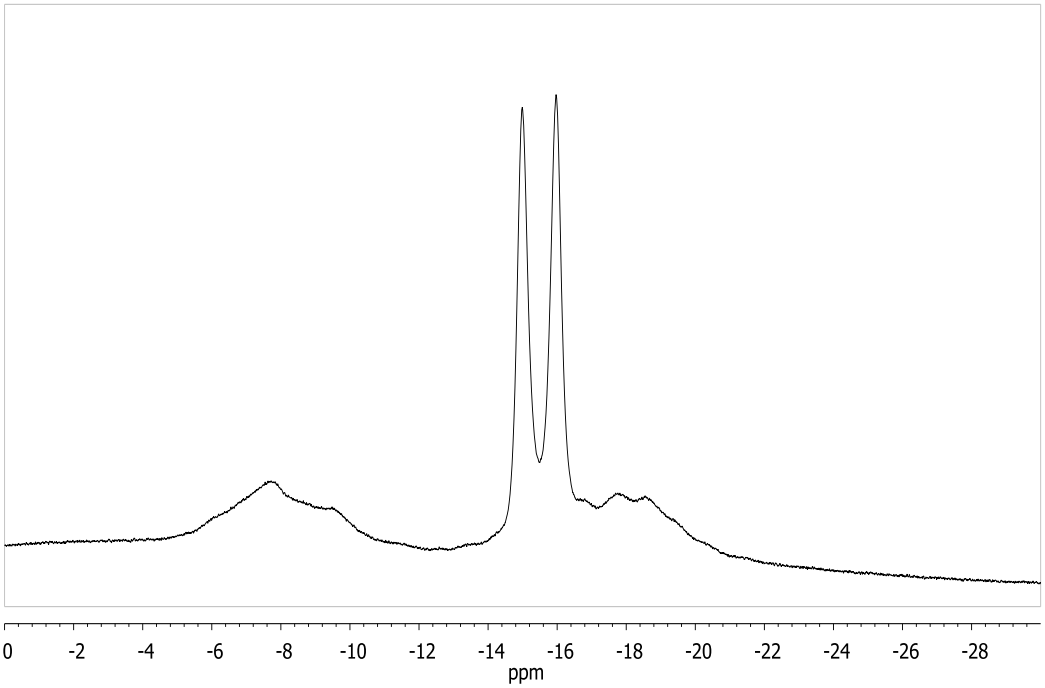

Figure 3-15. ^{11}B NMR spectrum for reaction of $Cs_2[B_{12}H_{12}]$ with reflux SO_2Cl_2 for 24 h.

$[Et_3NH]_2[B_{12}H_{12}]$. To a white suspension of $Cs_2[B_{12}H_{12}]$ (170 mg, 0.42 mmol) in 15 mL water was added 0.5 mL hydrochloric acid and Et_3N (0.6 mL, 4.3 mmol). The mixture was stirred at room temperature for 1 h. The white percipiate was collected on a medium frit, washed with water and then dried under vacuum at 100 ℃ overnight. Yield: 130 mg (91%). ^{1}H NMR (299.9 MHz, d_6-acetone): 3.05 (m, NCH_2CH_3, 6H), 1.14 (t, J_{H-H}= 7.2 Hz, NCH_2CH_3, 9H). ^{11}B NMR (128.2 MHz, d_6-acetone): δ -14.7 (d, J_{B-H}= 130 Hz).

Reaction of $[Et_3NH]_2[B_{12}H_{12}]$ with SO_2Cl_2: A suspension of $[Et_3NH]_2[B_{12}H_{12}]$ (120 mg, 0.35 mmol) in SO_2Cl_2 (8 mL, 99 mmol) in a Schlenk flask was heated to reflux for 24 h. Removal of all volatiles gave a white solid which was redissolved in water

for ^{11}B NMR study. ^{11}B NMR (128.2 MHz, aceotne): δ -11.8 (m), -17.8 (m) (Figure 3-16). SO_2Cl_2 used in this reaction was purchased from Aldrich and used as received.

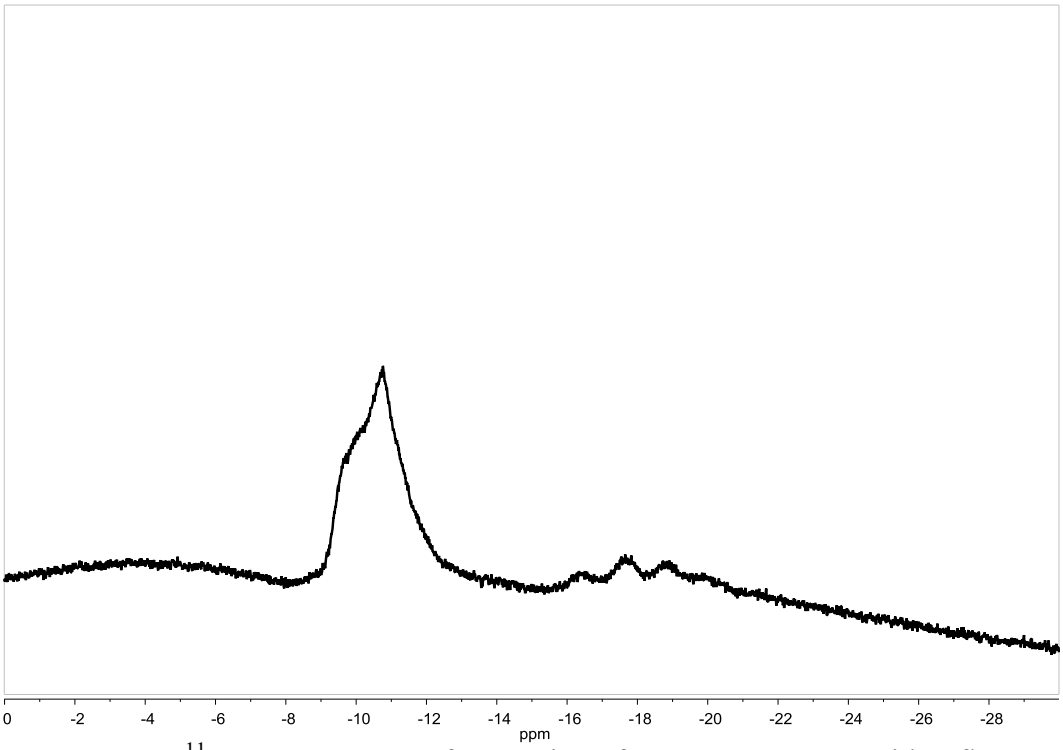

Figure 3-16. ^{11}B NMR spectrum for reaction of $[Et_3NH]_2[B_{12}H_{12}]$ with reflux SO_2Cl_2 for 24 h.

Reaction of $Cs_2[B_{12}H_{12}]$ with SO_2Cl_2 and MeCN (1 g scale): SO_2Cl_2 used in this reaction was purchased from Aldrich and used as received. MeCN was purchased from VWR and used as received. $Cs_2[B_{12}H_{12}]$ used in this reaction was purchased from Strem and used as received. To a suspension of $Cs_2[B_{12}H_{12}]$ (1.00 g, 2.45 mmol) in acetonitrile (30 mL) in a Schlenk flask was slowly added SO_2Cl_2 (30 mL, 370

mmol). The mixture soon became a clear solution and was heated to reflux for 24 h. Removal of all volatiles gave a white solid which was redissolved in CD_3CN for NMR study (Fig. 3-17). ^1H NMR (299.9 MHz, d_3-acetonitrile): 5.90 (t, $J_{N-H} = 54$ Hz). ^{11}B NMR (128.2 MHz, d^3-acetonitrile): δ -12.7 (s).

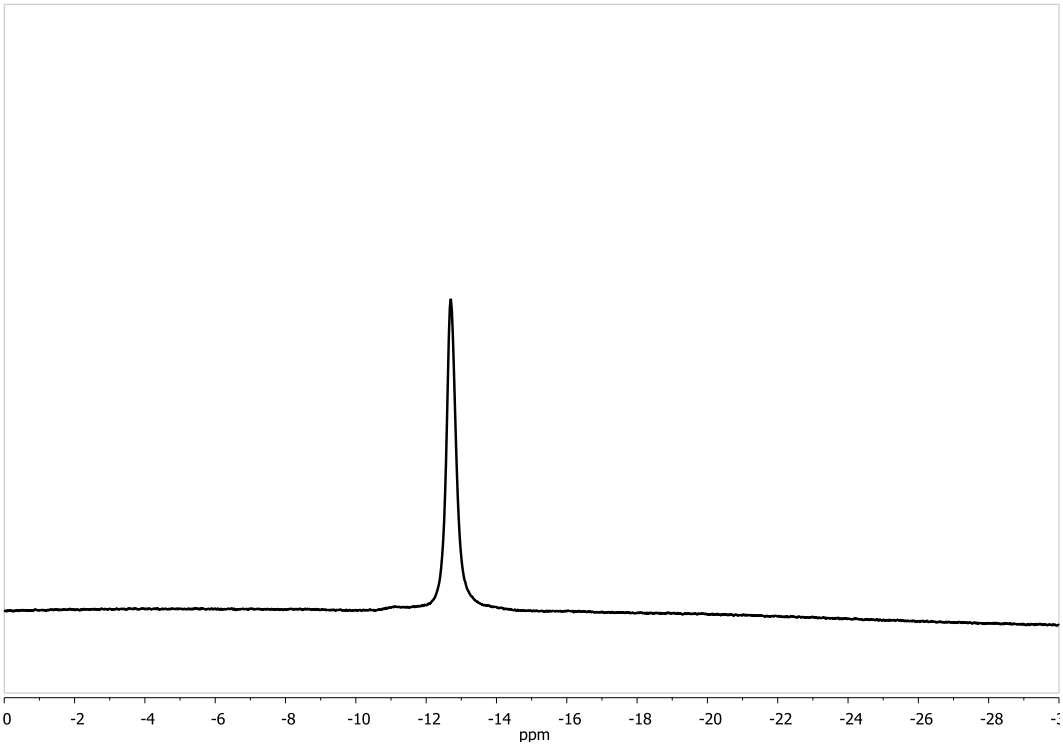

Figure 3-17. ^{11}B NMR spectrum for reaction of $Cs_2[B_{12}H_{12}]$ with reflux SO_2Cl_2 and acetonitrile for 24 h without workup. (Top: ^{11}B NMR in CD_3CN; Bottom: ^1H NMR in CD_3CN)

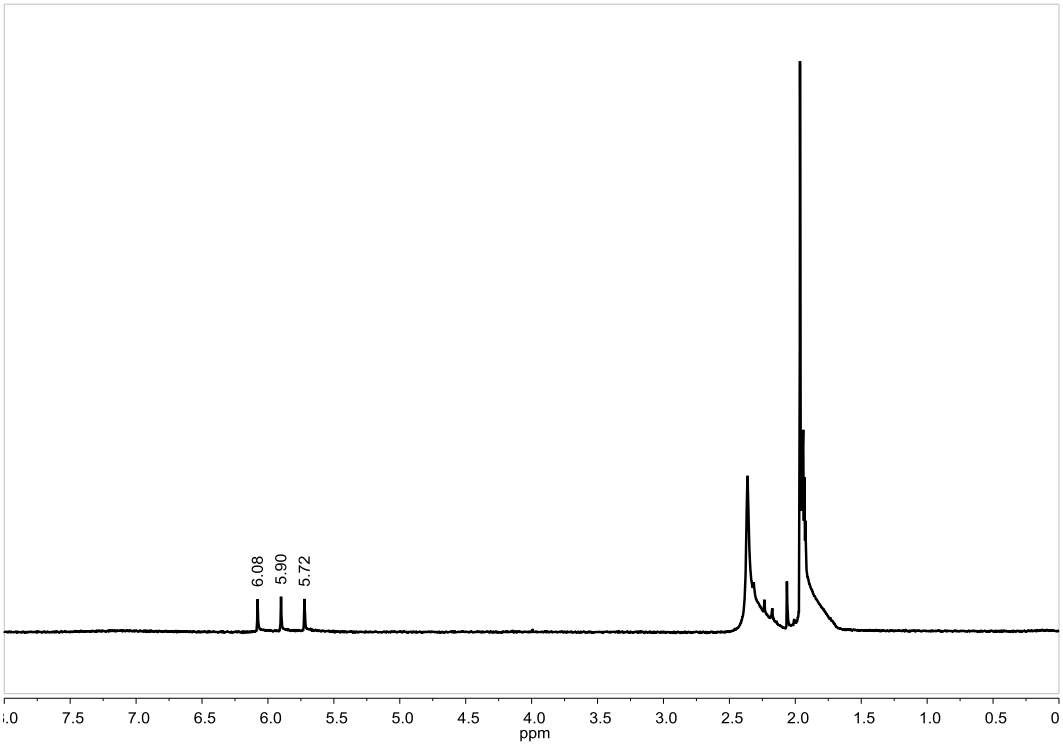

Figure 3-17. Continued

We surmised that the 1:1:1 triplet observed in the ^{1}H NMR belonged to NH_4^+, likely from the degradation of acetonitrile. The following steps assured removal of this impurity. The white solids obtained above were treated with 0.2 mL of 10% NaOH aqueous solution and then recrystallized from hot water with 1.5 g CsCl (8.9 mmol) to give $Cs_2[B_{12}Cl_{12}]$. Yield: 1.64 g (82%). ^{11}B NMR (128.2 MHz, H_2O): δ -12.1 (s). IR (cm^{-1}): ν= 1030 (vs), 534 (vs). (Figure 3-18) Elem. An. Found. (Calculated) for Cs2B12Cl12: Cl, 50.91 (51.82); B, 15.51 (15.80)%.

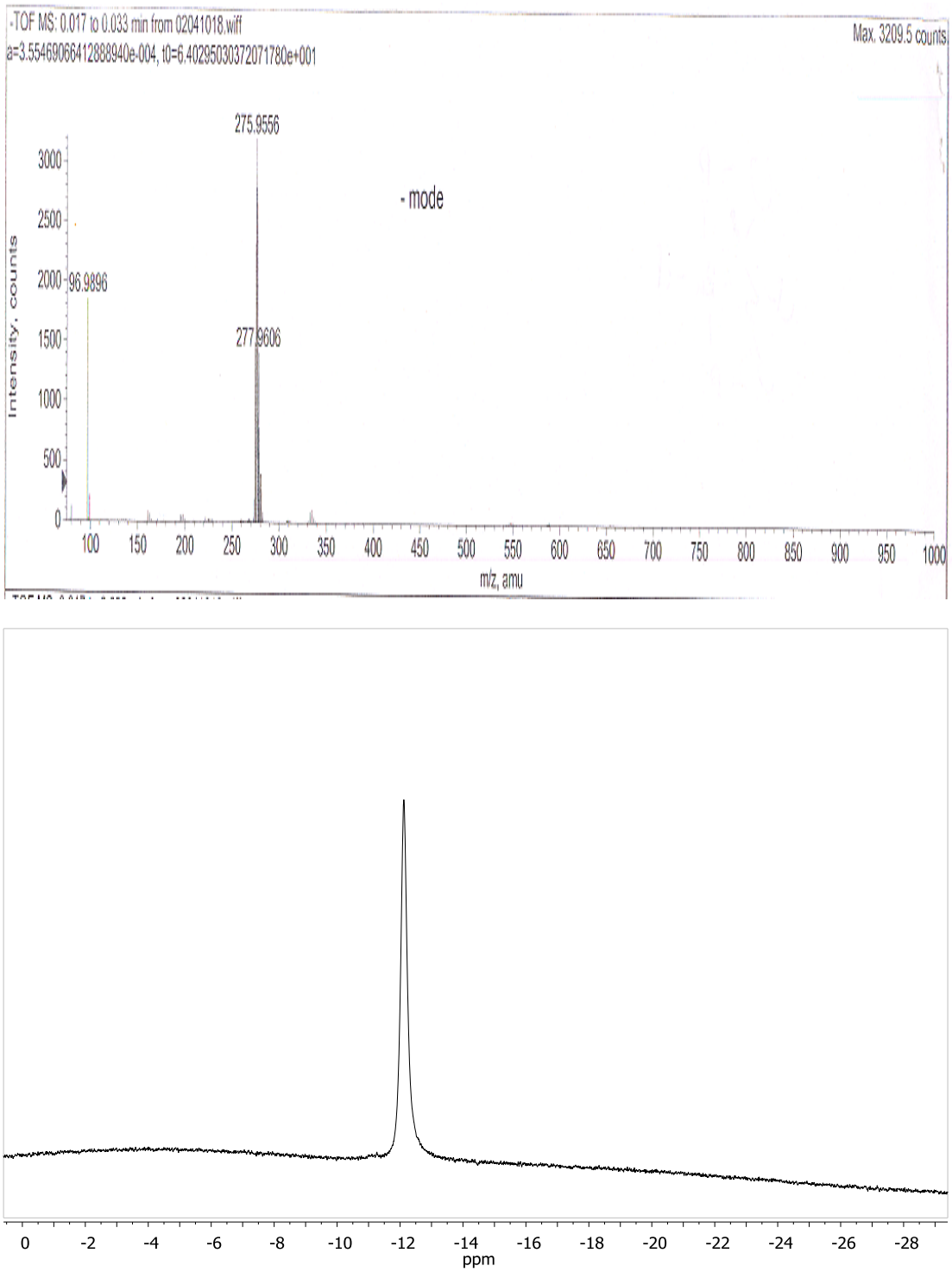

Figure 3-18. ^{11}B NMR spectrum for reaction of $Cs_2[B_{12}H_{12}]$ with reflux SO_2Cl_2 and acetonitrile for 24 h after workup. (Top: ESI-MS spectrum; Bottom: ^{11}B NMR in CD_3CN)

Reaction of $Cs_2[B_{12}H_{12}]$ with SO_2Cl_2 and MeCN (100 mg scale): To a suspension of $Cs_2[B_{12}H_{12}]$ (155 mg, 0.38 mmol) in acetonitrile (5 mL) in a Schlenk flask was slowly added SO_2Cl_2 (5 mL, 62 mmol). The mixture soon became a clear solution and was heated to reflux for 8 h. Removal of all volatiles gave a white solid which was treated with 0.05 mL of 10 % NaOH aqueous solution and then recrystallized from hot water with 0.3 g CsCl (1.8 mmol) to give $Cs_2[B_{12}Cl_{12}]$. Yield: 240 mg (78%). ^{11}B NMR (128.2 MHz, H_2O): δ -12.1 (s). SO_2Cl_2 used in this reaction was purchased from Aldrich and used as received. MeCN was purchased from VWR and used as received. $Cs_2[B_{12}H_{12}]$ used in this reaction was purchased from Strem and used as received.

Reaction of $Cs_2[B_{12}H_{12}]$ with SO_2Cl_2 (Acros) and MeCN: SO_2Cl_2 used in reaction was purchased from Acros. To a suspension of $Cs_2[B_{12}H_{12}]$ (97 mg, 0.24 mmol) in acetonitrile (3 mL) in a Schlenk flask was slowly added SO_2Cl_2 (3 mL, 37 mmol). The mixture soon became a clear solution and was heated to reflux for 8 h. Removal of all volatiles gave a white solid which was redissolved in water for ^{11}B NMR study. ^{11}B NMR (128.2 MHz, H_2O): δ -12.1 (s). SO_2Cl_2 used in this reaction was purchased from Acros and used as received. MeCN was purchased from VWR and used as received. $Cs_2[B_{12}H_{12}]$ used in this reaction was purchased from Strem and used as received.

Reaction of $Cs_2[B_{12}H_{12}]$ (recrystallized) with purified SO_2Cl_2 and MeCN in the absence of light: This reaction is protected from light. All of the flask and condenser were wrapped with aluminum foil during the reaction. $Cs_2[B_{12}H_{12}]$ used in this

reaction was recrsystallized from hot water and dried under vacuum at 80 ℃ for 8 h before use. MeCN used in this reaction was dried with CaH_2 and distilled under Ar and stored over molecular sieves in an Ar-filled glovebox. SO_2Cl_2 used in this reaction was purchased from Arcos and fractionally distilled before use. Starting with 100 mL SO_2Cl_2, the middle 50% (50 mL) was used in the reaction. To a suspension of $Cs_2[B_{12}H_{12}]$ (102 mg, 0.25 mmol) in acetonitrile (3 mL) in a Schlenk flask was slowly added SO_2Cl_2 (3 mL, 37 mmol). The mixture was heated to reflux. After 8 h, an aliquot was taken from the reation mixture. Removal of all volatiles gave a white solid which was redissolved in water for ^{11}B NMR study. After 24 h, all volatiles was removed under vacuum to give a white solid which was redissolved in water for ^{11}B NMR study. ^{11}B NMR (128 MHz, H_2O): δ -12.1 (s).

Reaction of $Cs_2[B_{12}H_{12}]$ (recrystallized) with purified SO_2Cl_2 and MeCN under Ar: This reaction is performed under Ar. $Cs_2[B_{12}H_{12}]$ used in this reaction was recrsystallized from hot water and dried under vacuum at 80 ℃ for 8 h before use. MeCN was dried with CaH_2 and distilled under Ar and stored over molecular sieves in an Ar-filled glovebox. SO_2Cl_2 used in this reaction was purchased from Arcos and fractionally distilled before use. Starting with 100 mL SO_2Cl_2, the middle 50% fraction (50 mL) was collected and used in the reaction. To a suspension of $Cs_2[B_{12}H_{12}]$ (102 mg, 0.25 mmol) in acetonitrile (3 mL) in a Schlenk flask was slowly added SO_2Cl_2 (3 mL, 37 mmol) under Ar. The mixture was heated to reflux. After 8 h, an aliquot was taken from the reation mixture. Removal of all volatiles gave a white solid which was redissolved in water for ^{11}B NMR study. After 24 h,

all volatiles was removed under vacuum to give a white solid which was redissolved in water for ^{11}B NMR study. ^{11}B NMR (128.2 MHz, H_2O): δ -12.1 (s).

CHAPTER IV

Sp^3 C-F BOND ACTIVATION MEDIATED BY SILYLIUM AND ALUMENIUM SPECIES*

4.1 Introduction

As presented in Chapter I, fluoroorganic compounds play an integral role in everyday life due to their special chemical, biological and mechanical properties. In the meantime, activation of C-F bonds under mild conditions remains as a great challenge. Early work on C-F bond activation mainly focused on redox chemistry mediated by transition metal complexes.[150] In 2005, Ozerov and coworkers reported an approach for hydrodefluorination of aliphatic C-F bonds in which the key step is a non-redox process of fluoride abstraction by highly electrophilic silylium species.[71a] The work was inspired by some early reports by Krause and Lampe in which they observed Si-H/C-F redistribution by mass spectroscopy while studying the reaction between SiH_3^+ and CF_4 in the gas phase.[151] Later, the Reed,[71b] Mueller[71c] and Siegel[152] groups reported similar C-F bond activation with silylium reagents paired with weakly coordinating anions.

---

* reprinted in part from *J. Am. Chem. Soc*., 131, Gu, W.; Haneline, M. R.; Douvris, C.; Ozerov, O. V. "Carbon−Carbon Coupling of C(sp^3)−F Bonds Using Alumenium Catalysis", 11203, copyright 2009 American Chemical Society and from *Inorg. Chem.*, 50, Gu, W.; Ozerov, O. V. "Exhaustive Chlorination of $[B_{12}H_{12}]^{2-}$ without Chlorine Gas and the Use of $[B_{12}Cl_{12}]^{2-}$ as Supporting Anion in Catalytic Hydrodefluorination of Aliphatic C-F Bonds", 2726, copyright 2011 American Chemical Society.

Scheme 4-1. Silylium and alumenium mediated C-F bond activations.

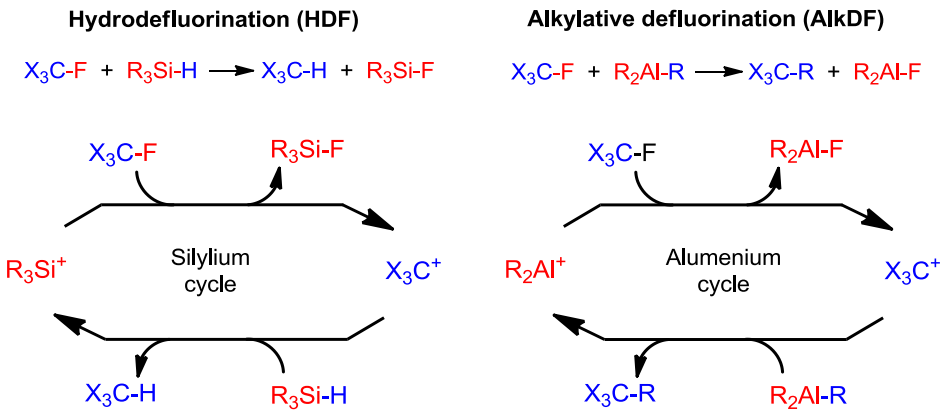

Recently, the reactivity and longevity of these silylium mediated C-F bond activations have been greatly improved by using halogenated carboranes as counterions.[71d,71f] Here we report a related "alkylative defluorination" (AlkDF) process mediated by R_2Al^+ equivalents (in place of R_3Si^+) paired with a carborane anion (Scheme 4-1). We expect the high polarity of the Al-C bonds would lead to facile and catalytic conversion of C-F to C-C, which is rare in the literature.

Several recent reports relevant to the use of aluminum compounds in C-F activation need to be highlighted. Akiyama[153] et al. have recently detailed activation of benzotrifluorides by the mixtures of $NbCl_5$ and $LiAlH_4$. However, it is not clear whether Al plays any role besides reducing Nb to a reactive state. Terao[154] and coworkers demonstrated that trialkylaluminums (without any added catalyst) could convert C-F bonds in primary fluorides or benzotrifluorides into C-C bonds. As our investigations demonstrate (*vide infra*), this reaction is largely limited to monofluoroalkanes.

Rosenthal and Krossing[101] used $^{i}Bu_2AlH$ as the source of H for hydrodefluorination (**HDF**) catalyzed by trityl salts of $B(C_6F_5)_4^-$, $Al(C_6F_5)_4^-$ or $Al(OC(CF_3)_3)_4^-$. Just as in the case of Si-based HDF with $B(C_6F_5)_4^-$,[71a,71b] these anions failed to sustain the catalysis for more than a few dozen turnovers. The groups of Sen and Reed[100] reported the preparation of $Et_2Al[HCB_{11}H_5Br_6]$ (**A**), a species with an alumenium (R_2Al^+) cation-like reactivity.

4.2 Results and Discussion

4.2.1 Alumenium Mediated Sp^3 C-F Bond Activation

In our hands, AlkDF reactions were performed with $Et_2Al[HCB_{11}H_5Br_6]$ (**A**), $Ph_3C[HCB_{11}H_5Br_6]$ (**B**) or $Ph_3C[B(C_6F_5)_4]$ (**C**) as (pre-)catalysts and substrates with sp^3 C-F bonds The results for catalytic AlkDF reactions are summarized in Table 4-1, Scheme 4-2 and Table 4-2. Given that **A** was originally prepared by Reed and his coworkers via reaction of **B** with Et_3Al,[100] it appears sound to assume that **B** and **C** are swiftly converted to the corresponding $Et_2Al[Anion]$ by the excess of Et_3Al in our catalytic reactions.

In the idealized form, we may refer to R_2Al^+ and R_3C^+ cations here. However, it is unlikely that true free cations exist in our catalytic reaction mixtures, especially in the less polar solvents. Except perhaps the more stabilized carbocations, the cations under study undoubtedly exist as adducts with the anion, solvent, one of the reactants or products. Nonetheless, considering the weakly coordinating nature of the hexa-bromocarborane anion or of the solvents employed here, it appears reasonable to treat these species in solution as close synthons of the requisite cations.

4.2.1.1 Reactions with Benzotrifluorides

We first examined the AlkDF reactivity with *p*-$FC_6H_4CF_3$ (**1**, Scheme 4-3). Due to the presence of the aromatic C-F moiety, it is easy to track both the substrate and the products by ^{19}F NMR. Similar to the results that were reported in the Si-mediated HDF chemistry, we saw no evidence of activation of the aromatic C-F bonds.[71a,71d] We used C_6F_6 as the internal integration standard for ^{19}F NMR.

Table 4-1. Summary of AlkDF reactions initiated at ambient temperature with Al/F ratio of 1.

No	Sub.	R_3Al	Cat.	Cat.%[a]	Solvent	% C-F[b]	% Al-F[b]	TON[c]
1	**1**	Me_3Al	**A**	0.33%	Hexanes	41(100)%	38(95)%	123
2	**1**	Et_3Al	**A**	0.33%	Hexanes	93%	87%	280
3	**1**	$^{i}Bu_3Al$	**A**	0.33%	Hexanes	100%	89%	300
4	**1**	$^{i}Bu_2AlH$	**A**	0.33%	Hexanes	96%	72%	290
5	**1**[d]	Et_3Al	**A**[e]	0.01%	Hexanes	98%	93%	9800
6	**1**	Et_3Al	**A**	0.33%	$C_6H_4Cl_2$	100%[f]	98%	300
7	**1**	Et_3Al	**B**	0.33%	Hexanes	21(90)%	18(82)%	63
8	**1**	Et_3Al	**C**	0.33%	Hexanes	16(50)%	13(45)%	48
9	**1**	Et_3Al	**B**	0.33%	$C_6H_4Cl_2$	100%[f]	88%	300
10	**1**	Et_3Al	**C**	0.33%	$C_6H_4Cl_2$	100%[f]	86%	300
11	**2**	Et_3Al	**A**	0.33%	Hexanes	90%	85%	270
12	**3**	Et_3Al	**A**	0.33%	Hexanes	25(93)%	21(89)%	75
13	**1**	Et_3Al	**A**[e]	0.33%	Hexanes	100%[f]	94%	300
14	**2**	Et_3Al	**A**[e]	0.33%	Hexanes	100%[f]	98%	300
15	**3**	Et_3Al	**A**[e]	0.33%	Hexanes	100%[f]	92%	300
16	**2**	Me_3Al	**A**	0.33%	Hexanes	35(94)%[g]	30(64)%	110
17	**4**[h]	Et_3Al	**A**	2.00%	$C_6H_4Cl_2$	23(100)%	NA	13
18	**4**[h]	Me_3Al	**A**[e]	2.00%	Hexanes	66(100)%	49(84)%	33
19	**4**[h]	Me_3Al	**A**[e]	0.33%	Hexanes	6(50)%	6(39)%	19
20	**5**[i]	Et_3Al	**A**	0.33%	$C_6H_4Cl_2$	51(92)%	50(90)%	150
21	**5**[i]	Me_3Al	**A**[e]	0.33%	Hexanes	39(82)%	37(80)%	120
22	**6**	Et_3Al	**A**	0.25%	$C_6H_4Cl_2$	100%[f]	95%	400
23[j]	**1**	Me_3Al/Et_3SiH	**B**	0.33%	Hexanes	100%	90%	300

[a] Catalyst loading, vs the number of C-F bonds; [b] Conversion after 3 h (after 24 h in parentheses) based on disappearance of C-F bonds or appearance of Al-F bonds, by ^{19}F NMR; [c] Turnover number after 3 h; [d] Reaction was carried out in a glass vial with stirring; [e] Catalyst introduced as a solution in *o*-$C_6H_4Cl_2$; [f] Reaction complete in <10 min; [g] 94% conversion after 36 h; [h] Reactions were carried out at 85 ℃ ; [i] Reactions were carried out at 50 ℃ . [j] only Al-F was observed by ^{19}F NMR, no Si-F observed.

Scheme 4-2. AlkDF reactions with benzotrifluorides.

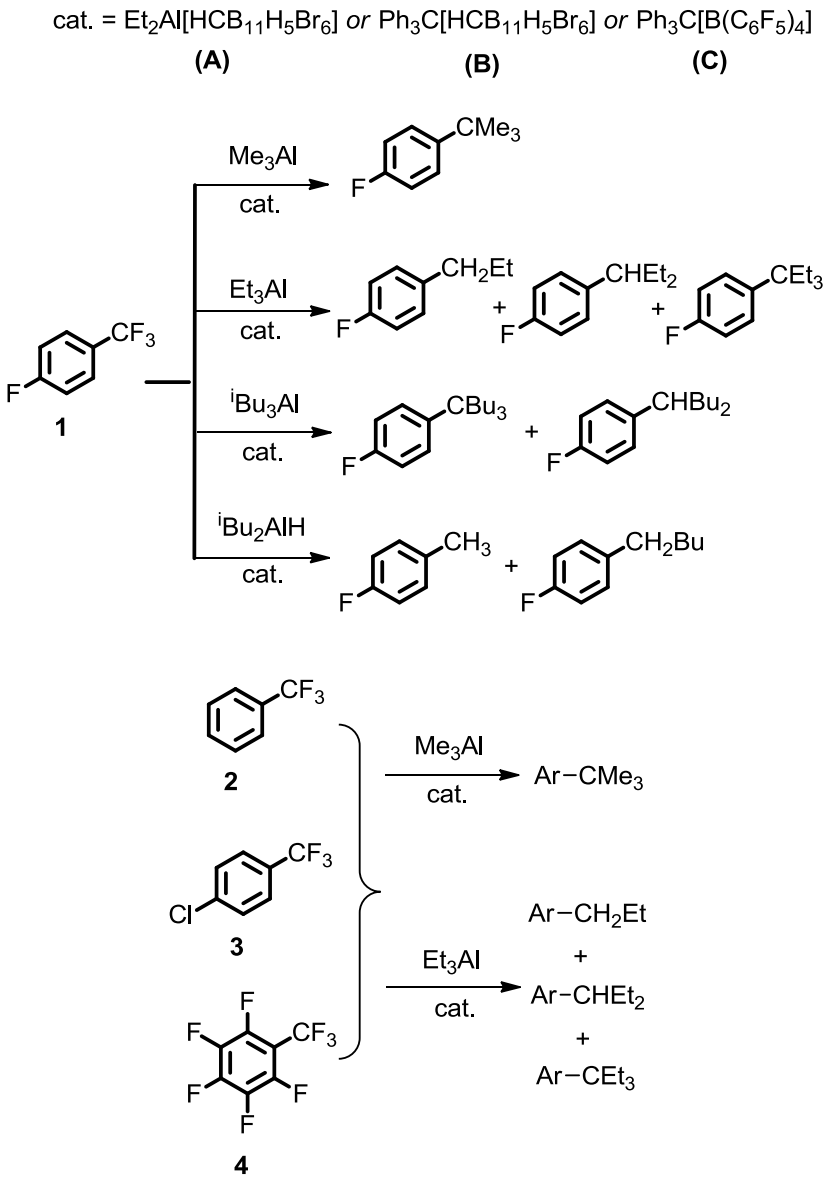

Table 4-2. Main organic products for the defluorination reactions.

No	substrate	aluminum reagents	Products
1	1	Me_3Al	*p*-$FC_6H_4CMe_3$
2	1	Et_3Al	*p*-$FC_6H_4CEt_3$, *p*-$FC_6H_4CHEt_2$, *p*-$FC_6H_4CH_2CH_2CH_3$
3	1	$^{i}Bu_3Al$	*p*-FC_6H_4-CHC_8H_{18}, *p*-FC_6H_4-$CC_{12}H_{27}$
4	1	$^{i}Bu_2AlH$	*p*-$FC_6H_4CH_3$, *p*-$FC_6H_4CH_2C_4H_9$
5	1	Et_3Al	*p*-$FC_6H_4CEt_3$, *p*-$FC_6H_4CHEt_2$, *p*-$FC_6H_4CH_2CH_2CH_3$
6	1	Et_3Al	*p*-$FC_6H_4CEt_3$, *p*-$FC_6H_4CHEt_2$, *p*-$FC_6H_4CH_2CH_2CH_3$
7	1	Et_3Al	*p*-$FC_6H_4CEt_3$, *p*-$FC_6H_4CHEt_2$, *p*-$FC_6H_4CH_2CH_2CH_3$
8	1	Et_3Al	*p*-$FC_6H_4CEt_3$, *p*-$FC_6H_4CHEt_2$, *p*-$FC_6H_4CH_2CH_2CH_3$
9	1	Et_3Al	*p*-$FC_6H_4CEt_3$, *p*-$FC_6H_4CHEt_2$, *p*-$FC_6H_4CH_2CH_2CH_3$
10	1	Et_3Al	*p*-$FC_6H_4CEt_3$, *p*-$FC_6H_4CHEt_2$, *p*-$FC_6H_4CH_2CH_2CH_3$
11	2	Et_3Al	$C_6H_5CEt_3$, $C_6H_5CHEt_2$, $C_6H_5CH_2CH_2CH_3$
12	3	Et_3Al	*p*-$ClC_6H_4CEt_3$, *p*-$ClC_6H_4CHEt_2$, *p*-$ClC_6H_4CH_2H_2CH_3$
13	1	Et_3Al	*p*-$FC_6H_4CEt_3$, *p*-$FC_6H_4CHEt_2$, *p*-$FC_6H_4CH_2CH_2CH_3$
14	2	Et_3Al	$C_6H_5CEt_3$, $C_6H_5CHEt_2$, $C_6H_5CH_2CH_2CH_3$
15	3	Et_3Al	*p*-$ClC_6H_4CEt_3$, *p*-$ClC_6H_4CHEt_2$, *p*-$ClC_6H_4CH_2CH_2CH_3$
16	2	Me_3Al	$C_6H_5CMe_3$
17	4	Et_3Al	$C_6F_5CEt_3$, $C_6F_5CHEt_2$, $C_6F_5CH_2CH_2CH_3$,
18	4	Me_3Al	$C_6F_5CMe_3$
19	4	Me_3Al	$C_6F_5CMe_3$
20	5	Et_3Al	III, IV and V in Scheme 4-5
21	5	Me_3Al	I, II in Scheme 4-5
22	6	$AlEt_3$	VI, VII in Scheme 4-11
23	1	Me_3Al/Et_3SiH	*p*-FC_6H_4-CH_3, *p*-FC_6H_4-CH_2Me, *p*-FC_6H_4-$CHMe_2$

Entries 1-4 of table 4-1 summarized the results for the reactions catalyzed by **A** (0.33% catalyst loading) in hexanes with various aluminum reagents. Although the reactions with Me_3Al were relatively slow, all reactions went to completion within 3-24 h with TON up to 300. The reactions worked well with lower catalyst loading as well. In one illustrative reaction (entry 5), we observed nearly 10^4 turnovers at 98% conversion in the catalyzed reaction of **1** with Et_3Al. Only the reactions with Me_3Al gave one clean product, where all sp^3 C-F bonds were replaced by C-Me bonds. On the other hand, for the reactions with Et_3Al, $^iBu_3Al$ or $^iBu_2AlH$, competitive reactions were observed between alkyl abstraction and β-hydride abstraction. Thus, multiple products were observed for entries 2-4 (Table 4-2). Release of the corresponding olefin were also observed in these reactions. Notably, the *β*-hydride abstraction from trialkylaluminum reagents was consistent with literature reports. In fact, catalyst **A** was synthesized via *β*-hydride abstraction from Et_3Al with **B**.[100]

Benzotrifluorides with differently substituted aryl rings were also tested with our AlkDF reactions. As we expected, benzotrifluorides with electronically similar aryl rings (substrate **2** and **3**) showed similar reactivity as substrate **1**. On the other hand, activation of the much more challenging substrate **4** required higher catalyst loading, longer reaction time and higher reaction temperature.

Scheme 4-3. Possible routes to generate multiple products in AlkDF reactions with $AlEt_3$. (Red: unobserved reaction intermediate; Blue: observed final products; Pink: unobserved theoretical product)

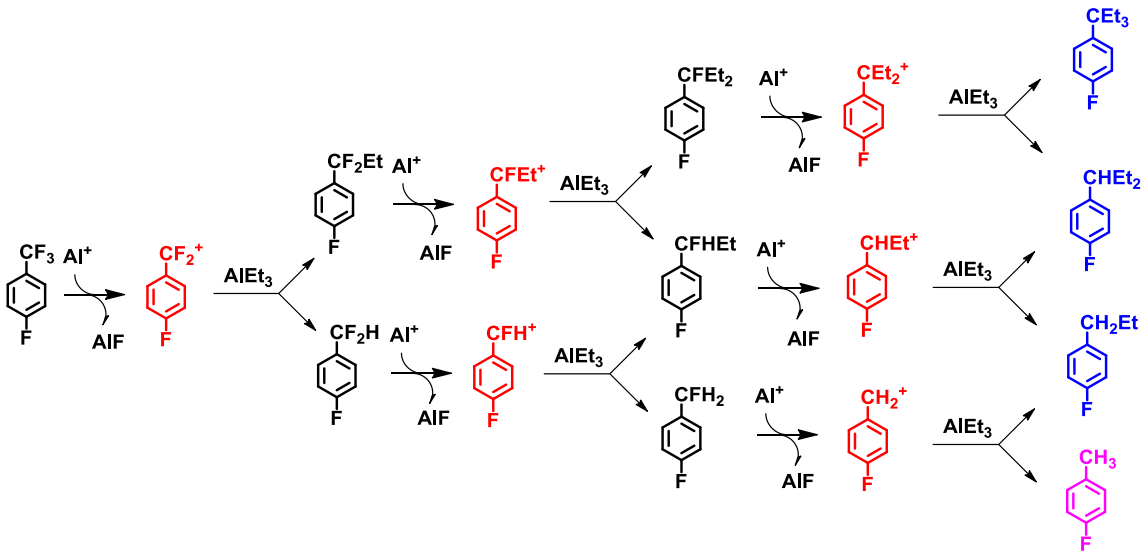

It is tempting to analyze why, in which cases, and by how much the transfer of hydride is favored over the transfer of the alkyl. However, the consideration of the system in full is daunting. Scheme 4-3 depicts four possible products for the defluorination reactions (only three observed). Yet, there are consecutively six carbocations, each of which can abstract an alkyl or a hydride from the aluminum compound. Furthermore, trialkylaluminum compounds in solution exist in equilibrium with their dimers. It is conceivable that both dimers and monomers can be donors of alkyl or hydride. As the reaction proceeds, alkyl groups on Al are replaced with fluorides. That introduces even more possibilities for structures of aluminum compounds that may exist in solution: the dimers (or even higher oligomers) may or may

not contain fluorides and fluorides or alkyls may be bridging. Little is known about structures of organoaluminum fluorides in solution; there is evidence in support of tetramers for Me_2AlF and Et_2AlF.[155] Even though it is likely that only some of the plausible Al compounds are capable of alkyl/hydride transfer,[156] the number of potential scenarios is difficult to digest. We suspect sterics plays a role in whether the carbocations prefer H abstraction or alkyl abstraction. On the one hand, the reactions between Et_3Al and benzotrifluorides do not produce $ArCH_3$. On the other hand, in the synthesis of the catalyst **A** itself, Ph_3C^+ cation (a very sterically encumbered cation) was reported to react with Et_3Al exclusively via abstraction of β-hydride and release of ethylene.[100] This is consistent with the preference for alkyl abstraction being greater for smaller carbocations and vice versa the hydride abstraction favored for larger carbocations.

C-F activation appears to proceed faster in more polar solvents. A reaction that gives 93% conversion in 1 h in hexanes is complete in 10 min or less in *o*-dichlorobenzene (entries 2, 6). We also found that introduction of the catalyst as a solution in $C_6H_4Cl_2$ (instead of a pure solid) to hexanes solutions led to a significant increase in rate. The reasons behind the solvent acceleration may be twofold. One, a more polar solvent may simply allow more of the catalyst to be dissolved or at least to be dissolved more rapidly. Two, a more polar solvent may lower the energy of the presumably polar transition state.

We found it possible to use **B** as (pre-)catalyst in place of isolated **A** in reactions with Et_3Al. The apparent rates of conversion were similar (cf. entries 7 and 9). The

results here are not surprising since **A** was reported before via reaction of **B** and Et_3Al. However, the reaction between **B** and Me_3Al was much slower and we did not use **B** as a (pre-)catalyst in reactions with Me_3Al. In our Si-based HDF work,[71a,71d] we demonstrated that $[B(C_6F_5)_4]^-$ can support some of the reactive cations involved, however, is ultimately destroyed during the course of the reaction. Rosenthal and Crossing recently reported HDF catalysis of primary alkyl fluorides and of $C_6H_5CF_3$ (**2**) using $^iBu_2AlH$ and **C** as a (pre-)catalyst, but their results were limited to 20 turnovers or less.[101] In our hands, **C** gave better results in reactions of **1** with Et_3Al. In $C_6H_4Cl_2$, it supported a 300 TON reaction to completion. The advantage of **C** is that it is a commercially available reagent. However, in contrast to an analogous reaction with **A** (entry 2), in hexanes **C** supported a reaction only to a maximum of 50% conversion (entry 8). It is reasonable to posit that a carborane anion is superior to $[B(C_6F_5)_4]^-$ in the Al-based AlkDF for the same reasons as in the Si-based HDF chemistry, although $[B(C_6F_5)_4]^-$ appears to more long-lived in the Al process.

4.2.1.2 Reactions with Non-benzylic C-F Bonds

Since the carbocation is more stable with an electronically average aryl group as substituent than with an alkyl group, it is safe to assume C-F bond activation should be easier at benzylic position if the rate-limiting step is fluoride abstraction and generation of carbocation. To extend the substrate scope, we tested several reactions with sp^3 C-F bonds at non-benzylic position. Rapid and complete conversion of C-F bonds in gem-difluorocyclopentane was observed with **A** as catalyst and Et_3Al as stoichiometric

reagents (Entry 22). Cyclopentane (33%) and ethylcyclopentane (67%) are the only products identified in this process.

On the other hand, the reactions with 3,3,3-trifluoropropylbenzene are much more complicated. Two products (**I** and **II** in Scheme 4-4) are obtained in 68:32 ratio when $AlMe_3$ is utilized as stoichiometric reagent. In Scheme 4-5 we proposed the possible Friedel-Crafts mechanism for the formation of indane derivatives **I**. The key step in the pathway is the intramolecular attack of a carbocation on the phenyl ring to yield the cyclization product. It echoes our proposal for the Friedel-Crafts pathways in the Si-based reactions.[71d] Terao and his coworkers also reported similar intramolecular Friedel-Crafts reaction in their non-catalytic C-F bond activation reactions.[154b] In Scheme 4-5, for the sake of argument, the intramolecular attack is shown to occur after the first C-F bond activation. We do not have enough evidence to determine whether the intramolecular attack occurs after the first, second or third C-F bond activation. When Et_3Al is used as stoichiometric reagent, more complicated products are observed since the carbocation intermediates participate in the competitive reactions between hydride abstractions, ethyl abstractions or cyclization reactions. The reaction rate of C-F activation of substrate **5** is much slower compared to similar reactions with **1-3**, which is consistent with our assumption that a carbocation with an aryl substituent group is more stable than a carbocation with an alkyl substituent group. The most challenging substrate that was activated in the Si-catalyzed HDF, nonafluorohexane (perfluorobutylethane),[71d] did not react with Et_3Al and catalyst **A** at all.

Scheme 4-4. Reactions of 3, 3, 3-trifluoropropylbenzene.

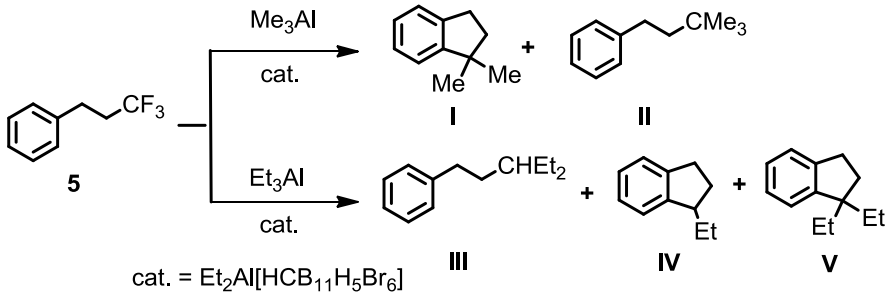

Scheme 4-5. Possible Friedel-Crafts mechanism for the formation of **I**.

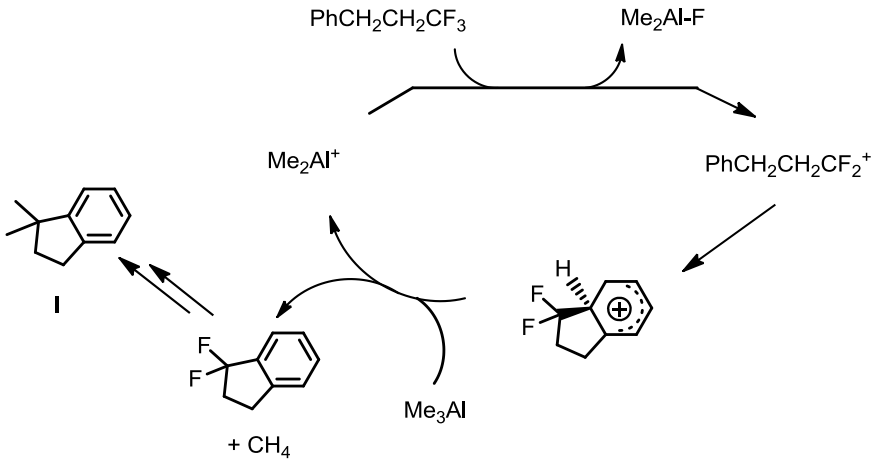

4.2.1.3 Competitive Reactions Between Et_3SiH and $AlMe_3$ Reagents

In order to test the reactivity difference between silylium and alumenium catalysis, we set up a competitive reaction with 1 equivalent of substrate **1**, 3 equivalents of Et_3SiH, 3 equivalents of $AlMe_3$ and 0.01 equivalent of catalyst **B** in hexanes (Entry 23). 4-fluoro-benzotrifluoride was completely consumed in 24 h and gave a mixture of three products (F-C_6H_4-CH_3, F-C_6H_4-CH_2Me, F-C_6H_4-$CHMe_2$) in a 28%, 57%, 14% ratio (Scheme 4-6). Thus, 71% of the C-F bonds were converted to C-H bonds and 29% of the C-F bonds were converted to C-C bonds. Mixing Et_3SiH and Me_3Al with or without catalyst **B** resulted in no change in the ^1H NMR spectrum after 24 h, indicating that there was no alkyl/hydride exchange between the Si and Al starting materials. However, only Al-F bonds (and no Si-F bonds) were observed upon the completion of the reaction, indicating that ligand exchange between Si and Al that involves fluoride can indeed occur. Because of this, although the hydrides transferred to C *ultimately* come from Si, we cannot ascertain whether all hydrides are transferred to C *directly* from Si. It is possible that hydrides are first transferred from Si to Al and only then to C. On the other hand, from the lack of *ethyl* transfer to C we can infer that alkyl transfer from Si to Al is negligible. Although the kinetic details remain obscured, this experiment shows that the hydride from Et_3SiH can be competitive with the Me from Me_3Al in replacing the F in C-F. The selectivity for a specific combination of hydride/alkyl transfer is low.

Scheme 4-6. Competitive reactions involving Me_3Al and Et_3SiH.

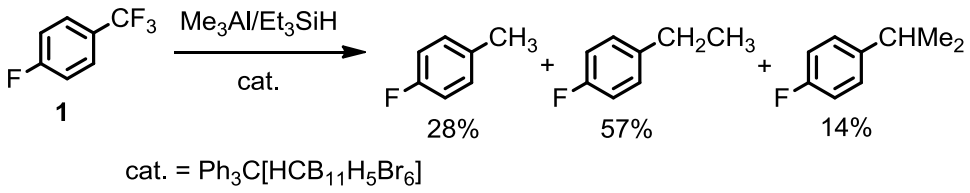

4.2.1.4 Efficiency of Utilization of the Trialkylaluminum Reagents

In our experiments, we typically used the same number of moles for the R_3Al reagent as the number of moles of C-F bonds to be consumed (1:1 Al:F ratio and 3:1 R:F ratio). If only one alkyl (or hydride) group from each R_3Al can be transferred to the carbon of the C-F substrate, this is an equimolar ratio. We set out to test how many R groups can indeed participate. We performed several experiments (Table 4-3) in which we used one equiv of R_3Al per molecule of **1**; in other words, one third of the usual amount so that the Al:F ratio is 1:3 and the R:F ratio is consequently 1:1. If only one R group from each R_3Al were to be transferred, 33% C-F conversion would be observed. The actual C-F conversions ranged from 37% to 47%, corresponding to 1.1 to 1.4 R groups from each R_3Al getting transferred (Scheme 4-7). Another corroborating datapoint (entry 5, Table 4-3) is the reaction with 3 equiv of $^{i}Bu_2AlF$ per molecule of **1**. In this case, the conversion was 42%, or, in other words, 0.14 of ^{i}Bu groups from each $^{i}Bu_2AlF$ was transferred. Since $^{i}Bu_2AlF$ is the product of a transfer of one ^{i}Bu group from $^{i}Bu_3Al$, the results are roughly equivalent.

Scheme 4-7. AlkDF reactions of **1** with deficiency of R_3Al in hexanes.

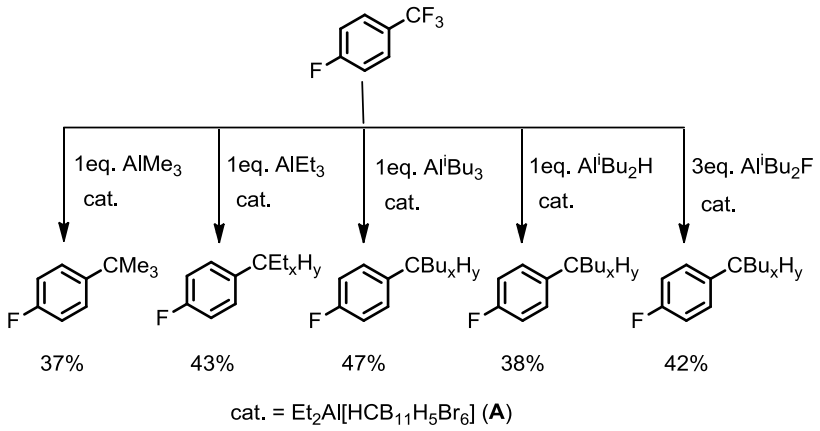

Table 4-3. AlkDF reactions of **1** with deficiency of R_3Al in hexanes.

No	Cat.%[a]	Al reagent	% C-F[b]
A1	0.33%	1 equivalent Me_3Al	37%
A2	0.33%	1 equivalent Et_3Al	43%
A3	0.33%	1 equivalent $^{i}Bu_3Al$	47%
A4	0.33%	1 equivalent $^{i}Bu_2AlH$	38%
A5	0.33%	3 equivalent $^{i}Bu_2AlF$	42%

[a] $Et_2Al[HCB_{11}H_5Br_6]$ (**A**) was used as catalyst, catalyst loading was calculated vs the number of C-F bonds; [b] Terminal conversion.

4.2.1.5 Trialkylaluminum Reagents Function as "Clean-up" Agent

Unlike trialkylsilanes, trialkylaluminums can serve as "clean-up" agents in the reaction mixture. In an illustrative experiment (Scheme 4-8), a mixture containing Et_3Al and **1** (4:1 Al:F ratio) was first treated with water (0.2 equivalent per F). Despite this, subsequent addition of catalyst **A** (0.01 equivalent per F, 1/20th the amount of water) initiated a 300-turnover reaction that proceeded with 100% conversion. In the presence of excess Et_3Al, water is converted to aluminoxanes, which are ostensibly not detrimental to the C-F activation. It was demonstrated before that organoaluminum reagents could be used as "clean-up" agents in olefin polymerization reactions.[70a,157]

Scheme 4-8. AlkDF reactions of **1** in the presence of water.

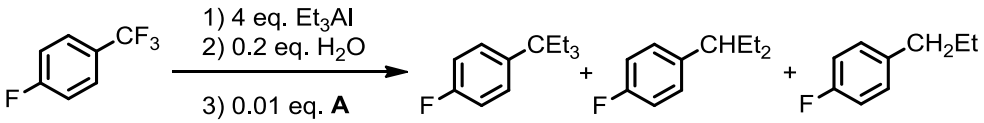

4.2.1.6 Reactions with MAO

Encouraged by the results that AlkDF reactions proceed successfully in the presence of aluminoxanes, we started to consider methylaluminoxane (MAO or $(MeAlO)_n$) as the reagent for AlkDF reactions. We found that commercial MAO (10% wt. in toluene) can effect C-F activation of **1**, even without any added alumenium catalyst (Table 4-4, Scheme 4-9). Multiple equivalents of Al per **1** are required for complete conversion, presumably because of the "Me-poor" nature of MAO compared to Me_3Al. MAO is an

ill-defined mixture of oligomers that possesses high Lewis acidity.[70a,157] It is often used in olefin polymerization catalysis as an activator that alkylates the metal halide precursor and abstracts an anionic ligand.[70a,157] The resultant highly electrophilic cationic olefin polymerization catalyst [158] is not unlike a silylium or alumenium cation in its requirements towards a compatible anion. Since the "[MAO+X]$^-$" anion is adequate to support electrophilic olefin polymerization catalysts, the reactivity observed with MAO here is thus not surprising.

Scheme 4-9. AlkDF reactions of **1** with MAO.

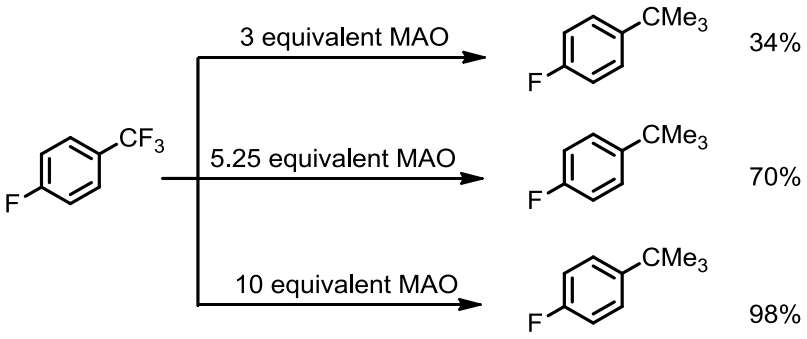

Table 4-4. AlkDF reactions of **1** with MAO without catalyst in toluene. ([a] Terminal conversion, reached after 3 h.)

No	Aluminum reagent	% C-F conversion[a]
B1	3 equivalent MAO	34%
B2	5.25 equivalent MAO	70%
B3	10 equivalent MAO	98%

4.2.1.7 Uncatalyzed Reactions with Et_3Al

Terao[154] et al. previously demonstrated that trialkylaluminum reagents can alkylate C-F bonds in primary alkyl fluorides without catalyst. We tested 1-fluorodecane (**7**) and **1** in uncatalyzed AlkDF reactions with Et_3Al (Table 4-5, Scheme 4-10). The reactions are much slower than with an alumenium catalyst and the reactions with **1** in hexanes at RT essentially do not proceed. Both substrates undergo defluorination faster in *o*-$C_6H_4Cl_2$. We also carried out an uncatalyzed reaction with substrate **6**. It is not only much slower, but also results in a qualitatively different outcome, producing 24% of 1-fluorocyclopentene as one of the products. The latter is an apparent product of formal HF loss[159] and is *not* observed in the defluorination of **6** with a catalyst. Notably, the C(sp^2)-F moiety in 1-fluorocyclopentene does not undergo further defluorination.

Scheme 4-10. AlkDF reactions with Et_3Al without a catalyst.

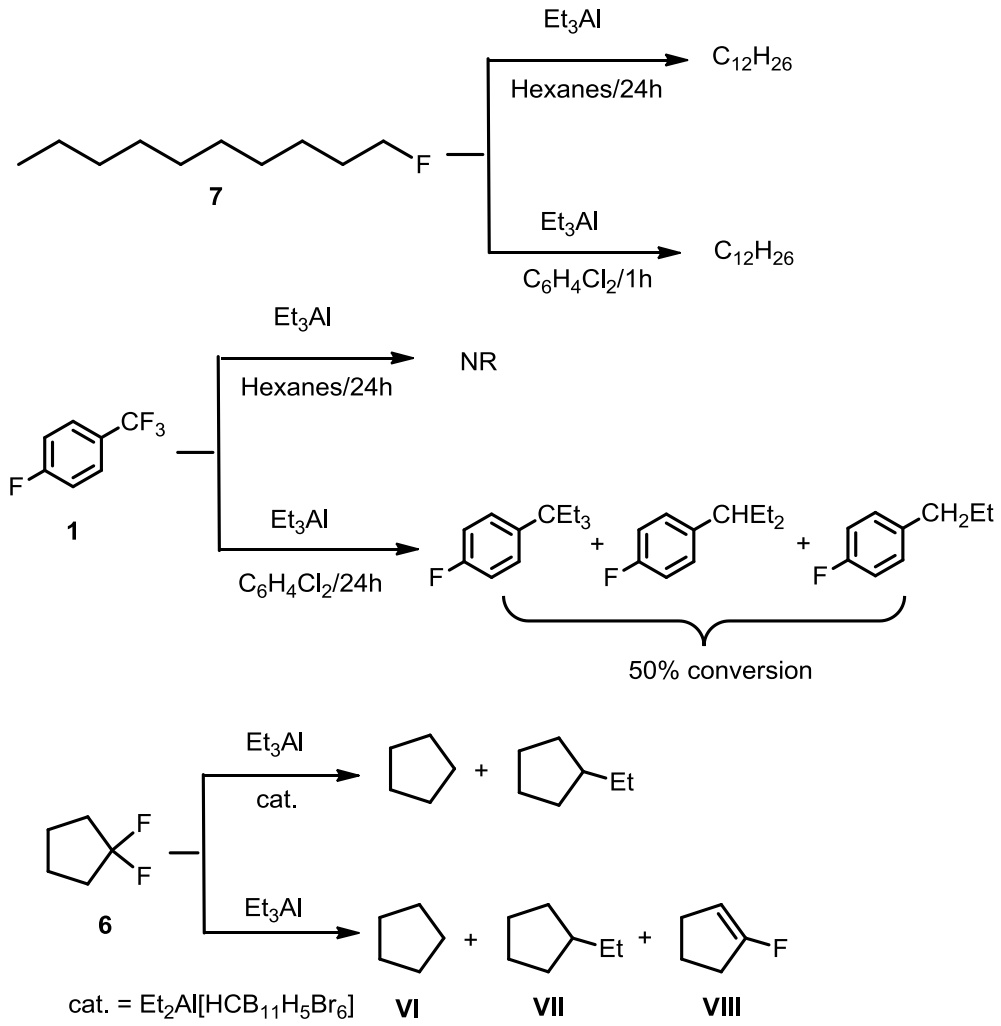

Table 4-5 AlkDF reactions with Et_3Al carried out without catalyst.

No	Substrate	Solvent	C-F conv.[a]	Al-F conv.[b]
C1	**7**	Hexanes	41% (100%)	35% (93%)
C2	**7**	$C_6H_4Cl_2$	100%	92%
C3	**1**	Hexanes	0% (1%)	0% (0%)
C4	**1**	$C_6H_4Cl_2$	2% (55%)	0% (44%)

[a] Conversion after 3 h (after 24 h in parentheses) based on the disappearance of substrate C-F by ^{19}F NMR; [b] Conversion after 3 h (after 24 h in parentheses) based on the appearance of Al-F by ^{19}F NMR.

4.2.2 Silylium Mediated Sp^3 C-F Bond Activation with $[B_{12}Cl_{12}]^{2-}$ as Counterion

Using literature cation exchange procedures,[102c,102d] we obtained $[Ph_3C]_2[B_{12}Cl_{12}]$. We have previously used trityl salts of $[B(C_6F_5)_4]^-$ and of halogenated carboranes as pre-catalysts for the hydrodefluorination (HDF) of aliphatic C-F bonds with Et_3SiH. The proposed HDF mechanism and the reactions under study in this work are outlined in Scheme 4-11 and Table 4-6. The trityl salts are convenient to store and are readily converted to triethylsilylium by reaction with excess triethylsilane in the reaction mixture.

Table 4-6. HDF results (Ar-CF_3 → Ar-CH_3).

No	Substrate	T (˚C)	Time (h)	Cat mol %[a]	Si-F Conv. %[b]	C-F Conv. %[b]	TON[c]
D1	1	22	0.5	0.049	87	>97	2040
D2	4	22	24	0.053	1	6	110
D3	4	50	24	0.052	82	96	1850
D4	4	80	1	0.052	90	>97	1920

[a] $[Ph_3C]_2[B_{12}Cl_{12}]$ was used as the catalyst in these reactions. Catalyst loading was calculated based on the moles of $[B_{12}Cl_{12}]^{2-}$ vs the moles of C-F bonds; [b] Conversion based on disappearance of C-F bonds or appearance of Si-F bonds by ^{19}F NMR; [c] Turnover number was calculated based on conversion of C-F bonds.

Scheme 4-11. The proposed mechanism of HDF and the reactions with benzotrifluorides under study in this work.

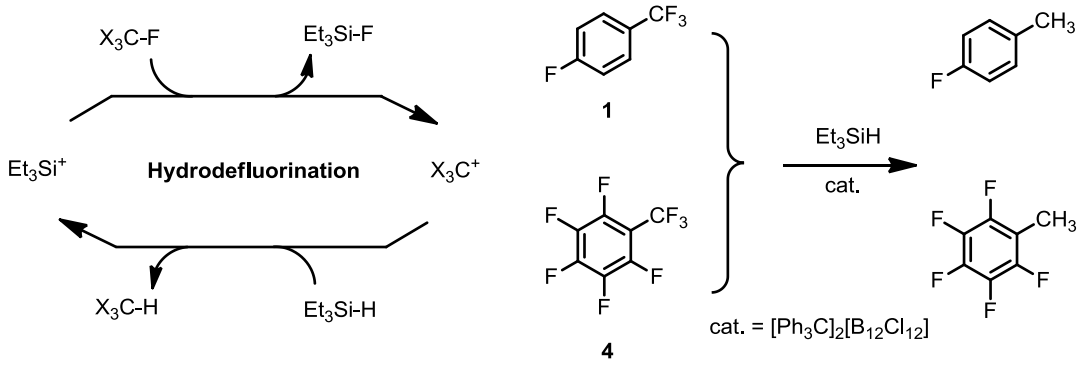

In all reactions, *o*-dichlorobenzene was used as solvent. Et_3SiF and Et_2SiF_2 were observed as the Si-F products. Along with the Ar-CH_3 HDF products, Friedel-Crafts products were also observed by ^{19}F NMR, as with other catalysts.[71d] The HDF reactions of *p*-$FC_6H_4CF_3$ worked well using $[Ph_3C]_2[B_{12}Cl_{12}]$ as (pre-)catalyst at 22 °C, with full consumption of the sp^3 C-F bonds, no conversion of the sp^2 C-F bond and TON[160] of ca. 2000. To further evaluate the competence of $[B_{12}Cl_{12}]^{2-}$, we performed HDF reactions

with the more challenging substrate $C_6F_5CF_3$ (D4, Table 4-6). At 22 °C, the reaction is fairly slow with consumption of only 6% of the C-F bonds in 24 h. However, the HDF reaction accelerated dramatically at elevated temperature. Complete or near-complete consumption of all sp^3 C-F bonds with TON of ca. 2000 was achieved within 24 h at 50 °C and within 1 h at 80 °C. The poor reactivity at room temperature may largely reflect the much lower solubility of $[Ph_3C]_2[B_{12}Cl_{12}]$ compared with carborane analogs. Nonetheless, these results illustrate that $[B_{12}Cl_{12}]^{2-}$ can be used as a WCA in HDF catalysis which sustains thousands of turnovers, similar to the results we reported with halogenated carboranes as supporting anions.[71d]

4.3 Conclusion

In summary, we have established that alumenium cation equivalent $Et_2Al[HCB_{11}H_5Br_6]$ functions as an efficient and long-lived catalyst for Lewis acid $C(sp^3)$-F bond activation with trialkylaluminums as stoichiometric reagents. The catalytic reactions showed superb longevity and turnover numbers of up to 10000 have been achieved. Conversion of C-F bonds only to C-Me bonds was accomplished when Me_3Al was used as the stoichiometric reagent. On the other hand, utilization of Et_3Al, $^iBu_3Al$ or $^iBu_2AlH$ results in the competitive replacement of C-F bonds either with C-Alkyl or C-H bonds. Moreover we demonstrate that alumenium mediated C-F bond activation process is tolerant of small quantities of water because trialkylaluminum compounds can act as "clean-up" agents in situ. It is also shown that $[B_{12}Cl_{12}]^{2-}$ can be used as a weakly coordinating anion for the C-F bond activation mediated by

electrophlic silylium species. The $[B_{12}Cl_{12}]^{2-}$ based catalysis showed longevity comparable to carborane-based catalysis in the HDF reactions.

4.4 Experimental Details

General considerations. Unless specified otherwise, all reactions were carried out under an argon atmosphere using glovebox or Schlenk line techniques. C_6F_6, C_6F_5Br, all the fluorinated substrates, and all the haloarene solvents were purchased from Oakwood products Inc. or Synquest lab Inc., dried with CaH_2 and distilled under Ar or vacuum transferred and stored over molecular sieves in an Ar-filled glovebox. All other chemicals were purchased from either Aldrich, Alfa Aesar or Acros and used as received unless otherwise noted. $Ph_3C[HCB_{11}Cl_{11}]$[98] and $[Ph_3C]_2[B_{12}Cl_{12}]$[102c] were synthesized from $Cs[HCB_{11}Cl_{11}]$ and $Cs_2[B_{12}Cl_{12}]$, respectively using literature cation exchange procedures. $Et_2Al[HCB_{11}Cl_{11}]$[100] was prepared using literature procedures.

NMR spectra were recorded on a Varian iNova 300 spectrometer (^{1}H NMR, 299.9 MHz, ^{19}F NMR, 282.2 MHz) or a Varian iNova 400 spectrometer (^{1}H NMR, 400.0 MHz, ^{11}B NMR, 128.5 MHz, ^{19}F NMR, 376.3 MHz) in noted solvents. Chemical shifts are given in δ (ppm). ^{11}B NMR spectra were referenced externally with BF_3 etherate at δ 0. ^{19}F NMR spectra were referenced externally with neat CF_3COOH at δ -78.5. Et_3SiF and Et_2SiF_2 were identified by ^{19}F NMR (in *o*-dichlorobenzene) at δ –176.2 and –144.5, respectively. ^{1}H NMR spectra were referenced using the solvent signals.

Caution: *In certain cases, C-F activation reactions may proceed very rapidly, self-accelerating and releasing dangerous amounts of heat. In addition, these reactions may generate hydrogen and possibly even other gases. Great care and preliminary testing of safety conditions are necessary for performing reactions in closed vessels.*

Determination of the Al-F products. The reactions described herein produce Al by-products. These are primarily of the stoichiometry R_2AlF. It is likely that the mixture contains a mixture of various dimers and possibly oligomers $R_{3-x}AlF_x$. These mixtures give rise to one or more broad resonances in the ^{19}F NMR spectra in the –145…-160 ppm range. The spectra obtained in our reactions bear close resemblance to the ^{19}F NMR spectrum of commercial $^{i}Bu_2AlF$ (Aldrich).

Calibration of ^{19}F NMR. The disappearance of the C-F bonds and the appearance of Al-F bonds were measured vs. the C_6F_6 internal standard. In each experiment, the initial (0% conversion or 100% starting material) intensity of the signal of the starting material vs the intensity of the C_6F_6 signal was recorded *before* the addition of the catalyst. As with any NMR integration-based method, errors on the order of 5-10% should be assumed. The relationship between the intensity of the C-F bonds in substrates and in C_6F_6 appears to be essentially the same within errors of measurement. In order to quantify the relationship between the integration values and concentrations involving Al-F bonds, we performed a calibration using commercial $^{i}Bu_2AlF$ and C_6F_6. It demonstrated that the ^{19}F NMR intensity of 1 mole of C_6F_6 is equal to the ^{19}F NMR intensity of 4.2 mol of Al-F bonds under the parameters of our ^{19}F NMR experiments (acq. time = 1.4 s, delay between scans = 2.0 s) (See table 4-7 & Scheme 4-12).

Table 4-7. ^{19}F NMR calibration: $^{i}Bu_2AlF$ (1 M in hexanes) vs C_6F_6.

Volume $^{i}Bu_2AlF$ (mL)	Moles $^{i}Bu_2AlF$ (mmol)	Volume C_6F_6 (µL)	Moles C_6F_6 (mmol)	Integral ratio $^{i}Bu_2AlF$ / C_6F_6	Molar ratio $^{i}Bu_2AlF$ / C_6F_6
0.40	0.40	5.0	0.043	2.1	9.2
0.60	0.60	5.0	0.043	3.4	13.9
0.80	0.80	5.0	0.043	4.4	18.5
1.00	1.00	5.0	0.043	5.4	23.1

Scheme 4-12. ^{19}F NMR calibration: $^{i}Bu_2AlF$ (A) vs C_6F_6 (B).

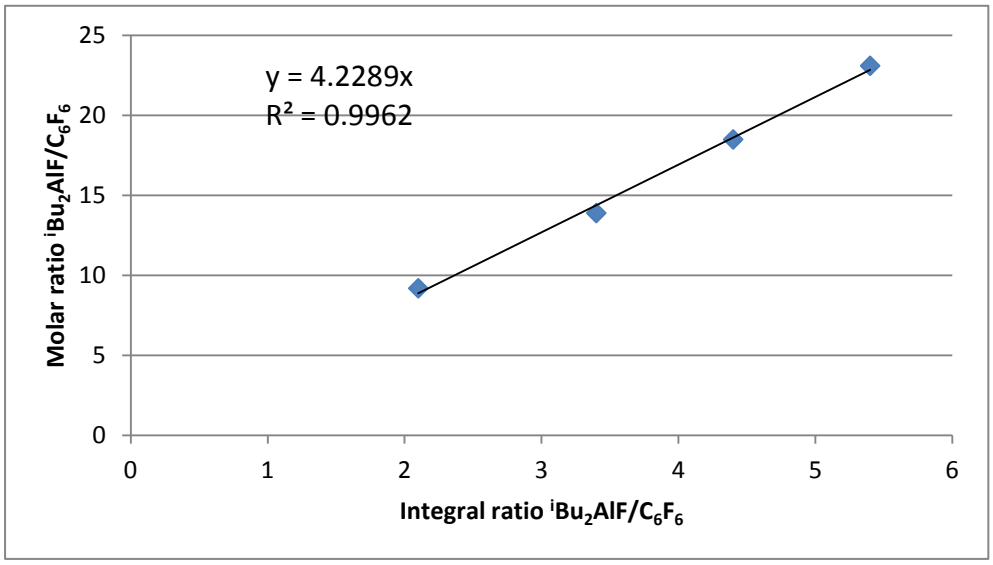

Calibration of GC/MS. C_6H_5Br was used as internal standard for GC experiment to measure the yield of products for the HDF reactions. Here five solutions containing $C_6H_5CMe_3$ and C_6H_5Br in different ratios were prepared and analyzed by GC/MS. Integration of the corresponding peaks in the resulting chromatogram gave the coefficient as 1.029 (Integral (A/B) versus Moles (A/B), see Table 4-8 and Scheme 4-13).

Table 4-8. Calibration of GC/MS ($C_6H_5CMe_3$ vs C_6H_5Br).

Vol. $C_6H_5CMe_3$ (μL)	Moles $C_6H_5CMe_3$ (μmol)	Vol. C_6H_5Br (μL)	Moles C_6H_5Br (μmol)	Integral ratio $C_6H_5CMe_3$ / C_6H_5Br	Molar ratio $C_6H_5CMe_3$ / C_6H_5Br
0.50	3.23	1.00	9.53	0.353	0.339
1.00	6.46	1.00	9.53	0.680	0.678
1.50	9.69	1.00	9.53	0.986	1.02
2.00	12.9	1.00	9.53	1.31	1.36
2.50	16.2	1.00	9.53	1.64	1.69

Scheme 4-13. Calibration of GC/MS ($C_6H_5CMe_3$ (A) vs C_6H_5Br (B)).

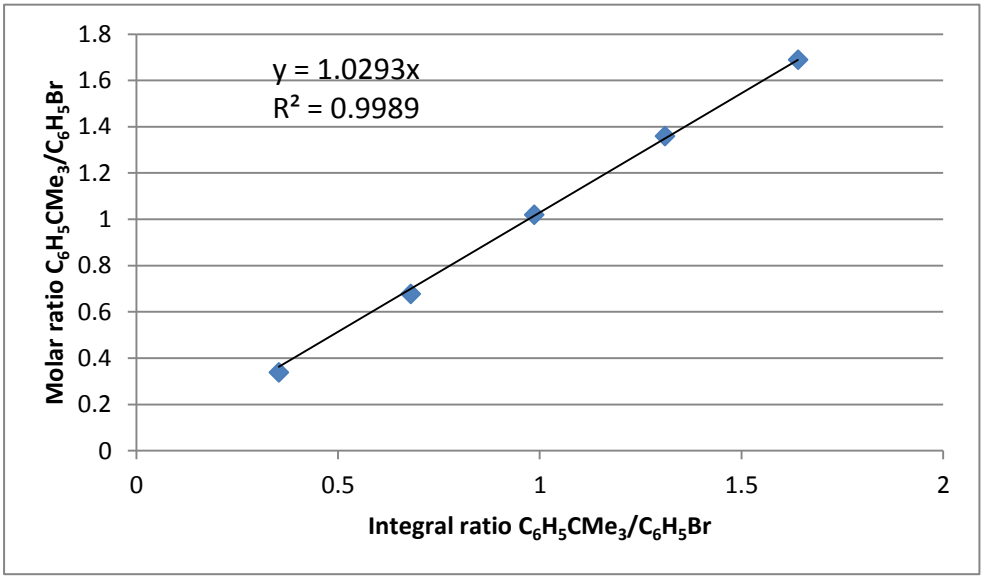

Entry 1: 40 µL (315 µmol) Substrate **1** was mixed with 475 µL (950 µmol) trimethylaluminum (2 M in hexanes), 5.0 µL (43 µmol) C_6F_6, 2.2 mg (3.2 µmol) $Et_2Al[HCB_{11}H_5Br_6]$ in a J. Young tube. A colorless solution was formed with a small amount of precipitate. The mixtures were allowed to stay at room temperature for 24 h. The reactions were monitored by detecting the increase in the intensity of ^{19}F NMR resonance of Al-F and decrease in the intensity of ^{19}F NMR resonance of F-substrates (δ -65.3 (p-FC_6H_4-CF_3), -110.1 (p-FC_6H_4-CF_3)). Yield (based on ^{19}F NMR, after 24 h): *p*-$FC_6H_4CMe_3$ 94%. ^{19}F NMR (376.3 MHz, hexanes): δ -120.7 (*F*-C_6H_4-CMe_3), -165.2 (C_6F_6). GC/MS: (F-C_6H_4-CMe_3; M/Z^+ 152).

Entry 2: 40 µL (315 µmol) Substrate **1** was mixed with 130 µL (950 µmol) triethylaluminum, 5.0 µL (43 µmol) C_6F_6, 2.2 mg (3.2 µmol) $Et_2Al[HCB_{11}H_5Br_6]$ in a J. Young tube. A colorless solution was formed with a small amount of precipitate. The mixtures were allowed to stay at room temperature for 24 h. The reactions were

monitored by detecting the increase in the intensity of ^{19}F NMR resonance of Al-F and decrease in the intensity of ^{19}F NMR resonance of F-substrates (δ -65.3 (p-FC_6H_4-CF_3), -110.1 (p-FC_6H_4-CF_3)). Yield (based on ^{19}F NMR, after 24 h): F-C_6H_4-$CH_2CH_2CH_3$ 18%, F-C_6H_4-$CHEt_2$ 61%, F-C_6H_4-CEt_3 15%. ^{19}F NMR (376.3 MHz, hexanes): δ -119.8 (*F*-C_6H_4-$CHEt_2$), -120.2 (*F*-C_6H_4-CEt_3), -120.8 (*F*-C_6H_4-$CH_2CH_2CH_3$), -165.2 (C_6F_6). GC/MS: (F-C_6H_4-$CH_2CH_2CH_3$; M/Z^+ 138), (F-C_6H_4-$CHEt_2$; M/Z^+ 166), (F-C_6H_4-CEt_3; M/Z^+ 194).

Identification and quantification of products in the reaction of Et_3Al and *p*-$FC_6H_4CF_3$ (1) by ^1H NMR (analogous to entry 2). 40 μL (315 μmol) Substrate **1** was mixed with 130 μL (950 μmol) Et_3Al, 5.0 μL (43 μmol) C_6F_6, 2.2 mg (3.2 μmol) $Et_2Al[HCB_{11}H_5Br_6]$ in 0.5 mL of C_6D_{12} in a J. Young tube. A colorless solution was formed. A small amount of precipitate was observed. The mixture was allowed to stay at room temperature for 24 h. The reaction was monitored by detecting the increase in the intensity of ^{19}F NMR resonance of Al-F and decrease in the intensity of ^{19}F NMR resonance of F-substrates (δ -65.3 (*p*-FC_6H_4-CF_3), -110.1 (*p*-*F*C_6H_4-CF_3)). After hydrolyzing the organoaluminum compounds, the mixture was dissolved in $CDCl_3$ for further analysis. Yield (based on ^{19}F NMR, after 24 h): F-C_6H_4-$CH_2CH_2CH_3$ 18%, F-C_6H_4-$CHEt_2$ 62% and F-C_6H_4-CEt_3 13%. GC/MS: (F-C_6H_4-$CH_2CH_2CH_3$; M/Z^+ 138), (F-C_6H_4-$CHEt_2$; M/Z^+ 166), (F-C_6H_4-CEt_3; M/Z^+ 194). ^{19}F NMR (376.3 MHz, $CDCl_3$): δ -119.8 (*F*-C_6H_4-$CHEt_2$), -120.2 (*F*-C_6H_4-CEt_3), -120.8 (*F*-C_6H_4-$CH_2CH_2CH_3$), -165.2 (C_6F_6). ^1H NMR (400.0 MHz, $CDCl_3$): 0.66 (t, $^3J_{H-H}$=7.2 Hz, F-C_6H_4-$C(CH_2CH_3)_3$), 0.77 (t, $^3J_{H-H}$=7.2 Hz, F-C_6H_4-$CH(CH_2CH_3)_2$), 0.94 (t, $^3J_{H-H}$=7.2 Hz, F-C_6H_4-

$CH_2CH_2CH_3$), 1.47-1.75 (m, F-C_6H_4-$C(CH_2CH_3)_3$, F-C_6H_4-$CH(CH_2CH_3)_2$, F-C_6H_4-$CH_2CH_2CH_3$), 2.30 (m, F-C_6H_4-$CH(CH_2CH_3)_2$), 2.57 (t, $^3J_{H-H}$=7.6 Hz, F-C_6H_4-$CH_2CH_2CH_3$), 6.93-7.13 (m, F-C_6H_4-$C(CH_2CH_3)_3$, F-C_6H_4-$CH(CH_2CH_3)_2$, F-C_6H_4-$CH_2CH_2CH_3$).

Entry 3: 40 μL (315 μmol) Substrate **1** was mixed with 950 μL (950 μmol) of $^iBu_3Al$ (1M in hexanes), 5.0 μL (43 μmol) C_6F_6, 2.2 mg (3.2 μmol) $Et_2Al[HCB_{11}H_5Br_6]$ in a J. Young tube. A colorless solution was formed with a small amount of precipitate. The mixtures were allowed to stay at room temperature for 24 h. The reactions were monitored by detecting the increase in the intensity of ^{19}F NMR resonance of Al-F and decrease in the intensity of ^{19}F NMR resonance of F-substrates (δ -65.3 (p-FC_6H_4-CF_3), -110.1 (p-FC_6H_4-CF_3)). The ratio of products in GC/MS is F-C_6H_4-CHC_8H_{18} 55% and F-C_6H_4-$CC_{12}H_{27}$ 45%. ^{19}F NMR (376.3 MHz, hexanes): δ -119.7, -119.8, -120.1, -120.3 (*F*-C_6H_4-R), -165.2 (C_6F_6). GC/MS: (F-C_6H_4-CHC_8H_{18}; M/Z^+ 222), (F-C_6H_4-$CC_{12}H_{27}$; M/Z^+ 278).

Entry 4: 40 μL (315 μmol) Substrate **1** was mixed with 820 μL (950 μmol) of $^iBu_2AlH$ (1.16M in hexanes), 5.0 μL (43 μmol) C_6F_6, 2.2 mg (3.2 μmol) $Et_2Al[HCB_{11}H_5Br_6]$ in a J. Young tube. A colorless solution was formed with a small amount of precipitate. The mixtures were allowed to stay at room temperature for 24 h. The reactions were monitored by detecting the increase in the intensity of ^{19}F NMR resonance of Al-F and decrease in the intensity of ^{19}F NMR resonance of F-substrates (δ -65.3 (p-FC_6H_4-CF_3), -110.1 (p-FC_6H_4-CF_3)). Yield (based on ^{19}F NMR, after 24 h): F-C_6H_4-CH_3 58%, F-C_6H_4-$CH_2C_4H_9$ 32%. ^{19}F NMR (376.3 MHz, hexanes): δ -120.3 (*F*-C_6H_4-$CH_2C_4H_9$), -

120.6 (*F*-C_6H_4-CH_3), -165.2 (C_6F_6). GC/MS: (F-C_6H_4-CH_3; M/Z^+ 110), (F-C_6H_4-$CH_2C_4H_9$; M/Z^+ 166).

Entry 5: 120 μL (945 μmol) *p*-$C_6H_4CF_3$ was mixed with 390 μL (2852 μmol) of triethylaluminum, 15.0 μL (129 μmol) C_6F_6, 21 μL of a $Et_2Al[HCB_{11}H_5Br_6]$ stock solution which was made by dissolving 10 mg of $Et_2Al[HCB_{11}H_5Br_6]$ in 1 mL of *o*-dichlorobenzene (0.21 mg, 0.29 μmol) in 1.5 mL hexanes in a 10 mL glass vial. A clear solution was formed. The mixture was stirred at room temperature for 24 h. The reaction was monitored by detecting the increase in the intensity of ^{19}F NMR resonance of Al-F and decrease in the intensity of ^{19}F NMR resonance of F-substrates (δ -65.3 (*p*F-C_6H_4-C*F*$_3$), -110.1 (*pF*-C_6H_4-CF_3)). Yield (based on ^{19}F NMR, after 24 h): F-C_6H_4-$CH_2CH_2CH_3$ 19%, F-C_6H_4-$CHEt_2$ 66%, F-C_6H_4-CEt_3 13%. ^{19}F NMR (376.3 MHz, hexanes): δ -119.8 (*F*-C_6H_4-$CHEt_2$), -120.2 (*F*-C_6H_4-CEt_3), -120.8 (*F*-C_6H_4-$CH_2CH_2CH_3$), -165.2 (C_6F_6). GC/MS: (F-C_6H_4-$CH_2CH_2CH_3$; M/Z^+ 138), (F-C_6H_4-$CHEt_2$; M/Z^+ 166), (F-C_6H_4-CEt_3; M/Z^+ 194).

Entry 6: 40 μL (315 μmol) Substrate **1** was with 130 μL (950 μmol) triethylaluminum, 5.0 μL (43 μmol) C_6F_6, 5.0 μL (43 μmol) C_6F_6, 2.2 mg (3.2 μmol) $Et_2Al[HCB_{11}H_5Br_6]$ in a J. Young tube. A colorless solution was formed. Dramatic elevation of temperature was observed at the beginning of the reaction. The mixtures were allowed to stay at room temperature for 24 h. The reactions were monitored by detecting the increase in the intensity of ^{19}F NMR resonance of Al-F and decrease in the intensity of ^{19}F NMR resonance of F-substrates (δ -65.3 (p-FC_6H_4-C*F*$_3$), -110.1 (p-*F*C_6H_4-CF_3)). Yield (based on ^{19}F NMR, after 24h): *F*-C_6H_4-CH_2-$C_6H_3Cl_2$ 10%, *F*-C_6H_4-$CH_2CH_2CH_3$ 8%, *F*-C_6H_4-

$CHEt_2$ 46%, *F*-C_6H_4-CEt_3 30%. ^{19}F NMR (376.3 MHz, *o*-$C_6H_4Cl_2$): δ -119.6 (might be *F*-C_6H_4-CH_2-$C_6H_3Cl_2$), -119.8 (*F*-C_6H_4-$CHEt_2$), -120.2 (*F*-C_6H_4-CEt_3), -120.8 (*F*-C_6H_4-$CH_2CH_2CH_3$), -165.2 (C_6F_6). GC/MS: (F-C_6H_4-$CH_2CH_2CH_3$; M/Z^+ 138), (F-C_6H_4-$CHEt_2$; M/Z^+ 166), (F-C_6H_4-CEt_3; M/Z^+ 194).

Entry 7: 40 μL (315 μmol) Substrate **1** was mixed with 130 μL (950 μmol) triethylaluminum, 5.0 μL (43 μmol) C_6F_6, 2.7 mg (3.2 μmol) of $Ph_3C[HCB_{11}H_5Br_6]$ in a J. Young tube. A colorless solution was formed with a small amount of precipitate. The mixtures were allowed to stay at room temperature for 24 h. The reactions were monitored by detecting the increase in the intensity of ^{19}F NMR resonance of Al-F and decrease in the intensity of ^{19}F NMR resonance of F-substrates (δ -65.3 (p-FC_6H_4-CF_3), -110.1 (p-*F*C_6H_4-CF_3)). Yield (based on ^{19}F NMR, after 24 h): F-C_6H_4-$CH_2CH_2CH_3$ 15%, F-C_6H_4-$CHEt_2$ 52%, F-C_6H_4-CEt_3 11%. ^{19}F NMR (376.3 MHz, hexanes): δ -65.3 (p-FC_6H_4-CF_3), -110.1 (p-*F*C_6H_4-CF_3), -119.8 (*F*-C_6H_4-$CHEt_2$), -120.2 (*F*-C_6H_4-CEt_3), -120.8 (*F*-C_6H_4-$CH_2CH_2CH_3$), -165.2 (C_6F_6). GC/MS: (F-C_6H_4-CF_3; M/Z^+ 164), (F-C_6H_4-$CH_2CH_2CH_3$; M/Z^+ 138), (F-C_6H_4-$CHEt_2$; M/Z^+ 166), (F-C_6H_4-CEt_3; M/Z^+ 194).

Entry 8: 40 μL (315 μmol) Substrate **1** was mixed with 130 μL (950 μmol) triethylaluminum, 5.0 μL (43 μmol) C_6F_6, 2.9 mg (3.2 μmol) of $Ph_3C[B(C_6F_5)_4]$ in a J. Young tube. A colorless solution was formed. The mixtures were allowed to stay at room temperature for 24 h. The reactions were monitored by detecting the increase in the intensity of ^{19}F NMR resonance of Al-F and decrease in the intensity of ^{19}F NMR resonance of F-substrates (δ -65.3 (p-FC_6H_4-CF_3), -110.1 (p-*F*C_6H_4-CF_3)). Yield (based on ^{19}F NMR, after 24 h): F-C_6H_4-$CH_2CH_2CH_3$ 8%, F-C_6H_4-$CHEt_2$ 28%, F-C_6H_4-CEt_3

6%. ^{19}F NMR (376.3 MHz, hexanes): δ -65.3 (p-FC$_6$H$_4$-C*F*$_3$), -110.1 (p-*F*C$_6$H$_4$-CF$_3$), -119.8 (*F*-C$_6$H$_4$-CHEt$_2$), -120.2 (*F*-C$_6$H$_4$-CEt$_3$), -120.8 (*F*-C$_6$H$_4$-CH$_2$CH$_2$CH$_3$), -165.2 (C$_6$*F*$_6$). GC/MS: (F-C$_6$H$_4$-CF$_3$; M/Z$^+$ 164), (F-C$_6$H$_4$-CH$_2$CH$_2$CH$_3$; M/Z$^+$ 138), (F-C$_6$H$_4$-CHEt$_2$; M/Z$^+$ 166), (F-C$_6$H$_4$-CEt$_3$; M/Z$^+$ 194).

Entry 9: 40 μL (315 μmol) Substrate **1** was with 130 μL (950 μmol) triethylaluminum, 5.0 μL (43 μmol) C$_6$F$_6$, 5.0 μL (43 μmol) C$_6$F$_6$, 2.7 mg (3.2 μmol) of Ph$_3$C[HCB$_{11}$H$_5$Br$_6$] in a J. Young tube. A colorless solution was formed. Dramatic elevation of temperature was observed at the beginning of the reaction. The mixtures were allowed to stay at room temperature for 24 h. The reactions were monitored by detecting the increase in the intensity of ^{19}F NMR resonance of Al-F and decrease in the intensity of ^{19}F NMR resonance of F-substrates (δ -65.3 (p-FC$_6$H$_4$-C*F*$_3$), -110.1 (p-*F*C$_6$H$_4$-CF$_3$)). Yield (based on ^{19}F NMR, after 24h): *F*-C$_6$H$_4$-CH$_2$CH$_2$CH$_3$ 8%, *F*-C$_6$H$_4$-CHEt$_2$ 51%, *F*-C$_6$H$_4$-CEt$_3$ 32%. ^{19}F NMR (376.3 MHz, *o*-C$_6$H$_4$Cl$_2$): δ -119.8 (*F*-C$_6$H$_4$-CHEt$_2$), -120.2 (*F*-C$_6$H$_4$-CEt$_3$), -120.8 (*F*-C$_6$H$_4$-CH$_2$CH$_2$CH$_3$), -165.2 (C$_6$*F*$_6$). GC/MS: (F-C$_6$H$_4$-CH$_2$CH$_2$CH$_3$; M/Z$^+$ 138), (F-C$_6$H$_4$-CHEt$_2$; M/Z$^+$ 166), (F-C$_6$H$_4$-CEt$_3$; M/Z$^+$ 194).

Entry 10: 40 μL (315 μmol) Substrate **1** was with 130 μL (950 μmol) triethylaluminum, 5.0 μL (43 μmol) C$_6$F$_6$, 5.0 μL (43 μmol) C$_6$F$_6$, 2.9 mg (3.2 μmol) of Ph$_3$C[B(C$_6$F$_5$)$_4$] in a J. Young tube. A colorless solution was formed. The mixtures were allowed to stay at room temperature for 24 h. The reactions were monitored by detecting the increase in the intensity of ^{19}F NMR resonance of Al-F and decrease in the intensity of ^{19}F NMR resonance of F-substrates (δ -65.3 (p-FC$_6$H$_4$-C*F*$_3$), -110.1 (p-*F*C$_6$H$_4$-CF$_3$)). Yield (based on ^{19}F NMR, after 24h): *F*-C$_6$H$_4$-CH$_2$CH$_2$CH$_3$ 8%, *F*-C$_6$H$_4$-CHEt$_2$ 48%, *F*-C$_6$H$_4$-CEt$_3$

29%. ^{19}F NMR (376.3 MHz, *o*-$C_6H_4Cl_2$): δ -119.8 (*F*-C_6H_4-$CHEt_2$), -120.2 (*F*-C_6H_4-CEt_3), -120.8 (*F*-C_6H_4-$CH_2CH_2CH_3$), -165.2 (C_6F_6). GC/MS: (F-C_6H_4-$CH_2CH_2CH_3$; M/Z^+ 138), (F-C_6H_4-$CHEt_2$; M/Z^+ 166), (F-C_6H_4-CEt_3; M/Z^+ 194).

Entry 11: 40 μL Substrate (326 μmol) was mixed with 135 μL (987 μmol) triethylaluminum, 5.0 μL (43 μmol) C_6F_6 and 2.3mg (3.3 μmol) $Et_2Al[HCB_{11}H_5Br_6]$ in 0.5 mL hexanes in a J. Young tube. A colorless solution with a small amount of precipitate was formed. Elevation of temperature was observed. The mixtures were allowed to stay at room temperature for 24 h. The reactions were monitored by detecting the increase in the intensity of ^{19}F NMR resonance of Al-F and decrease in the intensity of ^{19}F NMR resonance of F-substrates (δ -66.1 (C_6H_5-C*F*$_3$)). The ratio of products in GC/MS is C_6H_5-$CH_2CH_2CH_3$ 16%, C_6H_5-$CHEt_2$ 66% and C_6H_5-CEt_3 18%. ^{19}F NMR (376.3 MHz, hexanes): δ -165.2 (C_6F_6). GC/MS: (C_6H_5-$CH_2CH_2CH_3$; M/Z^+ 120), (C_6H_5-$CHEt_2$; M/Z^+ 148), (C_6H_5-CEt3; M/Z^+ 176).

Entry 12: 40 μL Substrate (300 μmol) was mixed with 125 μL (914 μmol) of triethylaluminum, 5.0 μL (43 μmol) C_6F_6 and 2.1 mg (3.0 μmol) $Et_2Al[HCB_{11}H_5Br_6]$ in 0.5 mL hexanes in a J. Young tube. A colorless solution with a small amount of precipitate was formed. The mixtures were allowed to stay at room temperature for 24 h. The reactions were monitored by detecting the increase in the intensity of ^{19}F NMR resonance of Al-F and decrease in the intensity of ^{19}F NMR resonance of F-substrates (δ -66.0 (Cl-C_6H_4-C*F*$_3$). The ratio of products in GC/MS is Cl-C_6H_4-$CH_2CH_2CH_3$ 7%, Cl-C_6H_4-$CHEt_2$ 71 % and Cl-C_6H_4-CEt_3 21%. ^{19}F NMR (376.3 MHz, hexanes): δ -165.2

(C_6F_6). GC/MS: (Cl-C_6H_4-$CH_2CH_2CH_3$; M/Z^+ 154, 156), (Cl-C_6H_4-$CHEt_2$; M/Z^+ 182, 184), (Cl-C_6H_4-CEt_3; M/Z^+ 210, 212).

Entry 13: 40 μL of (315 μmol) substrate **1** was mixed with 130 μL (950 μmol) of triethylaluminum, 5.0 μL (43 μmol) C_6F_6, 66 μL of $Et_2Al[HCB_{11}H_5Br_6]$ solution (predissolved in *o*-dichlorobenzene 1 mg/30 μL, 3.2 μmol) in a J. Young tube. A colorless solution was formed. Dramatic elevation of temperature was observed. The mixtures were allowed to stay at room temperature for 24 h. The reactions were monitored by detecting the increase in the intensity of ^{19}F NMR resonance of Al-F and decrease in the intensity of ^{19}F NMR resonance of F-substrates (δ -65.3 (*p*F-C_6H_4-C*F*$_3$), -110.1 (*pF*-C_6H_4-CF_3). Yield (based on ^{19}F NMR, after 24 h): F-C_6H_4-$CH_2CH_2CH_3$ 13%, F-C_6H_4-$CHEt_2$ 77% and F-C_6H_4-CEt_3 7%. ^{19}F NMR (376.3 MHz, hexanes): δ -119.8 (*F*-C_6H_4-$CHEt_2$), -120.2 (*F*-C_6H_4-CEt_3), -120.8 (*F*-C_6H_4-$CH_2CH_2CH_3$), -165.2 (C_6F_6). GC/MS: (F-C_6H_4-$CH_2CH_2CH_3$; M/Z^+ 138), (F-C_6H_4-$CHEt_2$; M/Z^+ 166), (F-C_6H_4-CEt_3; M/Z^+ 194).

Entry 14: 40 μL of (326 μmol) substrate **2** was mixed with 135 μL (987 μmol) of triethylaluminum, 5.0 μL (43 μmol) C_6F_6, 70 μL of $Et_2Al[HCB_{11}H_5Br_6]$ solution (predissolved in *o*-dichlorobenzene 1 mg/30 μL, 3.3 μmol) in a J. Young tube. A colorless solution was formed. Dramatic elevation of temperature was observed. The mixtures were allowed to stay at room temperature for 24 h. The reactions were monitored by detecting the increase in the intensity of ^{19}F NMR resonance of Al-F and decrease in the intensity of ^{19}F NMR resonance of F-substrates (δ -66.1 (C_6H_5-C*F*$_3$)). The ratio of products in GC/MS is C_6H_5-$CH_2CH_2CH_3$ 14%, C_6H_5-$CHEt_2$ 71% and C_6H_5-

CEt_3 15%. ^{19}F NMR (376.3 MHz, hexanes): δ -165.2 (C_6F_6). GC/MS: (C_6H_5-$CH_2CH_2CH_3$; M/Z^+ 120), (C_6H_5-$CHEt_2$; M/Z^+ 148), (C_6H_5-CEt_3; M/Z^+ 176).

Entry 15: 40 μL of (300 μmol) substrate **3** was mixed with 125 μL (914 μmol) of triethylaluminum, 5.0 μL (43 μmol) C_6F_6, 62 μL of $Et_2Al[HCB_{11}H_5Br_6]$ solution (predissolved in *o*-dichlorobenzene 1 mg/30 μL, 3 μmol) in a J. Young tube. A colorless solution was formed. The mixtures were allowed to stay at room temperature for 24 h. The reactions were monitored by detecting the increase in the intensity of ^{19}F NMR resonance of Al-F and decrease in the intensity of ^{19}F NMR resonance of F-substrates (δ -66.0 (Cl-C_6H_4-CF_3)). The ratio of products in GC/MS is Cl-C_6H_4-$CH_2CH_2CH_3$ 13%, Cl-C_6H_4-$CHEt_2$ 68% and Cl-C_6H_4-CEt_3 19%. ^{19}F NMR (376.3 MHz, hexanes): δ -165.2 (C_6F_6). GC/MS: (Cl-C_6H_4-$CH_2CH_2CH_3$; M/Z^+ 154, 156), (Cl-C_6H_4-$CHEt_2$; M/Z^+ 182, 184), (Cl-C_6H_4-CEt_3; M/Z^+ 210, 212).

Entry 16: Five solutions containing $C_6H_5CMe_3$ and C_6H_5Br in different ratios were prepared and analyzed by GC/MS. Integration of the corresponding peaks in the resulting chromatogram gave the coefficient as 1.029 (See detail in SI). The reaction (entry 17) was set up using 40 μL (326 μmol) of substrate **2** with 2.3 mg (3.3 μmol) $Et_2Al[HCB_{11}H_5Br_6]$, 5.0 μL (43 μmol) C_6F_6 and 490 μL $AlMe_3$ (980 μmol, 2 M in hexanes) in 0.5 mL hexanes. After 36 h, ^{19}F NMR indicated that 94% of C-F was converted. 60 μL (572 μmol) bromobenzene was added into the reaction mixture, the mixture was filtered through Celite, diluted by hexanes and analyzed by GC/MS. Integration of the resulting chromatogram gave a ratio of 0.48:1.00 corresponding to the

formation of 283 (0.48×1.029×572) μmol $C_6H_5CMe_3$. Yield: 87%. ^{19}F NMR (376.3 MHz, hexanes): δ -147.8 ($(CH_3)_2AlF$), -165.2 (C_6F_6). GC/MS: (C_6H_5-CMe_3; M/Z^+ 134).

Entry 17: 40 μL (280 μmol) Substrate **4** was mixed with 115 μL (840 μmol) $AlEt_3$, 5.0 μL (43 μmol) C_6F_6, 11.8 mg (16.8 μmol) of $Et_2Al[HCB_{11}H_5Br_6]$ in a J. Young tube. A clear solution was formed. The mixture was heated at 85 ℃ for 24 h. The reactions were monitored by detecting the increase in the intensity of ^{19}F NMR resonance of Al-F and decrease in the intensity of ^{19}F NMR resonance of F-substrates (δ -58.9 (C_6F_5-CCF_3), -142.4 (C_6F_5-CCF_3), -149.8 (C_6F_5-CCF_3), -162.4 (C_6F_5-CCF_3)). The ratio of products in GC/MS is C_6F_5-$CH_2CH_2CH_3$ 31%, C_6F_5-$CHEt_2$ 61% and C_6F_5-CEt_3 8%. GC/MS: (C_6F_5-$CH_2CH_2CH_3$; M/Z^+ 210), (C_6F_5-$CHEt_2$; M/Z^+ 238), (C_6F_5-CEt_3; M/Z^+ 266).

Entry 18: 40 μL (280 μmol) Substrate **4** was mixed with 420 μL (840 μmol) of $AlMe_3$ (2 M in hexanes), 5.0 μL (43 μmol) C_6F_6, 360 μL (16.8 μmol) $Et_2Al[HCB_{11}H_5Br_6]$ solution (1 mg/30 μL *o*-dichlorobenzene), a J. Young tube. A clear solution was formed. The mixture was heated at 85 ℃ for 24 h. The reactions were monitored by detecting the increase in the intensity of ^{19}F NMR resonance of Al-F and decrease in the intensity of ^{19}F NMR resonance of F-substrates (δ -58.9 (C_6F_5-CCF_3), -142.4 (C_6F_5-CCF_3), -149.8 (C_6F_5-CCF_3), -162.4 (C_6F_5-CCF_3)). Yield (based on ^{19}F NMR, after 24 h): C_6F_5-CMe_3 84%. ^{19}F NMR (376.3 MHz, hexanes): δ -140.7 (C_6F_5-CMe_3), -161.6 (C_6F_5-CMe_3), -165.2 (C_6F_6), -166.1 (C_6F_5-CMe_3). GC/MS: (C_6F_5-CMe_3; M/Z^+ 224).

Entry 19: 40 μL (280 μmol) Substrate **4** was mixed with 420 μL (840 μmol) of $AlMe_3$ (2 M in hexanes), 5.0 μL (43 μmol) C_6F_6, 60 μL (2.8 μmol) $Et_2Al[HCB_{11}H_5Br_6]$ solution

(1 mg/30 μL *o*-dichlorobenzene), a J. Young tube. A clear solution was formed. The mixture was heated at 85 ℃ for 24 h. The reactions were monitored by detecting the increase in the intensity of ^{19}F NMR resonance of Al-F and decrease in the intensity of ^{19}F NMR resonance of F-substrates (δ -58.9 (C_6F_5-CCF_3), -142.4 (C_6F_5-CCF_3), -149.8 (C_6F_5-CCF_3), -162.4 (C_6F_5-CCF_3)). Yield (based on ^{19}F NMR, after 24 h): C_6F_5-CMe_3 38%. ^{19}F NMR (376.3 MHz, hexanes): δ -58.9 (C_6F_5-CCF_3), -162.4 (C_6F_5-CCF_3), -140.7 (C_6F_5-CMe_3), -142.4 (C_6F_5-CCF_3), -149.8 (C_6F_5-CCF_3), -161.6 (C_6F_5-CMe_3), -162.4 (C_6F_5-CCF_3), -165.2 (C_6F_6), -166.1 (C_6F_5-CMe_3). GC/MS: (C_6F_5-CMe_3; M/Z^+ 224).

Entry 20: 40 μL (260 μmol) Substrate **5** was mixed with 110 μL (804 μmol) $AlEt_3$, C_6F_6 1.8 mg (2.6 μmol) of $Et_2Al[HCB_{11}H_5Br_6]$ in a J. Young tube. A clear solution was formed. The mixture was heated at 50 ℃ for 24 h. The reactions were monitored by detecting the increase in the intensity of ^{19}F NMR resonance of Al-F and decrease in the intensity of ^{19}F NMR resonance of F-substrates (δ -70.2 ($C_6H_5CH_2CH_2CF_3$). The ratio of products in GC/MS is C_6H_4-C_5H_{10} 34%, C_6H_4-C_7H_{14} 30% and C_6H_5-C_7H_{15} 36%. ^{19}F NMR (376 MHz, *o*-$C_6H_4Cl_2$): δ -70.2 (C_6H_5-$CH_2CH_2CF_3$), -165.2 (C_6F_6). GC/MS: (C_6H_5-$CH_2CH_2CF_3$; M/Z^+ 174), (C_6H_4-C_5H_{10}; M/Z^+ 146, possible structure Scheme 4-5 **IV**), (C_6H_4-C_7H_{14}; M/Z^+ 174, possible structure Scheme 4-5 **V**), (C_6H_5-C_7H_{15}; M/Z^+ 176, possible structure Scheme 4-5 **III**).

Entry 21: 40 μL (260 μmol) Substrate **5** was mixed with 390 μL (780 μmol) $AlMe_3$ (2 M in hexanes), 5.0 μL (43 μmol) C_6F_6, 54 μL of $Et_2Al[HCB_{11}H_5Br_6]$ solution (predissolved in *o*-dichlorobenzene 1 mg/30 μL, 2.6 μmol) in a J. Young tube. A clear

solution was formed. The mixture was heated at 50 ℃ for 24 h. The reactions were monitored by detecting the increase in the intensity of ^{19}F NMR resonance of Al-F and decrease in the intensity of ^{19}F NMR resonance of F-substrates (δ -70.2 ($C_6H_5CH_2CH_2C\mathit{F}_3$). The ratio of products in GC/MS is C_6H_4-C_5H_{10} 68% and C_6H_5-C_6H_{13} 32%. ^{19}F NMR (376.3 MHz, hexanes): δ -70.2 (C_6H_5-$CH_2CH_2C\mathit{F}_3$), -165.2 ($C_6\mathit{F}_6$). GC/MS: (C_6H_5-$CH_2CH_2CF_3$; M/Z^+ 174), (C_6H_4-C_5H_{10}; M/Z^+ 146, possible structure Scheme 4-5 **I**), (C_6H_5-C_6H_{13}; M/Z^+ 162, possible structure Scheme 4-5 **II**).

Entry 22: 40 μL (450 μmol) Substrate **6** was mixed with 125 μL (914 μmol) $AlEt_3$, 5.0 μL (43 μmol) C_6F_6, 1.6 mg (2.3 μmol $Et_2Al[HCB_{11}H_5Br_6]$, in *o*-$C_6H_4Cl_2$ in a J. Young tube. An orange color solution formed. Dramatic elevation of temperature was observed. The mixture was allowed to stay at room temperature for 24 h. The reactions were monitored by detecting the increase in the intensity of ^{19}F NMR resonance of Al-F and decrease in the intensity of ^{19}F NMR resonance of F-substrate δ -94.8 ($C\mathit{F}_2C_4H_8$). The ratio of products in GC/MS is Cyclopentane 33% and Ethylcyclopentane 67%. ^{19}F NMR (376.3 MHz, *o*-$C_6H_4Cl_2$: -165.2 ($C_6\mathit{F}_6$). GC/MS: (Cyclopentane; M/Z^+ 70), (Ethylcyclopentane; M/Z^+ 98). GC/MS sample was dissolved in *o*-dichlorobenzene, no solvent delay.

Entry 23: 40 μL (315 μmol) of **1** was mixed with 90 μL (940 μmol) Me_3Al and 150 μL (940 μmol) Et_3SiH, 5.0 μL (43 μmol) C_6F_6, 2.7 mg (3.2 μmol) $Ph_3C[HCB_{11}H_5Br_6]$ in 0.4 ml hexanes in a J. Young tube. A colorless solution was formed with little amount of precipitate. The mixtures were allowed to stay at room temperature for 24h. The reactions were monitored by detecting the increase in the intensity of ^{19}F NMR

resonance of Al-F and decrease in the intensity of ^{19}F NMR resonance of F-substrates (δ -65.3 (*p*F-C_6H_4-C*F*$_3$), -110.1 (*pF*-C_6H_4-CF_3)). The ratio of products in GC/MS is F-C_6H_4-CH_3 28%, F-C_6H_4-CH_2Me 57% and F-C_6H_4-$CHMe_2$ 14%. ^{19}F NMR (376.3 MHz, hexanes): δ -120.0 (*F*-C_6H_4-$CHMe_2$) -120.2 (*F*-C_6H_4-CH_2Me), -120.6 (*F*-C_6H_4-CH_3), -165.2 (C_6F_6). Yield (based on ^{19}F NMR, after 24 h): F-C_6H_4-CH_3 24%, F-C_6H_4-CH_2Me 49%, F-C_6H_4-$CHMe_2$ 13%. GC/MS: (F-C_6H_4-CH_3; M/Z$^+$ 110), (F-C_6H_4-CH_2Me; M/Z$^+$ 124), (F-C_6H_4-$CHMe_2$; M/Z$^+$ 138).

Reaction of 6 with $AlEt_3$ without catalyst: 40 μL (450 μmol) Substrate **6** was mixed with 155 μL (900 μmol) $AlEt_3$, 5.0 μL (43 μmol) C_6F_6 in 0.3 mL C_6D_{12} in a J. Young tube. An orange color solution formed. The mixture was allowed to stay at room temperature for 24 h. The reaction was monitored by detecting the increase in the intensity of ^{19}F NMR resonance of Al-F and decrease in the intensity of ^{19}F NMR resonance of F-substrate (δ -94.8 ($CF_2C_4H_8$). Yield (based on ^{19}F NMR, after 24 h): 1-fluoro-cyclopentene 24%. ^{19}F NMR (376.3 MHz, C_6D_{12}: -124.3 (1-fluoro-cyclopenene), -165.2 (C_6F_6).

Entry A1: 40 μL (315 μmol) Substrate **1** was mixed with 160 μL (320 μmol) Me_3Al (2 M in hexanes), 5.0 μL (43 μmol) C_6F_6, 2.2 mg (3.2 μmol) $Et_2Al[HCB_{11}H_5Br_6]$ in hexanes in a J. Young tube. A colorless solution was formed. A small amount of precipitate was observed. The mixtures were allowed to stay at room temperature for 5 d. The reactions were monitored by detecting the increase in the intensity of ^{19}F NMR resonance of Al-F and decrease in the intensity of ^{19}F NMR resonance of F-substrates (δ -65.3 (*p*F-C_6H_4-C*F*$_3$), -110.1 (*pF*-C_6H_4-CF_3)). Maximum conversion of C-F bond was

reached after 3 d. Yield (based on ^{19}F NMR, after 3 days): *p*-$FC_6H_4CMe_3$ 30%. ^{19}F NMR (376.3 MHz, hexanes): δ -65.3 (*p*F-C_6H_4-C*F*$_3$), -110.1 (*pF*-C_6H_4-CF_3), -120.7 (*F*-C_6H_4-CMe_3), -165.2 (C_6F_6). GC/MS: (F-C_6H_4-CMe_3; M/Z$^+$ 152, (F-C_6H_4-CF_3; M/Z$^+$ 164).

Entry A2: 40 μL (315 μmol) Substrate **1** was mixed with 45 μL (329 μmol) Et_3Al, 5.0 μL (43 μmol) C_6F_6, 2.2 mg (3.2 μmol) $Et_2Al[HCB_{11}H_5Br_6]$ in hexanes in a J. Young tube. A colorless solution was formed. A small amount of precipitate was observed. The mixtures were allowed to stay at room temperature for 5 d. The reactions were monitored by detecting the increase in the intensity of ^{19}F NMR resonance of Al-F and decrease in the intensity of ^{19}F NMR resonance of F-substrates (δ -65.3 (*p*F-C_6H_4-C*F*$_3$), -110.1 (*pF*-C_6H_4-CF_3)). Maximum conversion of C-F bond was reached after 3 d. Yield (based on ^{19}F NMR, after 3 days): F-C_6H_4-$CH_2CH_2CH_3$ 4%, F-C_6H_4-$CHEt_2$ 18%, F-C_6H_4-CEt_3 6%. ^{19}F NMR (376.3 MHz, hexanes): δ -65.3 (*p*F-C_6H_4-C*F*$_3$), -110.1 (*pF*-C_6H_4-CF_3), -119.8 (*F*-C_6H_4-$CHEt_2$), -120.2 (*F*-C_6H_4-CEt_3), -120.8 (*F*-C_6H_4-$CH_2CH_2CH_3$), -165.2 (C_6F_6). GC/MS: (F-C_6H_4-$CH_2CH_2CH_3$; M/Z$^+$ 138), (F-C_6H_4-$CHEt_2$; M/Z$^+$ 166), (F-C_6H_4-CEt_3; M/Z$^+$ 194), (F-C_6H_4-CF_3; M/Z$^+$ 164).

Entry A3: 40 μL (315 μmol) Substrate **1** was mixed with 315 μL (315 μmol) ^{i}Bu$_3$Al (1M in hexanes), 5.0 μL (43 μmol) C_6F_6, 2.2 mg (3.2 μmol) $Et_2Al[HCB_{11}H_5Br_6]$ in hexanes in a J. Young tube. A colorless solution was formed. A small amount of precipitate was observed. The mixtures were allowed to stay at room temperature for 5 d. The reactions were monitored by detecting the increase in the intensity of ^{19}F NMR resonance of Al-F and decrease in the intensity of ^{19}F NMR resonance of F-substrates (δ

-65.3 (*p*F-C_6H_4-C*F*$_3$), -110.1 (*pF*-C_6H_4-CF_3)). Maximum conversion of C-F bonds was reached after 3 d. The ratio of products in GC/MS is F-C_6H_4-CF_3 54%, F-C_6H_4-CHC_8H_{18} 25% and F-C_6H_4-$CC_{12}H_{27}$ 20%. ^{19}F NMR (376.3 MHz, hexanes): δ -65.3 (*p*F-C_6H_4-C*F*$_3$), -110.1 (*pF*-C_6H_4-CF_3), -119.7, -119.8, -120.1, -120.3 (*F*-C_6H_4-R), -165.2 (C_6F_6). GC/MS: (F-C_6H_4-CHC_8H_{18}; M/Z$^+$ 222), (F-C_6H_4-$CC_{12}H_{27}$; M/Z$^+$ 278), (F-C_6H_4-CF_3; M/Z$^+$ 164).

Entry A4: 40 μL (315 μmol) Substrate **1** was mixed with 275 μL (319 μmol) ^{i}Bu$_2$AlH (1.16M in hexanes), 5.0 μL (43 μmol) C_6F_6, 2.2 mg (3.2 μmol) Et$_2$Al[$HCB_{11}H_5Br_6$] in hexanes in a J. Young tube. A colorless solution was formed. A small amount of precipitate was observed. The mixtures were allowed to stay at room temperature for 5 d. The reactions were monitored by detecting the increase in the intensity of ^{19}F NMR resonance of Al-F and decrease in the intensity of ^{19}F NMR resonance of F-substrates (δ -65.3 (*p*F-C_6H_4-C*F*$_3$), -110.1 (*pF*-C_6H_4-CF_3)). Maximum conversion of C-F bond was reached after 3 d. Yield (based on ^{19}F NMR, after 3 days): F-C_6H_4-CH_3 20%, F-C_6H_4-$CH_2C_4H_9$ 13%. ^{19}F NMR (376.3 MHz, hexanes): δ -65.3 (*p*F-C_6H_4-C*F*$_3$), -110.1 (*pF*-C_6H_4-CF_3), -120.3 (*F*-C_6H_4-$CH_2C_4H_9$), -120.6 (*F*-C_6H_4-CH_3), -165.2 (C_6F_6). GC/MS: (F-C_6H_4-CH_3; M/Z$^+$ 110), (F-C_6H_4-$CH_2C_4H_9$; M/Z$^+$ 166), (F-C_6H_4-CF_3; M/Z$^+$ 164).

Entry A5: 40 μL (315 μmol) Substrate **1** was mixed with 950 μL (950 μmol, 1 M in hexanes) *i*Bu$_2$AlF, 5.0 μL (43 μmol) C_6F_6, 2.2 mg (3.15 μmol) Et$_2$Al[$HCB_{11}H_5Br_6$] in hexanes in a J. Young tube. A colorless solution was formed. A small amount of precipitate was observed. The mixture was allowed to stay at room temperature for 5 d. The reactions were monitored by detecting the increase in the intensity of ^{19}F NMR

resonance of Al-F and decrease in the intensity of ^{19}F NMR resonance of F-substrates (δ -65.3 (*p*F-C_6H_4-C*F*$_3$), -110.1 (*pF*-C_6H_4-CF_3)). Maximum conversion of C-F bond was reached after 3 d. The ratio of products in GC/MS is F-C_6H_4-CF_3 57%, F-C_6H_4-$CH_2C_4H_9$ 15%, F-C_6H_4-$CH_2C_4H_9$ (isomer) 14% and F-C_6H_4-CHC_8H_{18} 14%. ^{19}F NMR (376.3 MHz, hexane): δ -65.3 (*p*F-C_6H_4-C*F*$_3$), -110.1 (*pF*-C_6H_4-CF_3), -119.7, -119.8, -120.3 (*F*-C_6H_4-$CH_2C_4H_9$), -165.2 (C_6F_6). GC/MS: (F-C_6H_4-$CH_2C_4H_9$; M/Z$^+$ 166), (F-C_6H_4-$CH_2C_4H_9$ (isomer); M/Z$^+$ 166), (F-C_6H_4-CHC_8H_{18}; M/Z$^+$ 222), (F-C_6H_4-CF_3; M/Z$^+$ 164).

Entry B1: 20 μL (157 μmol) Substrate **1** was mixed with 470 μL (470 μmol) methylaluminoxane (1M in Toluene), 5.0 μL (43 μmol) C_6F_6 in a J. Young tube. A colorless solution was formed. The mixtures were allowed to stay at room temperature for 3 days or until no changes could be observed by ^{19}F NMR. The reactions were monitored by detecting the increase in the intensity of ^{19}F NMR resonance of Al-F and decrease in the intensity of ^{19}F NMR resonance of F-substrates (δ -65.3 (*p*F-C_6H_4-C*F*$_3$), -110.1 (*pF*-C_6H_4-CF_3)). ^{19}F NMR (376.3 MHz, toluene): δ -65.3 (*p*F-C_6H_4-C*F*$_3$), -110.1 (*pF*-C_6H_4-CF_3), -120.7 (*F*-C_6H_4-CMe_3), -165.2 (C_6F_6). GC/MS: (F-C_6H_4-CMe_3; M/Z$^+$ 152).

Entry B2: 20 μL (157 μmol) Substrate **1** was mixed with 820 μL (820 μmol) methylaluminoxane (1M in Toluene), 5.0 μL (43 μmol) C_6F_6 in a J. Young tube. A colorless solution was formed. The mixtures were allowed to stay at room temperature for 3 days or until no changes could be observed by ^{19}F NMR. The reactions were monitored by detecting the increase in the intensity of ^{19}F NMR resonance of Al-F and

decrease in the intensity of ^{19}F NMR resonance of F-substrates (δ -65.3 (*p*F-C_6H_4-C*F*$_3$), -110.1 (*pF*-C_6H_4-CF_3)). ^{19}F NMR (376.3 MHz, toluene): δ -65.3 (*p*F-C_6H_4-C*F*$_3$), -110.1 (*pF*-C_6H_4-CF_3), -120.7 (*F*-C_6H_4-CMe_3), -165.2 (C_6F_6). GC/MS: (F-C_6H_4-CMe_3; M/Z^+ 152).

Entry B3: 20 μL (157 μmol) Substrate **1** was mixed with 1570 μL (1570 μmol) methylaluminoxane (1M in Toluene), 5.0 μL (43 μmol) C_6F_6 in a J. Young tube. A colorless solution was formed. The mixtures were allowed to stay at room temperature for 3 days or until no changes could be observed by ^{19}F NMR. The reactions were monitored by detecting the increase in the intensity of ^{19}F NMR resonance of Al-F and decrease in the intensity of ^{19}F NMR resonance of F-substrates (δ -65.3 (*p*F-C_6H_4-C*F*$_3$), -110.1 (*pF*-C_6H_4-CF_3)). ^{19}F NMR (376.3 MHz, toluene): δ -120.7 (*F*-C_6H_4-CMe_3), -165.2 (C_6F_6). GC/MS: (F-C_6H_4-CMe_3; M/Z^+ 152).

Entry C1: 40 μL of $^{n}C_{10}H_{21}F$ (200 μmol) was mixed with 28 (200 μmol) triethylaluminum, 5.0 μL (43 μmol) C_6F_6 in hexanes in a J. Young tube. A colorless solution was formed with small amount of precipitate. The mixtures were allowed to stay at room temperature for 24 h. The reactions were monitored by detecting the increase in the intensity of ^{19}F NMR resonance of Al-F and decrease in the intensity of ^{19}F NMR resonance of F-substrates (δ -220.6 *F*-$(CH_2)_9CH_3$). GC/MS: ($CH_3(CH_2)_{10}CH_3$; M/Z^+ 170).

Entry C2: 40 μL of **7** (200 μmol) was mixed with 28 (200 μmol) triethylaluminum, 5.0 μL (43 μmol) C_6F_6 in $C_6H_4Cl_2$ in a J. Young tube. A colorless solution was formed. The mixtures were allowed to stay at room temperature for 24 h. The reactions were

monitored by detecting the increase in the intensity of ^{19}F NMR resonance of Al-F and decrease in the intensity of ^{19}F NMR resonance of F-substrates (δ -220.6 *F*-$(CH_2)_9CH_3$). GC/MS: ($CH_3(CH_2)_{10}CH_3$; M/Z^+ 170).

Entry C3: 40 μL of **1** (200 μmol) was mixed with 130 μL (950 μmol) triethylaluminum, 5.0 μL (43 μmol) C_6F_6 in hexanes in a J. Young tube. A colorless solution was formed with small amount of precipitate. The mixtures were allowed to stay at room temperature for 24 h. The reactions were monitored by detecting the increase in the intensity of ^{19}F NMR resonance of Al-F and decrease in the intensity of ^{19}F NMR resonance of F-substrates (δ -65.3 (*p*F-C_6H_4-C*F*$_3$), -110.1 (*pF*-C_6H_4-CF_3)). No product was detected by ^{19}F NMR or GC/MS.

Entry C4: 40 μL of **1** (200 μmol) was mixed with 130 μL (950 μmol) triethylaluminum, 5.0 μL (43 μmol) C_6F_6 in $C_6H_4Cl_2$ in a J. Young tube. A colorless solution was formed. The mixtures were allowed to stay at room temperature for 24 h. The reactions were monitored by detecting the increase in the intensity of ^{19}F NMR resonance of Al-F and decrease in the intensity of ^{19}F NMR resonance of F-substrates (δ -65.3 (*p*F-C_6H_4-C*F*$_3$), -110.1 (*pF*-C_6H_4-CF_3)). Yield (based on ^{19}F NMR, after 24h): F-C_6H_4-$CH_2CH_2CH_3$ 3%, F-C_6H_4-$CHEt_2$ 12%, F-C_6H_4-CEt_3 30%. ^{19}F NMR (376.3 MHz, *o*-$C_6H_4Cl_2$): δ -119.8 (*F*-C_6H_4-$CHEt_2$), -120.2 (*F*-C_6H_4-CEt_3), -120.8 (*F*-C_6H_4-$CH_2CH_2CH_3$), -165.2 (C_6F_6). GC/MS: (F-C_6H_4-$CH_2CH_2CH_3$; M/Z^+ 138), (F-C_6H_4-$CHEt_2$; M/Z^+ 166), (F-C_6H_4-CEt_3; M/Z^+ 194).

Reaction in 'wet' solvent. 1 μL H_2O (56 μmol) was added to 40 μL 4-fluorobenzotrifluoride (315 μmol), 170 μL triethylaluminum (1243 μmol) and

hexafluorobenzene (5.0 μL, 43 μmol) in 0.5 ml hexanes in a Schlenk flask under a flow of argon. $Et_2Al[HCB_{11}H_5Br_6]$ (2.2 mg, 3.2 μmol) was added to the mixture, after it was stirred at room temperature for 6 h. ^{19}F NMR spectra were recorded every hour to monitor the reaction. 100% conversion of C-F was reached in 6 h. Yield (based on ^{19}F NMR, after 24h): F-C_6H_4-$CH_2CH_2CH_3$ 20%, F-C_6H_4-$CHEt_2$ 58%, F-C_6H_4-CEt_3 15%. ^{19}F NMR (376 MHz, hexanes): δ -119.8 (*F*-C_6H_4-$CHEt_2$), -120.2 (*F*-C_6H_4-CEt_3), -120.8 (*F*-C_6H_4-$CH_2CH_2CH_3$), -165.2 (C_6F_6). ^{19}F NMR (376.3 MHz, hexanes): δ -119.8 (*F*-C_6H_4-$CHEt_2$), -120.2 (*F*-C_6H_4-CEt_3), -120.8 (*F*-C_6H_4-$CH_2CH_2CH_3$), -165.2 (C_6F_6). GC/MS: (F-C_6H_4-$CH_2CH_2CH_3$; M/Z^+ 138), (F-C_6H_4-$CHEt_2$; M/Z^+ 166), (F-C_6H_4-CEt_3; M/Z^+ 194).

$Ag_2[B_{12}Cl_{12}]$. $Cs_2[B_{12}Cl_{12}]$ (1.04 g, 1.26 mmol) and $AgNO_3$ (0.86 g, 5.06 mmol) were dissolved in 25 mL of water, then CH_3CN (5 drops) was added dropwise into the solution, forming some white precipitates. The white solids were collected on a medium frit and washed by 2 ml of water 3 times. The products were then put in a schlenk flask and dried under vaccum at 80 ℃ for 6 hours. Yield: 0.89 g (91%).

$[Ph_3C]_2[B_{12}Cl_{12}]$. In an Ar-filled glove box, $Ag_2[B_{12}Cl_{12}]$ (0.89 g, 1.15 mmol) and Ph_3CCl (350 mg, 1.26 mmol) were mixed in 20 mL of CH_3CN, forming a orange red solution with white precipitates. The mixture was stirred at room temperature for 1 hour before it was filtered through a medium frit. Removal of the volatiles gave a orange yellow solid which was then washed with 5 ml of toluene once and 5 ml of pentane three times. The products were recrystallized from CH_3CN/n-pentane solution at -30 ℃ . Yield: 0.97 g. (81%). ^{11}B NMR (128.5 MHz, CD_3CN): δ -12.7

(s).

Entry D1: 500 μL (3.9 mmol) $C_6H_5CF_3$, 2.0 mL (12.5 mmol) triethylsilane, 50 μL (430 μmol) C_6F_6 and 3 ml *o*-dichlorobenzene was added to a glass vial equipped with a stir bar. 6.0 mg (5.7 μmol) $[Ph_3C]_2[B_{12}Cl_{12}]$ was slowly added to the solution. The mixture was stirred at room temperature for 30 min. After 30 min, Bu_4NBH_4 was added to stop the reaction. 0.5 ml of the mixture was transfer to a J. Young tube and analyzed by ^{19}F NMR. ^{19}F NMR (282.2 MHz, ODCB): δ -119.3 (m, p-*F*C_6H_4-CH_3),), -144.5 (br, $Et_2Si\mathit{F}_2$), -163.2 (s, $C_6\mathit{F}_6$), -176.1 (br, $Et_3Si\mathit{F}$). Other unidentified peaks appeared at -117.8, -119.3, -124.2 (presumably Friedel-Crafts products).

Entry D2: 500 μL (3.5 mmol) $C_6F_5CF_3$, 2.0 mL (12.5 mmol) triethylsilane, 250 μL (511 μmol) C_6F_5Br and 3 ml *o*-dichlorobenzene was added to a glass vial equipped with a stir bar. 5.9 mg (5.6 μmol) $[Ph_3C]_2[B_{12}Cl_{12}]$ was slowly added to the solution. A colorless solution was formed with a small amount of precipitate. The mixture was allowed to stir at room temperature for 24 h. The reaction was monitored by detecting the increase in the intensity of ^{19}F NMR resonance of Si-F and decrease in the intensity of ^{19}F NMR resonance of F-substrates (δ -57.4 (C_6F_5-$C\mathit{F}_3$), -140.8, -147.8, -160.5 ($C_6\mathit{F}_5$-CF_3). ^{19}F NMR (282.2 MHz, ODCB): δ -57.4 (m, C_6F_5-$C\mathit{F}_3$), -133.5 (m, $C_6\mathit{F}_5Br$), -140.8 (m, $C_6\mathit{F}_5$-CF_3), -144.2 (m, $C_6\mathit{F}_5$-CH_3), -144.5 (br, $Et_2Si\mathit{F}_2$), -147.8 (m, $C_6\mathit{F}_5$-CF_3), -155.6 (m, $C_6\mathit{F}_5Br$), -157.4 (m, $C_6\mathit{F}_5$-CH_3), -160.5 (m, $C_6\mathit{F}_5$-CF_3), -161.4 (m, $C_6\mathit{F}_5Br$), -163.0 (m, $C_6\mathit{F}_5$-CH_3), -176.1 (br, $Et_3Si\mathit{F}$). Other unidentified peaks appeared at -142.7, -157.3, -163.4 (presumably Friedel-Crafts products).

Entry D3: 500 μL (3.5 mmol) $C_6F_5CF_3$, 2.0 mL (12.5 mmol) triethylsilane, 250 μL (511 μmol) C_6F_5Br and 3 ml *o*-dichlorobenzene were added to a sealed flask equipped with a stir bar. 5.7 mg (5.5 μmol) $[Ph_3C]_2[B_{12}Cl_{12}]$ was slowly added to the solution. A colorless solution was formed with a small amount of precipitate. The mixture was allowed to stir at 50 ℃ for 24 h. The reaction was monitored by detecting the increase in the intensity of ^{19}F NMR resonance of Si-F and decrease in the intensity of ^{19}F NMR resonance of F-substrates (δ -57.4 (C_6F_5-C*F*$_3$), -140.8, -147.8, -160.5 (C_6*F*$_5$-CF_3). ^{19}F NMR (282.2 MHz, ODCB): δ -57.4 (m, C_6F_5-C*F*$_3$), -133.5 (m, C_6*F*$_5$Br), -140.8 (m, C_6*F*$_5$-CF_3), -144.2 (m, C_6*F*$_5$-CH_3), -144.5 (br, Et_2Si*F*$_2$), -147.8 (m, C_6*F*$_5$-CF_3), -155.6 (m, C_6*F*$_5$Br), -157.4 (m, C_6*F*$_5$-CH_3), -160.5 (m, C_6*F*$_5$-CF_3), -161.4 (m, C_6*F*$_5$Br), -163.0 (m, C_6*F*$_5$-CH_3), -176.1 (br, Et_3Si*F*). Other unidentified peaks appeared at -142.7, -157.3, -163.4 (presumably Friedel-Crafts products).

Entry D4: 500 μL (3.5 mmol) $C_6F_5CF_3$, 2.0 mL (12.5 mmol) triethylsilane, 250 μL (511 μmol) C_6F_5Br and 3 ml *o*-dichlorobenzene were added to a sealed flask equipped with a stir bar. 5.7 mg (5.5 μmol) $[Ph_3C]_2[B_{12}Cl_{12}]$ was slowly added to the solution. A colorless solution was formed with a small amount of precipitate. The mixture was allowed to stir at 80 ℃ for 24 h. The reaction was monitored by detecting the increase in the intensity of ^{19}F NMR resonance of Si-F and decrease in the intensity of ^{19}F NMR resonance of F-substrates (δ -57.4 (C_6F_5-C*F*$_3$), -140.8, -147.8, -160.5 (C_6*F*$_5$-CF_3). ^{19}F NMR (282.2 MHz, ODCB): δ -57.4 (m, C_6F_5-C*F*$_3$), -133.5 (m, C_6*F*$_5$Br), -140.8 (m, C_6*F*$_5$-CF_3), -144.2 (m, C_6*F*$_5$-CH_3), -144.5 (br,

$Et_2Si\mathit{F}_2$), -147.8 (m, $C_6\mathit{F}_5$-CF_3), -155.6 (m, $C_6\mathit{F}_5Br$), -157.4 (m, $C_6\mathit{F}_5$-CH_3), -160.5 (m, $C_6\mathit{F}_5$-CF_3), -161.4 (m, $C_6\mathit{F}_5Br$), -163.0 (m, $C_6\mathit{F}_5$-CH_3), -176.1 (br, $Et_3Si\mathit{F}$). Other unidentified peaks appeared at -142.7, -157.3, -163.4 (presumably Friedel-Crafts products).

CHAPTER V

DESIGN AND SYNTHESIS OF TETRADENTATE TPB LIGANDS AND THEIR METAL COMPLEXES WITH GROUP 10 METALS

5.1 Introduction

Three ways could be used to analyze a 2ē bond between a metal and a ligand (Figure 5-1). If the 2ē metal-ligand bond is broken by giving the 2ē to the ligand and the resultant ligand species is a stable neutral species, than the ligand is considered as "L" type ligand. If it is an anion, it is considered as "X" type ligand. If the two electrons are given to the metal center and the resultant ligand species remains as neutral species, it is considered as "Z" type ligand.[22] Unlike the well documented X and L type ligands, Z-type ligands which function as σ-acceptor are relatively less developed since transition metals are usually more electropositive than the ligands.[161]

---

* reprinted in part from *Angew. Chem., Int. Ed*., 47, Bontemps, S.; Bouhadir, G.; Gu, W.; Mercy, M.; Chen, C.-H.; Foxman, B. M.; Maron, L.; Ozerov, O. V.; Bourissou D. "Metallaboratranes Derived from a Triphosphanyl-Borane: Intrinsic C_3 Symmetry Supported by a Z-Type Ligand ", 1481, copyright 2008 German Chemical Society and from *J. Am. Chem. Soc.,* 130, Sircoglou, M.; Bontemps, S.; Bouhadir, G.; Saffon, N.; Miqueu, K.; Gu, W.; Mercy, M.; Chen, C.-H.; Foxman, B.; Maron, L.; Ozerov, O. V.; Bourissou, D. "Group 10 and 11 Metal Boratranes (Ni, Pd, Pt, CuCl, AgCl, AuCl and Au^+) Derived from a Triphosphine–Borane", 16729, copyright 2008 American Chemical Society.

Significant progress has been made in the past decade,[162] especially with boranes as the Z-ligand.[163] Early work on the metal borane chemistry focused on halo- and arylborane complexes, in which the M→B interaction was studied by infrared and NMR spectroscopy.[164] The ^{11}B NMR resonances tend to shift upfield when the coordination number at boron increases.[165]

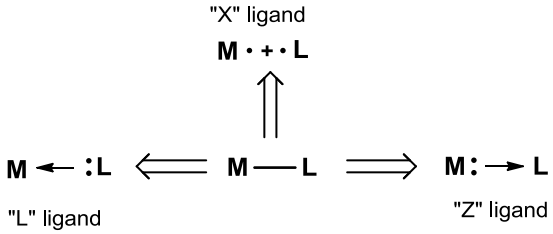

Figure 5-1. Definition of "L", "X" and "Z" ligand.

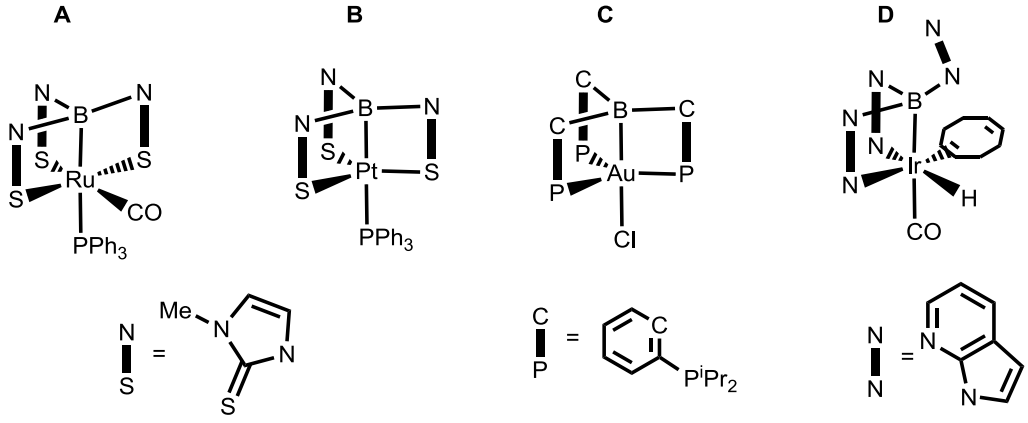

Figure 5-2. Metallaboratrane complexes.

Strong M→B interactions are often observed when transition metals are coordinated with ambiphilic ligands which contain both donor and acceptor coordination sites. In

1999, the first structural confirmation of M→B interactions[166] was reported in a ruthenium borane complex (**A**) (Figure 5-2) supported by three thione donor groups in a framework which is now commonly referred to as metallaboratrane, due to their structural similarity the more familiar boratrane cages (Figure 5-3).[167] Since then, many examples have been published in the metallaboratrane area with sulfur[168] (**B**), phosphorus[129,169] (**C**) or nitrogen[170] (**D**) as side arms and with metals from group 8,[168b-d] 9,[129,169b,170,171] 10[169a,b] and 11.[169a]

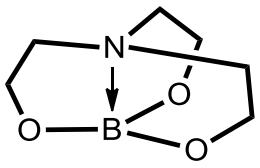

Figure 5-3. General scheme for boratrane species.

Recently, Bourissou and coworkers have demonstrated the M→B interactions with a series of ambiphilic ligands containing both phosphine and borane functional groups.[129,169] Bisphosphinophenyl-borane **BPB** (Figure 5-4) afforded 16ē square pyramidal complexes with d^8 metals,[172] in which the two phosphine arms were trans[169b] (**E**) or cis[129,173] (**F**) to each other and the lewis acidic boron center occupied the axial position. 16ē square planar complexes[169c] (**G**) were observed with BPB ligand and d^{10} metals,[171] the BPB ligand here adopted a meridional geometry. The formation of T-shape complexes[169a] (**H)** from the related monophosphinophenyl-borane MPB illustrated

the possibility for M→B interactions to occur in 14ē complexes, even when supported by a single donor buttress.

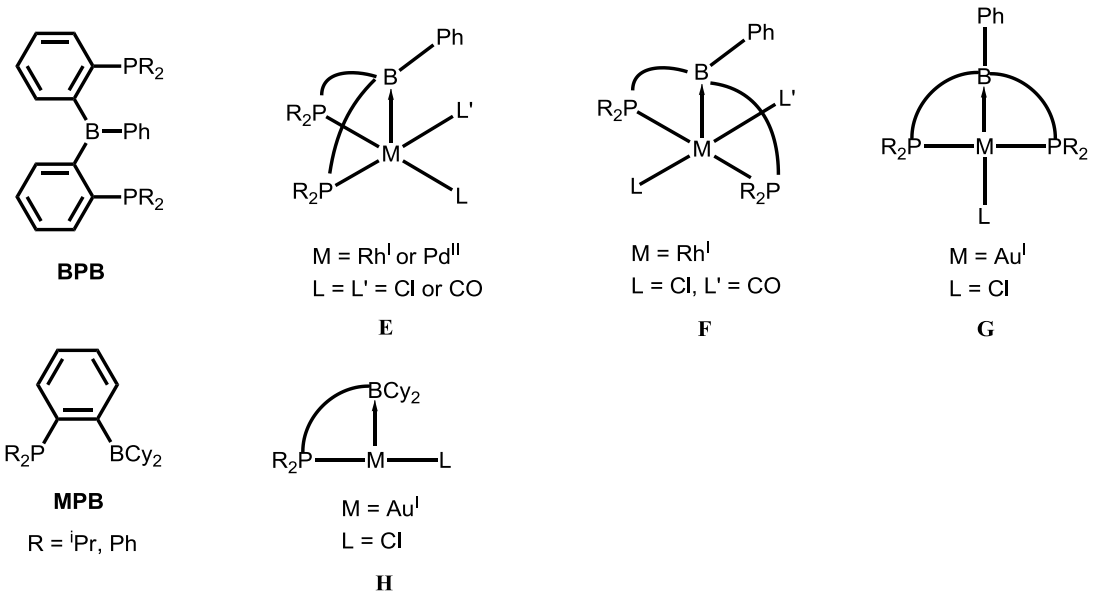

Figure 5-4. Phosphinophenyl-borane complexes with M→B interactions.

With the synthesis of stable metallaboratrane complexes, it became possible to explore their reactivity. Oxidative cleavage of metal boron bonds have been reported on Fe and Ni compounds (Scheme 5-1).[168c,d] Moderate and strong oxidants, such as XeF_2, $CHBr_3$ or $[PhC(O)O]_2$ were employed to oxidatively cleave Fe-B or Ni-B bonds to form corresponding haloborate metal halides. In all cases, the more electron-withdrawing halogens prefer to bind with boron center. Peters and coworkers recently reported the synthesis of Fe imide from the iron boratrane complex via redox chemistry with a metallaboratrane complex (Scheme 5-2).[174]

Scheme 5-1. Oxidative cleavage of the M-B bond in Ni and Fe boratrane complexes.

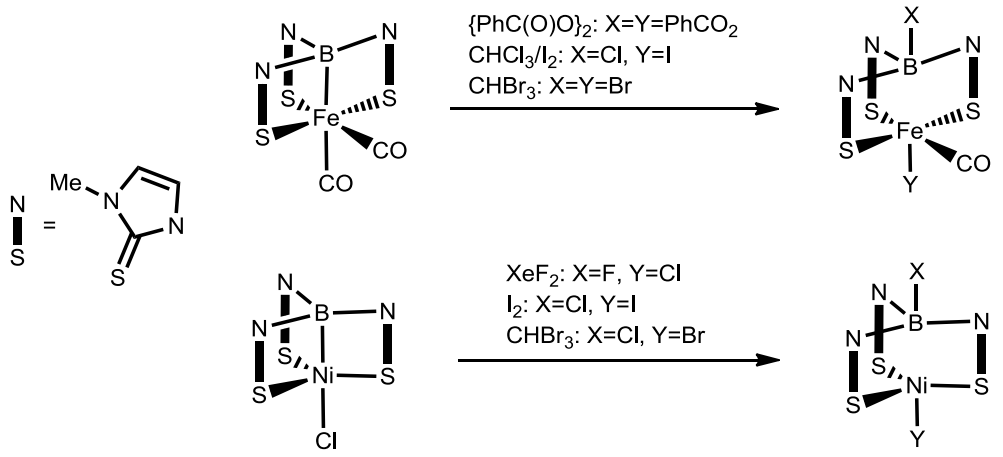

Scheme 5-2. Synthesis of iron imide.

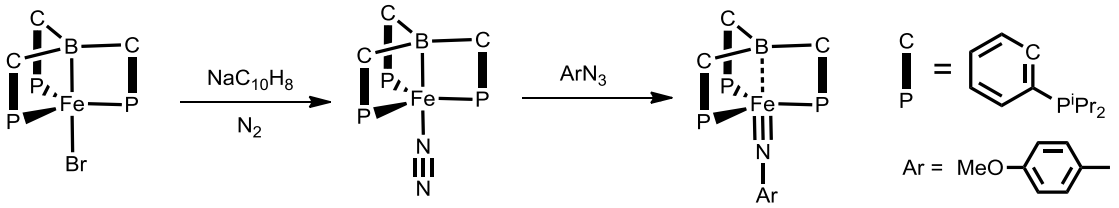

5.2 Results and Discussion

5.2.1 Synthesis and Characterization of Group 10 Metal Boratranes with Triphosphino-borane (TPB) Ligand.

We are interested in the synthesis of a series of (TPB)M complexes(M = Ni, Pd, Pt), so that we could evaluate the effect of cage structure on the metal borane interactions. The nickel boratrane **501** was readily obtained by reaction of **209** with [Ni(cod)$_2$] at 80

°C in toluene for 6 h (Scheme 5-3). After removal of the volatiles and washing with pentane, complex **501** was isolated in 82% yield. The unique signal observed at 35.0 ppm in the ^{31}P NMR spectrum and two distinctive sets of resonances for *iso*-propyl groups in the ^{1}H NMR spectrum of **501** are consistent with symmetric coordination of the three phosphorus atoms and C_3 symmetry of the molecule in solution. The high-field ^{11}B NMR chemical shift at 15.9 ppm strongly suggests the presence of a dative Ni→B interaction.[175] The related palladium boratrane **502** was isolated in 80% yield via reaction of **209** with $Pd(P^tBu_3)_2$ at room temperature for 6 h. Thermolysis of sterically hindered $Pt(P^tBu_3)_2$ with **209** in toluene at 100°C for 7 days led to the formation of **503** which was isolated as a red powder in 72% yield. The spectroscopic data of **502** and **503** displayed high similarity to that of **501** with ^{11}B NMR chemical shift at 27.3 and 15.9 ppm respectively, which indicates strong metal→B interaction. The spectroscopic features of **501**, **502** and **503** were summarized in Table 5-2.

Scheme 5-3. Synthesis of group 10 metal boratranes.

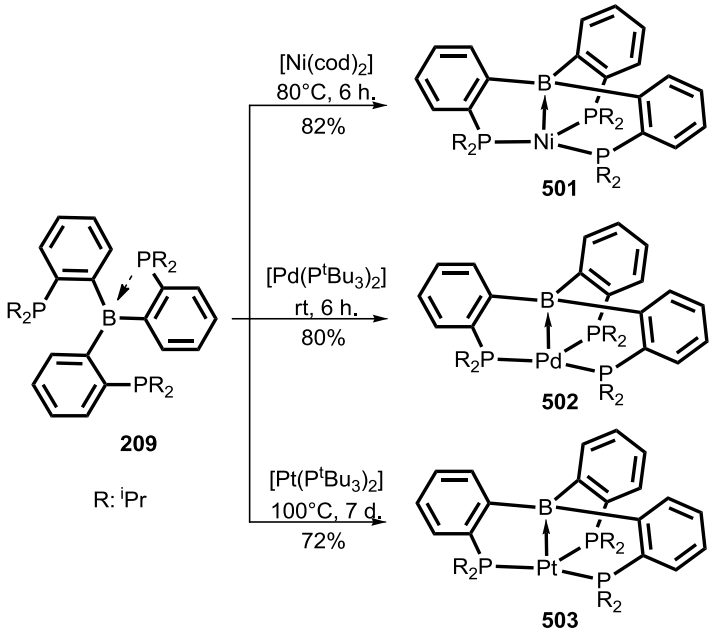

X-ray quality crystals of **501**, **502** [176] and **503** [177] were obtained from the corresponding toluene/pentane solution at -35 °C (Figures 5-5, 5-6 and 5-7). The overall structure of **501**, **502** and **503** are consistent with their observed NMR data, with the metal center adopting a trigonal pyramidal geometry and only slightly deviating from the basal plane formed by the three phosphorus atoms. The structural features of **501**, **502** and **503** were summarized in the table of p. 167.

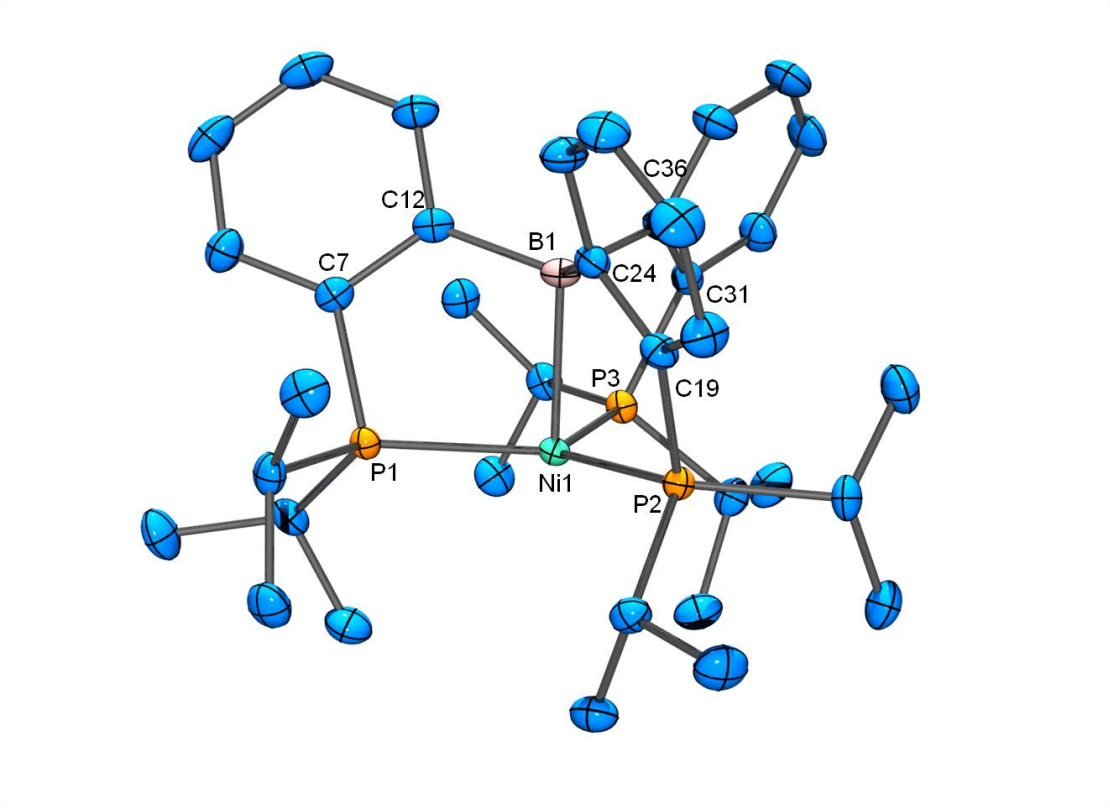

Figure 5-5. ORTEP[128] drawing (50% probability ellipsoids) of **501.** Omitted for clarity: H atoms and toluene molecule.

Selected distance (Å) and angles (deg) follow: Ni1-B1, 2.168(2); Ni1-P1, 2.2043(7); Ni1-P2: 2.1944(5); Ni1-P3. 2.1977(5); B1-Cl2, 1.613(3); B1-C24, 1.616(2); B1-C36, 1.618(2); P1-Ni1-B1, 87.96(5); P2-Ni1-B1, 86.85(5); P3-Ni1-B1, 87.17(5); P1-Ni1-P2, 119.53(3); P1-Ni1-P3, 119.90(3); P2-Ni1-P3, 119.93(3); Ni1-B1-C12, 104.8(1); Ni1-B1-C24, 106.1(1); Ni1-B1-C36, 106.0(1); Ni1-P1-C7, 102.42(5); Ni1-P2-C19, 103.49(5); Ni1-P3-C31, 103.05(5).

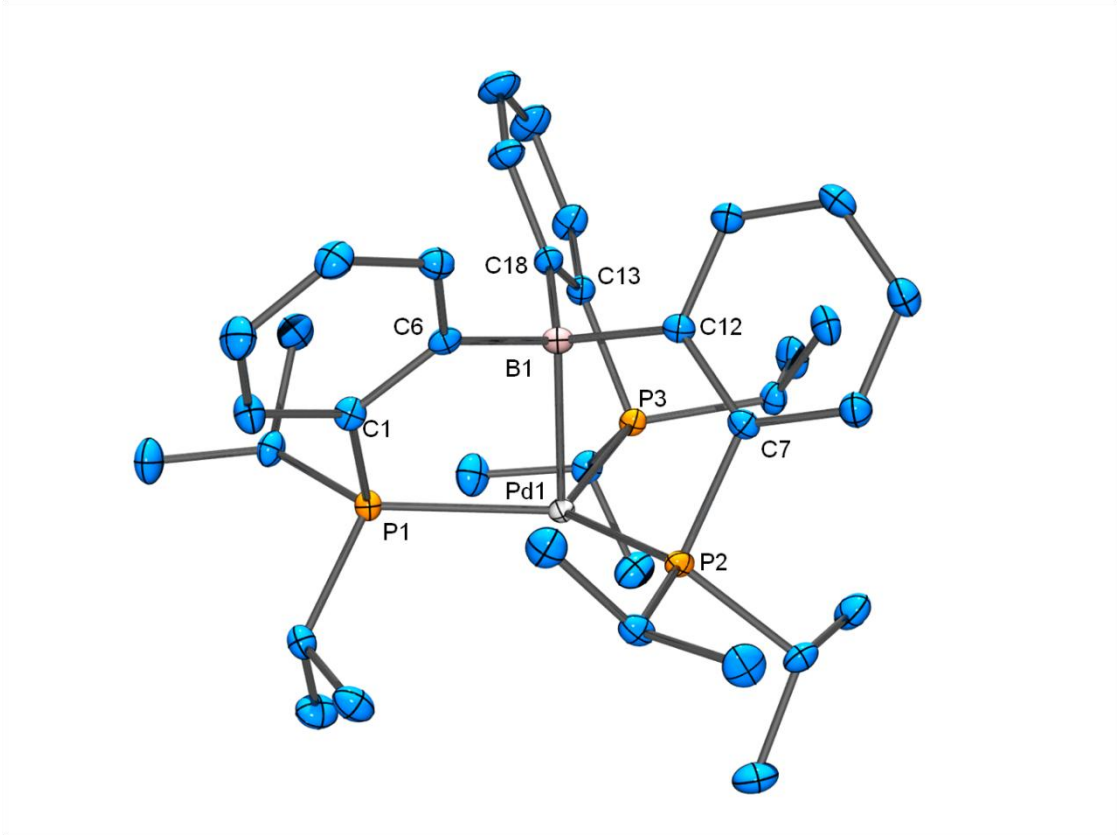

Figure 5-6. ORTEP[128] drawing (50% probability ellipsoids) of **502.** Omitted for clarity: H atoms.

Selected distance (Å) and angles (deg) follow: Pd1-B1, 2.254(2); Pd1-P1, 2.3470(5); Pd1-P2: 2.3527(4); Pd1-P3. 2.3459(6); B1-C6, 1.621(4); B1-C12, 1.624(2); B1-Cl8, 1.626(3); P1-Pd1-B1, 85.63(5); P2-Pd1-B1, 84.78(5); P3-Pd1-B1, 84.82(5); P1-Pd1-P2, 117.42(2); P1-Pd1-P3, 120.28(2); P2-Pd1-P3, 120.11(2); Pd1-B1-C6, 104.3(1); Pd1-B1-C12, 104.4(1); Pd1-B1-C18, 104.8(1); Pd1-P1-C1, 100.21(6); Pd1-P2-C7, 99.87(6); Pd1-P3-C13, 100.44(6).

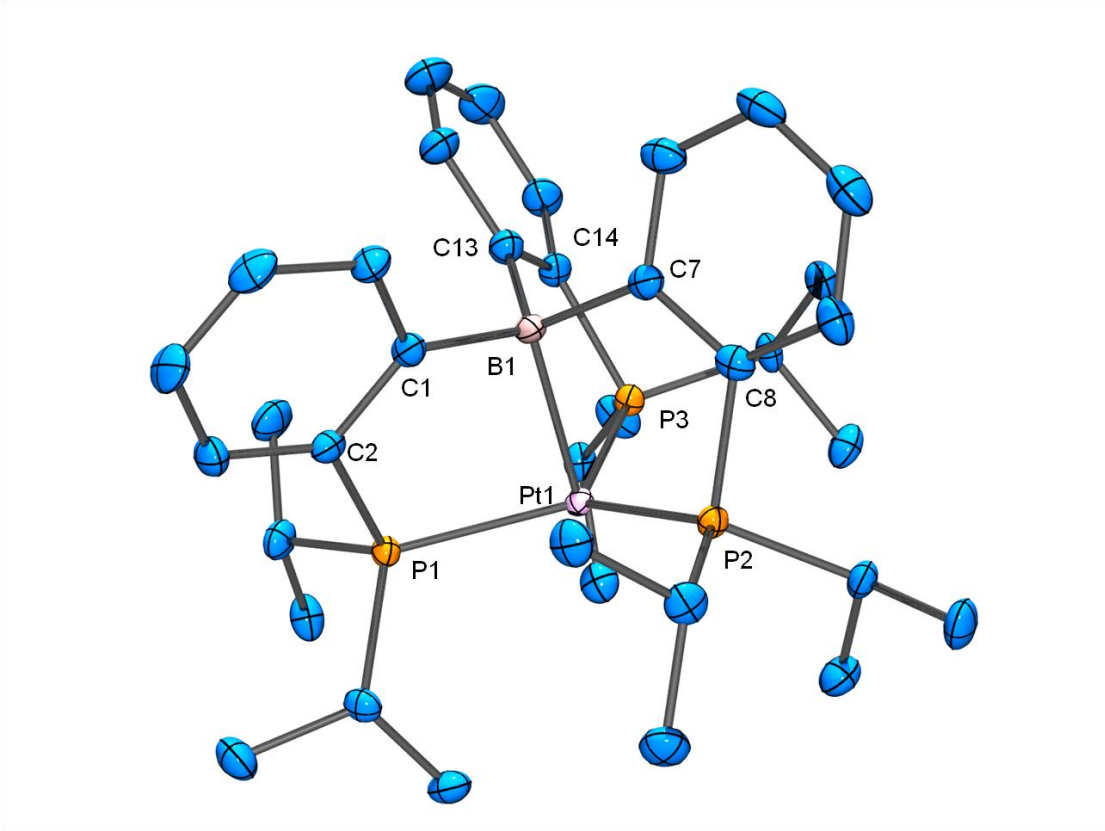

Figure 5-7. ORTEP[128] drawing (50% probability ellipsoids) of **503.** Omitted for clarity: H atoms and toluene molecule.

Selected distance (Å) and angles (deg) follow: Pt1-B1, 2.223(4); Pt1-P1, 2.300(1); Pt1-P2: 2.294(1); Pt1-P3. 2.294(1); B1-Cl, 1.618(6); B1-C7, 1.625(6); B1-Cl3, 1.625(5); P1-Pt1-B1, 86.0(1); P2-Pt1-B1, 85.6(1); P3-Pt1-B1, 85.6(1); P1-Pt1-P2, 119.82(4); P1-Pt1-P3, 118.92(4); P2-Pt1-P3, 119.62(4); Pt1-B1-C1, 106.1(2); Pt1-B1-C7, 106.4(2); Pt1-B1-C13, 106.7(2); Pt1-P1-C2, 102.8(1); Pt1-P2-C8, 102.7(1); Pt1-P3-C14, 103.0(1).

5.2.2 Comparison of TPB Group 10 Metal Complexes

M-B distances are one reflection of the strength of M→B interaction, however M-B distances are largely dependent on the sizes of the metals as well. In order to take into account the different sizes of the metals involved, these MB distances were compared with the sum of covalent atomic radii, which have been recently revisited by S. Alvarez and coworkers.[178] Accordingly, the ratio r = d(M-B) / $\Sigma(R_{cov})$ only slightly exceeds 1 for all complexes (Table 5-1), which suggests rather strong M→B dative interaction in our group 10 metallaboratranes. However, in these cases the MB bond length cannot be considered a reliable parameter to compare the magnitude of these M→B interactions due to the existence of the cage structure.

Table 5-1. Structural data for the group 10 metal boratranes.

	501	**502**	**503**
M-B bond length (Å)	2.168(2)	2.254(2)	2.223(4)
r[a]	1.04	1.01	1.01
ΣB_α	339.1°	341.8°	336.7°
torsion angle q	26.2°.	28.3°.	24.3°.
D_1[b] (Å)	0.102	0.202	0.171
D_2[c] (Å)	0.435	0.407	0.458

[a]: r = d(M-B) / $\Sigma(R_{cov})$; [b]: D_1 represents the distance between metal center and the plane formed by three phosphorus atoms; [b]: D_2 represents the distance between boron center and the plane formed by three *ipso* carbons.

The pyramidalization of the boron environment was employed to estimate the degree of M→B interaction independently of the size of the metal. In all of the metal boratranes **501-503**, the geometry around boron strongly deviates from planarity, with ΣB_α ranging from 336 to 342° and the distance from boron center to the plane formed by three *ipso*-Carbons (D_2) ranging from 0.407-0.458 Å. The slight decrease of ΣB_α from Pd (341.8°), to Ni (339.1°), and Pt (336.7°) is consistent with the increase of the D_2 from Pd (0.407 Å), to Ni (0.435 Å), and Pt (0.458 Å). The structure information indicates the strength of M→B interaction increases in the order of Pd, Ni and Pt.[179]

The ^{11}B NMR chemical shift can also be considered an interesting spectroscopic probe for the interaction of boranes with Lewis bases. Generally speaking, relatively high field ^{11}B chemical shift (20-50 ppm) represents higher degree of shielding for the boron center, which is a result from the stronger M→B interaction. The ^{11}B chemical shifts of our group 10 metallaboratranes fall in the range from 15 ppm to 28 ppm (Table 5-2), which are rather high filed compared to metallaboratranes known in the literatures.[169,173] The spectroscopic data further supports the presence of strong M→B interactions in the group 10 metal boratranes. In addition, the slightly higher ^{11}B NMR chemical shift obtained for the Pd complex **3** (27.3 ppm compared with 18.2 ppm for the Pt complex **4**, and with 15.9 ppm for the Ni complex **2**) suggests that the Pd→B interaction would be somewhat weaker than Pt→B and Ni→B interactions.

Table 5-2. Spectroscopic features for the group 10 metal boratranes.

	501	**502**	**503**
^{31}P (δ, ppm)	35	41.3	79.4
^{11}B (δ, ppm)	15.9	27.3	15.9

All of the metallaboratranes we obtained adopt trigonal pyramidal geometry, which is fairly unusual for four coordinated group 10 metal complexes. One early example of such geometry was reported by Pierpont with their $(PPh_3)_3Pt(SO_2)$ complex.[180] In their case, the platinum center is 0.33 Å away from the plane formed by three phosphorus atoms, which is much longer than the platinum to plane distance at 0.171 Å in **503**. Therefore, our metallaboratranes adopt a structure closer to a standard trigonal pyramidal geometry which is forced by the rigid cage structure.

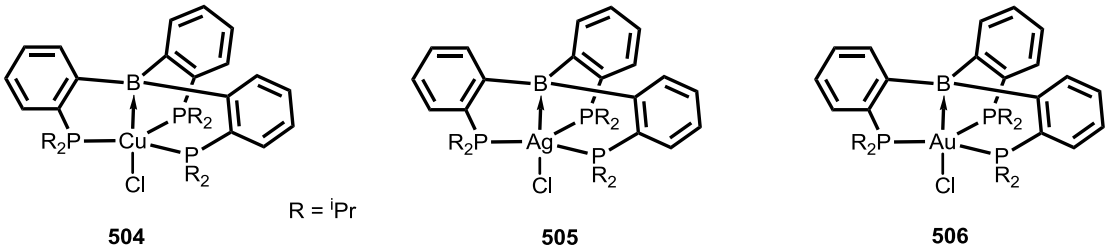

Figure 5-8. Group 11 metallaboratranes.

Compared to the isoelectronic group 11 metallaboratranes with the same ligand set (Figure 5-8),[181] group 10 metallaboratranes display stronger M→B interactions than the group 11 analogs based on structural information (Table 5-3). The variation is rather pronounced for the Ni/Cu and Pd/Ag, but much less significant for the Pt/Au.

Table 5-3. Structural data for the group 11 metal boratranes.

	504	**505**	**506**
M-B bond length	2.508(2)	2.540(2)	2.318(8)
r[a]	1.16	1.11	1.05
ΣB_α	347.0°	347.4°	339.3°
torsion angle q	29.4°	29.8°	27.0°

[a]: $r = d(M\text{-}B) / \Sigma(R_{cov})$.

5.3 Conclusion

In summary, a series of group 10 metal boratranes was synthesized and spectroscopically and structurally characterized with the aim of extending further the scope of M→B interactions. **TPB** ligand was shown to form robust boratrane complexes which exhibited M→B interaction. All metal boratrane species were found to adopt a trigonal pyramidal geometry with only a marginal deviation from the basal plane formed by the three phosphorus atoms which was likely largely imposed by the cage structure of TPB. Pt was shown to form stronger M→B interactions than their lighter analogs. Compared to the isoelectronic group 11 metallaboratranes, stronger M→B interactions were found with the metals with lower oxidation state.

5.4 Experimental Details

General considerations. Unless specified otherwise, all reactions and manipulations were carried out under an argon atmosphere using glove box or Schlenk line techniques. Dry, oxygen–free solvents were employed. Toluene, Pentane, diethyl ether, THF and

C_6D_6 were dried over NaK–/Ph_2CO–/18-crown-6, distilled and stored over molecular sieves in an Ar-filled glove box. $Ni(COD)_2$, $Pd(PBu^t_3)_2$ and $Pt(PBu^t_3)_2$ were purchase from Strem and used as received. Synthesis of ligand **204** was described in Chapter II. All other chemicals were used as received from commercial vendors unless otherwise noted.

Physical Methods. NMR spectra were recorded on a Varian iNova 400 spectrometer (^{1}H NMR, 400.0 MHz, ^{13}C NMR, 100.5 MHz, ^{31}P NMR, 161.9 MHz) and a Varian iNova 500 spectrometer (^{11}B NMR, 160.5 MHz) in noted solvents. Chemical shifts are given in δ (ppm). ^{11}B NMR spectra were referenced externally with BF_3 etherate at δ 0. ^{31}P NMR spectra were referenced externally with 85% phosphoric acid at δ 0. ^{1}H NMR and ^{13}C NMR spectra were referenced using the solvent signals. Elemental analyses were performed by CALI, Inc. (Parsippany, NJ). UV-vis spectra of complexes **501**, **502**, **503** were collected by Bourissou group. The solid state structure of **502** and **503** were solved by Prof. Bruce M. Foxman and Dr. Chun-Hsing Chen.

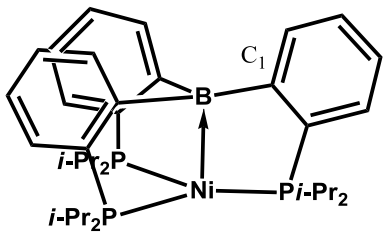

Synthesis of (TPB)Ni (501). To a solution of $Ni(COD)_2$ (54.7 mg, 0.20 mmol) in toluene (2 mL) was added TPB (117 mg, 0.20 mmol) at room temperature. After subsequent stirring for 6 hours at 80°C, volatiles were removed and the residue was

washed with 3 times 2 mL of cold n-pentane. Dark blue powder of (TPB)Ni (106.5 mg, 82%) was obtained from a saturated toluene solution at -35 °C. X-ray quality crystals were obtained by recrystallization from a toluene/pentane mixed solution at -35°C. $^{31}P\{^{1}H\}$ NMR (161.8 MHz, 296 K, C_6D_6): δ 35.0. $^{11}B\{^{1}H\}$ NMR (160.5 MHz, 298 K, C_6D_6): δ 15.9. $^{13}C\{^{1}H\}$ NMR (100.5 MHz, 296 K, C_6D_6): δ 164.3 (br, C_1), 140.2 (m, aromatic-C), 129.7 (m, aromatic-C), 127.9(s, aromatic-C), 127.6(s, aromatic-C), 124.6(s, aromatic-C), 29.7 (br, *C*HCH$_3$), 27.3 (br, *C*HCH$_3$), 25.8 (br, CH*C*H$_3$), 19.9 (br, CH*C*H$_3$), 19.4 (br, 2CH*C*H$_3$). ^{1}H NMR (399.8 MHz, 296 K, C_6D_6): δ 7.48 (br, 3H; aromatic-H), 7.28 (br, 3H; aromatic-H), 7.04 (br, 6H; aromatic-H), 2.66 (br, 3H, C*H*CH$_3$), 2.28 (br, 3H, C*H*CH$_3$),1.39 (br, 9H, CHC*H*$_3$), 1.29 (br, 9H, CHC*H*$_3$), 1.05 (br, 9H, CHC*H*$_3$), 0.34 (br, 9H, CHC*H*$_3$).

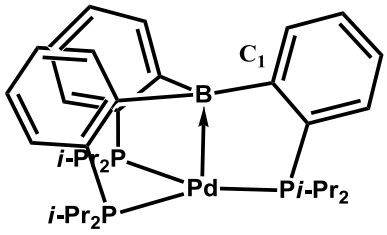

Synthesis of (TPB)Pd (502). To a solution of Pd(PBu$^{t}_3$)$_2$ (53.8 mg, 0.106 mmol) in toluene (2 mL) was added TPB (68.3 mg, 0.116 mmol) at room temperature. After subsequent stirring for 6 hours at room temperature, volatiles were removed and the residue was washed with 3 times 2 mL of cold n-pentane. Red powder of (TPB)Pd (58.5 mg, 80%) was obtained from a saturated toluene solution at -35°C. X-ray quality crystals were obtained by recrystallization from a toluene/pentane mixed solution at -35°C. $^{31}P\{^{1}H\}$ NMR (161.8 MHz, 296 K, C_6D_6): δ 41.3. $^{11}B\{^{1}H\}$ NMR (160.5 MHz, 298 K,

C_6D_6): δ 27.3. $^{13}C\{^1H\}$ NMR (100.5 MHz, 296 K, C_6D_6): δ 167.2 (br, C_1), 138.5 (m, aromatic-C), 133.2 (m, aromatic-C), 129.1(s, aromatic-C), 125.0(s, aromatic-C), 28.6(br, *C*HCH$_3$), 27.9 (br, *C*HCH$_3$), 24.0 (br, CH*C*H$_3$), 20.2 (br, CH*C*H$_3$), 19.9 (br, CH*C*H$_3$), 19.0 (br, CH*C*H$_3$); ^1H NMR (399.8 MHz, 296 K, C_6D_6): δ 7.35 (m, 6H; aromatic-H), 7.05 (m, 6H; aromatic-H), 2.44 (br, 3H, C*H*CH$_3$), 2.17 (br, 3H, C*H*CH$_3$), 1.43 (br, 9H, CHC*H*$_3$), 1.31 (br, 9H, CHC*H*$_3$), 0.78 (br, 9H, CHC*H*$_3$), 0.55 (br, 9H, CHC*H*$_3$). (One carbon resonance in aromatic range might be overlapped with the solvent peak.)

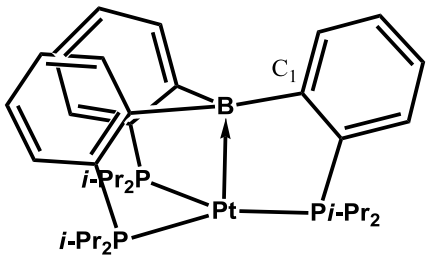

Synthesis of (TPB)Pt (503). To a solution of $Pt(Bu^t_3)_2$ (51.5 mg, 0.086 mmol) in toluene (5 mL) was added TPB **1** (55 mg, 0.094 mmol) at room temperature. After subsequent stirring for 7 days at 100 °C, volatiles were removed and the residue was washed with 3x2 mL of cold n-pentane. Red powder of (TPB)Pt **3** (48 mg, 72%) were obtained from a saturated toluene solution at -35 °C. Red crystals of **3** were obtained from a toluene/pentane mixed solution at -35 °C. $^{31}P\{^1H\}$ NMR (161.8 MHz, 296 K, C_6D_6): δ 79.4 ($^1J_{P\text{-}Pt}$=3578Hz). $^{11}B\{^1H\}$ NMR (160.5 MHz, 298 K, C_6D_6): δ 18.2. $^{13}C\{^1H\}$ NMR (100.5 MHz, 296 K, C_6D_6): δ 164.8 (br, C_1), 138.9 (m, aromatic-C), 130.0 (m, aromatic-C), 124.1 (s, aromatic-C), 34.1 (br, *C*HCH$_3$), 29.4 (br, *C*HCH$_3$), 23.4 (br, CH*C*H$_3$), 20.4 (br, CH*C*H$_3$), 19.3 (br, CH*C*H$_3$), 18.9 (br, CH*C*H$_3$). ^1H NMR (399.8 MHz, 296 K,

C_6D_6): δ 7.52 (d, 3H, $^3J_{H\text{-}H}$ = 7.6 Hz; H_6), 7.43 (br, 3H; H_3), 7.05 (m, 6H; H_4 and H_5), 2.65 (br, 6H, C*H*CH_3), 1.38 (br, 18H, CHC*H*$_3$), 0.96 (br, 9H, CHC*H*$_3$), 0.34 (br, 9H, CHC*H*$_3$).

CHAPTER VI

SYNTHESIS AND REACTIVITY OF PINCER PSiP LIGANDS AND OF THEIR METAL COMPLEXES WITH Pd AND Pt

6.1 Introduction

6.1.1 Pincer Ligands with Silicon as the Central Donor Atom

Phosphine based "PCP" ligand have been the subject of intense study for the past thirty years, due to their superb stoichiometric and catalytic reactivity.[4,5] On the other hand, only a few examples have been reported with the PSiP type of ligand, which contains flanking phosphine arms and a central silyl donor (Scheme 6-1). Stobart and coworkers pioneered the area of polydentate silyl ligands with a series of late transition metal complexes with bi, tri, and tetradentate phosphinosilyl ligands (Scheme 6-2).[112] A tetradentate SiP_3 ligand was reported by the Peters group (**D**, Scheme 6-2), which was used to form unusual Ru(I) and Os(I) complexes.[182] In 2007 Turculet and coworkers reported a pincer "PSiP" ligand with a rigid diphenylsilyl framework (Scheme 6-3).[17a] Access to different substituents on the silicon center and phosphine arms on these "PSiP" ligands provides tunability on both electronic and steric properties of the resulting metal complexes,[17,124] which have already been used as the catalyst in some catalytic transformations, such as dehydrogenative borylation and hydrocarboxylation of allenes with CO_2.[17f,g]

Scheme 6-1. PSiP (silyl) and P_2Si= (silylene) metal complexes.

Scheme 6-2. Metal complexes with bi, tri, and tetradentate phosphinosilyl ligands.

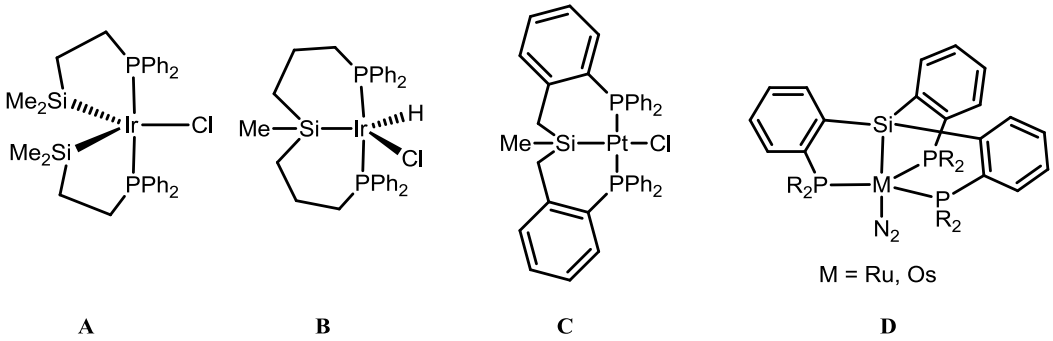

Scheme 6-3. PSiP ligands with diphenylsilyl backbone.

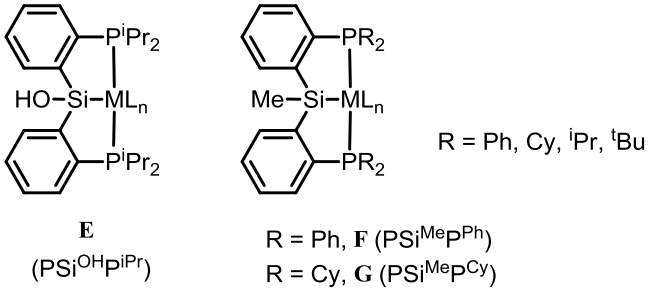

In theory, incorporation of strongly *σ*-donating and *trans*-labilizing silyl ligand may promote the formation of coordinatively unsaturated complexes which were often proposed as the reactive intermediates for (PCP)Ir and (PNP)Rh (for PCP and PNP ligand framework, see scheme 1-1 A and **D**) mediated oxidative addition reactions (Scheme 6-4).[33,183] These assumptions have recently been materialized by reports of C-H and N-H bond oxidative addition reactions by (PSiP)Ir complexes via unsaturated 14ē intermediates (Scheme 6-5).[9c,17b]

Scheme 6-4. Single bond activation via 14ē metal complexes as intermediates.

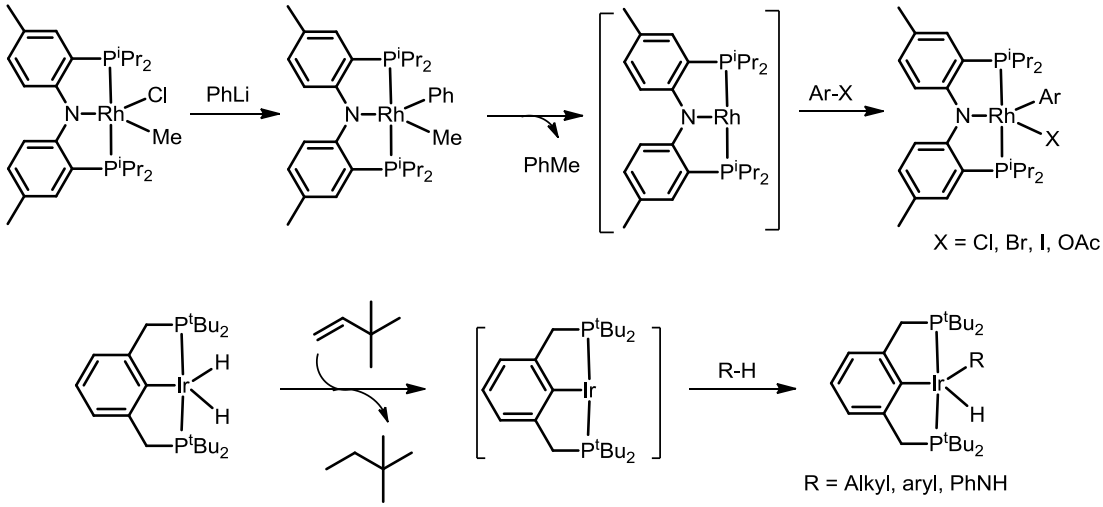

Scheme 6-5. Bond activation mediated by PSiP metal species.

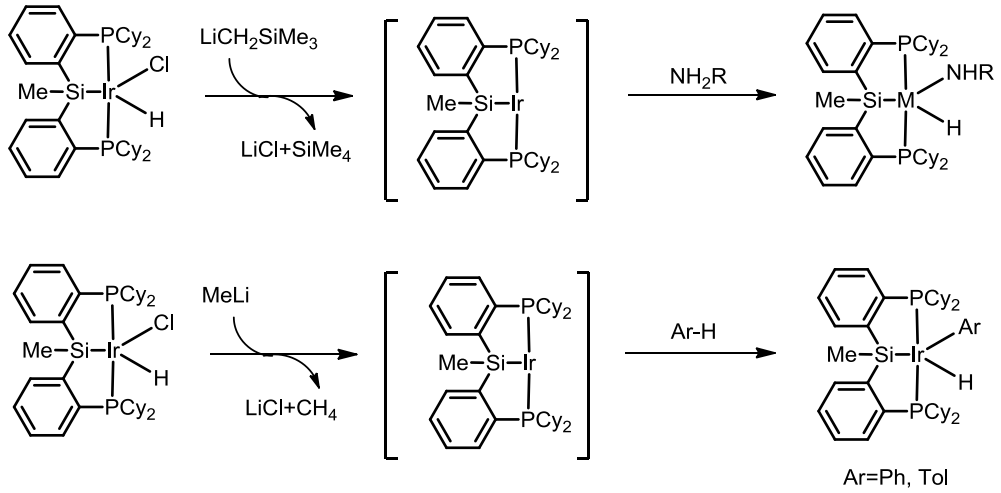

Unlike the pincer silyl species, pincer metal complexes featuring a silylene donor in the pincer remain unknown (Scheme 6-1). The silylene ligand in pincer complexes will feature σ-donor and π-acceptor property as well as strong Lewis acidity on silicon center.[118]

6.1.2 Metal Silylene Species

Carbene ligands are one of the most versatile and fruitful ligands in organometallic chemistry.[113] The importance of metal carbene compounds was highlighted by the 2005 Nobel Prize in chemistry for their use in olefin metathesis reactions.[184] Motivated by the close analogy of carbon and silicon,[185] metal silylene compounds have been targeted since the 1960s.[118] Free silylenes are electron-deficient species, with only six electrons in the outer shell of silicon (Figure 6-1). Therefore, silylenes are highly electrophilic in their reactions, especially when they have electron withdrawing substituents.[186]

Compared to carbene species, silylenes display higher Lewis acidity in reactions, for two key reasons: i) Silicon is more electropositive[187] (1.8 vs 2.5 for carbon), which localizes the partial positive charge on the silicon center in the $R_2Si=$ species; ii) The size of silicon is significantly larger than that of carbon,[188] which makes its tendency toward higher coordination numbers much greater. Due to the high reactivity of the highly Lewis acidic silylene center, not until 1987 had the first so-called base-stabilized silylene compound been reported (Scheme 6-6).[189] Since then, base-stabilized silylene compounds have been prepared with many transition metals.[190] Most of these compounds possess relatively downfield ^{29}Si NMR resonances between 90-150 ppm.[118]

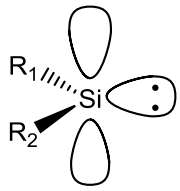

Figure 6-1. General scheme for silylene.

Scheme 6-6. Base-stabilized metal silylene species.

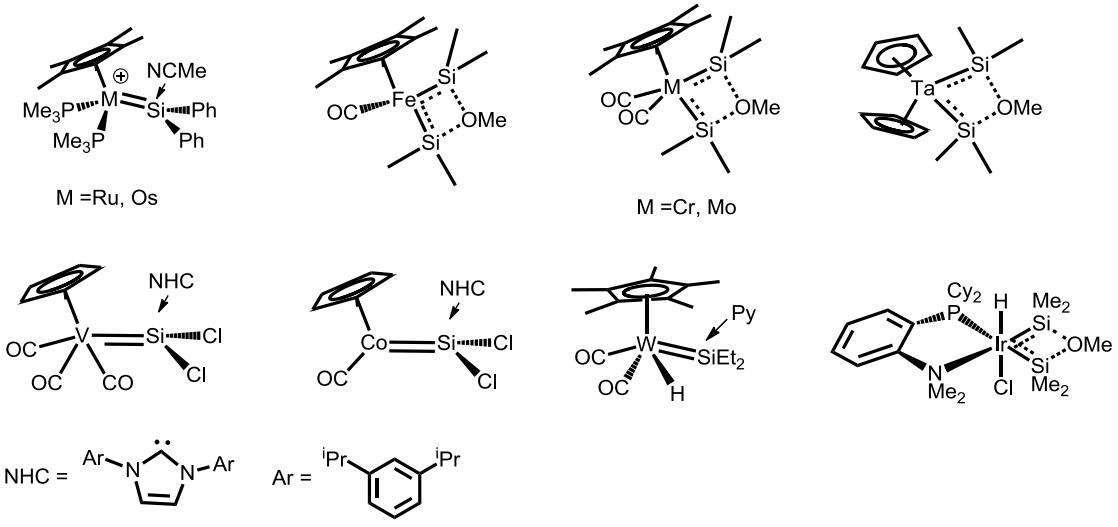

Significant progress in metal silylene chemistry came in 1990[191] when a base-free silylene compound was isolated with Ru (Scheme 6-7). In the ruthenium case, the thiolate group was employed to stabilize the cationic silylene species, which could donate electron to the empty p orbital on Si. Typical base-free metal silylene compounds possess a three-coordinate silicon center and their ^{29}Si NMR resonances are found at a characteristic downfield chemical shift, between 200-370 ppm.[118]

Scheme 6-7. Base-free ruthenium silylene species.

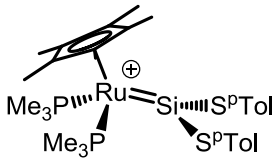

Scheme 6-8. Synthetic routes to silylene species.

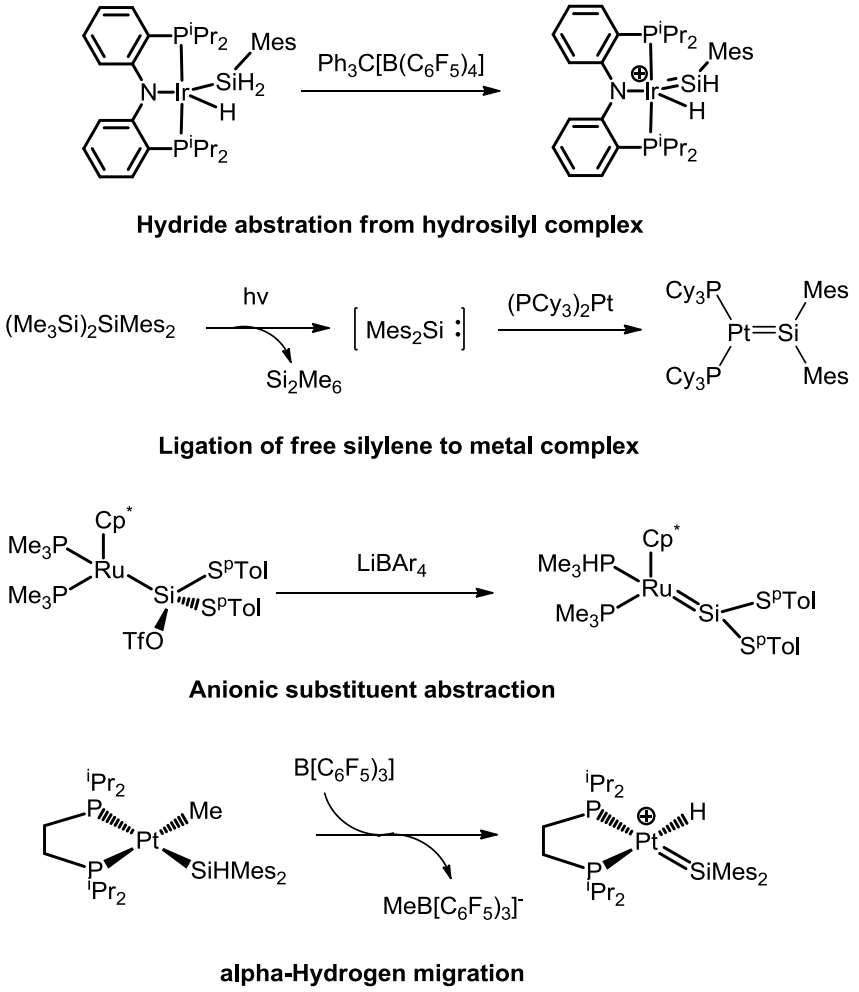

Typical synthetic routes to base-free metal silylene species are shown in Scheme 6-8.[118] Hydride abstraction, α-hydrogen migration or anionic substituent abstraction have been used to prepared metal silylene complexes with metals from group 8, 9 and 10. These approaches result in cationic (usually more electrophilic) silylene complexes. Therefore, weakly coordinating anions, such as BARF anions, are often used as the counterion for these silylene species.[192]

Scheme 6-9. Proposed route to access pincer silylene complexes.

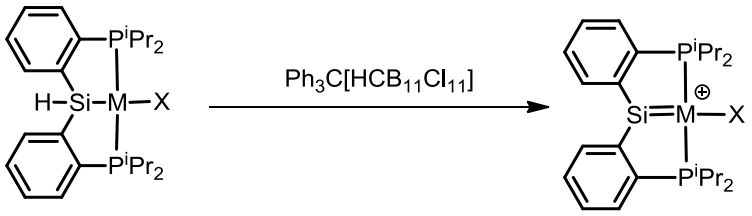

6.1.3 Reactivity of Silylene Complexes

Although some reactivities of metal silylene species show similarity to the corresponding metal carbene species, silylenes also display some unique reactivity due to the Lewis acidity at silicon center.[193] Cycloaddition reaction with unsaturated substrates, a common reaction for carbene species, is rare in the literature for silylene species.[10] One of the few examples of such reaction is a "2+2" cycloaddition reaction of cationic ruthenium silylene species with isocyanate (Scheme 6-10).[194] Interestingly, the same compound does not undergo "2+2" cycloaddition with ethylene. Mechanistic studies showed that the cycloaddition reaction with isocyanate was initiated by the coordination of isocyanate to the Lewis acidic silicon center via the lone pair of nitrogen, followed by the electron rich Ru(II) center adding to the CO group to form the metallacycle. The strong Lewis acidity of the silylene species also led to their reactions with various nucleophiles, such as water, alcohol and polar unsaturated compounds (Scheme 6-11).[192a,195]

Scheme 6-10. Cycloaddition reaction with metal silylene complexes.

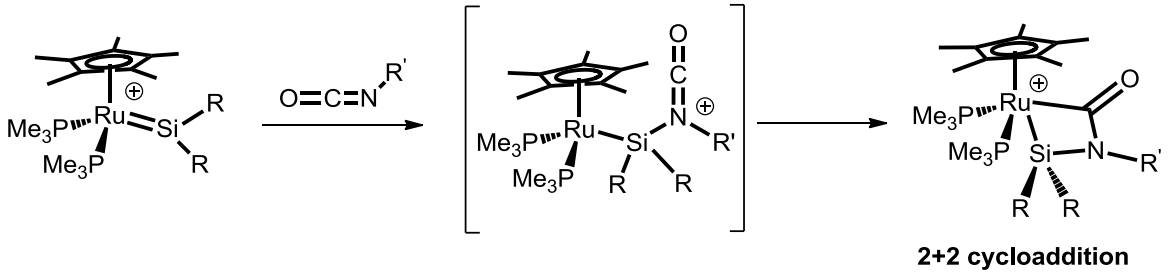

Scheme 6-11. Reactions of metal silylene with nucleophiles.

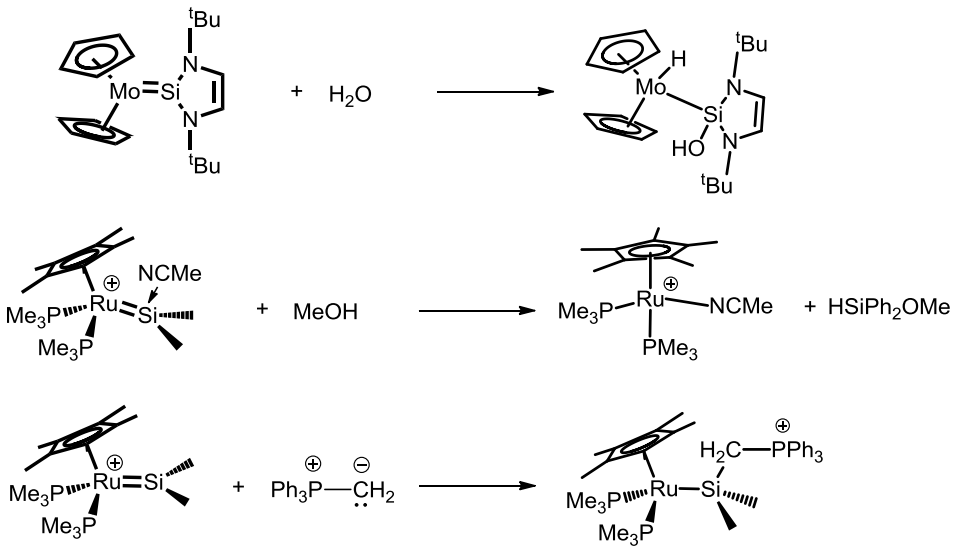

In contrast to the carbene complexes, only a few examples can be found in the literature about catalytic reactions mediated by metal silylene species. Most of these reactions center on the transfer of $SiMe_2$ group[196] as well as hydrosilylation of alkenes[197] and ketones.[198] An example of silylene-catalyzed $SiMe_2$ group transfer is shown in Scheme 6-12. Double $SiMe_2$ group transfer was accomplished with a Pd silylene compound as the catalyst. The first $SiMe_2$ group transfer was accomplished via 4+1

cycloaddition. The second $SiMe_2$ group transfer was accomplished by a sequence of oxidative addition of allylic C-H bond to Pd silylene, 1,2-migration and reductive elimination.[196d] Although Pd silylene species was not observed in this reaction, mechanistic study suggested it to be the active catalyst in this transformation.[196d]

Scheme 6-12. Catalytic reactions mediated by metal silylene species.

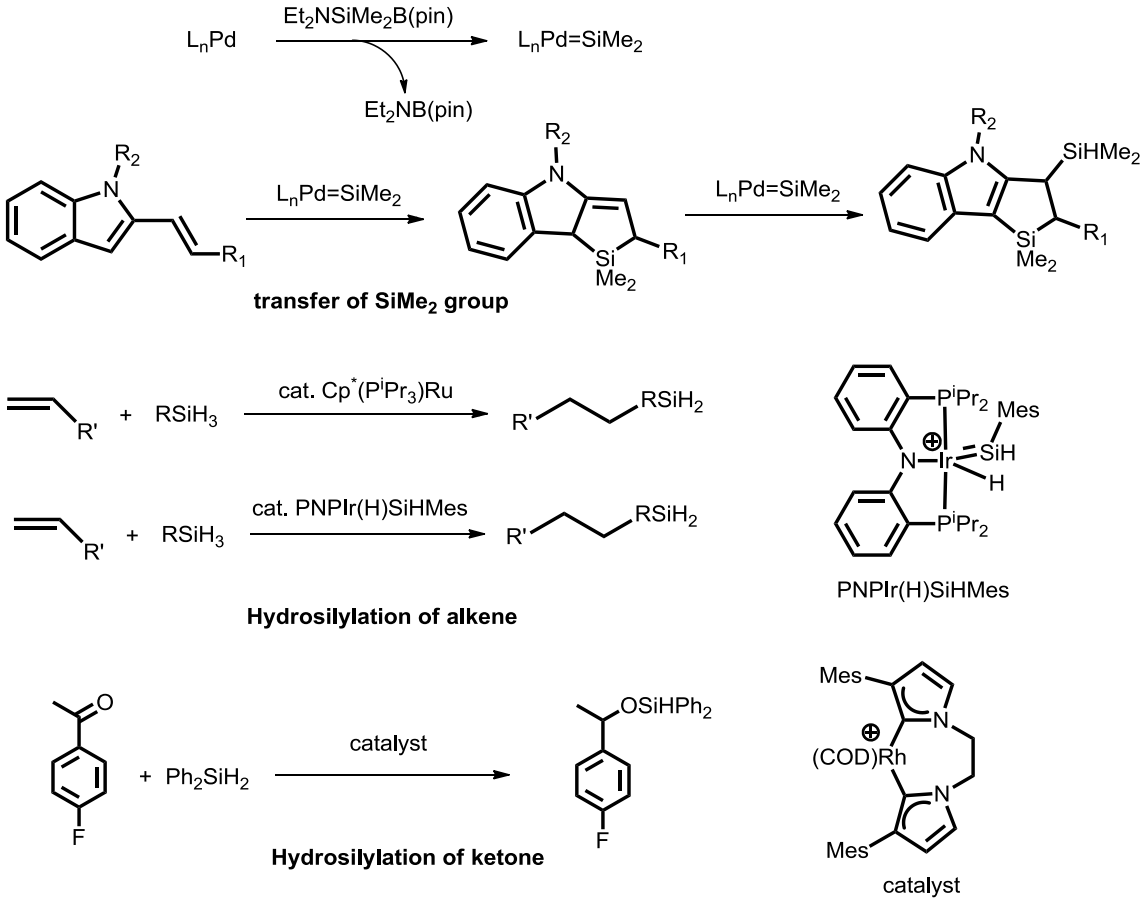

Hydrosilylation of alkenes or ketones is another type of catalytic transformation mediated by metal silylene species. As depicted in Scheme 6-12 hydrosilylation of alkene is catalyzed by either Ru silylene or Ir silylene species. Only primary silanes could be used as the silane in this reaction and only anti-Markovnikov products were obtained.[197a] Tilley and coworkers therefore proposed the following mechanism for this catalysis (Scheme 6-13) which featured double Si-H activation to form the silylene specie, direct insertion of alkene into the Si-H, 1,2-migration of the hydride and sequential reductive elimination.[197b] The key Si-C bond formation step was proposed to occur via a concerted addition process similar to B-C bond formation step in hydroboration of alkene.[199] Hydrosilylation of ketones with secondary silanes was reported to be catalyzed by a bis-carbene Rh(I) compound (Scheme 6-12). Although the Rh silylene compound was not isolated, experimental evidence was provided for the formation of the silylene intermediate.[198] The key step in this catalysis was the coordination of carbonyl to the electron deficient silylene silicon center.

Scheme 6-13. Proposed mechanism for the hydrosilylation of alkene catalyzed by Ru silylene complex.

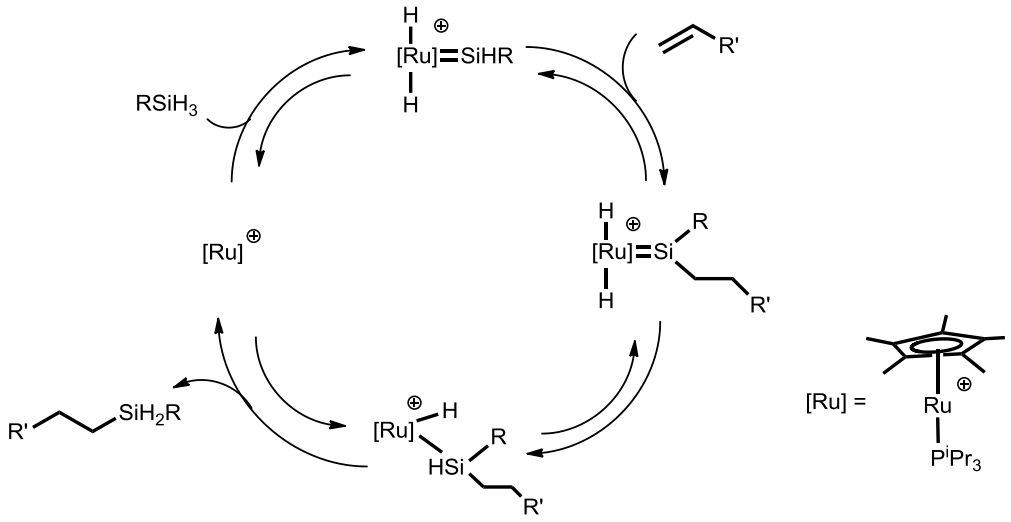

In this chapter, we decided to use hydride abstraction by $[Ph_3C][HCB_{11}Cl_{11}]$ to access a pincer P_2Si= metal complex with a silylene central donor (Scheme 6-9). Ph_3C^+ was shown previously to be able to abstract hydride from silanes[97] and $[HCB_{11}Cl_{11}]^-$ was shown in Chapter II to be a robust weakly coordinating anion partner for highly electrophilic cationic species.[63]

6.2 Results and Discussion

6.2.1 Synthesis of (PSiP)PtCl

(PSi^HP^{iPr})PtCl (**601**) was synthesized in 85% isolated yield via reaction of **207** with $Pt(COD)Cl_2$ in the presence of 2,6-lutidine (Scheme 6-14). Low reaction yield was observed when Et_3N was used as the base for this reaction, likely due to the decomposition to Pt metal. Notably, the key to reaching a high yield for this reaction

was the order of adding ligand **207** and base to the solution of metal precursors. If **207** was added before 2,6-lutidine, **602** was observed as the other product, presumably due to the reaction of HCl and the Si-H bond.[200] HCl was likely released from the of **207** and $Pt(COD)Cl_2$. **601** was characterized by multi-nuclear NMR spectroscopy, X-ray crystallography and elemental analysis. The $^1J_{Pt-P}$ at 2888 Hz is typical for *trans* phosphine ligands in cyclometalated Pt(II) complexes.[201] Virtual coupling for the isopropyl groups was observed in ^1H NMR spectra which indicated that the two phosphine groups were *trans* to each other.[23] Therefore the whole molecule adopts the square planar geometry common for d^8 16-electron metal complexes. Two different methine and four different methyl resonances were observed for the isopropyl groups on the phosphines, which indicated the molecule adopts C_s symmetry in solution.

Scheme 6-14. Synthetic procedure for $(PSi^HP^{iPr})PtCl$ (**601**).

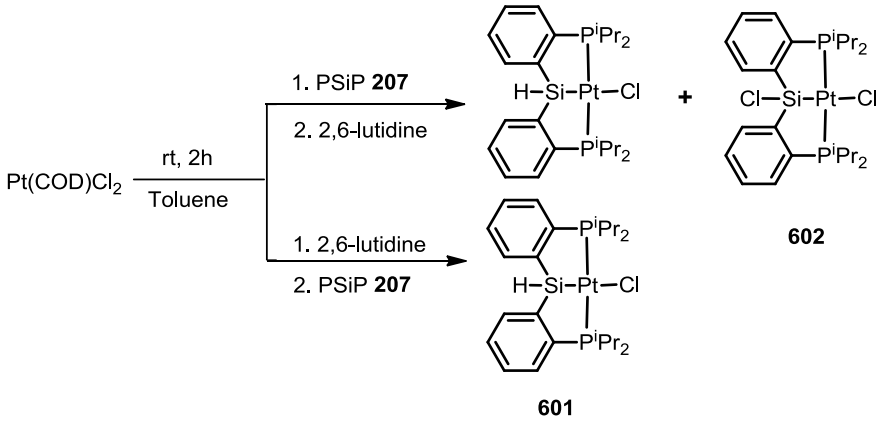

Crystals of **601** suitable for single-crystal X-ray diffraction were obtained by slow diffusion of pentane to a saturated toluene solution. The solid-state structure[202] of **601** is shown in Figure 6-2. The square planar geometry with C_s symmetry of **601** is consistent with the NMR data we observed. The sum of the bond angles of C1-Si-Pt, C7-Si-Pt and C1-Si-C7 is 330.7°, indicating the silicon center adopts a tetrahedral geometry. The Pt-Cl bond length at 2.452(2) Å and the Pt-Si bond length at 2.276(2) Å for **601** are similar to those in ($PSi^{OH}P^{iPr}$)PtCl[124] (2.47 Å for Pt-Cl, 2.277 Å for Pt-Si, (**E**)PtCl in Scheme 6-3) and ($PSi^{Me}P^{Ph}$)PtCl[17c] (2.44 Å for Pt-Cl, 2.278 Å for Pt-Si, (**F**)PtCl in Scheme 6-3).

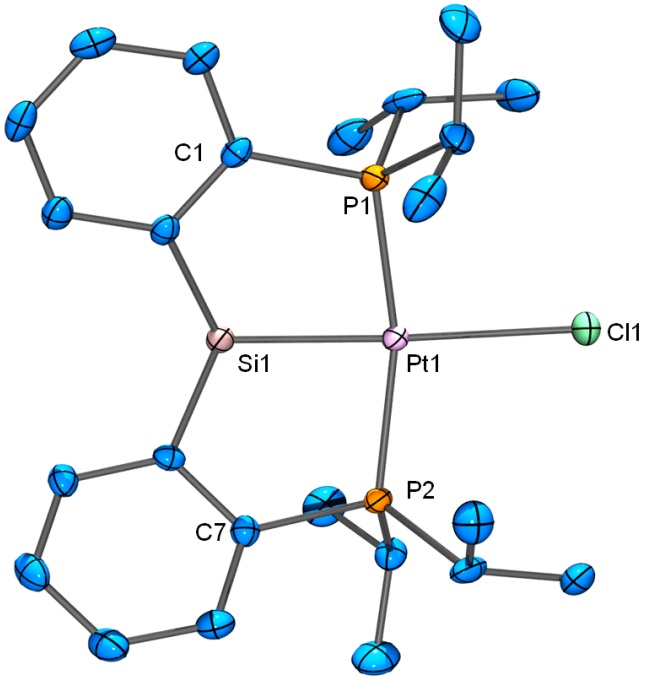

Figure 6-2. ORTEP[128] drawing (50% probability ellipsoids) of **601.** Omitted for clarity: H atoms. Selected distance (Å) and angles (deg) follow: Pt1-Si1, 2.276 (2); Pt1-P1, 2.297 (2); Pt1-P2: 2.296 (2); Pt1-Cl1, 2.452 (2); P1-Pt1-Si1, 84.41 (4); P2-Pt1-Si1, 84.05 (4); P1-Pt1-P2, 162.41 (4); C1-Si1-Pt1, 107.8 (1); C1-Si1-C7, 114.8

(2); C7-Si1-Pt1, 108.1 (1); Cl1-Pt1-Si1, 177.13 (4); Cl1-Pt-P2, 98.69 (4); Cl1-Pt-P1, 93.11 (4).

6.2.2 Synthesis of (PSiP)PtX

Scheme 6-14 depicts the methods we used to synthesize a series of (PSiP)PtX complexes from **601**. Pure ($PSi^{H}P^{iPr}$)PtI (**603**) was obtained via direct reaction with **601** and 10 equiv of iodotrimethylsilane (Me_3SiI). Smaller amounts (as low as 3 equiv) of Me_3SiI could be used to obtain clean **603**, if multiple cycles of addition of Me_3SiI and removal of volatiles were applied. **603** was isolated as a white powder in 61% yield after recrystallization from pentane at -35 ℃. ($PSi^{H}P^{iPr}$)PtOTf (**604**) was synthesized via direct reaction with **601** and 10 equiv of Me_3SiOTf. **604** was isolated as a white powder in 71% yield after workup.

Scheme 6-15. Synthesis of (PSiP)PtX compound from for **601**.

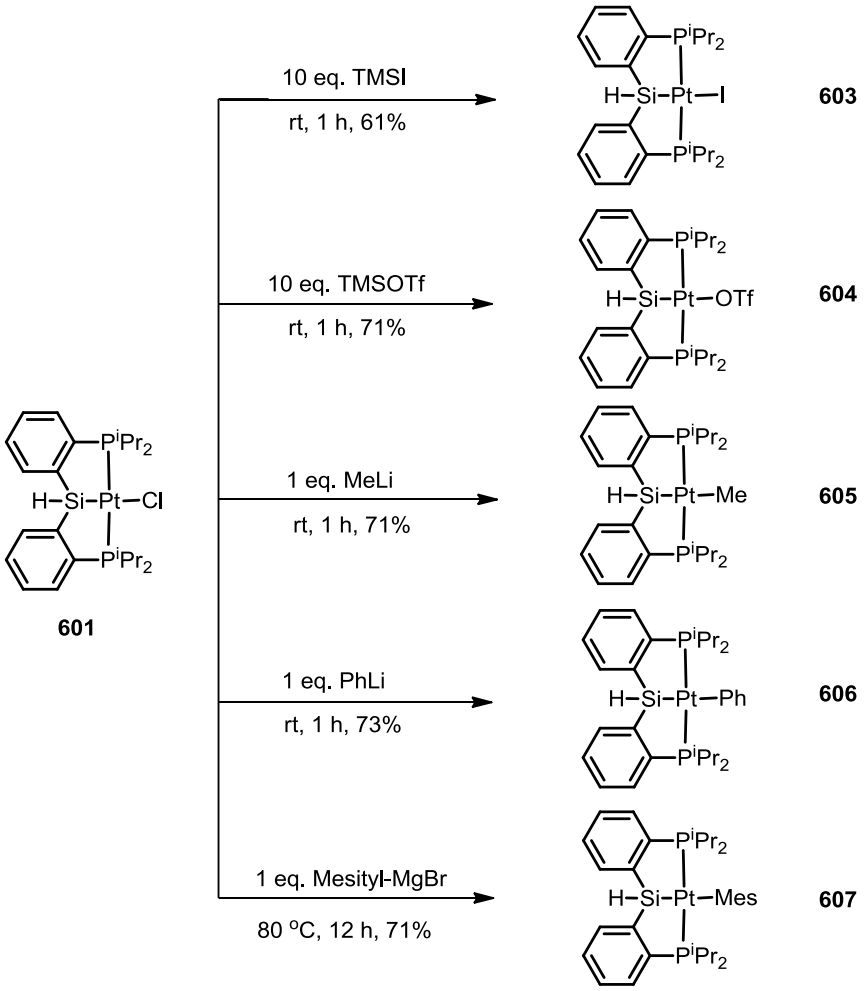

Complexes **605**, **606** and **607** were obtained via reactions of **601** with corresponding lithium reagents or Grignard Reagents. Metathesis of **601** with MeLi at room temperature for 1 h cleanly yielded ($PSi^{H}P^{iPr}$)PtMe (**605**). **605** was isolated as a white solid with 71% yield after recrystallization from pentane at -35 °C. **606** was obtained as a white powder with 73% isolated yield via similar reaction of **601** with PhLi. The synthesis of ($PSi^{H}P^{iPr}$)PtMes **607** was first attempted via reaction of **601** with mesityl

lithium (MesLi), but this approach did not yield the desired product. **607** was then successfully isolated in 71% yield via reaction of **601** and MesMgBr at 80 °C overnight.

Table 6-1. Selected NMR data for the neutral (PSiP)PtX species in C_6D_6, δ ppm.

No.	$^{31}P\{^1H\}$ ($^1J_{Pt\text{-}P}$)	$^{29}Si(^1J_{Si\text{-}H}, ^1J_{Pt\text{-}Si})$	$^{195}Pt\{^1H\}$	^{19}F
601	68.1 (2888 Hz)	11.7 (182 Hz, 1192 Hz)	-5031	N/A
603	67.9 (2846 Hz)	19.6 (184 Hz, 1160 Hz)	-5285	N/A
604	72.9 (2941 Hz)	-1.5 (193 Hz, 1373 Hz)	-5057	77.7
605	67.1 (2863 Hz)	43.1 (166 Hz, 660 Hz)	-4936	N/A
606	64.9 (2848 Hz)	34.5 (167 Hz, 632 Hz)	-5025	N/A
607	63.0 (2860 Hz)	34.3 (170 Hz, 608 Hz)	-4910	N/A

All of the neutral complexes **601** and **603-607** were characterized by ^1H, ^{31}P, ^{13}C, ^{195}Pt and ^{19}F (where applicable) NMR (Tables 6-1, 6-2, 6-3). **601** and **603-607** each possess one singlet with Pt satellites in the $^{31}P\{^1H\}$ NMR spectra, one doublet with Pt satellites in the ^{29}Si NMR spectra, one triplet with P coupling in the $^{195}Pt\{^1H\}$ NMR spectra (Table 6-1). ^1H NMR spectra of these compounds show two different isopropyl groups on the phosphine arms on the NMR timescale (Table 6-2). All the spectroscopic features of these neutral compounds in solution indicate they adopt a Cs symmetric square-planar geometry with the X ligand *trans* to the silicon center.

Table 6-2. Selected ^{1}H NMR data for the neutral (PSiP)PtX species in C_6D_6, δ ppm. (only the $PSi^{H}P$ ligand resonance shown, coupling constant in Hz)

No.	SiH ($^{2}J_{Pt-H}$)	CH_{Ar}	CH_{iPr}	CMe_{iPr}
601	5.74 (39)	8.05(d), 7.31(m), 7.21(t), 7.11(t)	3.39(m), 2.46(m)	1.41(m), 1.10(m), 0.93(m)
603	5.73 (41)	8.03(d), 7.35(m), 7.21(t), 7.09(t)	3.51(m), 2.66(m)	1.49(m), 1.27(m), 1.02(m), 0.93(m)
604	5.53 (60)	7.87(d), 7.20-7.09(m)	3.05-2.80(m)	1.47(m), 1.22(m), 0.96-0.81(m)
605	6.36 (21)	8.27(d), 7.42(m), 7.25(t), 7.14(t)	2.95(m), 2.46(m)	1.18(m), 0.99(m)
606	6.47 (20)	8.26(d), 7.44(t), 7.34(m), 7.25(t)	2.88(m), 2.40(m)	1.08(m), 0.99(m), 0.88(m)
607	6.38 (23)	8.23(d), 7.28-7.22(m), 7.15-7.07(m)	3.51(m), 2.66(m)	1.49(m), 1.27(m), 1.02(m), 0.93(m)

The ^{1}H NMR data unambiguously establish the presence of the Pt-Me functionality in **605**, the Pt-Ph functionality in **606** and Pt-Mes functionality in **607** (Table 6-3). The Pt-*Me* group in **605** was observed at 1.32 as a triplet with J_{P-H} of 5 Hz in its ^{1}H NMR spectrum and at -3.7 as a triplet with J_{P-C} of 8 Hz and $^{1}J_{Pt-C}$ of 505 Hz in its $^{13}C\{^{1}H\}$ NMR spectrum. Three distinctive methyl resonances of the mesityl groups were observed in the ^{1}H NMR spectrum and the $^{13}C\{^{1}H\}$ NMR spectrum of **607**, suggesting the C_s symmetry of the molecule and the mesityl group being perpendicular to the PSiPPt plane It also indicates the rotation of aryl group along the Pt-C_{ipso} bond is inhibited on the NMR time scale due to the steric crowding around the Pt center. Notably, only two sets of proton resonances for the phenyl group were observed for **606**, indicating the free rotation of the phenyl group along the Pt-C_{ipso} bond on the NMR time

scale. The differences of aryl groups in the ^{1}H NMR spectra of **606** and **607** highlighted the steric bulkiness of mesityl group compared to phenyl group.

Table 6-3. Selected ^{1}H NMR data for the (PSiP)PtX with R species in C_6D_6, δ ppm. (only Pt-*R* group resonance shown, coupling constant in Hz)

No.	Pt-R
605	1.32(t, $J_{P-H} = 5$)
606	7.88(d, $J_{P-H} = 7$, $J_{Pt-H} = 40$), 7.14(m)
607	7.28-7.22(m), 2.76(s), 2.49(s),2.40(s)

Table 6-4. Selected NMR data for ($PSi^{Me}P^{Cy}$)PtX species reported by Turculet group in C_6D_6, δ ppm.

No.	$^{31}P\{^{1}H\}$ ($^{1}J_{Pt-P}$)	$^{29}Si(^{1}J_{Pt-Si})$
(**G**)PtCl	59.4 (2984 Hz)	32.3 (1183 Hz)
(**G**)PtOTf	65.9 (3055 Hz)	18.8 (1381 Hz)
(**G**)PtMe	57.9 (2938 Hz)	63.9 (696 Hz)
(**G**)PtPh	56.2 (2921 Hz)	59.7 (646 Hz)

Table 6-5. Selected NMR data for *trans*-$(PCy_3)_2PtHX$ species reported by Stahl Labinger and Bercaw in CD_2Cl_2, δ ppm. (only Pt-*H* group resonance shown, coupling constant in Hz)

Complex	Pt-*H* ($^1J_{Pt-H}$, $^2J_{P-H}$)
trans-$(PCy_3)_2Pt(Cl)(H)$	-18.86 (1300, 12)
trans-$(PCy_3)_2Pt(Br)(H)$	-17.58 (1356, 12)
trans-$(PCy_3)_2Pt(I)(H)$	-14.65 (1390, 11)
trans-$(PCy_3)_2Pt(OTf)(H)$	-27.6 (1585, 14)
trans-$(PCy_3)_2Pt(Me)(H)$	-6.47 (660, 17)
trans-$(PCy_3)_2Pt(Ph)(H)$	-8.01 (595, 17)
trans-$(PCy_3)_2Pt(H)(H)$	-3.97 (796, 17)
trans-$(PCy_3)_2Pt(SiH_3)(H)$	-0.97 (760, 11)

Since a series of neutral (PSiP)PtX compounds were obtained, it is interesting to make an assessment of the effect of the X ligand on the spectroscopic properties of the molecule (Table 6-1). Although the $^{31}P\{^1H\}$ and $^{195}Pt\{^1H\}$ NMR data are very similar for these neutral silyl species, they could be easily separated into two groups. With weak *trans* influence groups as the X ligand, such as halide or pseudo-halide, the $^1J_{Pt-Si}$ is fairly large which indicates strong Pt-Si interactions.[203] On the other hand, the strong *trans* influence groups such as methyl and aryl decrease the Pt-Si interaction which results in a much smaller $^1J_{Pt-Si}$. Strong trans-influence ligands also result in the more downfield shift for Si-*H* resonance and smaller J_{Pt-H}. Indeed, a general trend of increasing $^1J_{Pt-Si}$, increasing $^1J_{Pt-H}$, increasing $^2J_{Pt-H}$ and decreasing δ of Si-*H* in ^1H NMR

with decreasing *trans* influence of X ligand in (PSiP)PtX compounds was found in Table 6-1 and Table 6-2. Turculet[17c] reported a similar trend of increasing $^{1}J_{Pt\text{-}Si}$ and decreasing δ in ^{29}Si NMR with decreasing *trans* influence of X ligand in their ($PSi^{Me}P^{Cy}$)PtX complexes ([**G**]PtX, Scheme 6-3, Table 6-4). Similar trend has also been reported by Stahl, Labinger and Bercaw[204] (Table 6-5). They found in a series of *trans*-$(PCy_3)_2$PtHX complexes, stronger *trans* influence group as X ligand resulted in more downfield chemical shift for the hydride on Pt as well as smaller $^{1}J_{Pt\text{-}H}$.

Crystals suitable for single-crystal X-ray diffraction[202] for **607** were obtained by slow diffusion of pentane into a saturated toluene solution (Figure 6-3). **607** adopts a square planar geometry with C_s symmetry in solid state, which is consistent with the NMR data. The sum of the bond angles of C1-Si-Pt, C7-Si-Pt and C1-Si-C7 is around 335.1°, indicating the silicon center adopts a tetrahedral geometry. The Pt-Si bond distance of **607** is 2.3123(9) Å, which is slightly shorter than the Pt-Si bond distance of **601** at 2.276(2) Å. The slightly longer Pt-Si bond distance in **607** is likely the result of the aryl group being a stronger trans-influence ligand. As expected from the NMR data, the mesityl group is perpendicular to the PSiPPt plane with the average P-Pt-C_{Mes}-C_{Mes} torsion angle about 90°.

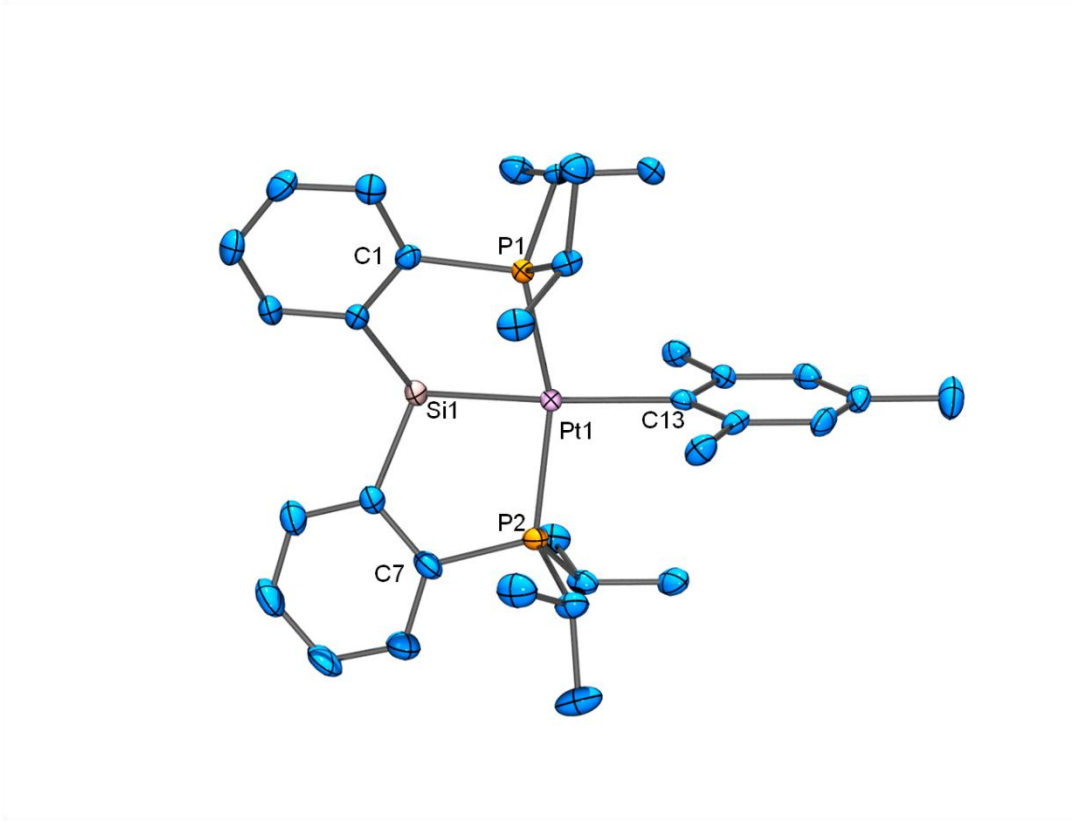

Figure 6-3. ORTEP[128] drawing (50% probability ellipsoids) of **607.** Omitted for clarity: H atoms. Selected distance (Å) and angles (deg) follow: Pt1-Si1, 2.3123 (9); Pt1-P1, 2.2845 (7); Pt1-P2: 2.2876 (7); Pt1-C13, 2.154 (3); P1-Pt1-Si1, 83.66 (3); P2-Pt1-Si1, 83.20 (3); P1-Pt1-P2, 156.52 (3); C1-Si1-Pt1, 108.6 (1); C1-Si1-C7, 116.1 (1); C7-Si1-Pt1, 110.4(1); C13-Pt1-Si1, 168.02 (8); C13-Pt-P2, 99.48 (8); C13-Pt-P1, 97.40 (8).

6.2.3 Hydride Abstraction of (PSiP)PtX

$Ph_3C[HCB_{11}Cl_{11}]$ was used to abstract the hydride from **601** in fluorobenzene (Scheme 6-16). Successful hydride abstraction by the trityl salt was illustrated by the the loss of the Si-*H* resonance and the appreance of the Ph_3C-*H* resonance in the ^1H NMR spectrum. One singlet (with ^{195}Pt satellites) in the $^{31}P\{^1H\}$ NMR spectrum and one triplet in the $^{195}Pt\{^1H\}$ NMR spectrum with J_{Pt-P} of 2957 Hz indicateed the formation of only one new metal complex which was likely a Pt(II) complex[201] with two phosphine arms *trans* to each other. However, the relatively high-field ^{29}Si NMR resonance at 32.7 was consistent with the product being a silyl species. We therefore proposed **608** to be the product for this reaction. It is likely that after the hydride abstraction, the chloride undergoes an inter- or intramolecular migration from Pt to Si due to the high lewis acidity of the silylene group. Halogen abstraction reactions by silylene groups have been previously reported by the Tilley group.[205] In their osmium silylene complex the readily oxidized (electron-rich) osmium center with a Lewis-acidic silylene ligand promotes the cleavage of the carbon-halogen bond. However, the reaction was reported to proceed via radical abstraction mechansim, which is unlikely for our chloride migration reaction.

Scheme 6-16. Hydride abstraction reactions of (PSiP)PtX with $Ph_3C[HCB_{11}Cl_{11}]$.

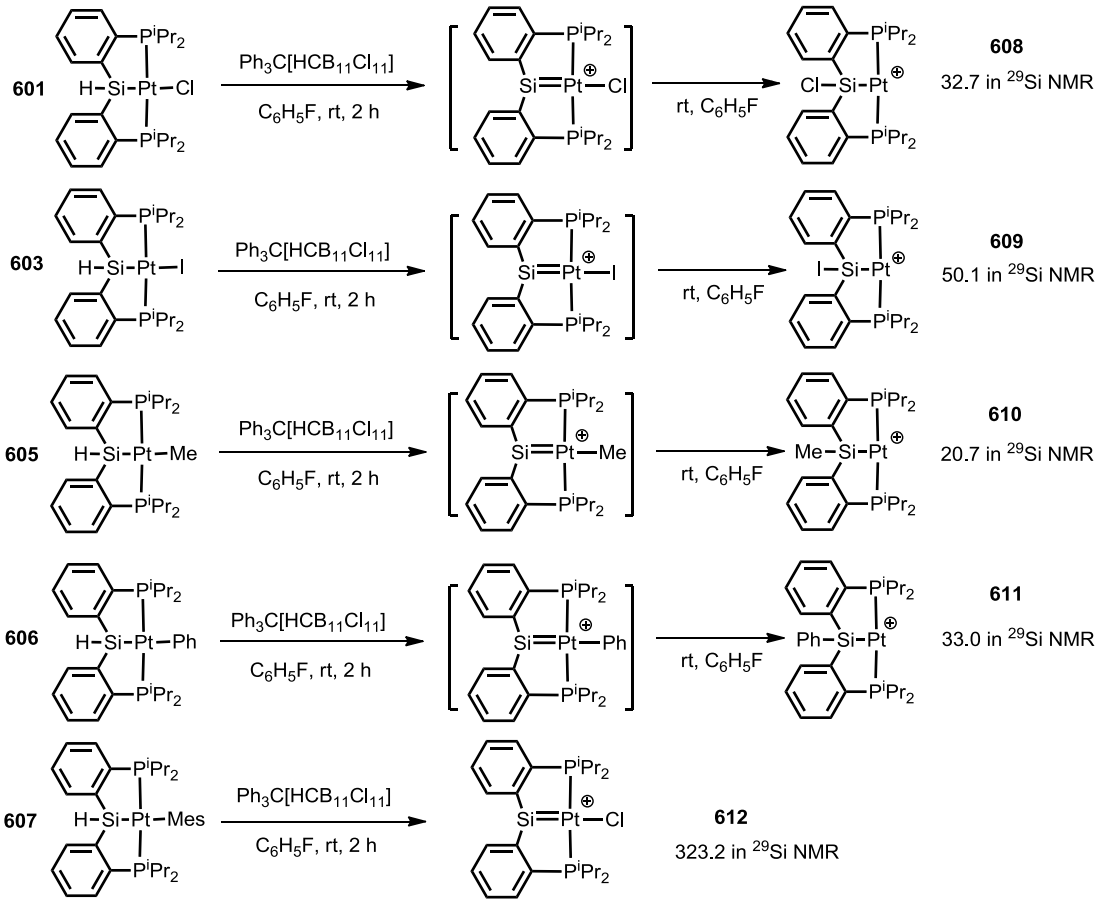

Hydride abstraction reactions by $Ph_3C[HCB_{11}Cl_{11}]$ have been tested with **603** and **605** (Scheme 6-16), which yielded the corresponding silyl products **609** and **610** with ^{29}Si resonance at 50.1 and 20.7 ppm, respectively. The Si-*Me* group of **610** was found at 0.48 ppm with no observable coupling to phosphorus or platinum which is consisten with the methyl group being bound to Si instead of Pt. Similar (PSiP)Pt(II) cationic species have been reported by the Turculet group (Figure 6-1) and displayed

^{29}Si NMR resonances between 26-32 ppm and the Si-*Me* ^{1}H NMR resonances between 0.19-0.36 ppm (Figure 6-4).[17c]

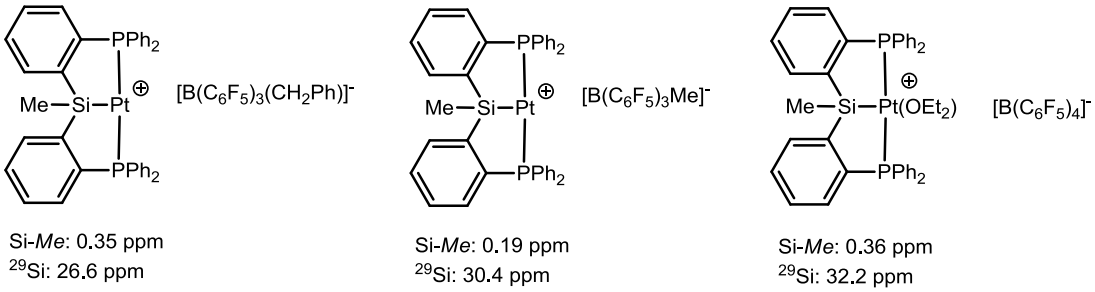

Figure 6-4. Cationic pincer silyl platinum species reported by Turculet group and their ^{29}Si NMR resonance and Si-*Me* resonance in ^{1}H NMR spectra.

611 was obtained as a silyl complex with ^{29}Si resonance at 33.0 ppm via reaction of **606** with $Ph_3C[HCB_{11}Cl_{11}]$ (Scheme 6-16). We noticed that all the cationic silyl species **608**, **609**, **610** and **611** appeared colorless in the C_6H_5F solution. However, in the reaction of **606** with $Ph_3C[HCB_{11}Cl_{11}]$, a deep red solution was initially observed. We were not able to isolate or spectroscopically characterize the intermediate, since the color quickly disappeared in 30 min and the only metal complex we isolated was **611**.

The reaction between **607** and $Ph_3C[HCB_{11}Cl_{11}]$ yielded a deep red product (**612**) which was stable in solution at room temperature (Scheme 6-16). Although the ^{31}P{^{1}H}, ^{29}Si and ^{195}Pt{^{1}H} NMR spectra were all broad for **612** at room temperature, well resolved spectra were obtained at -30 °C (Figure 6-6). The signature resonance at 323.2 ppm in the ^{29}Si NMR spectrum is consistent with **612** being a silylene complex, as all known base-free platinum silylene species display resonances between 300-400 ppm in

their ^{29}Si NMR spectra (Figure 6-5).[192b,192e,206] The $^{1}J_{Pt\text{-}Si}$ for **612** is 896 Hz, which is much greater than that in **611** (606 Hz), indicating a stronger Pt-Si interaction. The $^{1}J_{Pt\text{-}P}$ in **612** is 2526 Hz which is significantly smaller than that of all the PSiPPt species we have obtained (Table 6-6). The smaller $^{1}J_{Pt\text{-}P}$ may be an indication of lower electron density at the platinum center, owing to the d_{π}-p_{π} donation from the platinum center to the electron-poor :SiR_2 group. All spectroscopic data point to that we have obtained the (P_2Si=)Pt complex with silylene as the central donor.

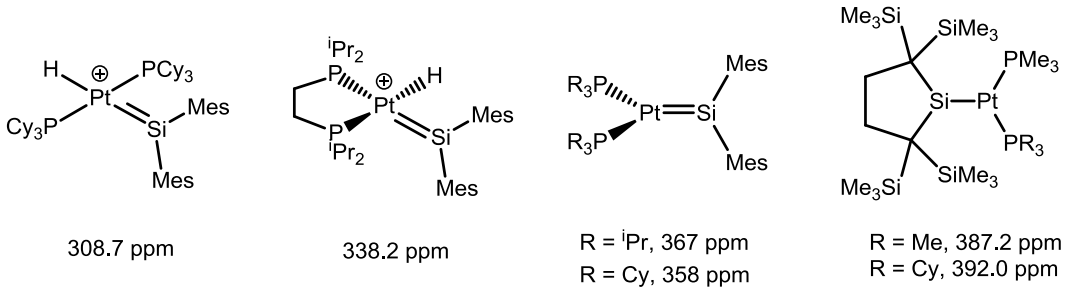

Figure 6-5. Platinum silylene complexes know in the literature and their ^{29}Si resonance.

Table 6-6. Selected NMR data for the cationic (PSiP)PtX species in C_6H_5F. (Coupling constant in Hz)

No.	$^{31}P\{^{1}H\}$ ($^{1}J_{Pt\text{-}P}$)	$^{29}Si(^{1}J_{Si\text{-}Pt})$	$^{195}Pt\{^{1}H\}$
608	71.5 (2957 Hz)	32.7 (1599 Hz)	-4985
609	69.3 (2837 Hz)	50.1	
610	81.8 (2960 Hz)	20.7	
611	71.0 (2942 Hz)	33.0	
612	69.2 (2526 Hz)	323.2 (896 Hz)	-5050

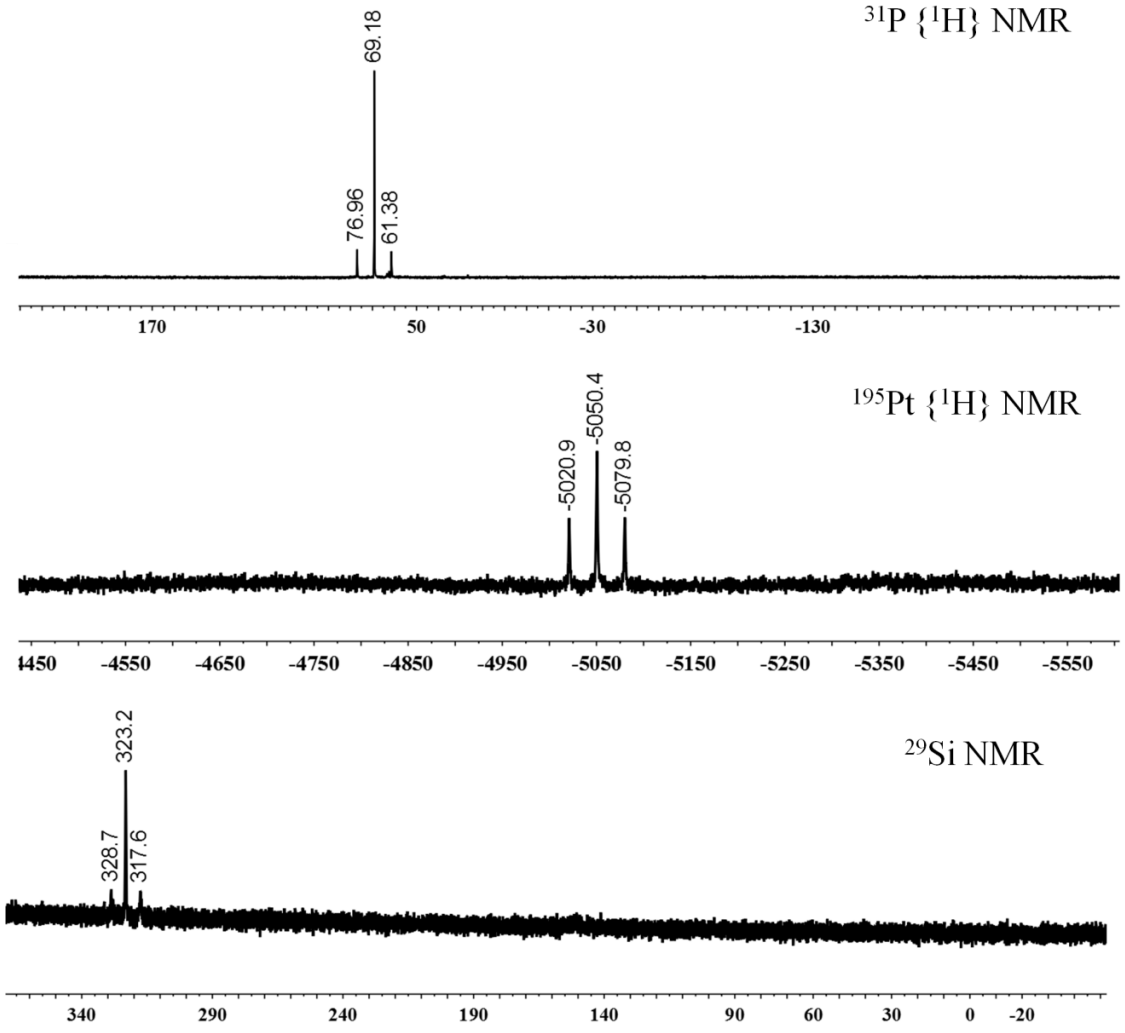

Figure 6-6. NMR spectra for **612.** (Top: ^{31}P{^{1}H} NMR; Middle: ^{195}Pt{^{1}H} NMR; Bottom: ^{29}Si NMR)

6.2.4 Synthesis and Reactivity of (PSiP)PdCl

The synthesis of (PSiP)PdCl (**613**) is described in Scheme 6-17. Unlike the Pt case, although 2,6-lutidine was added before **207**, ($PSi^{Cl}P^{iPr}$)PdCl (**614**) was always observed as a byproduct in this reaction. **614** was removed from **613** by recrystallization from a toluene/pentane solution at -30 °C. The ^{1}H, $^{31}P\{^{1}H\}$ and ^{29}Si NMR spectra of **613** are consistent with the formation of C_s symmetric square-planar complex with Cl *trans* to Si center.

Scheme 6-17. Synthetic procedure for $PSi^{H}P^{iPr}PdCl$ (**613**).

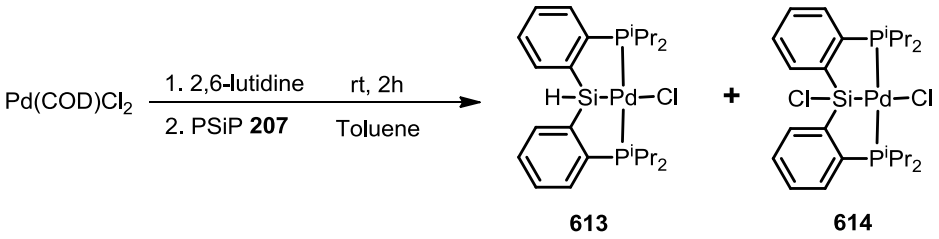

Hydride abstraction reaction (Scheme 6-18) with $Ph_3C[HCB_{11}Cl_{11}]$ was performed with **613** which yielded one single compound (**615**) with a ^{29}Si NMR resonance around 56 ppm. Hence, **615** is likely a silyl complex. Reactions of **613** with Me_3SiI, MeLi or PhLi have been explored with the goal of access to the corresponding ($PSi^{H}P^{iPr}$)PdI, ($PSi^{H}P^{iPr}$)PdMe or ($PSi^{H}P^{iPr}$)PdPh products. However, none of these reactions proceeded to give clean products.

Scheme 6-18. Synthetic procedure for $PSi^{Cl}P^{iPr}Pt^{+}$ (**615**) from **613**.

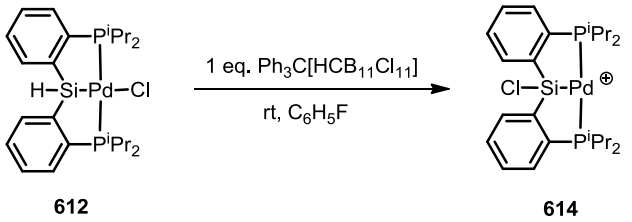

612 **614**

6.3 Conclusion

In this chapter, $(PSi^{H}P^{iPr})PtCl$ was synthesized from $Pt(COD)Cl_2$ and $PSi(H_2)P$ ligand via Si-H bond activation in the presence of base. Direct X ligand exchange methods yielded a series of $(PSi^{H}P^{iPr})PtX$ (X=I, OTf, Me, Ph, Mes) compounds from $(PSi^{H}P^{iPr})PtCl$. $Ph_3C[HCB_{11}Cl_{11}]$ was shown to be able to used to abstract the hydride from the silicon center on these $(PSi^{H}P^{iPr})PtX$ compounds. The resulting platinum silylene complexes displayed silylium character, which was exemplified by the X ligand abstraction with Cl, I, Me and Ph. However, the mesityl group was resistant towards abstraction by silylene center, which is probably attributed to the steric bulkiness of mesityl group. Hence, a pincer metal silylene species was observed after the hydride abstraction which was the first reported PSiP metal species with a central silylene donor.

6.4 Experimental Details

General considerations. Unless specified otherwise, all reactions and manipulations were carried out under an argon atmosphere using glovebox or Schlenk line techniques. Dry, oxygen–free solvents were employed. Toluene, n-pentane, diethyl ether and C_6D_6

were dried over NaK/Ph_2CO/18-crown-6, distilled and stored over molecular sieves in an Ar-filled glove box. Fluorobenzene and C_6D_5Br were dried over CaH_2, distilled and stored over molecular sieves in an Ar-filled glove box. $Si(OEt)_4$ and 2,6-lutidine were fractionally distilled prior to use. $Ph_3C[HCB_{11}Cl_{11}]$,[98] Pt[COD]Cl_2 [207] and Pd[COD]Cl_2[207] were prepared according to published procedures. $PSi(H_2)P$ was prepared acoording to methods described in Chapter II. All other chemicals were used as received from commercial vendors unless otherwise noted.

Physical Methods. NMR spectra were recorded on a Varian iNova 300 spectrometer (^{1}H NMR, 299.9 MHz, ^{13}C NMR, 75.4 MHz, ^{31}P NMR, 121.4 MHz), a Varian iNova 400 spectrometer (^{1}H NMR, 400.0 MHz, ^{13}C NMR, 100.5 MHz, ^{31}P NMR, 161.9 MHz ^{29}Si NMR, 79.4 MHz, ^{195}Pt NMR, 85.9 MHz) and a Varian iNova 500 spectrometer (^{1}H NMR, 400.0 MHz, ^{13}C NMR, 125.7 MHz, ^{31}P NMR, 202.4 MHz) in noted solvents. Chemical shifts are given in δ (ppm). ^{29}Si NMR spectra were referenced externally with $SiMe_4$ at δ 0. $^{31}P\{^1H\}$ NMR spectra were referenced externally with 85% phosphoric acid at δ 0. ^{1}H NMR and $^{13}C\{^1H\}$ NMR spectra were referenced using the solvent signals. Elemental analyses were performed by CALI, Inc. (Parsippany, NJ). The solid state structures of **601** and **607** were solved by Dr. David E. Herbert.

(PSiP)PtCl (601). To a solution of Pt(COD)Cl_2 (1.80 g, 4.76 mmol) and 2,6-lutidine (0.56 mL, 4.81 mmol) in toluene (30 mL) was added a solution of **207** (1.94 g, 4.67 mmol) in 10 mL toluene. The resulting white suspension was stirred at room temperature for 3 h, then the reaction mixtures were filtered through a short plug of Celite. After removal of all volatiles, the crude products were purified by

recrystallization from toluene/pentane solution at -30 °C. X-ray quality crystals were obtained by slow diffusion of pentane to a saturated toluene solution of **601**. Yield: 2.6 g (85%). $^{31}P\{^{1}H\}$ NMR (121.4 MHz, C_6D_6): δ 68.1 (s, J_{Pt-P} = 2887 Hz). ^{1}H NMR (299.9 MHz, C_6D_6): δ 8.05 (d, J_{H-H} = 7 Hz, 2H, Ar-*H*), 7.31 (m, 2H, Ar-*H*), 7.21 (t, J_{H-H} = 7 Hz, 2H, Ar-*H*), 7.11 (t, J_{H-H} = 7 Hz, 2H, Ar-*H*), 5.74 (s, J_{Pt-H} = 39 Hz, J_{Si-H} = 182 Hz, 1H, Si-*H*), 3.39 (m, 2H, C*H*Me_2), 2.46 (m, 2H, C*H*Me_2), 1.41 (m, 12H, CH*Me*$_2$), 1.10 (dvt, J_{P-H} = 7 Hz, J_{H-H} = 7 Hz, 6H, CH*Me*$_2$), 0.93 (dvt, J_{P-H} = 7 Hz, J_{H-H} = 7 Hz, 6H, CH*Me*$_2$). $^{13}C\{^{1}H\}$ NMR (100.5 MHz, C_6D_6): δ 151.4 (t, J_{P-C} = 21 Hz), 141.6 (t, J_{P-C} = 26 Hz), 134.1 (m), 131.1 (br m, J_{Pt-C} = 44 Hz), 130.7 (br m), 128.9 (t, J_{P-C} = 4 Hz), 27.7 (vt, J_{P-C} = 14 Hz, *C*HMe_2), 25.9 (vt, J_{P-C} = 14 Hz, *C*HMe_2), 19.2 (vt, J_{P-C} = 2 Hz, CH*Me*$_2$), 19.0 (br m, J_{Pt-C} = 20 Hz, CH*Me*$_2$), 18.6 (br, CH*Me*$_2$), 18.2 (br m, J_{Pt-C} = 22 Hz, CH*Me*$_2$). $^{195}Pt\{^{1}H\}$ NMR (85.9 MHz, C_6D_6): δ -5051.4 (t, J_{Pt-P} = 2885 Hz). ^{29}Si NMR (79.4 MHz, C_6D_6): δ 11.7 (d, J_{Si-H} = 180 Hz, J_{Pt-Si} = 1192 Hz). Elem. An. Found (Calculated) for $C_{24}H_{37}ClP_2PtSi$: C, 44.64 (44.61); H, 5.82 (5.77)%.

(PSiP)PtI (603). To a solution of **601** (53 mg, 0.08 mmol) in 2 mL toluene (30 mL) was added iodotrimethylsilane (17.5 μL, 0.12 mmol). The reaction mixtures were stirred at room temperature for 1 h before all volatiles were removed under vacuum. The residue was redissolved in 2 mL toluene, mixed with second portion of iodotrimethylsilane (17.5 μL, 0.12 mmol) and stirred at room temperature for 1 h. After removal of all volatiles, the crude products were recrystallized from toluene/pentane solution at -30 ℃ and dried under vaccuum. Yield: 36 mg (61%).

$^{31}P\{^{1}H\}$ NMR (121.4 MHz, C_6D_6): δ 67.9 (s, J_{Pt-P} = 2846 Hz). ^{1}H NMR (299.9 MHz, C_6D_6): δ 8.03 (d, J_{H-H} = 7 Hz, 2H, Ar-*H*), 7.35 (m, 2H, Ar-*H*), 7.21 (dt, J_{H-H} = 7 Hz, J_{P-H} = 1 Hz, 2H, Ar-*H*), 7.09 (t, J_{H-H} = 7 Hz, 2H, Ar-*H*), 5.73 (s, J_{Pt-H} = 41 Hz, J_{Si-H} = 184 Hz, 1H, Si-*H*), 3.51 (m, 2H, C*H*Me$_2$), 2.66 (m, 2H, C*H*Me$_2$), 1.49 (dvt, J_{P-H} = 7 Hz, J_{H-H} = 7 Hz, 6H, CH*Me*$_2$), 1.27 (dvt, J_{P-H} = 7 Hz, J_{H-H} = 7 Hz, 6H, CH*Me*$_2$), 1.02 (dvt, J_{P-H} = 7 Hz, J_{H-H} = 7 Hz, 6H, CH*Me*$_2$), 0.93 (dvt, J_{P-H} = 7 Hz, J_{H-H} = 7 Hz, 6H, CH*Me*$_2$). $^{13}C\{^{1}H\}$ NMR (100.5 MHz, C_6D_6): δ 151.3 (t, J_{P-C} = 21 Hz), 141.6 (t, J_{P-C} = 25 Hz), 133.9 (m), 131.3 (br m, J_{Pt-C} = 43 Hz), 130.6 (br m), 129.0 (t, J_{P-C} = 4 Hz), 28.6 (vt, J_{P-C} = 14 Hz, *C*HMe$_2$), 28.2 (vt, J_{P-C} = 14 Hz, *C*HMe$_2$), 20.2 (m, CH*Me*$_2$), 19.0 (m, CH*Me*$_2$), 18.8 (br, CH*Me*$_2$), 18.4 (m, J_{Pt-C} = 24 Hz, CH*Me*$_2$). $^{195}Pt\{^{1}H\}$ NMR (85.9 MHz, C_6D_6): δ -5284.9 (t, J_{Pt-P} = 2845 Hz). ^{29}Si NMR (79.4 MHz, C_6D_6): δ 19.6 (d, J_{Si-H} = 183 Hz, J_{Pt-Si} = 1160 Hz).

(PSiHP)PtOTf (Compound 604). To a solution of **601** (27 mg, 0.04 mmol) in 0.5 mL C_6D_6 was slowly added trimethylsilyl triflate (75 μL, 0.41 mmol). The reaction mixtures were stayed at room temperature for 1 h. After all volatiles were removed under vacuum, another portion of C_6D_6 (0.5 mL) and Me_3SiOTf (75 μL) was added into the mixtures. The mixtures were stayed at room temperature for 1 h. After removal of all volatiles, the crude products were washed with cold pentane and dried under vacuum at 80 ℃ for 3 h. Yield: 22 mg (71%). $^{31}P\{^{1}H\}$ NMR (121.4 MHz, C_6D_6): δ 72.9 (s, J_{Pt-P} = 2941 Hz). ^{1}H NMR (299.9 MHz, C_6D_6): δ 7.87 (d, J_{H-H} = 7 Hz, 2H, Ar-*H*), 7.20-7.09 (m, 6H, Ar-*H*), 5.53 (s, J_{Pt-H} = 60 Hz, J_{Si-H} = 193 Hz, 1H, Si-*H*), 3.05-2.80 (m, 4H, C*H*Me$_2$), 1.47 (dvt, J_{P-H} = 7 Hz, J_{H-H} = 7 Hz, 6H, CH*Me*$_2$), 1.22 (dvt, J_{P-H} = 7 Hz, J_{H-H} = 7

Hz, 6H, CH*Me*$_2$), 0.96-0.81 (m, 12H, CH*Me*$_2$). ^{19}F NMR (282.2 MHz, C_6D_6): δ -77.7 (s). ^{195}Pt{^{1}H} NMR (85.9 MHz, C_6D_6): δ -5056.6 (t, J_{Pt-P} = 2941 Hz). ^{29}Si NMR (79.4 MHz, C_6D_6): δ -1.5 (d, J_{Si-H} = 193 Hz, J_{Pt-Si} = 1373 Hz).

(PSiHP)PtMe (Compound 605). To a solution of **601** (76 mg, 0.12 mmol) in 2 mL toluene was slowly added MeLi (80 μL, 1.6 M in diethyl ether, 0.13 mmol). The reaction mixtures were stirred at room temperature for 1 h and then filtered through a short plug of Celite. After removal of all volatiles, the crude products were recrystallized from toluene/pentane solution at -30 ℃ and dried under vaccuum. Yield: 52 mg (71%). ^{31}P{^{1}H} NMR (121.4 MHz, C_6D_6): δ 67.1 (s, J_{Pt-P} = 2863 Hz). ^{1}H NMR (299.9 MHz, C_6D_6): δ 8.27 (d, J_{H-H} = 7 Hz, 2H, Ar-*H*), 7.42 (m, 2H, Ar-*H*), 7.25 (t, J_{H-H} = 7 Hz, 2H, Ar-*H*), 7.14 (t, J_{H-H} = 7 Hz, 2H, Ar-*H*), 6.36 (s, J_{Pt-H} = 21 Hz, J_{Si-H} = 166 Hz, 1H, Si-*H*), 2.95 (m, 2H, C*H*Me$_2$), 2.46 (m, 2H, C*H*Me$_2$), 1.32 (t, J_{P-H} = 5 Hz, 3H, Pt*Me*), 1.18 (m, 12H, CH*Me*$_2$), 0.99 (m, 12H, CH*Me*$_2$). ^{13}C{^{1}H} NMR (100.5 MHz, C_6D_6): δ 154.8 (t, J_{P-C} = 21 Hz), 144.8 (t, J_{P-C} = 26 Hz), 135.0 (t, J_{P-C} = 10 Hz), 130.8 (br m, J_{Pt-C} = 30 Hz), 129.8 (br m), 128.1 (br m), 28.2 (vt, J_{P-C} = 14 Hz, *C*HMe$_2$), 25.7 (vt, J_{P-C} = 14 Hz, *C*HMe$_2$), 19.6 (m, CH*Me*$_2$), 19.2 (m, CH*Me*$_2$), 18.4 (m, CH*Me*$_2$), 18.3 (m, CH*Me*$_2$), -3.7 (t, J_{P-C} = 8 Hz, J_{Pt-C} = 505 Hz, Pt*Me*). ^{195}Pt{^{1}H} NMR (85.9 MHz, C_6D_6): δ -4935.5 (t, J_{Pt-P} = 2862 Hz). ^{29}Si NMR (79.4 MHz, C_6D_6): δ 43.1 (d, J_{Si-H} = 166 Hz, J_{Pt-Si} = 660 Hz).

(PSiHP)PtPh (Compound 606). To a solution of **601** (102 mg, 0.16 mmol) in 2 mL toluene was slowly added PhLi (90 μL, 1.8 M in dibutyl ether, 0.16 mmol). The reaction mixtures were stirred at room temperature for 3 h and then filtered through a

short plug of Celite. After removal of all volatiles, the crude products were recrystallized from toluene/pentane solution at -30 ℃ and dried under vaccuum at 80 ℃ for 12 h. Yield: 80 mg (73%). $^{31}P\{^{1}H\}$ NMR (121.4MHz, C_6D_6): δ 64.9 (s, J_{Pt-P} = 2848 Hz). ^{1}H NMR (299.9 MHz, C_6D_6): δ 8.26 (d, J_{H-H} = 7 Hz, 2H, Ar-*H*), 7.88 (d, J_{H-H} = 7 Hz, J_{Pt-H} = 40 Hz, 2H, Ar-*H*), 7.44 (t, J_{H-H} = 7 Hz, 2H, Ar-*H*), 7.34 (m, 2H, Ar-*H*), 7.25 (t, J_{H-H} = 7 Hz, 2H, Ar-*H*), 7.14 (m, 3H, Ar-*H*), 6.47 (s, J_{Pt-H} = 20 Hz, J_{Si-H} = 167 Hz, 1H, Si-*H*), 2.88 (m, 2H, C*H*Me_2), 2.40 (m, 2H, C*H*Me_2), 1.08 (dvt, J_{P-H} = 7 Hz, J_{H-H} = 7 Hz, 6H, CH*Me*$_2$), 0.99 (m, 12H, CH*Me*$_2$), 0.88 (dvt, J_{P-H} = 7 Hz, J_{H-H} = 7 Hz, 6H, CH*Me*$_2$). $^{13}C\{^{1}H\}$ NMR (100.5 MHz, C_6D_6): δ 174.6 (t, J_{P-C} = 10 Hz, J_{Pt-C} = 690 Hz, Pt*Ph*), 154.3 (t, J_{P-C} = 21 Hz), 143.8 (t, J_{P-C} = 26 Hz), 141.1 (br m), 134.8 (br m, J_{Pt-C} = 150 Hz, Pt*Ph*), 131.0 (m), 130.1 (m), 129.9 (m), 122.2 (m, Pt*Ph*), 122.0 (m, Pt*Ph*), 28.0 (vt, J_{P-C} = 14 Hz, *C*HMe_2), 24.3 (m, *C*HMe_2), 19.2 (m, CH*Me*$_2$), 18.8 (m, CH*Me*$_2$), 18.0 (m, CH*Me*$_2$), 17.6 (m, CH*Me*$_2$). $^{195}Pt\{^{1}H\}$ NMR (85.9 MHz, C_6D_6): δ -5024.6 (t, J_{Pt-P} = 2846 Hz). ^{29}Si NMR (79.4 MHz, C_6D_6): δ 34.5 (d, J_{Si-H} = 166 Hz, J_{Pt-Si} = 632 Hz).

(PSiHP)PtMesityl (Compound 607). To a solution of **601** (200 mg, 0.30 mmol) in 5 mL toluene was slowly added 2- mesitylmagnesium bromide (300 μL, 1.0 M in diethyl ether, 0.30 mmol). The reaction mixtures were stirred at 80 ℃ for 12 h and then filtered through a short plug of Celite and silica gel. After removal of all volatiles, the crude products were recrystallized from toluene/pentane solution at -30 ℃ and dried under vaccuum at 80 ℃ for 12 h. Yield: 155 mg (71%). X-ray quality crystals were obtained by slow diffusion of pentane to a saturated toluene solution of

607. $^{31}P\{^{1}H\}$ NMR (121.4 MHz, C_6D_6): δ 63.0 (s, J_{Pt-P} = 2861 Hz). ^{1}H NMR (299.9 MHz, C_6D_6): δ 8.23 (d, J_{H-H} = 7 Hz, 2H, Ar-*H*), 7.28-7.22 (m, 4H, Ar-*H*), 7.15-7.07 (m, 4H, Ar-*H*), 6.37 (s, J_{Pt-H} = 22 Hz, J_{Si-H} = 168 Hz, 1H, Si-*H*), 2.76 (s, 3H, Ar-*Me*), 2.74 (m, 2H, C*H*Me$_2$), 2.49 (s, 3H, Ar-*Me*), 2.45 (m, 2H, C*H*Me$_2$), 2.40 (s, 3H, Ar-*Me*), 1.11-0.93 (m, 18H, CH*Me*$_2$), 0.80 (dvt, J_{P-H} = 7 Hz, J_{H-H} = 7 Hz, 6H, CH*Me*$_2$). $^{13}C\{^{1}H\}$ NMR (125.7 MHz, C_6D_6): δ 163.7 (m, Pt-*Ar*), 153.2 (t, J_{P-C} = 20 Hz), 145.3 (m), 144.9 (s, J_{Pt-C} = 26 Hz), 143.6 (t, J_{P-C} = 26 Hz, J_{Pt-C} = 26 Hz), 134.7 (t, J_{P-C} = 10 Hz), 131.7 (s), 130.7 (s, J_{Pt-C} = 30 Hz), 130.0 (s), 128.3 (m), 29.1 (m, Ar-*Me*), 29.0 (m, Ar-*Me*), 26.2 (m, J_{Pt-C} = 54 Hz, *C*HMe$_2$), 24.1 (m, J_{P-C} = 16 Hz, *C*HMe$_2$), 21.3 (s, Ar-*Me*), 19.0 (m, CH*Me*$_2$), 18.4 (m, J_{Pt-C} = 21 Hz, CH*Me*$_2$), 17.8 (m, J_{Pt-C} = 17 Hz, CH*Me*$_2$), 17.6 (m, CH*Me*$_2$). $^{195}Pt\{^{1}H\}$ NMR (85.9 MHz, C_6D_6): δ -4910.1 (t, J_{Pt-P} = 2846 Hz). ^{29}Si NMR (79.4 MHz, C_6D_6): δ 36.1 (d, J_{Si-H} = 170 Hz, J_{Pt-Si} = 608 Hz). Elem. An. Found (Calculated) for $C_{30}H_{48}P_2PtSi$: C, 54.38 (54.31); H, 6.68 (6.63)%.

(PSi^{Cl}P)Pt[HCB$_{11}$Cl$_{11}$] (608). To a solution of **601** (67 mg, 0.10 mmol) in 0.5 mL fluorobenzene was slowly added $Ph_3C[HCB_{11}Cl_{11}]$ (78 mg, 0.10 mmol). The resulting yellow solution was stayed at room temperature for 1 h and then filtered through a short plug of Celite. After removal of all volatiles, the crude pale yellow products were washed with pentane three times and dried under vacuum for 30 m. Yield: 95 mg (79 %). $^{31}P\{^{1}H\}$ NMR (121.4 MHz, 295 K, C_6H_5F): δ 71.5 (s, J_{Pt-P} = 2957 Hz). $^{195}Pt\{^{1}H\}$ NMR (85.9 MHz, 295 K, C_6H_5F): δ -4985 (t, J_{Pt-P} = 2960Hz). ^{29}Si NMR (79.4 MHz, 295 K, C_6H_5F): δ 32.7 (s, J_{Pt-Si} = 1599 Hz).

(PSi^{I}P)Pt[HCB$_{11}$Cl$_{11}$] (609). To a solution of **603** (20 mg, 0.027 mmol) in 0.3 mL fluorobenzene was slowly added $Ph_3C[HCB_{11}Cl_{11}]$ (21 mg, 0.027 mmol). The resulting yellow solution was stayed at room temperature for 1 h. $^{31}P\{^1H\}$ NMR (121.4 MHz, 295 K, C_6H_5F): δ 69.3 (s, J_{Pt-P} = 2837 Hz). ^{29}Si NMR (79.4 MHz, 295 K, C_6H_5F): δ 50.1 (s).

(PSi^{Me}P)Pt[HCB$_{11}$Cl$_{11}$] (610). To a solution of **605** (45 mg, 0.074 mmol) in 0.5 mL fluorobenzene was slowly added $Ph_3C[HCB_{11}Cl_{11}]$ (56 mg, 0.704 mmol). The resulting yellow solution was stayed at room temperature for 2 h and then filtered through a short plug of Celite. After removal of all volatiles, the crude yellow products were washed with pentane three times and dried under vacuum 3 h. Yield: 76 mg (74%). $^{31}P\{^1H\}$ NMR (121.4 MHz, 295 K, C_6H_5F): δ 81.8 (s, J_{Pt-P} = 2960 Hz). ^{29}Si NMR (79.4 MHz, 295 K, C_6H_5F): δ 20.7 (s).

(PSi^{Ph}P)Pt[HCB$_{11}$Cl$_{11}$] (611). To a solution of **606** (45 mg, 0.065 mmol) in 0.5 mL fluorobenzene was slowly added $Ph_3C[HCB_{11}Cl_{11}]$ (50 mg, 0.065 mmol). The resulting deep red solution was stayed at room temperature for 2 h. $^{31}P\{^1H\}$ NMR (121.4 MHz, 295 K, C_6H_5F): δ 65.5 (s, J_{Pt-P} = 2828 Hz), 71.0 (s, J_{Pt-P} = 2942 Hz). During the time, the deep red solution slowly became a pale yellow solution. $^{31}P\{^1H\}$ NMR (121.4 MHz, 243 K, C_6H_5F): δ 71.0 (s, J_{Pt-P} = 2942 Hz). ^{29}Si NMR (79.4 MHz, 295 K, C_6H_5F): δ 30.0 (s).

(PSiP)PtMesityl[HCB$_{11}$Cl$_{11}$] (612). To a solution of **607** (115 mg, 0.16 mmol) in 0.5 mL fluorobenzene was slowly added $Ph_3C[HCB_{11}Cl_{11}]$ (120 mg, 0.16 mmol). The resulting deep red solution was stayed at room temperature for 2 h and then filtered

through a short plug of Celite. After removal of all volatiles, the crude deep red products were washed with pentane three times and dried under vacuum 3 h. Yield: 145 mg (74%). $^{31}P\{^{1}H\}$ NMR (161.9 MHz, 243 K, C_6H_5F): δ 69.2 (s, J_{Pt-P} = 2526 Hz). $^{195}Pt\{^{1}H\}$ NMR (85.9 MHz, 243 K, C_6H_5F): δ -5050 (t, J_{Pt-P} = 2526 Hz). ^{29}Si NMR (79.4 MHz, 243 K, C_6H_5F): δ 323.2 (s, J_{Pt-Si} = 896 Hz).

(PSiP)PdCl (613). To a solution of $Pd(COD)Cl_2$ (136 mg, 0.48 mmol) and 2,6-lutidine (0.28 mL, 2.4 mmol) in toluene (5 mL) was added a solution of **207** (200 mg, 0.48 mmol) in 10 mL toluene. The resulting white suspension was stirred at room temperature for 3 h, then the reaction mixtures were filtered through a short plug of Celite. After removal of all volatiles, the crude products were purified by recrystallization from toluene/pentane solution at -30 ℃. Yield: 180 mg (64%). $^{31}P\{^{1}H\}$ NMR (121.4 MHz, C_6D_6): δ 66.2 (s). ^{1}H NMR (299.9 MHz, C_6D_6): δ 7.97 (d, J_{H-H} = 7 Hz, 2H, Ar-*H*), 7.08-7.27 (m, 6H, Ar-*H*), 6.11 (s, J_{Si-H} = 182 Hz, 1H, Si-*H*), 3.08 (m, 2H, C*H*Me_2), 2.11 (m, 2H, C*H*Me_2), 1.42 (m, 12H, CH*Me*$_2$), 1.04 (dvt, J_{P-H} = 7 Hz, J_{H-H} = 7 Hz, 6H, CH*Me*$_2$), 0.93 (dvt, J_{P-H} = 7 Hz, J_{H-H} = 7 Hz, 6H, CH*Me*$_2$). ^{29}Si NMR (79.4 MHz, C_6D_6): δ 29.4 (d, J_{Si-H} = 186 Hz).

(PSi^{Cl}P)Pd[$HCB_{11}Cl_{11}$] (615). To a solution of **613** (88 mg, 0.17 mmol) in 0.5 mL fluorobenzene was slowly added $Ph_3C[HCB_{11}Cl_{11}]$ (110 mg, 0.15 mmol). The resulting orange solution was stayed at room temperature for 1 h and then filtered through a short plug of Celite. After removal of all volatiles, the crude pale yellow products were washed with pentane three times and dried under vacuum 3 h. $^{31}P\{^{1}H\}$ NMR (121.4 MHz, 295 K, C_6D_5Br): δ 66.8 (s). ^{29}Si NMR (79.4 MHz, 295 K, C_6D_5Br): δ 55.7 (s).

Attempted preparation of (PSiP)PdI. Similar procedure as in the synthesis of **603** was applied in an attempt to make **(PSiP)PdI.** Treatment of **613** (40 mg, 0.07 mmol) with Me_3SiI (15 μL , 0.11 mmol) afforded mutiple products.

Attempted preparation of (PSiP)PdMe. Similar procedure as in the synthesis of **605** was applied in an attempt to make **(PSiP)PdMe.** Treatment of **613** (93 mg, 0.17 mmol) with MeLi (104 μL, 1.6 M in diethyl ether, 0.17 mmol) afforded mutiple products based on $^{31}P\{^{1}H\}$ NMR spectra.

Attempted preparation of (PSiHP)PdPh. Similar procedure as in the synthesis of **606** was applied in an attempt to make **(PSiHP)PdPh.** Treatment of **613** (100 mg, 0.18 mmol) with PhLi (100 μL, 1.8 M in dibutyl ether, 0.18 mmol) afforded two products based on ^{31}P NMR spectra.

CHAPTER VII

DESIGN AND SYNTHESIS OF PINCER PBP Rh COMPLEXES

7.1 Introduction

7.1.1 Metal Boryl Complexes

"Boryl" refers to an sp^2-hybridized BX_2 species.[163c] Boryls are very strong σ-donors, and therefore are ligands of very strong *trans* influence.[208] Their effects have been studied theoretically[209] and experimentally.[210] Unlike organolithium or Grignard reagents, stable source of BX_2^- hardly exists due to the coordinating unsaturation of the boron atom as well as the large difference of electronegativities between boron and lithium (2.04 vs 0.96).[211] Hence, compared to the corresponding metal alkyl species, metal boryl complexes are far less common in the literature. Of the existing metal boryl compounds, the two X atoms on the boron are normally good π-donors, such as oxygen, nitrogen or halogen.[163c]

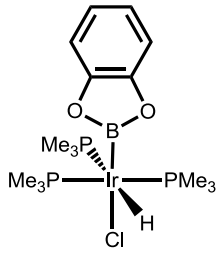

Figure 7-1. First structurally characterized metal boryl compound.

The first structurally characterized metal boryl species (Figure 7-1) with two-center-two-electron metal-boron σ-bond was published in 1990.[212] Most early examples of metal boryl compounds were limited to mid-transition metals.[213] There has been a recent surge in the studies of metal boryl compounds with group 10 metals, since they are often regarded as key intermediates in the catalytic diboration and borylation reactions.[214]

7.1.2 Pincer Boryl Ligands

Although metal boryl species have been widely used in catalytic borylation reactions, in these cases the boryl ligands functioned as "active ligands".[163c] It would be interesting to develop pincer boryl ligands, which could take advantage of the strong *trans*-labilizing effect of the boryl group to promote the formation of coordinatively unsaturated metal complexes. The first pincer ligand with central monoanionic boryl unit was reported by the Nozaki group in 2009[16] (**A**, Figure 7-2), in which the chelating diamino substituents were used to stabilize the electron-deficient boryl unit.[16] The slightly longer Ir-Cl bond length in (P^NB^NP)Ir(H)(Cl)(CO) compared to that in similar (PCP)Ir(H)(Cl)(CO) species revealed the stronger σ-donor ability of P^NB^NP ligand than that of PCP.[16a]

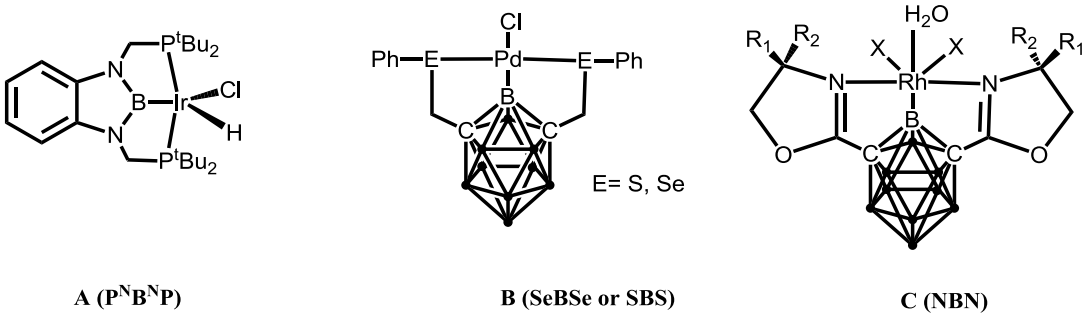

A (P^NB^NP) **B (SeBSe or SBS)** **C (NBN)**

Figure 7-2. Pincer boryl complexes known in the literature. (Each dot on the cage represnts one BH group)

Scheme 7-1. Ir-Cl bond distances (in Å) of (PCP)Ir(H)(Cl)(CO) and (P^NB^NP)Ir(H)(Cl)(CO) complexes.

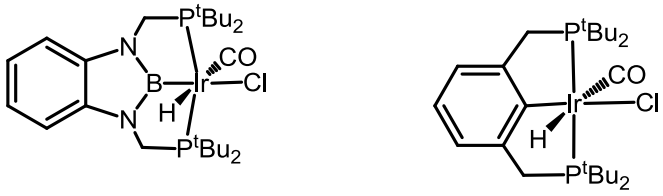

Ir-Cl: 2.53 Ir-Cl: 2.48

Later, Mirkin and coworkers developed carborane-based tridentate ligands with a central boryl unit (**B**, Figure 5-2).[114] The bis(selenophenyl)carborane (SeBSe) and bis(thiophenylether)carborane (SBS) have been employed to make Pd complexes via B-H bond activation. However, the boryl unit here is not a classical sp^2 hybridized BX_2 species, the electrons of the boron atoms are delocalized throughout the boron cluster cage, which contributes to the stability of these boron cluster based pincer complexes. Recently, Nakamura and coworkers developed carborane-based NBN chiral ligands (**C**, Figure 5-2) and their metal complexes with Pd, Ni and Rh.[115] The (NBN)Rh complexes

were shown to be an effective catalyst for asymmetric reduction of α,β-unsaturated esters and asymmetric reductive aldol reaction of *tert*-butyl acrylate and benzaldehyde with diethoxymethylsilane as the reductant (Scheme 7-2).

Scheme 7-2. Reactions catalyzed by (NBN)Rh complexes.

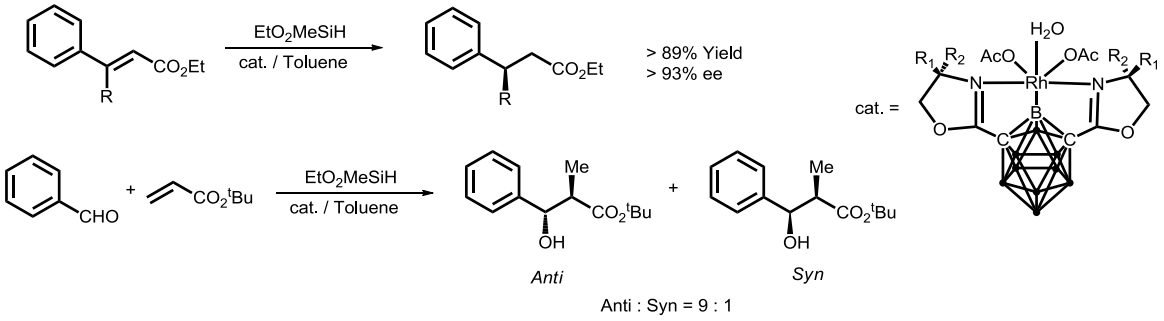

We decided to obtain **702** type of pincer boryl complexes which not only eliminate the potentially reactive methylene protons in reported P^NB^NP complexes , but also mimic the rigid backbone set our group reported before in PNP and PSiP complexes, which would be easier in the future to evaluate the electronic effect of boryl central donor in pincer boryl complexes. We expected to obtain **702** via activation of B-Ph of **701**, which is a known compound reported by Bourissou group.[129] We reasoned **701** might dissociate at elevated temperature to its monomer species which would open a *cis* empty site for potential oxidative addition of B-Ph bond (Scheme 7-3).[22]

Scheme 7-3. Potential pathway to pincer boryl compound via activation of B-Ph bond.

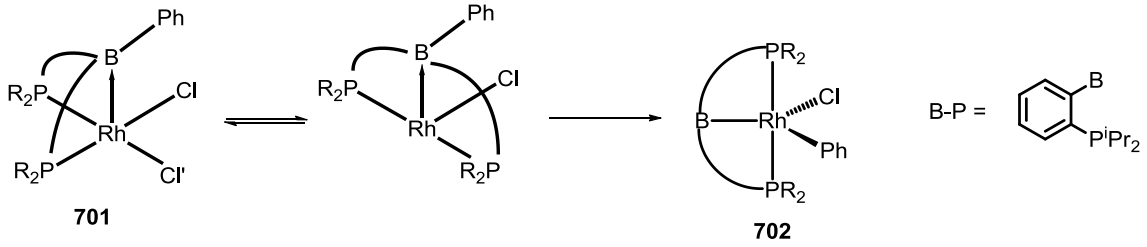

7.2 Results and Discussion

7.2.1 Bisphosphino-borane ($PB^{Ph}P$) Ligand and its Complexes with Rh

Synthesis of the $PB^{Ph}P$ ligand **210** was described in Chapter II. **701** $[(PB^{Ph}P)RhCl]_2$ was readily obtained via the method developed by Bourissou and coworkers (Scheme 7-4).[129] After workup, **701** was isolated as yellow powder with 95% yield which displayed spectroscopic features consistent with the literature report with two isomers observed in ^1H and $^{31}P\{^1H\}$ NMR spectrum. X-ray[215] quality crystals of one of the isomers of **701** were obtained by slow diffusion of *n*-pentane into a saturated $CHCl_3$ solution of **701** at room temperature (Figure 7-3). The structure for the isomer we obtained for **701** was consistent with the structure Bourissou reported in 2006.[129]

Scheme 7-4. Synthesis of **701** from **210** and $[Rh(COD)Cl]_2$.

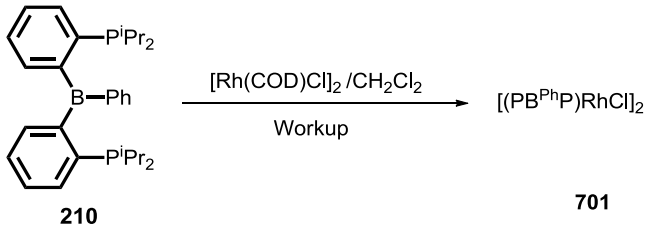

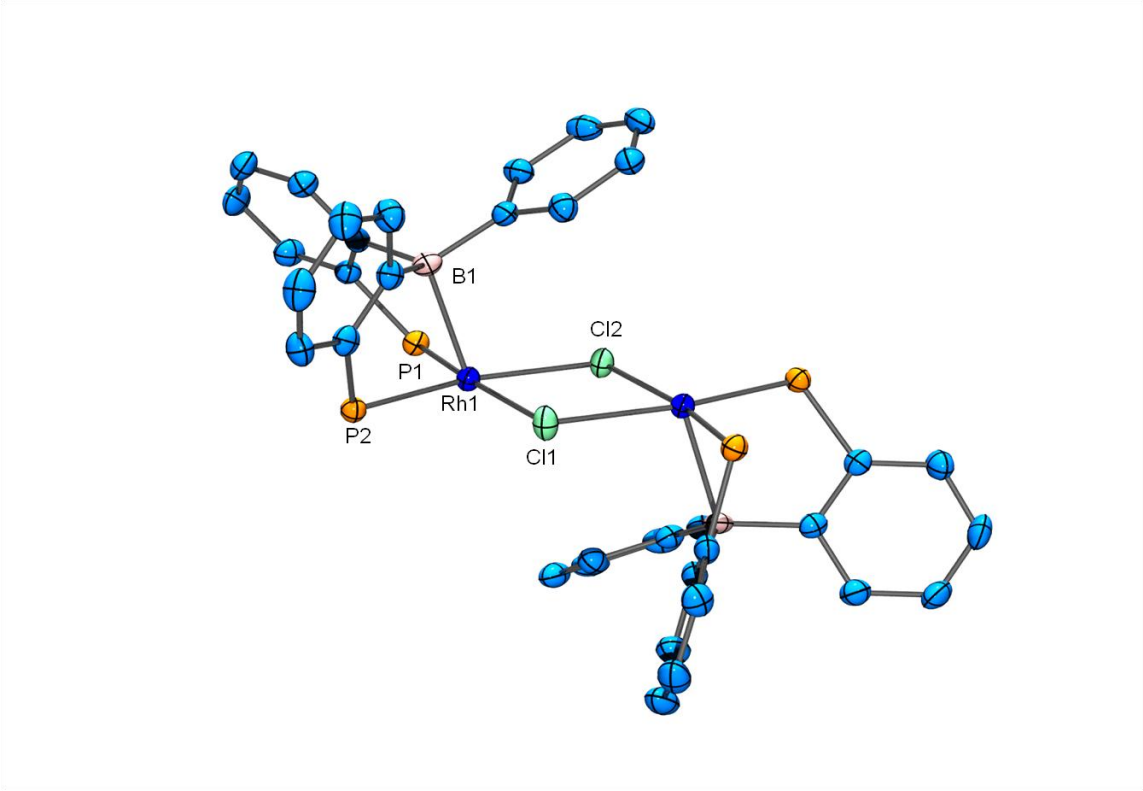

Figure 7-3. ORTEP[128] drawing (50% probability ellipsoids) of **701.** Omitted for clarity: H atoms and *iso*-propyl groups on the phosphorus atoms. Selected distance (Å) and angles (deg) follow: Rh1-B1, 2.303 (3); Rh1-P1, 2.2509 (9); Rh1-P2: 2.2637 (9); Rh1-Cl1. 2.4316 (6); Rh1-Cl2, 2.4380 (6); Cl1-Rh1-Cl2, 77.97 (2); P1-Rh1-P2, 98.38 (3); Cl1-Rh1-P1, 172.27 (3); Cl2-Rh1-P2, 166.46 (3); P1-Rh1-B1, 81.68 (8); P2-Rh1-B1, 80.26 (8); Cl1-Rh1-B1, 102.57 (8); Cl2-Rh1-B1, 105.08 (8).

Thermolysis of **701** at 170 ℃ in *o*-dichlorobenzene (ODCB) for 7 d gave one metal complex **703** (Scheme 7-5), which was characterized by multinuclear NMR spectroscopy after workup. **703** displayed one doublet in the $^{31}P\{^{1}H\}$ NMR spectrum at 45.1 ppm with a much smaller $^{1}J_{Rh\text{-}P}$ at 106 Hz compared to that of **701**, which is consistent with a Rh complex with lower electron density on the Rh center.[183b] The ^{1}H and $^{13}C\{^{1}H\}$ NMR spectra indicated the loss of the phenyl group which was originally

on the boron center. One methine and two methyl resonances were observed for the *iso*-propyl groups, suggesting C_{2v} symmetry for **703**. Based on the spectroscopic data, **703** was proposed to be (PBP)$RhCl_2$. However, no structural evidence has yet been obtained for **703**. We suspect that **703** was formed by a series sequence of B-Ph oxidative addition, reductive elimination of PhCl, C-Cl oxidative addition of ODCB, and then *β*-chloride elimination.

Scheme 7-5. Thermolysis of **701** to obtain **703**.

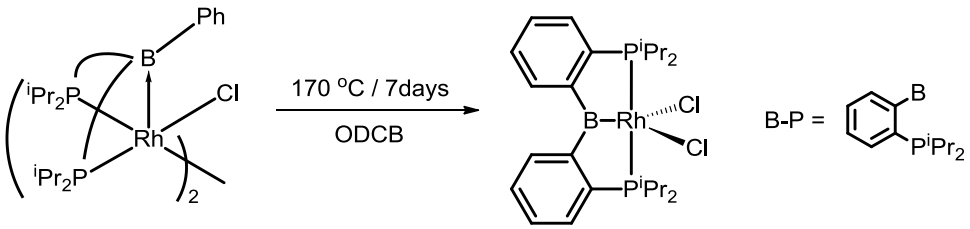

701 **703**

7.2.2 $PB^{Ph}PRhX$ Complexes

Although thermolysis of **701** produced boryl compound **703** (spectroscopic evidence), the reaction was not clean since a brownish powder was collected as the product and multiple organic byproducts was observed in the aromatic region in the ^1H NMR spectra. Given the fact that the reaction was heated at such a high temperature for extended period of time, it is quite possible that some decomposition reactions might occur. We therefore decided to synthesize $PB^{Ph}PRhX$ compounds with more donating

X-ligand, which might make the Rh center more electron rich to favor the oxidative addition of B-Ph bond at relatively low temperature.[22]

Scheme 7-6. Synthesis of complexes **704**, **706** and **708** from **701**.

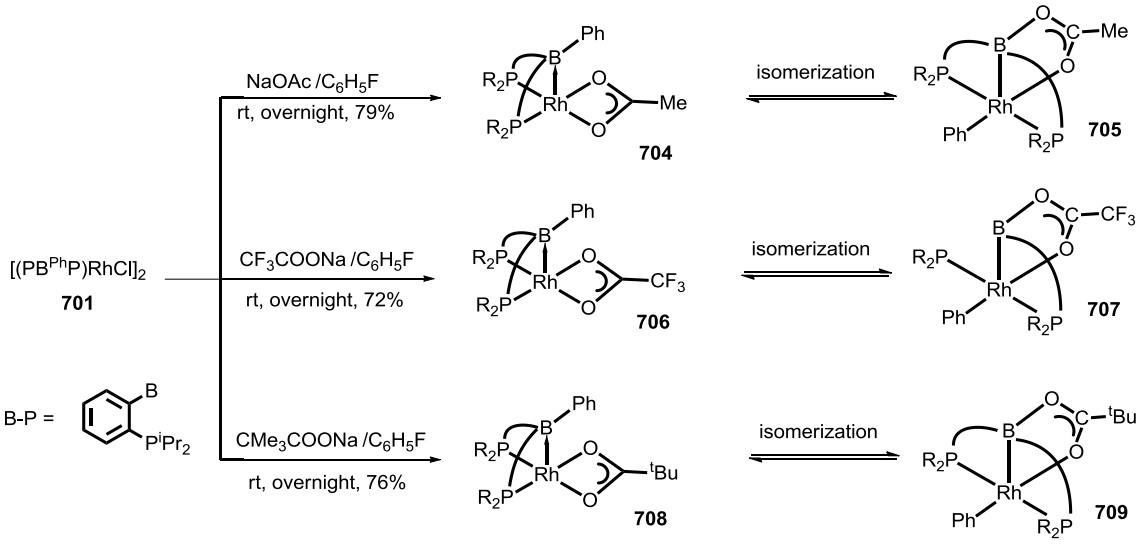

A series of (PB^{Ph}P)Rh carboxylate complexes (**704**, **706** and **708**) were obtained via reaction of **701** and corresponding sodium carboxylate in 72%-79% yield (Scheme 7-6).[216] Complexes **704**, **706** and **708** were characterized by ^{1}H, ^{31}P, ^{13}C, and ^{19}F (where applicable) NMR (Tables 7-1, 7-2). All of them possess one doublet with $^{1}J_{Rh-P}$ around 170 Hz in the $^{31}P\{^{1}H\}$ NMR spectra. ^{1}H NMR spectra of these compounds show two different isopropyl groups on the phosphine arms on the NMR timescale (Table 7-2). All the spectroscopic features of Rh carboxylate complexes in solution indicate they adopt C_s symmetry. The signals of **704** and **706** in $^{11}B\{^{1}H\}$ NMR spectra are very weak. Nevertheless, satisfied $^{11}B\{^{1}H\}$ NMR spectrum was collected for **708** which displayed a

broad signal at 20.0 ppm. The relatively upfield chemical shift suggests the boron center being four coordinated,[163c] which means the phenyl group is likely to be bound to the boron. Moreover, C_{ipso} of phenyl group in **704** and **708** displayed broad signals in $^{13}C\{^{1}H\}$ NMR spectra which is probably owing to the quadrupolar effect of boron atom. Notably, only two sets of the proton resonances for the phenyl group were observed for **704**, **706** and **708**, indicating the free rotation of the phenyl group along the B-C_{ipso} bond on the NMR time scale.

Table 7-1. Selected NMR data for the ($PB^{Ph}P$)Rh carboxylate species in $CDCl_3$, δ ppm. (coupling constant in Hz)

No.	$^{31}P\{^{1}H\}$ (^{1}JRh-P)	RhO(O)C*R*	RhO(O)*C*R
704	74.8 (168)	^{1}H: 1.52 (s, 3H)	$^{13}C\{^{1}H\}$:190.4
706	78.5 (176)	^{19}F: 76.8(s)	not obtained
708	75.5 (168)	^{1}H: 0.83 (s, 9H)	$^{13}C\{^{1}H\}$:197.4

Table 7-2. Selected ^{1}H NMR data for the ($PB^{Ph}P$)Rh carboxylate species in $CDCl_3$, δ ppm. (only the $PB^{Ph}P$ ligand resonance shown, coupling constant in Hz)

No.	aromatic region	aliphatic region
704	7.76 (m, 2H), 7.71 (d, 2H), 7.22 (m, 2H), 7.18-7.13 (m, 5H), 7.00 (t, 2H)	2.49 (m, 2H), 1.88 (m, 2H), 1.36 (m, 12H), 1.18 (dvt, 6H), 0.78 (dvt, 6H)
706	7.56-7.50 (m, 4H), 7.36 (m, 2H), 7.19 (t, 2H, 7.15-7.05 (m, 5H),)	2.56 (m, 2H), 2.09 (m, 2H), 1.43 (m, 12H), 1.31 (m, 6H), 1.01 (m, 6H)
708	7.46 (d, 2H), 7.34 (t, 2H), 7.28 (d, 2H), 7.21 (t, 2H), 7.08 (m, 3H), 7.02 (t, 2H)	2.55 (m, 2H), 2.05 (m, 2H), 1.41 (dvt, 12H), 1.27 (dvt, 6H), 0.99 (dvt, 6H)

X-ray quality crystals of **708** were obtained by slow diffusion of *n*-pentane to a saturated $CHCl_3$ solution of **708** (Figure 7-4). The solid state structure[215] of **708** is consistent with its spectroscopic data. The rhodium center adopts a square pyramidal geometry and only slightly deviates from the basal plane formed by the 2 phosphorus atoms and 2 oxygen atoms (0.071 Å in **708**). The pivalate functions as a κ^2-ligand, while the PBP moiety adopts a facial geometry. The boron atom occupies the axial position with Rh-B distance at 2.28 Å. Compared to ($PB^{Ph}P$)Rh complexes in the literature,[129,137,169b] the Rh-B distance in **708** is similar to that in compounds **A**, **B** and **D**, indicating a strong Rh→B interaction (Figure 7-5). While in compounds **C** and **E**, the Rh-B bond distance are much longer due to the coordination of CO which results in a weaker Rh→B interaction. Although we have not obtained solid state structures for **704** and **706**, the high similarity in spectroscopic data strong suggests **708**, **706** and **704** to display similar structures.

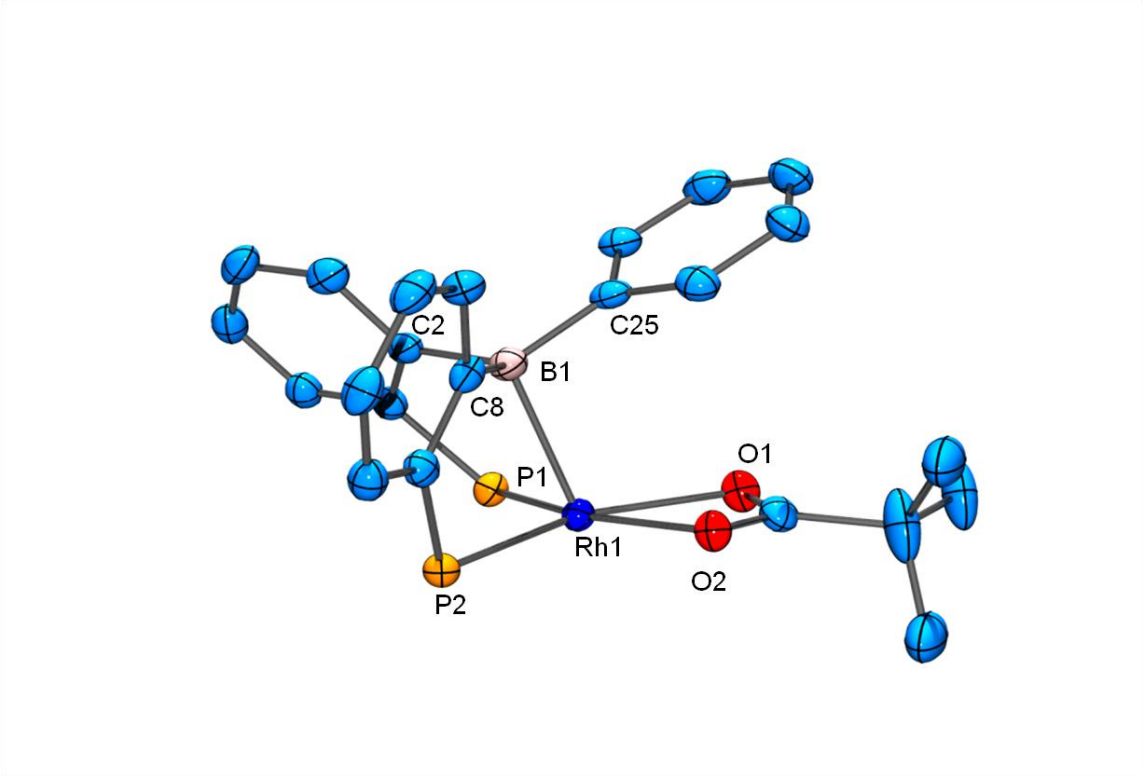

Figure 7-4. ORTEP[128] drawing (50% probability ellipsoids) of **708.** Omitted for clarity: H atoms and *iso*-propyl groups on phosphorus atoms. Selected distance (Å) and angles (deg) follow: Rh1-B1, 2.281 (5); Rh1-P1, 2.213 (1); Rh1-P2: 2.223 (1); Rh1-O1. 2.174 (2); Rh1-O2, 2.155 (3); B1-C2, 1.619 (6); B1-C8, 1.615 (5); B1-C25, 1.598 (5); O1-Rh1-O2, 60.8 (1); P1-Rh1-P2, 99.82 (4); O1-Rh1-P2, 157.42 (8); O2-Rh1-P1, 162.47 (7); P1-Rh1-B1, 82.7 (1); P2-Rh1-B1, 82.2 (1); O1-Rh1-B1, 107.2 (1); O2-Rh1-B1, 101.6 (1); C2-B1-C8, 109.3 (3); C2-B1-C25, 117.0 (3); C8-B1-C25, 116.1 (3); C2-B1-Rh1, 108.1 (2); C8-B1-Rh1, 103.1 (3); C25-B1-Rh1, 101.6 (2); C2-B1-Rh1-P1, 21.4 (2); C8-B1-Rh1-P2, 36.1 (2).

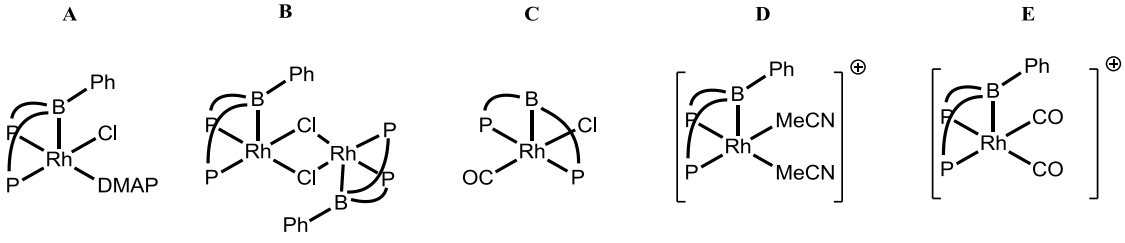

Figure 7-5. Rh-B bond distance (in Å) of (PBP)Rh complexes in literature.

704 slowly isomerized to **705** in $CDCl_3$ at room temperature (Scheme 7-5). The transformation appeared to reach equilibrium in $CDCl_3$ at room temperature in 12 h, with approximately 3 to 1 ratio of **705** to **704**. The equilibrium favored **705** at higher temperature with approximately 5 to 1 ratio of **705** to **704** at 50 ℃ , however the ratio returned to 3:1 once the mixture was cooled down to room temperature which confirmed this was indeed a equilibrium system. The same isomerization was much faster for **706.** In fact, **706** was observed to isomerize to **707** in C_6H_5F. Therefore **706** was always obtained as a mixture of **706** and **707**, since C_6H_5F was used as the solvent for the synthesis of **706**. **708**, on the other hand isomerized much more slowly to **709**. The equilibrium was reached at room temperature after 3 days, or at 60 ℃ in 12 hours with approximately 20:1 ratio of **709** versus **708** at room temperature.

The spectroscopic data of **705**, **707** and **709** was summarized in table 7-3, table 7-4 and table 7-5. All of them possess one doublet with $^1J_{Rh\text{-}P}$ around 140 Hz in the $^{31}P\{^1H\}$ NMR spectra. The smaller $^1J_{Rh\text{-}P}$ compared to those of **704**, **706** and **708** suggests less electron density on the Rh center of **705**, **707** and **709,** which might be a result of oxidative addition of B-Ph bond.[183b] ^1H NMR spectra of these compounds showed two different *iso*-propyl groups on the phosphine arms on the NMR timescale (Table 7-2), which indicates C_s symmetry for complexes **705**, **707** and **709** in solution. The C_{ipso} of the phenyl group appeared as doublet of triplets in $^{13}C\{^1H\}$ NMR spectrum with a large $J_{Rh\text{-}C}$, which unambiguously revealed Ph group has transferred to the metal center. Five sets of proton resonances for the phenyl group were observed for **705**, **707** and **709**, indicating the rotation of the phenyl group along the Rh-C_{ipso} bond has been inhibited on

the NMR time scale due to the steric crowding around Rh center. The relatively upfield chemical shift of **709** at 18.2 ppm in $^{11}B\{^1H\}$ NMR spectrum suggests the boron center being four coordinated.[163c]

Table 7-3. Selected NMR data for the (PBP)Rh(Ph) carboxylate species in $CDCl_3$, δ ppm. (coupling constant in Hz)

No.	$^{31}P\{^1H\}$ (^{1}JRh-P)	RhO(O)C*R*	RhO(O)*C*R
705	48.6 (140)	^1H: 1.88 (s, 3H)	$^{13}C\{^1H\}$ 177.2
707	51.3 (133)	^{19}F: 75.5(s)	not obtained
709	48.2 (142)	^1H: 0.88 (s, 9H)	$^{13}C\{^1H\}$ 184.2

Table 7-4. Selected ^1H NMR data for the (PBP)Rh(Ph) carboxylate species in $CDCl_3$, δ ppm. (only the PBP ligand resonance shown, coupling constant in Hz)

No.	aromatic region	aliphatic region
705	8.23 (d, 2H), 7.41 (t, 2H), 7.36-7.31 (m, 2H), 7.28 (t, 2H),	2.45 (m, 2H), 1.93 (m, 2H), 1.23-1.36 (m, 18H), 0.08 (dvt, 6H)
707	8.03 (d, 2H), 7.54 (m, 2H), 7.42 (br, 2H), 7.29 (m, 2H)	2.35 (m, 2H), 2.18 (m, 2H), 1.18 (dvt, 12H), 0.94 (dvt, 6H), 0.40 (dvt, 6H)
709	8.11 (d, 2H), 7.37 (t, 2H), 7.31-7.29 (m, 2H), 7.19 (t, 2H),	2.31 (m, 2H), 1.96 (m, 2H), 1.39 (dvt, 6H),1.24 (dvt, 6H), 1.14 (dvt, 6H), 0.14 (dvt, 6H)

Table 7-5. Selected ^{1}H NMR and $^{13}C\{^{1}H\}$ NMR data for the (PBP)Rh(Ph) carboxylate species in $CDCl_3$, δ ppm. (only phenyl group resonance shown, coupling constant in Hz)

No.	^{1}H NMR	$^{13}C\{^{1}H\}$ NMR, only C_{ipso}
705	7.67 (d, 1H), 6.78 (t, 1H), 6.47 (t, 1H), 6.17 (t, 1H), 5.92 (d, 1H),	151.6 (dvt, $^{1}J_{Rh-C}$ = 22, $^{1}J_{Rh-C}$ = 12)
707	7.58 (br, 1H), 6.87 (br, 1H), 6.60 (t, 1H), 6.36 (br, 1H), 5.77 (br, 1H),	Not obtained
709	7.64 (d, 1H), 6.77 (t, 1H), 6.46 (t, 1H), 6.18 (t, 1H), 5.81 (d, 1H),	152.5 (dvt, $^{1}J_{Rh-C}$ = 34, $^{1}J_{Rh-C}$ = 12)

X-ray quality crystals of **709** were obtained from slow diffusion of *n*-pentane to a saturated $CHCl_3$ solution of **709** (Figure 7-8). The solid state structure[215] we obtained is consistent with its spectroscopic data. Rhodium center adopts a square pyramidal geometry and only slightly deviated from the basal plane formed by the 2 phosphorus atoms, one oxygen atom and one carbon atom (0.118 Å in **709**). The PBP moiety adopts a meridional geometry with the boron atom occupying the axial position with Rh-B distance at 2.14 Å. The Rh-B bond distance is significantly shorter than that of other (PBP)Rh species with a Rh→B interaction (Figure 7-6). [129,137,169b] The Rh-B bond distance is also considerably longer than that of Rh boryl complexes in the literature (Figure 7-6).[217] The carboxylate group is bridging between Rh-B bond. The two C-O bond distances of the carboxylate group are similar to each other (1.29 Å versus 1.24 Å). Carboxylate bridge has been previously studied with binuclear transition metal complexes, which displayed similar C-O bond length compared to the C-O bond length

in **709** (Figure 7-7).[218] Based on the solid state structure and upfield chemical shift $^{11}B\{^{1}H\}$ spectra, we assigned **709** as a carboxylate-substituted borane Rh complex.

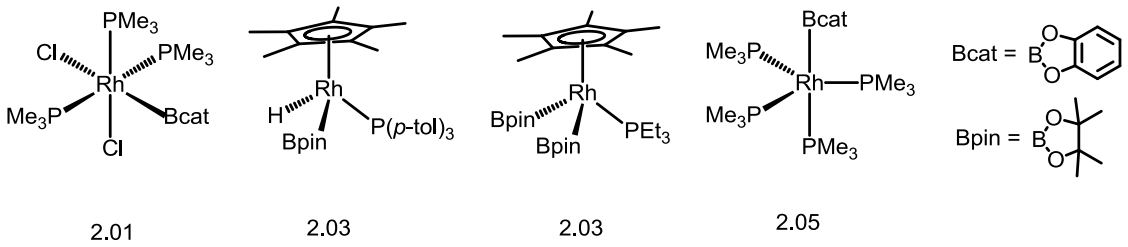

Figure 7-6. Rh-B bond distances (in Å) in Rh boryl complexes in literature.

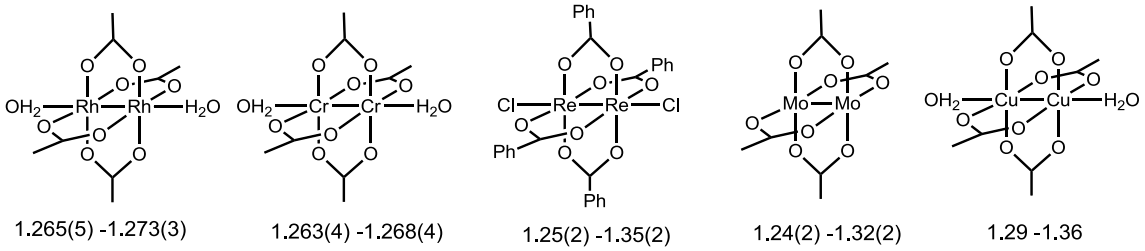

Figure 7-7. C-O bond distances (in Å) in carboxylate-bridging binuclear species.

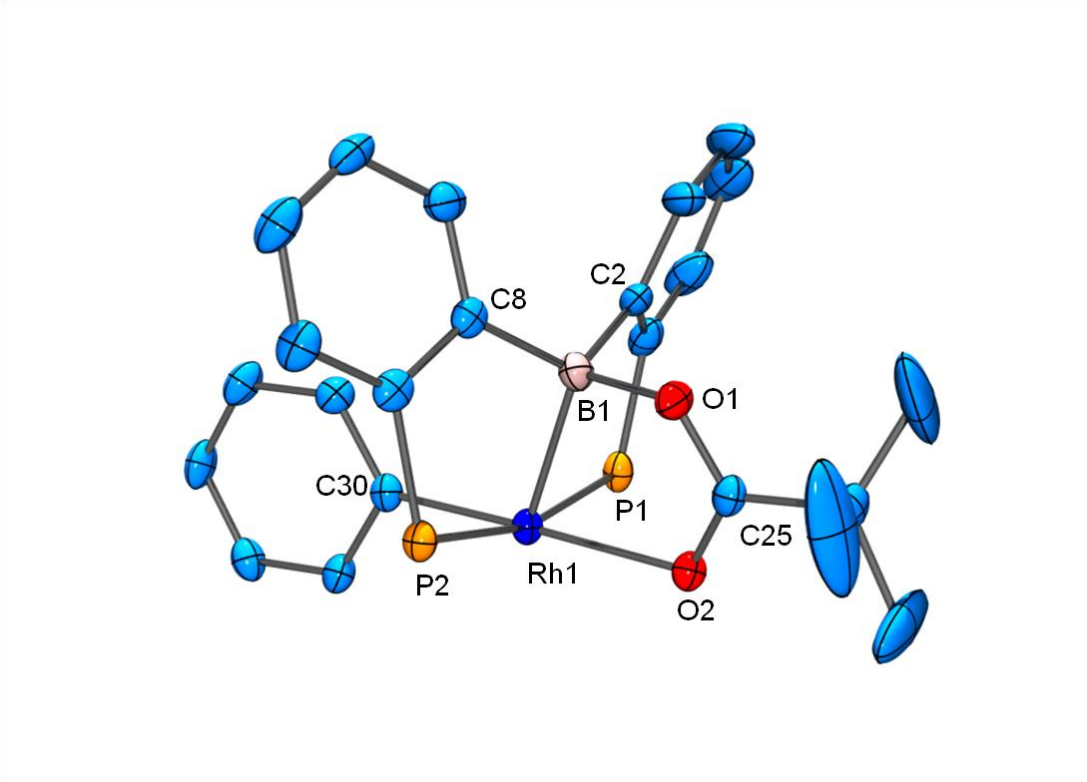

Figure 7-8. ORTEP[128] drawing (50% probability ellipsoids) of **709.** Omitted for clarity: H atoms and *iso*-propyl groups on phosphine arms. Selected distance (Å) and angles (deg) follow: Rh1-B1, 2.141 (5); Rh1-P1, 2.316 (1); Rh1-P2: 2.323 (1); Rh1-O2. 2.190 (2); Rh1-C30, 2.011 (3); B1-C2, 1.614 (6); B1-C8, 1.612 (5); B1-O1, 1.549 (5); C25-O1, 1.296 (3); C25-O2, 1.241 (4); O1-C25-O2, 122.0 (3); O1-Rh1-C30, 178.0 (1); P1-Rh1-P2, 166.16 (3); P1-Rh1-B1, 85.6 (1); P2-Rh1-B1, 82.1 (1); O2-Rh1-B1, 78.8 (1); C30-Rh1-B1, 103.1 (1); C2-B1-C8, 118.7 (3); C2-B1-O1, 105.2 (3); C8-B1-O1, 106.6 (3); C2-B1-Rh1, 112.3 (1); C8-B1-Rh1, 109.3 (3); O1-B1-Rh1, 103.4 (2); C2-B1-Rh1-P1, 5.7 (2); C8-B1-Rh1-P2, 34.0 (2); O1-B1-Rh1-O2, 15.0 (2) .

NMR spectra have been collected at different temperatures to investigate the thermodynamics for the isomerization between **704** and **705**. **704**/**705** were picked as the model to study the intramolecular B-Ph bond activation process, since the equilibrium between **704** and **705** was reached in relatively short amount of time

which made it easy to monitor by NMR spectroscopy. The equilibrium was reached and monitored by ^{1}H NMR spectroscopy at 5 different temperatures between 26 ℃ and 58 ℃ . The ratio of **705** and **704** was determined by their intergrations in the ^{1}H NMR spectra. The van't Hoff analysis of the experimental data (Figure 7-9) led to the determination of$\Delta H° = 8.9 \pm 1.2$ KJ/mol and $\Delta S° = 37.6 \pm 3.6$ J·mol^{-1}K $^{-1}$ for the transformation from **704** to **705**.[219]

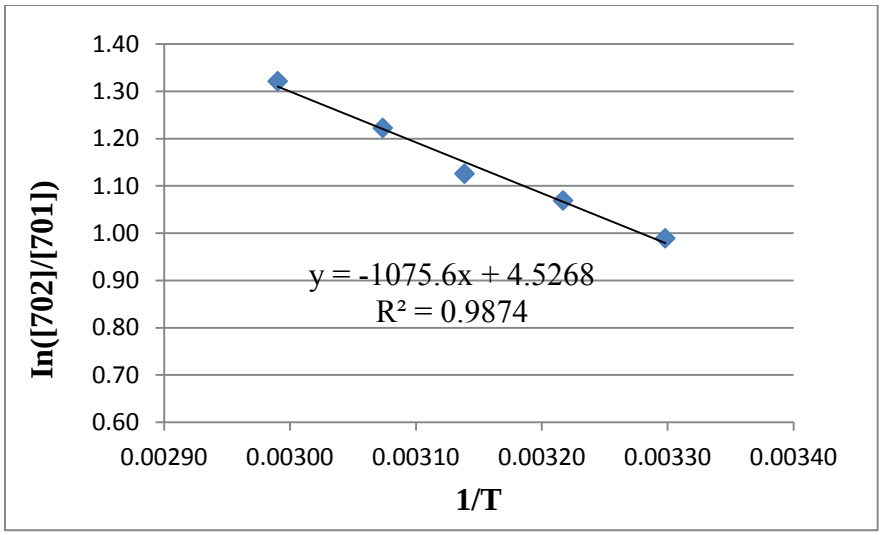

Figure 7-9. Van't Hoff Plot for the transformation between **705** and **704**.

In the (PB^{Ph}P)Rh pivalate species, **708** isomerized to form a pivalate-bridging Rh borane complex. We reasoned the acac group would disfavor the bridging with B-Rh bond due to geometric constraint. (PB^{Ph}P)Rh(acac) was synthesized (**710**) via reaction of **701** and Na(acac) at room temperature for 3 h. After workup, **710** was isolated as yellow powder with 79% yield (Scheme 7-7). One doublet was observed at 68.4 ppm

($^1J_{Rh\text{-}P}$ = 168 Hz) in the $^{31}P\{^1H\}$ NMR spectrum and two distinctive sets of resonances for *iso*-propyl groups in ^1H spectrum of **710** are consistent with symmetric coordination of the two phosphorus atoms. One methyl resonance was observed for the acac group suggesting the symmetric η^2 coordination of acac and C_s symmetry of the molecule in solution.

Scheme 7-7. Synthesis of complexes **710** and **711** from **701**.

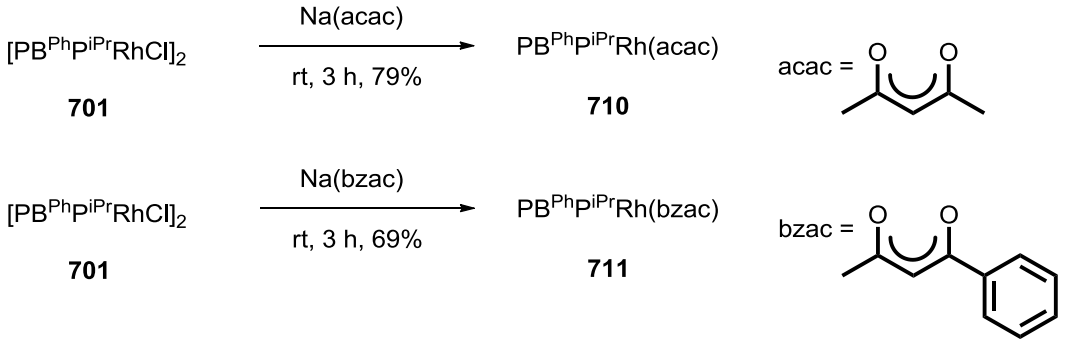

X-ray quality crystals of **710** were obtained by slow diffusion of *n*-pentane into a saturated fluorobenzene solution of **710** at room temperature (Figure 7-10). The solid state structure[215] we obtained is consistent with the spectroscopic data for **710**. The Rh center adopted a square pyramidal geometry and only slightly deviated from the basal plane formed by the 2 phosphorus atoms and two oxygen atoms. (0.019 Å in **710**). PBP moiety adopted facial geometry with boron occupying the axial position. The B-Rh bond distance is 2.27 Å which is very close to that of **708** and **701**. No B-Ph bond activation was observed at 60 ℃ in $CDCl_3$ for several days.

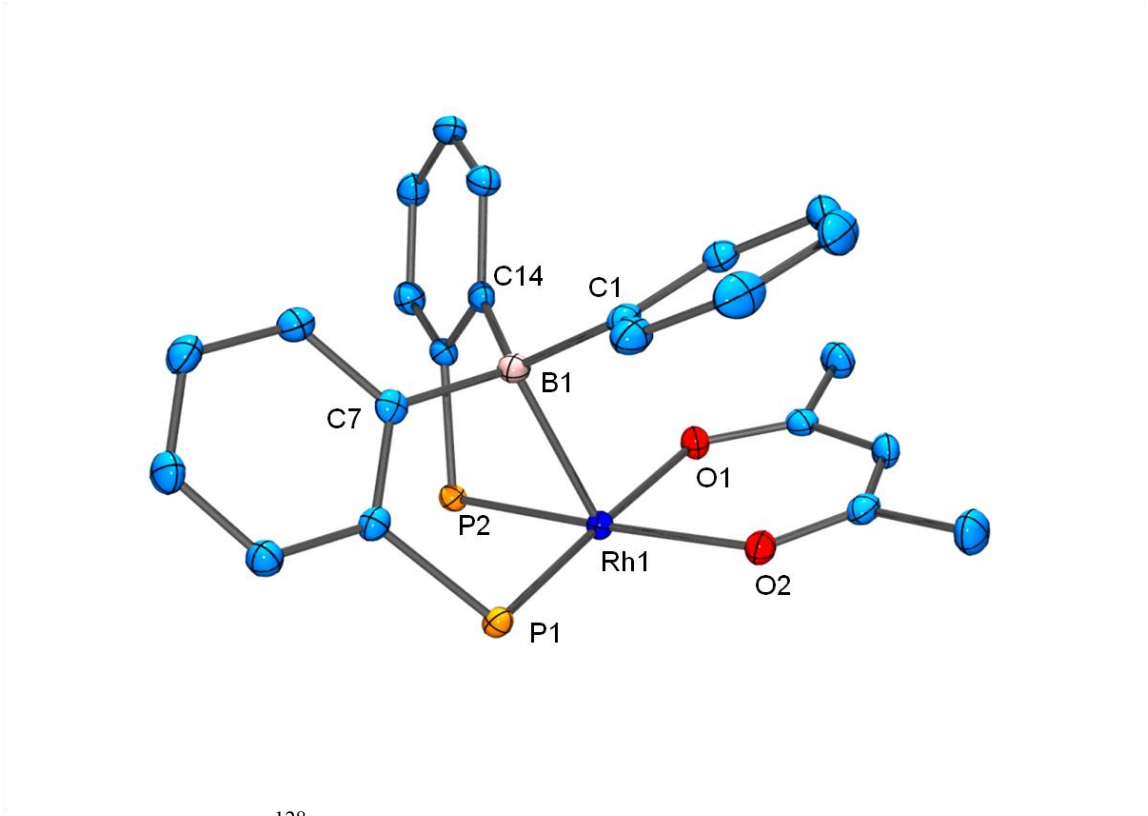

Figure 7-10. ORTEP[128] drawing (50% probability ellipsoids) of **710.** Omitted for clarity: H atoms and *iso*-propyl groups on phosphine arms. Selected distance (Å) and angles (deg) follow: Rh1-B1, 2.271 (2); Rh1-P1, 2.2394 (6); Rh1-P2: 2.2535 (6); Rh1-O1. 2.067 (1); Rh1-O2, 2.075 (1); B1-C1, 1.597 (3); B1-C7, 1.616 (3); B1-C14, 1.614 (2); O1-Rh1-O2, 87.83 (5); P1-Rh1-P2, 98.73 (2); O1-Rh1-P1, 176.51 (4); O2-Rh1-P2, 172.14 (4); P1-Rh1-B1, 83.74 (5); P2-Rh1-B1, 80.06 (5); O1-Rh1-B1, 96.49 (6); O2-Rh1-B1, 103.37 (6); C1-B1-C7, 113.5 (2); C1-B1-C14, 116.5 (2); C7-B1-C14, 112.4 (1); C1-B1-Rh1, 101.0 (1); C7-B1-Rh1, 108.2 (1); C14-B1-Rh1, 103.8 (1); C7-B1-Rh1-P1, 21.1(1); C14-B1-Rh1-P2, 40.6(1). 0.019 Å of the plane.

One interesting aspect from the NMR data for **704**, **706**, **708** and **710** is that the ^{1}H NMR spectra display virtual coupling with both ^{31}P nuclei. It exhibits most obviously for the methyl groups of *iso*-propyl groups on the phosphine arms, which appeared as doublet of triplets. This is unexpected because in the solid state structures of **708** and **710** the P-Rh-P angle is only ca. 98-100° (Figure 7-11). Virtual coupling requires two

equivalent phosphines with a large P-P coupling constant, which is normally achieved only when the phosphines are approximately *trans* to each other (Figure 7-12). [22,220] It was thus of interest to us to find out the P-P coupling constant in **704**, **706**, **708** and **710** to further understand the observed apparent virtual coupling. Obviously, we are not able to observe the P-P coupling in **704**, **706**, **708** and **710**, since the two phosphine groups are equivalent to each other on the NMR time scale. Therefore, we set to synthesize ($PB^{Ph}P$)Rh(acac) type of complex with different R groups. ($PB^{Ph}P$)Rh(bzac) **711** was obtained via reaction of **701** and Na(bzac) at room temperature for 3 h. After workup, **711** was isolated as yellow powder with 69% yield (Scheme 7-7). Two sets of doublet of doublets were observed at 71.1 ppm (dd, J_{Rh-P} = 164 Hz, J_{P-P} = 39 Hz) and 66.8 ppm (dd, J_{Rh-P} = 164 Hz, J_{P-P} = 39 Hz) in the $^{31}P\{^{1}H\}$ NMR spectrum. Four distinctive sets of resonances for *iso*-propyl groups observed in ^{1}H NMR spectrum of **711** are consistent with C_1 symmetry of the molecule. The fairly small P-P coupling constant at 39 Hz is rather unusually for the observation of virtual coupling. Nevertheless, simulation of ^{1}H NMR spectrum for **704** on Mestrec resulted close to observed spectrum when P-P coupling constant was set at 60 Hz (Figure 7-13).

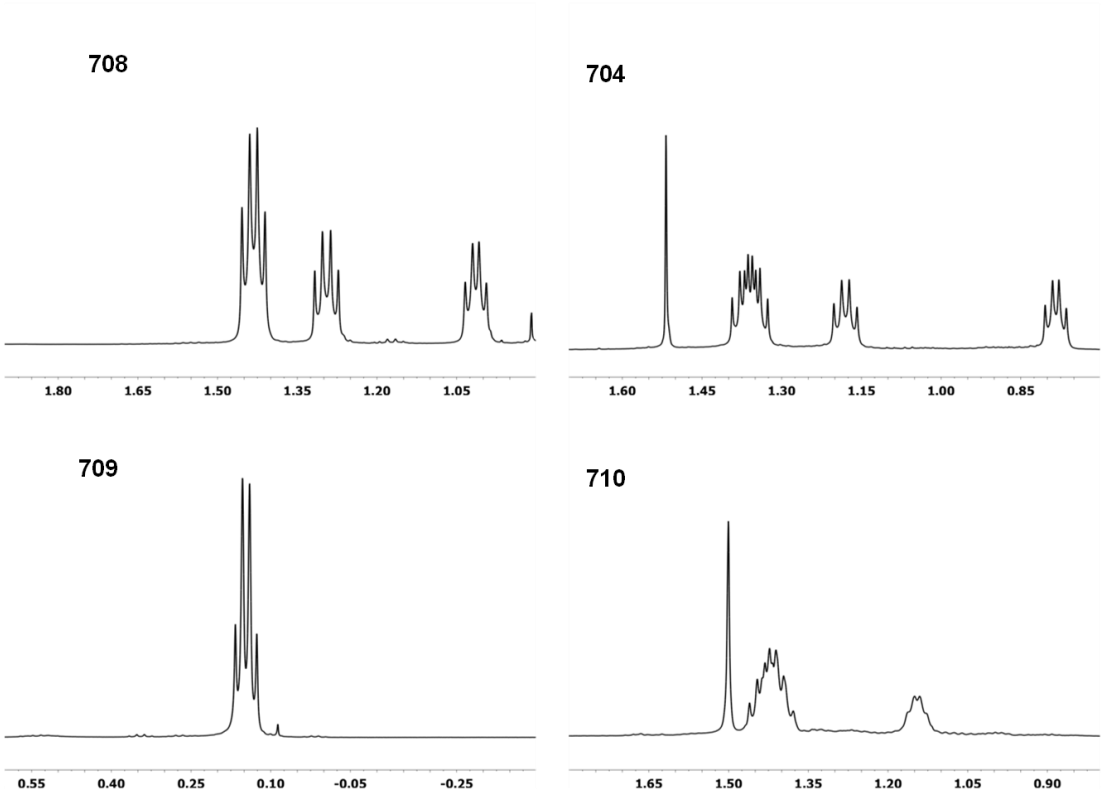

Figure 7-11. Selected ^{1}H NMR spectra for the methyl group of the *iso*-propyl.

Figure 7-12. Coupling pattern affected by the geometry of bisphosphine complexes.

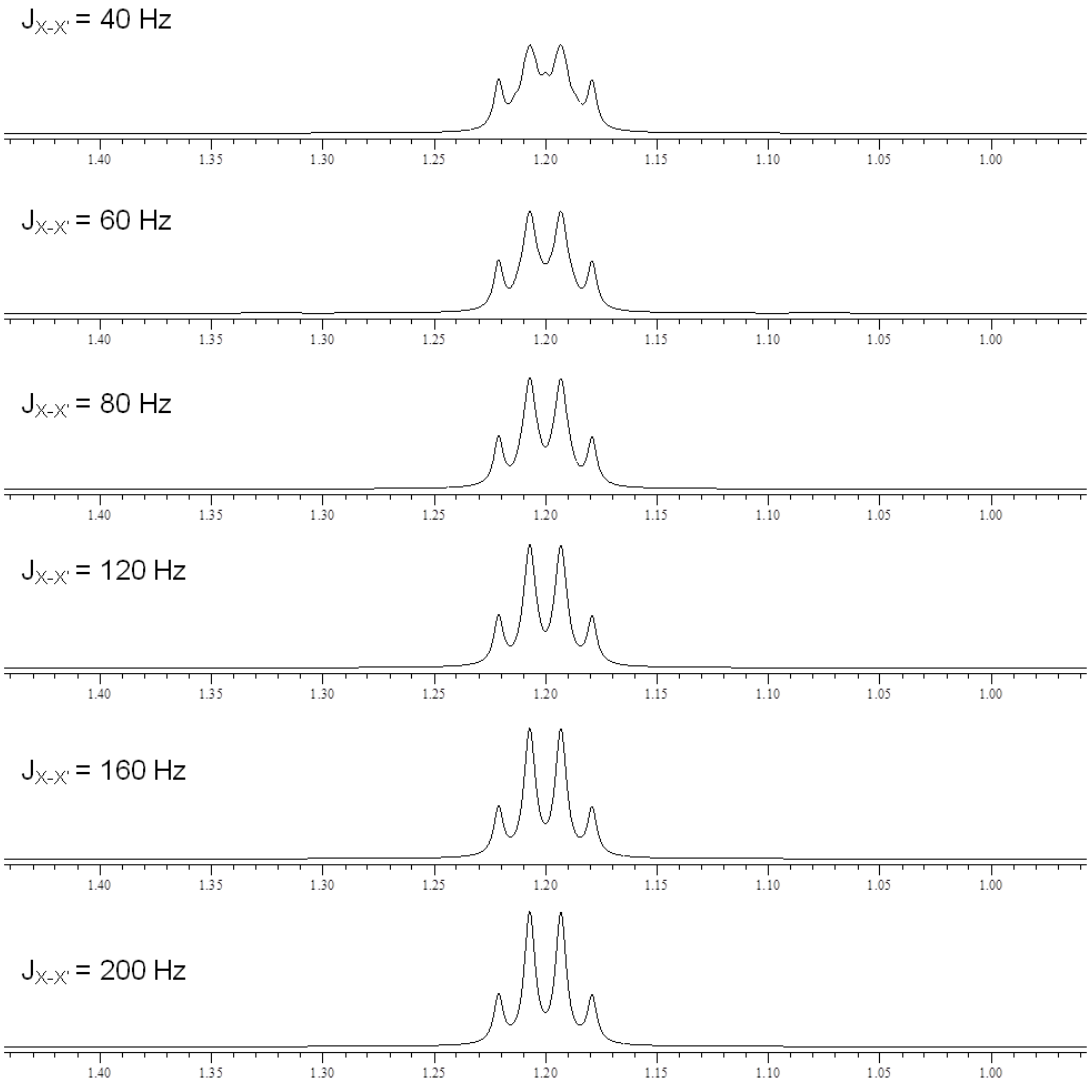

Figure 7-13. Simulation of the coupling pattern of the methyl group of the *iso*-propyl group. ABXX' system was used and the spectroscopic information was set as the following: spectrometer frequency 500 MHz, line width 2.5 Hz. A (methine), 2.5 ppm; B (methyl), 1.2 ppm; X (P1), 180.0 ppm; X' (P2), 180.0 ppm; J_{A-B} = 7 Hz; J_{A-X} = 12 Hz, J_{A-X} was set at 0 for simplicity. $J_{X-X'}$ was varied between 40 to 200 Hz.

7.3 Conclusion

In summary, a series of (PBP)RhX complexes were synthesized via salt metathesis reaction with (PBP)RhCl dimer and characterized by multi-nuclei NMR spectroscopy,

elemental analysis and X-ray crystallography. (PBP)Rh acetate, trifluoroacetate, pivalate and acetylacetonate species all showed strong Rh→B interaction. While the (PBP)Rh acetylacetonate specie was stable at room temperature in solution, the carboxylate species underwent reversible intramolecular B-Ph bond activation process. Preliminary studies for the thermodynamics of this transformation revealed that in the (PBP)Rh acetate species, the ΔH° for the isomerization of **704** is around 8.9 ± 1.2 KJ/mol and the ΔS° or the same transformation is around 37.6 ± 3.6 $J \cdot mol^{-1}K^{-1}$. A carboxylate-bridging Rh borane was observed after the phenyl migration. Therefore, we conclude carboxylate species is not suitable to be used as the X lihgand to obtain (PBP)Rh(X)(Ph) complex with three coordinated boryl unit via B-Ph bond activation of ($PB^{Ph}P$)Rh(X) species. Thermolysis of 701 gave access to (PBP)$RhCl_2$ (spectroscopic evidence). However the reaction is not clean which make it an undesirable method to access pincer boryl compounds as potential starting material for further study. One interesting observation from our research is that, although in **711** we only observed P-P coupling constant around 40 Hz for the two *cis* phosphines, we observed virtual coupling for the *iso*-propyl group for **704**, **706**, **708** and **710** despite the two phosphine groups being *cis* to each other.

7.4 Experimental Details

General considerations. Unless specified otherwise, all reactions and manipulations were carried out under an argon atmosphere using glove box or Schlenk line techniques. Dry, oxygen–free solvents were employed. Toluene, Pentane, diethyl ether, THF and

C_6D_6 were dried over NaK/Ph_2CO/18-crown-6, distilled and stored over molecular sieves in an Ar-filled glove box. CH_2Cl_2, $CDCl_3$, CD_2Cl_2, *o*-dichlorobenzene were dried over CaH_2, distilled and stored over molecular sieves in an Ar-filled glove box. $[Rh(COD)Cl]_2$[221] and $[Ir(COD)Cl]_2$[222] were prepared via literature procedures. Synthesis of ligand **210** were described in Chapter II. All other chemicals were used as received from commercial vendors unless otherwise noted.

Physical Methods. NMR spectra were recorded on a Varian iNova 300 spectrometer (^{1}H NMR, 299.9 MHz, ^{13}C NMR, 75.4 MHz, ^{31}P NMR, 121.4 MHz), a Varian iNova 400 spectrometer (^{1}H NMR, 400.0 MHz, ^{13}C NMR, 100.5 MHz, ^{31}P NMR, 161.9 MHz ^{11}B NMR, 120.4 MHz) and a Varian iNova 500 spectrometer (^{1}H NMR, 500.0 MHz, ^{13}C NMR, 125.7 MHz, ^{31}P NMR, 202.4 MHz, ^{19}F NMR, 469.9 MHz) in noted solvents. Chemical shifts are given in δ (ppm). ^{11}B NMR spectra were referenced externally with BF_3 etherate at δ 0. ^{31}P NMR spectra were referenced externally with 85% phosphoric acid at δ 0. ^{1}H NMR and ^{13}C NMR spectra were referenced using the solvent signals. Elemental analyses were performed by CALI, Inc. (Parsippany, NJ). Solid state structures of **701**, **708**, **709** and **710** were solved by Dr. David E. Herbert.

(PB^{Ph}P)RhCl (701). To a cold solution of **210** (1.54 g, 3.24 mmol) in CH_2Cl_2 (6 mL) was added $[Rh(COD)Cl]_2$ (800 mg, 1.62 mmol). The resulting orange solution was stirred at room temperature for 3 h, yellow compounds was slowly percipitated from the solution though the time. The yellow powder was collected on a "M" frit, washed with CH_2Cl_2 and dried under vacuum for 3h. Yield: 1.90 g (95%). Two isomers were observed in ^{31}P, ^{1}H NMR spectra. Isomer 1: ^{31}P{^{1}H} NMR (121.4

MHz, $CDCl_3$): δ 50.4 (d, J_{Rh-P} = 126 Hz). ^1H NMR (500.0 MHz, $CDCl_3$): δ 8.07 (m, 2H, Ar-*H*), 7.60 (m, 2H, Ar-*H*), 7.52 (m, 4H, Ar-*H*), 6.68 (m, 2H, Ar-*H*), 6.60 (m, 3H, Ar-*H*), 3.09 (m, 2H, C*H*Me_2), 2.39 (m, 2H, C*H*Me_2), 1.31 (m, 6H, CH*Me*$_2$), 1.10 (m, 6H, CH*Me*$_2$), 0.89 (m, 6H, CH*Me*$_2$), 0.34 (m, 6H, CH*Me*$_2$). Isomer 2: $^{31}P\{^1H\}$ NMR (121.4 MHz, $CDCl_3$): δ 88.8 (d, J_{Rh-P} = 194 Hz). ^1H NMR (500.0 MHz, $CDCl_3$): δ 7.91 (br, 2H, Ar-*H*), 7.59 (br, 6H, Ar-*H*), 7.08 (br, 2H, Ar-*H*), 6.96 (m, 3H, Ar-*H*), 2.48 (br, 2H, C*H*Me_2), 2.07 (br, 2H, C*H*Me_2), 1.49 (br, 12H, CH*Me*$_2$), 1.24 (br, 6H, CH*Me*$_2$), 0.88 (br, 6H, CH*Me*$_2$).

(PB^{Ph}P)RhCl$_2$ (703). A solution of **701** (18 mg, 0.015 mmol) in ODCB (0.5 mL) was heated to 170 ℃ in a J-Young tube for 7 days. After passed through a short plug of Celite and removal of all volatiles, brownish powder was obtained as the product. $^{31}P\{^1H\}$NMR (121.4 MHz, $CDCl_3$): δ 45.1 (d, J_{Rh-P} = 106 Hz). ^1H NMR (500.0 MHz, $CDCl_3$): δ 7.88 (m, 2H, Ar-*H*), 7.76 (m, 2H, Ar-*H*), 7.52 (m, 2H, Ar-*H*), 7.46 (m, 2H, Ar-*H*), 2.88 (br, 4H, C*H*Me_2), 1.38 (m, 12H, CH*Me*$_2$), 1.29 (m, 12H, CH*Me*$_2$). $^{13}C\{^1H\}$ NMR (125.6 MHz, $CDCl_3$): δ 170.1 (br), 135.7 (s), 131.5 (s), 131.4 (t, J_{P-C} = 10 Hz), 131.0 (s), 130.1(s), 24.8 (t, J_{P-C} = 13 Hz, *C*HMe_2), 20.8 (s, CH*Me*$_2$), 20.3 (s, CH*Me*$_2$).

(PB^{Ph}P)RhOAc (704). To a solution of **701** (50 mg, 0.041 mmol) in C_6H_5F (4 mL) was added potassium acetate (40 mg, 0.41 mmol). The resulting yellow suspension was stirred at room temperature overnight, then the reaction mixtures were filtered through a short plug of Celite. After removal of all volatiles, the crude products were washed with cold pentane 3 times and dried under vacuum for 3h. Yield: 52 mg

(79%). $^{31}P\{^{1}H\}$ NMR (121.4 MHz, C_6D_6): δ 74.8 (d, J_{Rh-P} = 168 Hz). ^{1}H NMR (500.0 MHz, C_6D_6): δ 7.76 (m, 2H, Ar-*H*), 7.71 (d, J_{H-H} = 8 Hz, 2H, Ar-*H*), 7.22 (m, 2H, Ar-*H*), 7.13-7.18 (m, 5H, Ar-*H*), 7.00 (t, J_{H-H} = 8 Hz, 2H, Ar-*H*), 2.49 (m, 2H, C*H*Me_2), 1.88 (m, 2H, C*H*Me_2), 1.52 (s, 3H, C*Me*(acetate)), 1.36 (m, 12H, CH*Me*$_2$), 1.18 (dvt, J_{H-H} = 7 Hz, J_{P-H} = 7 Hz, 6H, CH*Me*$_2$), 0.78 (dvt, J_{H-H} = 7 Hz, J_{P-H} = 7 Hz, 6H, CH*Me*$_2$). $^{13}C\{^{1}H\}$ NMR (125.6 MHz, $CDCl_3$): δ 190.4 (s, *C*=O (acetate)), 168.1 (m), 154.9 (m), 136.7 (s), 136.3 (s), 132.0 (t, J_{P-C} = 10 Hz), 128.9 (s), 127.9 (s), 126.4 (s), 126.0 (s), 124.1 (t, J_{P-C} = 4 Hz), 27.5 (t, J_{P-C} = 13 Hz, *C*HMe_2), 27.1 (t, J_{P-C} = 13 Hz, *C*HMe_2), 25.0 (s, C*Me*(acetate)), 22.4 (s, CH*Me*$_2$), 20.1 (s, C*Me*(acac)), 20.0 (s, CH*Me*$_2$), 19.6 (s, CH*Me*$_2$). Elem. An. Found (Calculated) for $C_{32}H_{44}BO_2P_2Rh$: C, 60.40 (60.38); H, 6.97 (6.91)%.

(PBP)Rh(Ph)OAc (705). Compound **704** was dissolved in $CDCl_3$ and slowly converted to compound **705** at room temperature. After 12 h, the equilibrium was established between compound **704** and compound **705** with 1:3 ratio. $^{31}P\{^{1}H\}$ NMR (121.4 MHz, $CDCl_3$): δ 48.6 (d, J_{Rh-P} = 140 Hz). ^{1}H NMR (500.0 MHz, $CDCl_3$): δ 8.23 (d, J_{H-H} = 8 Hz, 2H, Ar-*H*), 7.67 (d, J_{H-H} = 7 Hz, 1H, Ar-*H*), 7.41 (t, J_{H-H} = 8 Hz, 2H, Ar-*H*), 7.31-7.36 (m, 2H, Ar-*H*), 7.28 (t, J_{H-H} = 8 Hz, 2H, Ar-*H*), 6.78 (t, J_{H-H} = 7 Hz, 1H, Ar-*H*), 6.47 (t, J_{H-H} = 7 Hz, 1H, Ar-*H*), 6.17 (t, J_{H-H} = 7 Hz, 1H, Ar-*H*), 5.92 (d, J_{H-H} = 7 Hz, 1H, Ar-*H*), 2.45 (m, 2H, C*H*Me_2), 1.93 (m, 2H, C*H*Me_2), 1.88 (s, 3H, C*Me*(acetate)), 1.23-1.36 (m, 18H, CH*Me*$_2$), 0.08 (dvt, J_{H-H} = 7 Hz, J_{P-H} = 7 Hz, 6H, CH*Me*$_2$). $^{13}C\{^{1}H\}$ NMR (125.6 MHz, $CDCl_3$): δ 177.2 (s, *C*=O (acetate)), 161.3 (m), 151.6 (dvt, J_{Rh-C} = 22 Hz, J_{P-C}= 12 Hz), 140.5 (s), 137.7 (dvt, J_{Rh-C} = 3 Hz, J_{P-C}= 20

Hz), 132.9 (d, J_{Rh-C} = 2 Hz), 131.9 (t, J_{P-C} = 10 Hz), 130.8 (s), 128.3 (s), 125.5 (s), 125.2 (s), 124.0 (s), 120.2 (s), 27.3 (t, J_{P-C} = 9 Hz, *C*HMe$_2$), 22.0 (t, J_{P-C} = 11 Hz, *C*HMe$_2$), 21.4 (s, C*Me*(acetate)), 21.0 (t, J_{P-C} = 3 Hz, CH*Me*$_2$), 19.2 (s, J_{P-C} = 3 Hz, C*Me*(acac)), 18.4 (s, CH*Me*$_2$), 17.7 (s, CH*Me*$_2$).

(PB^{Ph}P)Rh(O(O)CCF$_3$) (706). To a solution of **701** (107 mg, 0.087 mmol) in C_6H_5F (10 mL) was added potassium trifluorocetate (130 mg, 0.86 mmol). The resulting yellow suspension was stirred at room temperature for 3 h, then the reaction mixtures were filtered through a short plug of Celite. After removal of all volatiles, the crude products were washed with cold pentane 3 times and dried under vacuum for 3 h. **706** was found to quickly convert to **707** in C_6H_5F, the equilibrium was established between compound **706** and compound **707** with 1:2 ratio. Therefore, the yellow powder we isolated is a mixture of **706** and **707**. Yield: 87 mg (72%). $^{31}P\{^1H\}$ NMR (121.4 MHz, $CDCl_3$): δ 78.5 (d, J_{Rh-P} = 176 Hz). ^{19}F NMR (469.9 MHz, $CDCl_3$): δ 76.8 (s). ^1H NMR (500.0 MHz, $CDCl_3$): δ 7.56-7.50 (m, 4H, Ar-*H*), 7.36 (m, 2H, Ar-*H*), 7.19 (t, J_{H-H} = 8 Hz, 2H, Ar-*H*), 7.05-7.15 (m, 5H, Ar-*H*), 2.56 (m, 2H, C*H*Me$_2$), 2.09 (m, 2H, C*H*Me$_2$), 1.43 (m, 12H, CH*Me*$_2$), 1.31 (m, 6H, CH*Me*$_2$), 1.01 (m, 6H, CH*Me*$_2$).

(PBP)Rh(Ph)(O(O)CCF$_3$) (707). $^{31}P\{^1H\}$ NMR (121.4 MHz, $CDCl_3$): δ 51.3 (d, J_{Rh-P} = 133 Hz). ^{19}F NMR (469.9 MHz, $CDCl_3$): δ 75.5 (s). ^1H NMR (500.0 MHz, $CDCl_3$): δ 8.03 (d, J_{H-H} = 8 Hz, 2H, Ar-*H*), 7.58 (br, 1H, Ar-*H*), 7.54 (m, 2H, Ar-*H*), 7.42 (br, 2H, Ar-*H*), 7.29 (m, J_{H-H} = 8 Hz, 2H, Ar-*H*), 6.87 (br, 1H, Ar-*H*), 6.60 (t, J_{H-H} = 7 Hz, 1H, Ar-*H*), 6.36 (br, 1H, Ar-*H*), 5.77 (br, 1H, Ar-*H*), 2.35 (m, 2H, C*H*Me$_2$), 2.18 (m,

2H, C*H*Me$_2$), 1.18 (dvt, J_{H-H} = 7 Hz, J_{P-H} = 7 Hz, 6H, CH*Me*$_2$), 0.94 (dvt, J_{H-H} = 7 Hz, J_{P-H} = 7 Hz, 12H, CH*Me*$_2$), 0.40 (dvt, J_{H-H} = 7 Hz, J_{P-H} = 7 Hz, 6H, CH*Me*$_2$).

(PB^{Ph}P)Rh(O(O)C^{t}Bu) (708). To a solution of **701** (93 mg, 0.15 mmol) in C_6H_5F (10 mL) was added potassium pivalate (105 mg, 0.75 mmol). The resulting yellow suspension was stirred at room temperature overnight, then the reaction mixtures were filtered through a short plug of Celite. After removal of all volatiles, the crude products were washed with cold pentane 3 times and dried under vacuum for 3 h. Yield: 78 mg (76%). X-ray quality crystals were obtained by slow diffusion of pentane to a saturated fluorobenzene solution of **708**. $^{31}P\{^1H\}$ NMR (121.4 MHz, $CDCl_3$): δ 75.5 (d, J_{Rh-P} = 168 Hz). ^1H NMR (500.0 MHz, $CDCl_3$): δ 7.46 (d, J_{H-H} = 8 Hz, 2H, Ar-*H*), 7.34 (t, J_{H-H} = 8 Hz, 2H, Ar-*H*), 7.28 (d, J_{H-H} = 8 Hz, 2H, Ar-*H*), 7.21 (t, J_{H-H} = 8 Hz, 2H, Ar-*H*), 7.08 (m, 3H, Ar-*H*), 7.02 (t, J_{H-H} = 8 Hz, 2H, Ar-*H*), 2.55 (m, 2H, C*H*Me$_2$), 2.05 (m, 2H, C*H*Me$_2$), 1.41 (dvt, J_{H-H} = 7 Hz, J_{P-H} = 7 Hz, 12H, CH*Me*$_2$), 1.27 (dvt, J_{H-H} = 7 Hz, J_{P-H} = 7 Hz, 6H, CH*Me*$_2$), 0.99 (dvt, J_{H-H} = 7 Hz, J_{P-H} = 7 Hz, 6H, CH*Me*$_2$), 0.83 (s, 9H, C*Me*$_3$). $^{13}C\{^1H\}$ NMR (125.6 MHz, $CDCl_3$): δ 197.4 (s, *C*=O (pivalate)), 168.7 (m), 155.3 (m), 136.8 (s), 136.5 (s), 132.0 (t, J_{P-C} = 10 Hz), 128.7 (s), 127.7 (s), 126.2 (s), 125.4 (s), 124.0 (t, J_{P-C} = 4 Hz), 39.8 (s, *C*Me$_3$), 27.4 (t, J_{P-C} = 13 Hz, *C*HMe$_2$), 27.2 (t, J_{P-C} = 13 Hz, *C*HMe$_2$), 26.6 (s, C*Me*$_3$), 22.3 (s, CH*Me*$_2$), 20.0 (s, CH*Me*$_2$), 19.8 (s, CH*Me*$_2$), 19.3 (s, CH*Me*$_2$). $^{11}B\{^1H\}$ NMR (120.4 MHz, $CDCl_3$): δ 20.0 (br). Elem. An. Found (Calculated) for $C_{35}H_{50}BO_2P_2Rh$: C, 61.96 (61.73); H, 7.43 (7.44)%.

(PBP)Rh(Ph)(O(O)C^{t}Bu) (709). Compound **708** was dissolved in $CDCl_3$ and

converted to compound **709** at 50 °C. After 12 h, the equilibrium was established between compound **708** and compound **709** with 1 : 20 ratio. X-ray quality crystals were obtained by slow diffusion of pentane to a saturated fluorobenzene solution of **709**. $^{31}P\{^{1}H\}$ NMR (121.4 MHz, $CDCl_3$): δ 48.2 (d, J_{Rh-P} = 142 Hz). ^{1}H NMR (500.0 MHz, $CDCl_3$): δ 8.11 (d, J_{H-H} = 8 Hz, 2H, Ar-*H*), 7.64 (d, J_{H-H} = 7 Hz, 1H, Ar-*H*), 7.37 (t, J_{H-H} = 8 Hz, 2H, Ar-*H*), 7.29-7.31 (m, 2H, Ar-*H*), 7.19 (t, J_{H-H} = 8 Hz, 2H, Ar-*H*), 6.77 (t, J_{H-H} = 7 Hz, 1H, Ar-*H*), 6.46 (t, J_{H-H} = 7 Hz, 1H, Ar-*H*), 6.18 (t, J_{H-H} = 7 Hz, 1H, Ar-*H*), 5.81 (d, J_{H-H} = 7 Hz, 1H, Ar-*H*), 2.31 (m, 2H, C*H*Me_2), 1.96 (m, 2H, C*H*Me_2), 1.39 (dvt, J_{H-H} = 7 Hz, J_{P-H} = 7 Hz, 6H, CH*Me*$_2$), 1.24 (dvt, J_{H-H} = 7 Hz, J_{P-H} = 7 Hz, 6H, CH*Me*$_2$), 1.14 (dvt, J_{H-H} = 7 Hz, J_{P-H} = 7 Hz, 6H, CH*Me*$_2$), 0.88 (s, 9H, C*Me*$_3$), 0.14 (dvt, J_{H-H} = 7 Hz, J_{P-H} = 7 Hz, 6H, CH*Me*$_2$). $^{13}C\{^{1}H\}$ NMR (125.6 MHz, $CDCl_3$): δ 184.2 (s, *C*=O (pivalate)), 161.3 (m), 152.5 (dvt, J_{Rh-C} = 34 Hz, J_{P-C} = 12 Hz), 140.3 (s), 137.8 (dvt, J_{Rh-C} = 3 Hz, J_{P-C} = 20 Hz), 132.7 (d, J_{Rh-C} = 2 Hz), 131.8 (t, J_{P-C} = 10 Hz), 130.5 (s), 128.0 (s), 125.4 (s), 124.9 (s), 124.0 (s), 120.1 (s), 38.0 (s, *C*Me_3), 26.9 (s, C*Me*$_3$), 26.3 (t, J_{P-C} = 9 Hz, *C*HMe_2), 21.3 (t, J_{P-C} = 4 Hz, *C*HMe_2), 21.2 (s, CH*Me*$_2$), 19.5 (br, CH*Me*$_2$), 18.5 (s, CH*Me*$_2$), 17.4 (s, CH*Me*$_2$). $^{11}B\{^{1}H\}$ NMR (120.4 MHz, $CDCl_3$): δ 18.2 (br).

(PB^{Ph}P)Rh(acac) (710). To a solution of **701** (60 mg, 0.049 mmol) in C_6H_5F (5 mL) was added sodium acetylacetonate (60 mg, 0.49 mmol). The resulting yellow suspension was stirred at room temperature for 3 h, then the reaction mixtures were filtered through a short plug of Celite. After removal of all volatiles, the crude products were purified by recrystallization from C_6H_5F solution at -30 ℃ . X-ray

quality crystals were obtained by slow diffusion of pentane to a saturated fluorobenzene solution of **710**. Yield: 52 mg (79%). $^{31}P\{^{1}H\}$ NMR (121.4 MHz, $CDCl_3$): δ 68.4 (d, J_{Rh-P} = 168 Hz). ^{1}H NMR (500.0 MHz, $CDCl_3$): δ 7.47 (br, 2H, Ar-*H*), 7.26 (t, J_{H-H} = 7 Hz, 2H, Ar-*H*), 7.11 (t, J_{H-H} = 7 Hz, 2H, Ar-*H*), 7.03 (t, J_{H-H} = 7 Hz, 2H, Ar-*H*), 6.94 (m, 3H, Ar-*H*), 6.88 (m, 2H, Ar-*H*), 5.14 (s, 1H, C-*H*(acac)), 2.78 (m, 2H, C*H*Me_2), 1.90 (m, 2H, C*H*Me_2), 1.50 (s, 6H, C*Me*(acac)), 1.42 (m, 18H, CH*Me*$_2$), 1.14 (m, 6H, CH*Me*$_2$). $^{13}C\{^{1}H\}$ NMR (125.6 MHz, $CDCl_3$): δ 183.9 (s, *C*=O (acac)), 168.7 (m), 154.8 (m), 139.5 (d, J_{Pt-C} = 48 Hz), 135.5 (s), 131.5 (m), 128.8 (s), 128.0 (s), 125.1 (s), 124.2 (s), 123.4 (s), 100.0 (s, *C*-H (acac)), 27.4 (m, *C*HMe_2), 26.7 (m, CH*Me*$_2$), 25.0 (m, *C*HMe_2), 22.5 (m, C*Me*(acac)), 22.0 (br, CH*Me*$_2$), 20.9 (br, CH*Me*$_2$), 20.7 (br m, J_{Pt-C} = 22 Hz, CH*Me*$_2$). Elem. An. Found (Calculated) for $C_{35}H_{48}BO_2P_2Rh$: C, 62.08 (62.15); H, 7.09 (7.15)%.

(PB^{Ph}P)Rh(benzoylacetonate) (711). To a solution of **701** (25 mg, 0.02 mmol) in C_6H_5F (2 mL) was added sodium benzoylacetonate (25 mg, 0.136 mmol). The resulting yellow suspension was stirred at room temperature for 3 h, then the reaction mixtures were filtered through a short plug of Celite. After removal of all volatiles, the crude products were purified by recrystallization from C_6H_5F solution at -30 ℃ . Yield: 20 mg (68%). $^{31}P\{^{1}H\}$ NMR (121.4 MHz, $CDCl_3$): δ 71.1 (dd, J_{Rh-P} = 164 Hz, J_{P-P} = 39 Hz), 66.8 (dd, J_{Rh-P} = 164 Hz, J_{P-P} = 39 Hz). ^{1}H NMR (500.0 MHz, $CDCl_3$): δ 7.65 (t, J_{H-H} = 7 Hz, 1H, Ar-*H*), 7.56 (t, J_{H-H} = 7 Hz, 1H, Ar-*H*), 7.42 (m, 1H, Ar-*H*), 7.31 (t, J_{H-H} = 7 Hz, 1H, Ar-*H*), 7.23-7.13 (m, 5H, Ar-*H*), 7.11-6.99 (m, 5H, Ar-*H*), 6.91 (m, 1H, Ar-*H*), 6.87 (br, 1H, Ar-*H*), 6.75 (br, 1H, Ar-*H*), 5.77 (s, 1H, C-

H(acac)), 2.92 (m, 1H, C*H*Me$_2$), 2.78 (m, 1H, C*H*Me$_2$), 2.22 (br, 2H, C*H*Me$_2$), 1.76 (dd, J_{P-H} = 14 Hz, J_{P-H} = 7 Hz, 3H, CH*Me*$_2$), 1.66 (br, 3H, CH*Me*$_2$), 1.55 (dd, J_{P-H} = 14 Hz, J_{P-H} = 7 Hz, 3H, CH*Me*$_2$), 1.50 (s, 3H, C*Me*), 1.44 (m, 6H, CH*Me*$_2$), 1.35 (dd, J_{P-H} = 14 Hz, J_{P-H} = 7 Hz, 3H, CH*Me*$_2$), 1.12 (dd, J_{P-H} = 14 Hz, J_{P-H} = 7 Hz, 3H, CH*Me*$_2$), 0.77 (m, 3H, CH*Me*$_2$).

CHAPTER VIII

CONCLUSION

In conclusion, we report two new, straightforward methods for the synthesis of valuable $[HCB_{11}Cl_{11}]^-$ with either Cl_2 or $SbCl_5$ as chlorination reagents. We obtained $[HCB_{11}Cl_{11}]^-$ product with SO_2Cl_2 as chlorination reagents and an unindentified catalyst. Amines, borane amine adducts and dry HCl have been tested as additives for the chlorination reactions with SO_2Cl_2. Although some of them shifted the reaction towards more chlorinated products, none of them gave pure $[HCB_{11}Cl_{11}]^-$ products. On the other hand, we were able to obtain useful $[B_{12}Cl_{12}]^{2-}$ from $[B_{12}H_{12}]^{2-}$ with SO_2Cl_2 as the chlorination reagent and acetonitrile as cosolvent. While the involved synthesis or the relatively high cost of the requisite parent anion $[HCB_{11}H_{11}]^-$ remain an issue, the syntheses we report here make the subsequent chlorination expedient, economical, and readily available to chemists at large without the need for specialized training or equipment.

We have established that alumenium cation equivalent $Et_2Al[HCB_{11}H_5Br_6]$ functions as an efficient and long-lived catalyst for Lewis acid $C(sp^3)$-F bond activation with trialkylaluminums as stoichiometric reagents. The catalytic reactions showed superb longevity and turnover numbers of up to 10000 have been achieved. Conversion of C-F bonds only to C-Me bonds was accomplished when Me_3Al was used as the stoichiometric reagent. On the other hand, utilization of Et_3Al, $^iBu_3Al$ or $^iBu_2AlH$ results in the competitive replacement of C-F bonds either with C-Alkyl or C-H bonds.

Moreover we demonstrate that alumenium mediated C-F bond activation process is tolerant of small quantities of water because trialkylaluminum compounds can act as "clean-up" agents in situ. It is also shown that $[B_{12}Cl_{12}]^{2-}$ can be used as a weakly coordinating anion for the C-F bond activation mediated by electrophlic silylium species. The $[B_{12}Cl_{12}]^{2-}$ based catalysis showed longevity comparable to carborane-based catalysis in the HDF reactions.

A series of group 10 metal boratranes was synthesized and spectroscopically and structurally characterized with the aim of extending further the scope of M→B interactions. **TPB** ligand was shown to form robust boratrane complexes which exhibited M→B interaction. All metal boratrane species were found to adopt a trigonal pyramidal geometry with only a marginal deviation from the basal plane formed by the three phosphorus atoms which was likely largely imposed by the cage structure of TPB. Pt was shown to form stronger M→B interactions than their lighter analogs. Compared to the isoelectronic group 11 metallaboratranes, stronger M→B interactions were found with the metals with lower oxidation state.

$(PSi^{H}P^{iPr})PtCl$ was synthesized from $Pt(COD)Cl_2$ and $PSi(H_2)P$ ligand via Si-H bond activation in the presence of base. Direct X ligand exchange methods yielded a series of $(PSi^{H}P^{iPr})PtX$ (X=I, OTf, Me, Ph, Mes) compounds from $(PSi^{H}P^{iPr})PtCl$. $Ph_3C[HCB_{11}Cl_{11}]$ was shown to be able to used to abstract the hydride from the silicon center on these $(PSi^{H}P^{iPr})PtX$ compounds. The resulting platinum silylene complexes displayed silylium character, which was exemplified by the X ligand abstraction with Cl, I, Me and Ph. However, the mesityl group was resistant towards abstraction by silylene

center, which is probably attributed to the steric bulkiness of mesityl group. Hence, a pincer metal silylene species was observed after the hydride abstraction which was the first reported PSiP metal species with a central silylene donor.

A series of (PBP)RhX complexes were synthesized via salt metathesis reaction with (PBP)RhCl dimer and characterized by multi-nuclei NMR spectroscopy, elemental analysis and X-ray crystallography. (PBP)Rh acetate, trifluoroacetate, pivalate and acetylacetonate species all showed strong Rh→B interaction. While the (PBP)Rh acetylacetonate specie was stable at room temperature in solution, the carboxylate species underwent reversible intramolecular B-Ph bond activation process. Preliminary studies for the thermodynamics of this transformation revealed that in the (PBP)Rh acetate species, the $\Delta H°$ for the isomerization of **704** is around 8.9 ± 1.2 KJ/mol and the $\Delta S°$ or the same transformation is around 37.6 ± 3.6 $J \cdot mol^{-1}K^{-1}$. A carboxylate-bridging Rh borane was observed after the phenyl migration. Therefore, we conclude carboxylate species is not suitable to be used as the X lihgand to obtain (PBP)Rh(X)(Ph) complex with three coordinated boryl unit via B-Ph bond activation of ($PB^{Ph}P$)Rh(X) species. Thermolysis of 701 gave access to (PBP)$RhCl_2$ (spectroscopic evidence). However the reaction is not clean which make it an undesirable method to access pincer boryl compounds as potential starting material for further study. One interesting observation from our research is that, although in **711** we only observed P-P coupling constant around 40 Hz for the two *cis* phosphines, we observed virtual coupling for the *iso*-propyl group for **704**, **706**, **708** and **710** despite the two phosphine groups being *cis* to each other.

REFERENCES

1. Moulton, C. J.; Shaw, B. L. *J. Chem. Soc. Dalton Trans.* **1976**, 1020.

2. van Koten, G. *Pure Appl. Chem.* **1989**, *61*, 1681.

3. a) Deuschel-Cornioley, C.; Ward, T.; von Zelewsky, A. *Helv. Chim. Acta* **1988**, *71*, 130. b) Cave, G. W. V.; Fanizzi, F. P.; Deeth, R. J.; Errington, W.; Rourke, J. P. *Organometallics* **2000**, *19*, 1355. c) Lu, W.; Chan, C. W.; Cheung, K.-K.; Che, C.-M. *Organometallics* **2001**, *20*, 2477; d) Peris, E.; Loch, J. A.; Mata, J.; Crabtree, R. H. *Chem. Commun.* **2001**, 201.

4 . Morales-Morales, D.; Jensen, C. M., *The Chemistry of Pincer Compounds*, Elsevier, Amsterdam, **2007**.

5. (a) Albrecht, K.; van Koten, G. *Angew. Chem. Int. Ed.* **2001**, *40*, 3750. (b) van der Boom, M. E.; Milstein, D. *Chem. Rev.* **2003**, *103*, 1759. (c) Liang, L. C. *Coord. Chem. Rev.* **2006**, *250*, 1152. (d) Gunanathan, C; Milstein, D. *Acc. Chem. Res.* **2011**, *44*, 588.

6. (a) Sundermann, A.; Uzan, O.; Martin, J. M. L. *Organometallics* **2001**, *20*, 1783. (b) Cohen, R.; van der Boom, M. E.; Shimon, L. J. W.; Rozenberg, H.; Milstein, D. *J. Am. Chem. Soc.* **2000**, *122*, 7723. (c) Sundermann, A.; Uzan, D.; Milstein, D. *J. Am. Chem. Soc.* **2000**, *122*, 7095. (d) Rybtchinski, B.; Oevers, S.; Montag, M.; Vigalok, A.; Rozenberg, H.; Martin, J. M. L.; Milstein, D. *J. Am. Chem. Soc*. **2001**, *123*, 9064.

7. (a) van der Boom, M. E.; Liou, S.-Y.; Ben-David, Y.; Vigalok, A.; Milstein, D. *Angew. Chem., Int. Ed. Engl.* **1997**, *36*, 625. (b) Gandelman, M.; Milstein, D. *Chem. Commun.* **2000**, 1603.

8. van der Boom, M. E.; Liou, S.-Y.; Ben-David, Y.; Shimon, L. J. W.; Milstein, D. *J. Am. Chem. Soc.* **1998**, *120*, 6531.

9. (a) Kanzelberger, M.; Zhang, X.; Emge, T. J.; Goldman, A. S.; Zhao, J.; Incarvito, C.; Hartwig, J. F. *J. Am. Chem. Soc.* **2003**, *125*, 13644. (b) Zhao, J.; Goldman, A. S.; Hartwig, J. F. *Science* **2005**, *307*, 1080. (c) Morgan E.; MacLean D. F.; McDonald R.; Turculet L. *J. Am. Chem. Soc.* **2009**, *131*, 14234.

10. (a) Vigalok, A.; Ben-David, Y.; Milstein, D. *Organometallics* **1996**, *15*, 1839. (b) Kaska, W. C.; Nemeh, S.; Shirazi, A.; Potuznik, S. *Organometallics* **1988**, *7*, 13. (c) McLoughlin, M. A.; Keder, N. L.; Harrison, W. T. A.; Flesher, R. J.; Mayer, H. A.; Kaska, W. C. *Inorg. Chem.* **1999**, *38*, 3223. (d) Steffey, B. D.; Miedaner, A.; Maciejewski-Farmer, M. L.; Bernatlis, P. R.; Herring, A. M.; Allured, V. S.; Carperos, V.; DuBois, D. L. *Organometallics* **1994**, *13*, 4844. (e) Jessop, P. G.; Ikariya, T.; Noyori, R. *Chem. Rev.* **1995**, *95*, 259.

11 . Jensen, C. M.; Trogler, W. C. *J. Am. Chem. Soc.* **1986**, *108*, 723.

12. Young, K. J. H.; Oxgaard, J.; Ess, D. H.; Meier, S. K.; Stewart, T.; Goddard, III, W. A.; Periana, R. A. *Chem. Commun.* **2009**, 3270.

13. (a) van der Zeijden, A. H.; van Koten, G.; Luijk, R.; Vrieze, K.; Slob, C.; Krabbendam, H.; Spek, A. L. *Inorg. Chem.* **1988**, *27*, 1014. (b) Albrecht, M.; James, S. L.; Veldman, N.; Spek, A. L.; van Koten, G. *Can. J. Chem.* **2001**, *79*, 709. (c) Dupont, J.; Beydoun, N.; Pfeffer, M. *J. Chem. Soc. Dalton Trans.* **1989**, *9*, 1715. Bedford, R. B.; Draper, S. M.; Noelle, S. P.; Welch, S. L. *New. J. Chem.* **2000**, *24*, 745.

14. Al-Salem, N. A.; Empsall, H. D.; Markham, R.; Shaw, B. L.; Weeks, B. *J. Chem. Soc. Dalton Trans.* **1979**, 1972.

15. (a) Fryzuk, M. D.; Macneil, P. A.; Rettig, S. J. *Organometallics* **1982**, *1*, 918. (b) Fan, L.; Foxman, B. M.; Ozerov, O. V. *Organometallics* **2004**, *23*, 326-328. (c) Liang, L. C.; Lin, J. M.; Hung, C. H. *Organometallics* **2003**, *22*, 3007-3009.

16. (a) Segawa Y.; Yamashita M.; Nozaki K. *J. Am. Chem. Soc.* **2009**, *131*, 26. (b) Segawa Y.; Yamashita M.; Nozaki K. *Organometallics* **2009**, *28*, 6234.

17. (a) MacInnis, M. C.; MacLean, D. F.; Lundgren, R. J.; McDonald, R.; Turculet, L. *Organometallics* **2007**, *26*, 6522. (b) MacLean D. F.; McDonald R.; Ferguson M. J.; Caddell A. J.; Turculet L. *Chem. Commun.* **2008**, **41**, 5146. (c) Mitton, S. J.; McDonald, R.; Turculet, L. *Organometallics* **2009**, *28*, 5122. (d) Mitton, S. J.; McDonald, R.; Turculet, L. *Angew. Chem. Int. Ed.* **2009**, *48*, 8568. (e) MacInnis, M. C.; McDonald, R.; Ferguson, M. J.; Tobisch, S.; Turculet, L. *J. Am. Chem. Soc.* **2011**, in press. (f) Takaya, J.; Kirai, N.; Iwasawa, N. *J. Am. Chem. Soc.* **2011**, *133*, 12980. (g) Takaya, J.; Iwasawa, N. *J. Am. Chem. Soc.* **2008**, *130*, 15254.

18. Mankad, N. P.; Rivard, E.; Harkins, S. B.; Peters, J. C.; *J. Am. Chem. Soc.* **2005**, *127*, 16032.

19. (a) Weng, W.; Parkin, S.; Ozerov, O. V. *Organometallics* **2006**, *25*, 5345. (b) Weng, W.; Chen, C.-H.; Foxman, B. M.; Ozerov, O. V. *Organometallics* **2007**, *26*, 3315.

20. (a) Zhang, J.; Leitus, G.; Ben-David, Y.; Milstein, D. *J. Am. Chem. Soc.* **2005**, *127*, 10840. (b) Ben-Ari, E.; Leitus, G.; Shimon, L. J.W.; Milstein, D. *J. Am. Chem. Soc.*

2006, *128*, 15390. (c) Zhang, J.; Leitus, G.; Ben-David, Y.; Milstein, D. *Angew. Chem., Int. Ed.* **2006**, *45*, 1113.

21. Ozerov, O. V.; Guo, C.; Fan, L.; Foxman, B. M. *Organometallics* **2004**, *23*, 5573.

22. Crabtree, R. H. *The Organometallic Chemistry of Transition Metals 4th Ed.* Wiley-VCH: Weinheim, Germany, 2007.

23. Grove, D. M.; van Koten, G.; Ubbels, H. J. C.; Zoet, R.; Spek, A L. *Organometallics* **1983**, *3*, 1003.

24. (a) Steenwinkel, P.; Gossage, R. A.; van Koten, G. *Chem. Eur. J.* **1998**, *4*, 759. (b) Ryabov, A. D. *Chem. Rev.* **1990**, *90*, 403. (c) Ozerov, O. V.; Guo, C.; Papkov, V. A.; Foxman, B. M. *J. Am. Chem. Soc*. **2004**, *126*, 4792-4793.

25. (a) Grove, D. M.; van Koten, G.; Louwen, J. N.; Notltes, J. G.; Spek, A.; Ubbels, H. J. *J. Am. Chem. Soc.* **1982**, *104*, 6609. (b) Koller, J.; Sarkar, S.; Abboud, K. A.; Veige, A. S. *Organometallics* **2007**, *26*, 5438. (c) Gerber, L. C. H.; Watson, L. A.; Parkin, S.; Weng, W.; Foxman, B. M.; Ozerov, O. V. *Organometallics* **2007**, *26*, 4866. (d) Weng, W.; Yang, L.; Foxman, B. M.; Ozerov, O. V. *Organometallics* **23**, *23*, 4700. (e) Harkins, S. B.; Peters, J. C. *J. Am. Chem. Soc.* **2004**, *126*, 2855. (f) Brammell, C. M.; Pelton, E. J.; Chen, C.-H.; Yakovenko, A. A.; Weng, W.; Foxman, B. M.; and Ozerov, O. V. *J. Organomet. Chem.* **2011**, in press.

26. Pape, A; Lutz, M.; Müller, G. *Angew. Chem., Int. Ed.* **1994**, *33*, 2281.

27. (a) Garrison, J. C.; Youngs, W. J. *Chem. Rev* **2005**, *105*, 3978. (b) DeMott, J. C.; Basuli, F.; Kilgore, U. J.; Foxman, B. M.; Huffman, J. C.; Ozerov, O. V., Mindiola, D. J. *Inorg. Chem*. **2007**, *46*, 6271-6276.

28. (a) Dani, M.; Albrecht, M.; van Klink, G. P. M.; van Koten, G. *Organometallics* **2000**, *19*, 4468. (b) Albrecht, M.; Dani, P.; Lutz, M.; Spek, A. L.; van Koten, G. *J. Am. Chem. Soc*. **2000**, *122*, 11822. (c) Albrecht, M.; James, S. L.; Veldman, N.; Spek, A. L.; van Koten, G. *Can. J. Chem.* **2001**, *79*, 709.

29. Dupont, J.; Beydoun, N.; Pfeffer, M. *J. Chem. Soc. Dalton Trans*. **1989**, 1715.

30 Maassarani, F.; Davidson, M. F.; Wehman-Ooyevaar, I. C. M.; Grove, D. M.; van Koten, M. A.; Smeets, W. J. J.; Spek, A. L.; van Koten, G. *Inorg. Chim. Acta* **1995**, *235*, 327.

31. (a) Roundhill, D. M. *Chem. Rev.* **1992**, *92*, 1. (b) Casalnuovo, A. L.; Calabrese, J. C.; Milstein, D. *J. Am. Chem. Soc.* **1988**, *110*, 6738. (c) Cowan, R. L.; Trogler, W. C. *J. Am. Chem. Soc.* **1989**, *111*, 4750.

32. Two reactions of ammonia are among the top 10 challenges for catalysis listed in this article: Haggin, J. *Chem. Eng. News.* **1993**, *71*, 23.

33. Kanzelberger, M.; Singh, B.; Czerw, M.; Krogh-Jespersen, K.; Goldman, A. S. *J. Am. Chem. Soc.* **2000**, *122*, 11017.

34. (a) Gupta, M.; Hagen, C.; Flesher, R. J.; Kaska, W. C.; Jensen, C. M. *Chem. Commun.* **1996**, 2083. (b) Gupta, M.; Hagen, C.; Kaska, W. C.; Cramer, R. E.; Jensen, C. M. *J. Am. Chem. Soc.* **1997**, *119*, 840. (c) Xu, W.; Rosini, G. P.; Gupta, M.; Jensen, C.

M.; Kaska, W. C.; Krogh-Jespersen, K.; Goldman, A. S. *Chem. Commun.* **1997**, 2273. (d) Goldman, A. S.; Roy, A. H.; Huang, Z.; Ahuja, R.; Schinski, W.; Brookhart, M. *Science* **2006**, *312*, 257. (e) Choi, J.; MacArthur, A. M. R.; Brookhart, M.; Goldman, A. S. *Chem. Rev.* **2011**, *111*, 1761.

35. (a) Weckhuysen, B. M.; Schoonheydt, R. A. *Catal. Today* **1999**, *51*, 223. (b) O'Connor, R. P.; Klein, E. J.; Henning, D.; Schmidt, L. D. *Appl. Catal., A* **2003**, *238*, 29. (c) Olsbye, U.; Virnovskaia, A.; Prytz, O.; Tinnemans, S. J.; Weckhuysen, B. M. *Catal. Lett.* **2005**, *103*, 143. (d) Adlhart, C.; Uggerud, E. *Chem. Eur. J.* **2007**, *13*, 6883. (e) Jackson, S. D.; Stair, P. C.; Gladden, L. F.; McGregor, *J. Met. Oxide Catal.* **2009**, *2*, 595.

36. (a) Baudry, D.; Ephritikhine, M.; Felkin, H.; Holmes-Smith, R. *J. Chem. Soc., Chem. Commun.* **1983**, 788. (b) Felkin, H.; Fillebeen-Khan, T.; Gault, Y.; Holmes-Smith, R.; Zakrzewski, J. *Tetrahedron Lett.* **1984,** *25*, 1279. (c) Felkin, H.; Fillebeen-Khan, T.; Holmes-Smith, R.; Lin, Y. *Tetrahedron Lett.* **1985**, *26*, 1999. (d) Burk, M. J.; Crabtree, R. H.; Parnell, C. P.; Uriarte, R. J. *Organometallics* **1984**, *3*, 816. (e) Burk, M. J.; Crabtree, R. H.; McGrath, D. V. *J. Chem. Soc., Chem. Commun.* **1985**, 1829. (f) Burk, M. J.; Crabtree, R. H. *J. Am. Chem. Soc.* **1987**, *109*, 8025.

37. Crabtree, R. H.; Mihelcic, J. M.; Quirk, J. M. *J. Am. Chem. Soc.* **1979**, *101*, 7738.

38. Jensen, C. M. *Chem. Commun.* **1999**, 2443.

39. Renkema, K. B.; Kissin, Y. V.; Goldman, A. S. *J. Am. Chem. Soc.* **2003**, *125*, 7770.

40. (a) Schrock R. R.; Murdzek J. S.; Bazan G. C.; Robbins, J.; Dimare, M.; O'Regen, M. *J. Am. Chem. Soc.* **1990**, *112*, 3875. (b) Schrock, R. R. *Chem. Commun.* **2005**, 2773.

41. (a) Hiyama, T. *Organofluorine Compounds Chemistry and Applications*, Springer, New York, **2000**. (b) Smart, B. E. in: Banks, R. E.; Smart, B. E.; Tatlow, J. C. (Eds.), *Organofluorine Chemistry: Principles and Commercial Applications*, Plenum Press, New York, **1994**, p. 57 (Chapter III).

42. (a) Műller, K.; Faeh, C.; Diederich, F. *Science* **2007**, *317*, 1881. (b) Purser, S.; Moore, P. R.; Swallow, S.; Gouverneur, V. *Chem. Soc. Rev.* **2008**, *37*, 320. (c) Jeschke, P. *ChemBioChem* **2004**, *5*, 570.

43. Hung, M. H.; Farnham, W. B.; Feiring, A. E.; Rozen, S.; in *Fluoropolymers: Synthesis* Vol. 1 (eds Hougham, G., Cassidy, P. E., Johns, K. & Davidson, T.) 51–66 (Plenum,1999).

44. (a) Wende, M.; Meier, R.; Gladysz, J. A. *J. Am. Chem. Soc*. **2001**, *123*, 11490. (b) Gladysz, J. A.; Curran, D. P. *Tetrahedron* **2002**, *58*, 3823. (c) Barthel-Rosa, L. P.; Gladysz, J. A. *Coord. Chem. Rev*. **1999**, *190-192*, 587. (d) Gladysz, J. A. *Science* **1994**, *266*, 55. (e) Horvath, I. T. *Acc. Chem. Res.* **1998**, *31*, 641. (f) Horvath, I. T.; Rabai, J. *Science* **1994**, *266*, 72.

45. Ametamey, S. M.; Honer, M.; Schubiger, P. A. *Chem. Rev.* **2008**, *108*, 1501.

46. (a) Molina, M. J.; Rowland, F. S. *Nature* **1974**, *249*, 810. (b) Rowland, F. S.; Molina, M. J. *Rev. Geophys. Space Phys.* **1975**, *13*, 1. (c) Rowland, F. S. *Environ. Sci.*

Technol. **1991**, *25*, 622. (d) Victor, D. G.; MacDonald, G. J. *Climatic Change* **1999**, *42*, 633. (e) Roehl, C. M.; Boglu, D.; Bruehl, C.; Moortgat, G. K. *Geophysical Research Letters* **1995**, *22*, 815. (f) Timms, P. L. *J. Chem. Soc., Dalton Trans*. **1999**, 815.

47. Hudlicky, M. *Chemistry of Organic Fluorine Compounds*; Prentice-Hall: New York, **1992**; p. 175.

48. (a) Kiplinger, J. L.; Richmond, T. G.; Osterberg, C. E. *Chem. Rev.* **1994**, *94*, 373. (b) Burdeniuc, J.; Jedlicka, B.; Crabtree, R. H. *Chem. Ber.* **1997**, *130*, 145. (c) Richmond, T. G. In *Topics in Organometallic Chemistry*; Murai, S., Ed.; Springer: New York, 1999; Vol. 3, p 243. (d) Reinhold, M.; McGrady, J. E.; Perutz, R. N. *J. Am. Chem. Soc.* **2004**, *126*, 5268. (e) Torrens, H. *Coord. Chem. Rev*. **2005**, *249*, 1957. (f) Amii, H.; Uneyama, K. *Chem. Rev*. **2009**, *109*, 2119. (f) Braun T.; Perutz, R. N. in *Comprehensive Organometallic Chemistry III*, Eds Crabtree R. H.; Mingos, D, M, P. Elsevier, Oxford, **2007.** (g) O'Hagan, D. *Chem Soc. Rev.* **2008**, *37*, 308.

49. Bosque, R.; Clot, E.; Fantacci, S.; Maseras, F.; Eisenstein, O.; Perutz, R. N.; Renkema, K. B.; Caulton, K. G. *J. Am. Chem. Soc.* **1998**, *120*, 12634.

50. Su, M. D.; Chu, S. Y. *J. Am. Chem. Soc.* **1997**, *119*, 10178.

51. (a) Fahey, D. R.; Mahan, J. E. *J. Am. Chem. Soc.* **1977**, *99*, 2501. (b) Cronin, L.; Higgitt, C. L.; Karch, R.; Perutz, R. N. *Organometallics* **1997**, *16*, 4920.

52. Whittlesey, M. K.;, R. N.; Moore, M. H. *Chem. Commun.* 1996, 787.

53. Aizenberg, M.; Milstein, D. *Science* **1994**, *265*, 359.

54. Aizenberg, M.; Milstein, D. *J. Am. Chem. Soc.* **1995**, *117*, 8674.

55. Vela, J.; Smith, J. M.; Yu, Y.; Ketterer, N. A.; Flaschenriem, C. J.; Lachicotte, R. J.; Holland, P. L. *J. Am. Chem. Soc.* **2005**, *127*, 7857.

56. Reade, S. P.; Mahon, M. F.; Whittlesey, M. K. *J. Am. Chem. Soc.* **2009**, *131*, 1874.

57. Amii, H.; Uneyama, K. *Chem. Rev.* **2009**, *109*, 2119.

58. (a) Böhm, V. P. W.; Gstttmayr, C. W. K.; Weskamp, T.; Herrmann, W. A. *Angew. Chem. Int. Ed.* **2001**, *40*, 3387. (b) Saeki, T.; Takashima, Y.; Tamao, K. *Synlett* **2005**, 1771. (c) Inada, K.; Miyaura, N. *Tetrahedron* **2000**, *56*, 8657. (d) Zhou, J.; Fu, G. C *J. Am. Chem. Soc.* **2004**, *126*, 1340. (e) Schaub, T.; Backes, M.; Radius, U. *J. Am. Chem. Soc.* **2006**, *128*, 15964. (f) Widdowson, D. A.; Wilhelm, R. *Chem. Commun.* **1999**, 2211. (g) Wilhelm, R.; Widdowson, D. A. *J. Chem. Soc., Perkin Trans. 1* **2000**, 3808. (h) Cahoez, G.; Lepifre, F.; Ramiandrasoa, P. *Synthesis* **1999**, 2138. (i) Guo, H.; Kong, F.; Kanno, K.; He, J.; Nakajima, K.; Takahashi, T. *Organometallics* **2006**, *25*, 2045. (j) Yamada, S.; Takahashi, T.; Konno, T.; Ishihara, T. *Chem. Commun.* **2007**, 3679.

59. (a) Kraft, B. M.; Lachicotte, R. J.; Jones, W. D. *J. Am. Chem. Soc.* **2000**, *122*, 8559. (b) Kraft, B. M.; Lachicotte, R. J.; Jones, W. D. *J. Am. Chem. Soc.* **2001**, *123*, 10973.

60. Choi, J.; Wang, D. Y.; Kundu, S.; Choliy, Y.; Emge, T. J.; Krogh-Jespersen, K.; Goldman, A. S. *Science*, **2011**, *332*, 1545.

61. (a) Strauss, S. H. *Chem. Rev.* **1993**, *93*, 927. (b) Krossing, I.; Raabe, I. *Angew. Chem. Int. Ed.* **2004**, *43*, 2066.

62. Rosenthal, M. R. *J. Chem. Edu.* **1973**, *50*, 331.

63. (a) Reed, C. A. *Acc. Chem. Res.* **1998**, *31*,133. (b) Reed, C. A. *Chem. Commun.* **2005**, 1669. (c) Krossing, I.; Reisinger, A. *Coord. Chem. Rev.* **2006**, *250*, 2771. (d) Körbe, S.; Schreiber, P. J.; Michl, J. *Chem. Rev.* **2006**, *106*, 5208. (d) Reed, C. A. *Acc. Chem. Res.* **2010**, *43*, 121.

64. (a) LeSuer, R. J.; Geiger, W. E. *Angew. Chem. Int. Ed.* **2000**, *39*, 248. (b) Barriere, F.; Camire, N.; Geiger, W. E.; Mueller-Westerhoff, U. T.; Sanders, R. *J. Am. Chem. Soc.* **2002**, *124*, 7262. (c) Camire, N.; Nafady, A.; Geiger, W. E.; *J. Am. Chem. Soc.* **2002**, *124*, 7260. (d) Camire, N.; Mueller-Westerhoff, U. T.; Geiger, W. E. *J. Organomet. Chem.* **2001**, *637–639*, 823. (e) Gassman, P. G.; Deck, P. A. *Organometallics* **1994**, *13*, 1934; (f) Hill, M. G.; Lamanna, W. M.; Mann, K. R. *Inorg. Chem.* **1991**, *30*, 4687. (g) Gassman, P. G.; Sowa, Jr. J. R.; Hill, M. G.; Mann, K. R. *Organometallics* **1995**, *14*, 4879. (h) Pospisil, L.; King, B. T.; Michl, J. *Electrochim. Acta* **1998**, *44*, 103.

65. (a) Wasserscheid, P.; Keim, W. *Angew. Chem. Int. Ed.* **2000**, *39*, 3772. (b) Holbrey, J. D. *Clean Prod. Processes* **1999**, *1*, 2071. (c) Welton, T. *Chem. Rev.* **1999**, *99*, 2071. (d) Wasserscheid, P. *Chem. Unserer Zeit* **2003**, *37*, 52. (e) Bösmann, A.; Francio, G.; Janssen, E.; Leitner, W.; Wasserscheid, P. *Angew. Chem. Int. Ed.* **2001**, *40*, 2697. (f) Larsen, A. S.; Holbrey, J. D.; Tham, F. S.; Reed, C. A. *J. Am. Chem. Soc.* **2000**, *122*, 7264.

66. Kita, F.; Sakata, H.; Sinomoto, S.; Kawakami, A.; Kamizori, H.; Sonoda, T.; Nagashima, H.; Nie, J.; Pavlenko, N. V.; Yagupolskii, Y. *J. Power Sources* **2000**, *90*, 27.

67. Suzuki, H.; Naganawa, H.; Tachimori, S. *Phys. Chem. Chem. Phys.* **2003**, *5*, 726.

68. (a) Castellanos, F.; Fouassier, J. P.; Priou, C.; Cavezzan, J. *J. Appl. Poly. Sci.* **1996**, *60*, 705. (b) Ren, K.; Mejiritski, A.; Malpert, J. H.; Grinevich, O.; Gu, H.; Neckers, D. C. *Tetrahedron Lett*. **2000**, *41*, 8669. (c) Li, H.; Ren, K.; Zhang, W.; Malpert, J. H.; Neckers, D. C. *Macromolecules* **2001**, *34*, 4161. (d) Gu, H.; Ren, K.; Mejiritski, A.; Grinevich, O.; Malpert, J. H.; Neckers, D. C. *J. Org. Chem.* **2001**, *66*, 4161. (e) Ren, K.; Malpert, J. H.; Li, H.; Gu, H.; Neckers, D. C. *Macromolecules* **2002**, *35*, 1632.

69. (a) Moss, S.; King, B. T.; de Meijere, A.; Kozushkov, S. I.; Eaton, P. E.; Michl, J. *Org. Lett.* **2001**, *3*, 2001. (b) Fujiki, K.; Ikeda, S.; Kobayashi, H.; Mori, A.; Nagira, A.; Nie, J.; Sonoda, T.; Yagupolskii, Y. *Chem. Lett.* **2000**, 66. (c) Kloster, G. M.; Dubaz, W. J.; Grieco, P. A.; Shriver, D. F.; Strauss, S. H. *Inorg. Chim. Acta* **1997**, *263*, 195. (d) Grieco, P. A.; DuBay, W. J.; Todd, L. J. *Tetrahedron Lett.* **1996**, *37*, 8707. (e) DuBay, W. J.; Grieco, P. A.; Todd, L. J. *J. Org. Chem.* **1994**, *59*, 6898.

70 (a) Chen, E. Y.-X.; Marks, T. J. *Chem. Rev.* **2000**, *100*, 1391. (b) Ittel, S. D.; Johnson, L. K.; Brookhart, M. *Chem. Rev.* **2000**, *100*, 1169. (c) Britovsek, G. J. P.; Gibson, V. C.; Wass, D. F. *Angew. Chem. Int. Ed.* **1999**, *38*, 429. (d) Mecking, S. *Coord. Chem. Rev.* **2000**, *203*, 305.

71. (a) Scott, V. J.; Çelenligil-Çetin, R.; Ozerov, O. V. *J. Am. Chem. Soc*. **2005**, *127*, 2852. (b) Panisch, R.; Bolte, M.; Mueller, T. *J. Am. Chem. Soc*. **2006**, *128*, 9676. (c) Douvris, C.; Stoyanov, E. S.; Tham, F. S.; Reed, C. A. *Chem. Commun*. **2007**, 1145. (d)

Douvris, C.; Ozerov, O. V. *Science* **2008**, *328*, 1188. (e) Gu, W.; Haneline, M. R.; Douvris, C.; Ozerov, O. V. *J. Am. Chem. Soc.* **2009**, *131*, 11203. (f) Douvris, C.; Nagaraja, C. M.; Chen, C.-H.; Foxman, B. M.; Ozerov, O. V. *J. Am. Chem. Soc.* **2010**, *132*, 4946

72. (a) Hill, M. G.; Lamanna, W. M.; Mann, K. R. *Inorg. Chem.* **1991**, *30*, 4687. (b) Bond, A. M.; Ellis, S. R.; Hollenkamp, A. F. *J. Am. Chem. Soc*. **1988**, *110*, 5293.(c) Appel, M.; Schloter, K.; Heidrich, J.; Beck, W. *J. Organomet. Chem.* **1987**, *322*, 77. (d) Rhodes, M. R.; Mann, K. R. *Znorg. Chem.* **1984**, *23*, 2053.

73. (a) Winter, C. H.; Zhou, X.-X.; Heeg, M. J. *Inorg. Chem.* **1992**, *31*, 1808. (b) Gorrell, I. B.; Parkin, G. *Inorg. Chem.* **1990**, *29*, 2452. (c) Klapdtke, T.; Gowik, P. *Monatsh. Chem.* **1989**, *120*, 711. (d) Bochmann, M.; Wilson, L. M.; Hursthouse, M. B.; Short, R. L. *Organometallics* **1987**, *6*, 2556. (e) Jordan, R. F.; Dasher, W. E.; Echols, S. F. *J. Am. Chem. Soc.* **1986**, *108*, 1718. (f) Reedijk, J. *Comments Inorg. Chem.* **1982**, *1*, 379.

74. (a) Seppelt, K. *Angew. Chem. Int. Ed.* **1993**, *32*, 1025. (b) Bochmann, M. *Angew. Chem. Int. Ed.* **1992**, *104*, 1181.

75. (a) Jordan, R. F. *Adv. Organomet. Chem*. **1991**, *32*, 325. (b) Horton, A. D.; Frijns, J. H. G. *Angew. Chem. Int. Ed.* **1991**, *30*, 1152. (c) Bochmann, M.; Jaggar, A. J.; Nicholls, J. C. *Angew. Chem., Int. Ed.* **1990**, *29*, 780. (d) Hlatky, G. G.; Turner, H. W.; Eckman, R. R. *J. Am. Chem. Soc.* **1989**, *111*, 2728. (e) Taube, R.; Krukowka, L. *J. Organomet. Chem.* **1988**, *347*, C9. (f) Turner, H. W. European Patent Appl. 277,004

(assigned to Exxon), 1988. (g) Lin, Z.; Le Marechall, J.-F.; Sabat, M.; Marks, T. J. *J. Am. Chem. Soc.* **1987**, *109*, 4127. (h) Jordan, R. F.; Bajgur, C. S.; Willett, R.; Scott, B. *J. Am. Chem. Soc.* **1986**, *108*, 7410.

76. Nishida, H.; Takada, N.; Yoshimura, M.; Sonoda, T.; Kobayashi, H. *Bull. Chem. Soc. Jpn.* **1984**, *57*, 2600.

77. Massey, A. G.; Park, A. J. *J. Organomet. Chem.* **1964**, *2*, 245.

78. Kaul, F. A. R.; Puchta, G. T.; Schneider, H.; Grosche, M.; Mihalios, D.; Herrmann, D. A. *J. Organomet. Chem.* **2001**, *621*, 177.

79. (a) Jia, L.; Jang, X.; Stern, C. L.; Marks, T. J. *Organometallics* **1997**, *16*, 842. (b) Jia, L.; Yang, X.; Ishihara, A.; Marks, T. J. *Organometallics* **1995**, *14*, 3135.

80. Rodriguez, G.; Brant, P. *Organometallics* **2001**, *20*, 2417.

81. van den Broeke, J.; Deelman, B.-J.; van Koten, G. *Tetrahedron Lett.* **2001**, *42*, 8085.

82. Fujiki, K.; Ichikawa, J.; Kobayashi, H.; Sonoda, A.; Sonoda, T. *J. Fluorine Chem.* **2000**, *102*, 293.

83. (a) Biagini, P.; Luigli, G.; Abis, L.; Andeussi P. (Enichem), US Patent 5602269, **1997**. (b) Bochmann, M.; Sarsfield, M. J. *Organometallics* **1998**, *17*, 5908.

84. (a) Ren, K.; Mejiritski, A.; Malpert, J. H.; Neckers, D. C. *Tetrahedron Lett.* **2000**, *41*, 8669. (b Ren, K.; Malpert, J. H.; Li, H.; Gu, H.; Neckers, D. C. *Macromolecules* **2002**, *35*, 1632.

85. King, R. B. *Chem Rev.* **2001**, *101*, 1119.

86. Romerosa, A. M. *Thermochim. Acta* **1993**, *217*, 123.

87. Ivanov, S. V.; Rockwell, J. J.; Polyakov, O. G.; Gaudinski, C. M.; Anderson, O. P.; Solntsev, K. A.; Strauss, S. H. *J. Am. Chem. Soc.* **1998**, *120*, 4224.

88. Xie, Z.; Tsang, C.; Sze, E. T.; Yang, Q.; Chan, D. T. W.; Mak, T. C. W. *Inorg. Chem.* **1998**, *37*, 6444.

89. Peymann, T.; Herzog, A.; Knobler, C. B.; Hawthorne, M. F. *Angew. Chem., Int. Ed.* **1999**, *38*, 1061.

90. King, B. T.; Janoušěk, Z.; Grüner, B.; Trammell, M.; Noll, B. C.; Michl, J. *J. Am. Chem. Soc.* **1996**, *118*, 3313.

91. Fete, M. G. *Ph.D. Dissertation*, University of Colorado, Boulder, CO, **2006**.

92. Knoth, W. H. *Inorg. Chem.* **1971**, *10*, 598.

93. It was found in our group that $[HCB_{11}Cl_{11}]^-$ could be deprotonated by NaOH or KO^tBu.

94. Xie, Z.; Tsang, C.; Xue, F.; Mak, T. C. W. *J. Organomet. Chem.* **1999**, *577*, 197.

95. Stasko D.; Reed, C. A. *J. Am. Chem. Soc*. **2002**, *124*, 1148.

96. Kato, T.; Reed, C. A. *Angew. Chem., Int. Ed.* **2004**, *43*, 2908.

97. (a) Reed, C. A. *Acc. Chem. Res.* **1998**, *31*, 325. (b) Kim, K.-C.; Reed, C. A.; Elliott, D. W.; Mueller, L. J.; Tham, F.; Lin, L.; Lambert, J. B. *Science* **2002**, *297*, 825.

98. Juhasz, M.; Hofmann, S.; Stoyanov, E.; Kim K.; Reed, C. A. *Angew. Chem. Int. Ed.* **2004**, *43*, 5352.

99. Fărcaşiu, D.; Ghenciu, A. *J. Am. Chem. Soc.* **1993**, *115*, 10901.

100. Kim, K.-C.; Reed, C. A.; Long, G. S.; Sen, A. *J. Am. Chem. Soc.* **2002**, *124*, 7662.

101. Klahn, M.; Fischer, C.; Spannenberg, A.; Rosenthal, U.; Krossing, I. *Tet. Lett.* **2007**, *48*, 8900.

102. (a) Bolli, C.; Derendorf, J.; Keβler, M.; Knapp, C.; Scherer, H.; Schulz, C.; Warneke, J. *Angew. Chem. Int. Ed.* **2010**, *49*, 3536. (b) Kessler, M.; Knapp, C.; Sagawe, V.; Scherer, H.; Uzun, R. *Inorg. Chem.* **2010**, *49*, 5223. (c) Avelar, A.; Tham, F. S.; Reed, C. A. *Angew. Chem. Int. Ed.* **2009**, *48*, 3491. (d) Geis, V.; Guttsche, K.; Knapp, C.; Scherer, H.; Uzun, R. *Dalton Trans.* **2009**, 2687.

103. Keβler, M.; Knapp, C.; Zogaj, A. *Organometallics* **2011**, *30*, 3786.

104. Gu, W.; Ozerov, O. V. *Inorg. Chem.* **2011**, *50*, 2726.

105. Miller, P. K.; Abney, K. D.; Rappé, A. K.; Anderson, O. P; Strauss, S. H. *Inorg. Chem.* **1988**, *28*, 2255.

106. Sanders, J. C. P.; Schrobilgen, G. J. J. *Chem. Soc. Chem. Commun.* **1989**, *1*, 1576.

107. (a) Van Seggan, D. M.; Hurtburt, P. K.; Noirot, M. D.; Anderson, O. P. Strauss, S. H. *Inorg. Chem.* **1992**, *31*, 1423. (b) Mercier, H. P. A.; Saunders, J. C. P.; Schrobilgen, G. T. *J. Am. Chem. Soc.* **1994**, *116*, 2921. (c) Van Seggen, D. M.; Hurlburt, P. K.; Anderson, O. P.; Strauss, S. H. *Inorg. Chem.* **1995**, *34*, 3453. (d) Cameron, T. S.; Krossing, I.; Passmore, J. *Inorg. Chem.* **2001**, *40*, 2001. (e) Moock, K.; Seppelt, K. *Z. Anorg. Allg. Chem.* **1988**, *561*, 132.

108. (a) Gerken, M.; Kolb, P.; Wegner, A.; Mercier, H. P. A.; Borrmann, H.; Dixon, D. A.; Schrobilgen, . J. *Inorg. Chem.* **2000**, *39*, 2813. (b) Casteel, Jr. W. J.; Kolb, P.; LeBlond, N.; Mercier, H. P. A.; Schrobilgen, G. J. *Inorg. Chem.* **1996**, *35*, 929.

109. Krossing, I. *Chem. Eur. J.* **2001**, *7*, 490.

110. Ren, P.; Vechorkin, O.; Csok, Z.; Salihu, I.; Scopelliti, R.; Hu, X. *Dalton Trans.* **2011**, *40*, 8906.

111. (a) Fryzuk, M. D.; MacNeil, P. A. *J. Am. Chem. Soc.* **1984**, *106*, 6993. (b) Ozerov, O. V.; Gerard, H. F.; Watson, L. A.; Huffman, J. C.; Caulton, K. G. *Inorg. Chem*. **2002**, *41*, 5615.

112. (a) Auburn, M. J.; Stobart, S. R. *Inorg. Chem.* **1985**, *24*, 318. (b) Joslin, F. L.; Stobart, S. R. J. Chem. Soc., *Chem. Commun.* **1989**, 504. (c) Auburn, M. J.; Holmes-Smith, R. D.; Stobart, S. R.; Bakshi, P. K.; Cameron, T. S. *Organometallics* **1996**, *15*, 3032. (d) Gossage, R. A.; McLennan, G. D.; Stobart, S. R. *Inorg. Chem.* **1996**, *35*, 1729. (e) Brost, R. D.; Bruce, G. C.; Joslin, F. L.; Stobart, S. R. *Organometallics* **1997**, *16*, 5669. (f) Zhou, X.; Stobart, S. R. *Organometallics* **2001**, *20*, 1898.

113. (a) Trnka, T. M.; Grubbs, R. H. *Acc. Chem. Soc.* **2001**, *34*, 18. (b) Herrmann, W. A. *Angew. Chem. Int. Ed.* **2002**, *41*, 1290. (c) Hahn, F. E.; Jahnke, M. C. *Angew. Chem. Int. Ed.* **2008**, *47*, 3122. (d) Peris, E.; Grubbs, R. H. *Coord. Chem. Rev.* **2004**, *248*, 2239. (e) Crudden, C. M.; Allen, D. P. *Coord. Chem. Rev.* **2004**, *248*, 2247.

114. Spokoyny, A. M.; Reuter, M. G.; Stern, C. L.; Ratner, M. A.; Seideman, T., Mirkin, C. A. *J. Am. Chem. Soc.* 2009, *131*, 9482.

115. El-Zaria, M. E.; Arii, H.; Nakamura, H.; *Inorg. Chem.* **2011**, *50*, 4149

116. (a) Charmant, J. P. H.; Cheng, F.; Norman, N. C; Pringle, P. G. *Dalton Trans.* **2007**, 114. (b) Liang, L.-C.; Lin, J.-M.; Lee, W.-Y. *Chem. Commun* **2005**, 2462. (c) Hu, J.; Xu, H.; Nguyen, M.-H.; Yip, J. H. K. *Inorg. Chem.* **2009**, *48*, 9684.

117. (a) Braunschweig, H.; Radacki, K.; Rais, D.; Uttinger, K. *Angew. Chem., Int. Ed.* **2006**, *45*, 162. (b) Braunschweig, H.; Green, H.; Radacki, K.; Uttinger, K. *Dalton Trans.* **2008**, 3531.

118. Waterman, R.; Hayes, P. G.; Tilley, T. D. *Acc. Chem. Res.* **2007**, *40*, 712.

119. Morales-Morales, D.; Grause, C.; Kasaoka, K.; Redón, R.; Cramer, R. E.; Jensen, C. M. *Inorg. Chim. Acta.* **2000**, *300*, 958.

120. Kawatsura, M.; Hartwig, J. F. *Organometallics* **2001**, *20*, 1960.

121. (a) Liang, L. -C.; Lin, J. -M.; Hung, C. -H. *Organometallics* **2003**, *22*, 3007. (b) Winter, A. M.; Eichele, K.; Mack, H. -G.; Potuznik, S.; Mayer, H. A.; Kaska, W. C. *J. Organomet. Chem.* **2003**, *682*, 149. (c) Fan, L.; Foxman, B. M.; Ozerov, O. V. Organometallics **2004**, 23, 326.

122. (a) Katz, H. E. *J. Am. Chem. Soc.*, **1985**, 107, 1421. (b) Tour, J. M.; John, J. A.; Stephens, E. B. *Organomet. Chem.* **1992**, *429*, 301. (c) Hinke, A.; Kuchen, W. *Chem. Ber.* **1983**, *116*, 3003.

123. (a) Talay, R.; Rehder, D. *Zeit. f. Natur., B: Anorg. Chemie.* **1981**, *36*, 451. (b) Tamm, M.; Dreßel, B.; Baum, K.; Lűgger, T.; Pape, T. *J. Organomet. Chem.* **2003**, *677*,

1. (c) Chiswell, B.; Venanzi, L. M. *J. Chem. Soc. (A)* **1966**, 417. (d) Tunney, S. E.; Stille, J. K. *J. Org. Chem.* **1987**, *52*, 748.

124. Korshin, E. E.; Leitus, G.; Shimon, L. J. W.; Konstantinovski, L.; Milstein, D. *Inorg. Chem.* **2008**, *47*, 7177.

125. Chen, L. S.; Chen, G. J. *J. Organomet. Chem.* **1980**, *193*, 283.

126. The solid state structure of **209** was solved by Prof. Bruce M. Foxman and Dr. Chun-Hsing Chen.

127. Bontemps, S.; Bouhadir, G.; Dyer, P. W.; Miqueu, K.; Bourissou, D. *Inorg. Chem.* **2007**, *46*, 5149.

128 . (a) Persistence of Vision Ray Tracer (POV-Ray), available at http://www.Povray.org/ (b) Ortep-3 for Windows: Farugia, L. J. *J. Appl. Crystallogr*. **1997**, *30*, 56.

129. Bontemps, S.; Gornitzka, H.; Bouhadir, G.; Miqueu, K.; Bourissou, D. *Angew. Chem. Int. Ed.* **2006**, *45*, 1611.

130. Zhang, Y.; Shibatomi, K.; Yamamoto, S. *Synlett*. **2005**, *18*, 2837.

131. (a) Knoth, W. H. *J. Am. Chem. Soc.* **1967**, *89*, 1274. (b) Knoth, W. H. *Inorg. Chem.* **1971**, *10*, 598.

132. Mueller, T.; Juhasz, M.; Reed, C. A. *Angew. Chem., Int. Ed*. **2004**, *43*, 1543.

133. Bolskar, R. D.; Mathur R. S.; Reed, C. A. *J. Am. Chem. Soc.* **1996**, *118*, 13093.

134. (a) Mueller, T. *Adv. Organomet. Chem*. **2005**, *53*, 155. (b) Kueppers, T.; Bernhardt, E.; Eujen, R.; Willner, H.; Lehmann, C. W. *Angew. Chem. Int. Ed*. **2007**, *46*, 6346.

135. (a) Reed, C. A.; Xie, Z.; Bau, R.; Benesi, A. *Science* **1993**, *262*, 402.

136. Schleyer, P.; Najafian, K. *Inorg. Chem.* **1998**, *37*, 3454.

137. (a) Plešek, J.; Plzák, Z.; Stuchlík, J.; Heřmánek, S. *Collect. Czech. Chem. Commun.* **1981**, *46*, 1748. (b) Jelínek, T.; Plešek, J.; Mareš, F.; Heřmánek, S.; Štíbr, B. *Polyhedron* **1987**, *6*, 1981.

138. Jelínek, T.; Plešek, J.; Heřmánek, S.; Štíbr, B. *Collect. Czech. Chem. Commun.* **1986**, *51*, 819.

139. Approximate prices from the Aldrich catalog are $0.20/g for SbCl5 and $0.06/g for SO2Cl2 vs. $1/g for CF3SO3H and $0.6/g for ICl.

140. For use of SO2Cl2 in chlorination: (a) Silberrad, O. *J. Chem. Soc.* **1921**, *119*, 2029. (b) Silberrad, O.; Silberrad, C. A.; Parke, B. *J. Chem. Soc.* **1925**, *127*, 1724.

141. For use of SbCl5 in chlorination (a) Müller, H. *J. Chem. Soc.* **1862**, *15*, 41. (b) Kovacic, P.; Sparks, A. K. *J. Am. Chem. Soc.* **1960**, *82*, 5740.

142. Lebedev V. N.; Zakharkin, L. I. *Izu. Akad. Nauk SSSR, Ser. Khim.*, **1986**, *1*, 253.

143. Sivaev, I. B.; Bregadze,V. I.; Sjöberg, S. *Collect. Czech. Chem. Commun.* **2002**, *67*, 679.

144. Knoth, W. H.; Miller, H. C.; Sauer, J. C.; Chia, Y. T.; Muetterties, E. L. *Inorg. Chem.* **1964**, *3*, 159.

145. The solid state structure of $Cs[HCB_{11}Cl_9(O_3SCF_3)_2]$was solved by Prof. Bruce M. Foxman.

146. Ballester, M.; Molinet, C.; Castaner, J. *J. Am. Chem. Soc.* **1960**, *82*, 4254.

147. In our hands, sometimes we got complete chlorination with SbCl5 in as low as 3 days.

148. Peryshkov, D. V.; Popov, A. A.; Strauss, S. H. J. Am. Chem. Soc. 2009, 131, 18393 and references within.

149. In our hands, sometimes we got complete chlorination with SO2Cl2 and MeCN in as low as 8 hours.

150. T. Braun, R. N. Perutz, in *Comprehensive Organometallic Chemistry III*, R. H. Crabtree, D. M. P. Mingos, Eds. (Elsevier, Oxford, 2006).

151. Krause, J. R.; Lampe, F. W. *J. Phys. Chem*. **1977**, *81*, 281.

152. (a) Duttwyler, S.; Douvris, C.; Fackler, N. L.; Tham, F. S.; Reed, C. A.; Baldridge, K. K.; Siegel, J. S. *Angew. Chem. Int. Ed.* **2010**, *49*, 7519. (b) Allemann, O.; Duttwyler, S.; Romanato, P.; Baldridge, K. K.; Siegel, J. S. *Science* **2011**, *332*, 574.

153. (a) Fuchibe, K.; Akiyama, T. *J. Am. Chem. Soc*. **2006**, *128*, 1434. (b) Fuchibe, K.; Mitomi, K.; Suzuki, R.; Akiyama, T. *Chem. Asian J*. **2008**, *3*, 261.

154. (a) Terao, J.; Begum, S. A.; Shinohara, Y.; Tomita, M.; Naitoh, Y.; Kambe, N. *Chem. Commun.* **2007**, 855. (b) Terao, J.; Nakamura, M.; Kambe, N. *Chem. Commun.* **2009**, 855.

155. (a) Gundersen, G.; Haugen, T.; Haaland, A. *J. Organomet. Chem.* **1973**, *54*, 77. (b) Laubengayer, A. W.; Lengnick, G. F. *Inorg. Chem.* **1966**, *5*, 5037.

156. (a) Gundersen, G.; Haugen, T.; Haaland, A. *J. Organomet. Chem*. **1973**, *54*, 77. (b) Laubengayer, A. W.; Lengnick, G. F. *Inorg. Chem*. **1966**, *5*, 5037.

157. Zurek, E.; Ziegler, T. *Prog. Polym. Sci*. **2004**, *29*, 107.

158. Bochmann, M. *J. Chem. Soc., Dalton Trans*. **1996**, 255.

159. Strobach, D. R.; Boswell, G. A. *J. Org. Chem.* **1971**, *36*, 818.

160. We calculate TON based on the amount of the [B12Cl12]2- counterion. It is not clear whether both cations associated with it can be catalytically engaged simultaneously at all times. If they are, then our TON values should be divided by two.

161. (a) King, R. B. *Adv. Chem. Ser.* **1967**, *62*, 203. (b) Green, M. L. H. *J. Organomet. Chem.* **1995**, *500*, 127.

162. (a) Kubas, G. J. *Acc. Chem. Res.* **1994**, *27*, 183. (a) Burlitch, J. M.; Leonowicz, M. E.; Petersen, R. B.; Hughes, R. E. *Inorg. Chem.* **1979**, *18*, 1097. (b) Golden, J. T.; Peterson, T. H.; Holland, P. L.; Bergman, R. G.; Andersen, R. A. *J. Am. Chem. Soc.* **1998**, *120*, 223. (c) Braunschweig, H.; Gruss, K.; Radacki, K. *Angew. Chem., Int. Ed.* **2007**, *46*, 7782. (d) Braunschweig, H.; Gruss, K.; Radacki, K. *Inorg. Chem.* **2008**, *47*, 8595.

163. (a) Braunschweig, H.; Kollann, C.; Rais, D. *Angew. Chem., Int. Ed.* **2006**, *45*, 5254. (b) Fontaine, F.-G.; Boudreau, J.; Thibault, M.-H. *Eur. J. Inorg. Chem.* **2008**, 5439. (c) Braunschweig, H.; Dewhurst, R. D.; Schneider. A. *Chem. Rev.* **2010**, *110*, 3924.

164. Gilbert, K. B.; Boocock, S. K.; Shore, S. G. In *Comprehensive Organometallic Chemistry*; Abel, E. W., Stone, F. G. A., Wilkinson, G., Eds.; Pergamon: Oxford, 1982; Vol. 6, p 880.

165. Burlitch, J. M.; Burk, J. H.; Leonowicz, M. E.; Hughes, R. E. *Inorg. Chem.* **1979**, *18*, 1702.

166. Hill, A. F.; Owen, G. R.; White, A. J. P.; Williams, D. J. *Angew. Chem., Int. Ed.* **1999**, *38*, 2759.

167. Brown, H. C.; Fletcher, E. A. *J. Am. Chem. Soc.* **1951**, *73*, 2808.

168 . (a) Trofimenko, S. Scorpionates: *The Coordination Chemistry of Poly-(pyrazolyl)borate Ligands*; Imperial College Press: London, 1999. (b) Foreman, M. R. St.-J.; Hill, A. F.; White, A. J. P.; Williams, D. J. *Organometallics* **2004**, *23*, 913. (c) Figueroa, J. S.; Melnick, J. G.; Parkin, G. *Inorg. Chem.* **2006**, *45*, 7056. (d) Crossley, I. R.; Foreman, M. R. St.-J.; Hill, A. F.; Owen, G. R.; White, A. J. P.; Williams, D. J.; Willis, A. C. *Organometallics* **2008**, *27*, 381.

169. (a) Bontemps, S.; Bouhadir, G.; Miqueu, K.; Bourissou, D. *J. Am. Chem. Soc.* **2006**, *128*, 12056. (b) Bontemps, S.; Sircoglou, M.; Bouhadir, G.; Puschmann, H.; Howard, J. A. K.; Dyer, P. W.; Miqueu, K.; Bourissou, D. *Chem.-Eur. J.* **2008**, *14*, 731.

(c) Sircoglou, M.; Bontemps, S.; Mercy, M.; Saffron, N.; Takahashi, M.; Bouhadir, G.; Maron, L.; Bourissou, D. *Angew. Chem. Int. Ed*. **2007**, *46*, 8583.

170. (a) Tsoureas, N.; Haddow, M. F.; Hamilton, A.; Owen, G. R. Chem. Commun. **2009**, 2538. (b) Tsoureas, N.; Bevis, T.; Butts, C. P.; Hamilton, A.; Owen, G. R. *Organometallics* **2009**, *28*, 5222.

171. (a) Crossley, I. R.; Hill, A. F.; Willis, A. C. *Organometallics* **2005**, *24*, 1062. (b) Crossley, I. R.; Hill, A. F.; Willis, A. C. *Organometallics* **2007**, *26*, 3891.

172. We understand it is debatable whether to treat borane ligand as neutral ligand or dianionic ligand when counting the oxidation state of the transition metal. Here, for the sake of argument, we treat it as neutral ligand.

173. Conifer, C. M.; Law, D. J.; Sunley, G. J.; White, A. J. P.; Britovsek, G. J. P. *Organometallics* **2011**, *30*, 4066.

174. Moret, M.-E.; Peters, J. C. *Angew. Chem. Int. Ed*. **2011**, *50*, 2063.

175. Transition metal complexes of phosphino-boranes featuring M→B interactions typically display 11B NMR chemical shifts from 18 to 55 ppm.[162c, 169]

176. The solid state structure of **502** was solved by Prof. Bruce M. Foxman and Dr. Chun-Hsing Chen.

177. The solid state structure of **503** was solved by Prof. Bruce M. Foxman and Dr. Chun-Hsing Chen.

178. Cordero, B.; Gómez, V.; Pletro-Prats, A. E.; Revés, M.; Echeverría, J.; Cremades, E.; Barragán, F.; Alvarez, S. *Dalton Trans.* **2008**, 2832.

179. The order is consistent with the results from theoretical studies performed by Bourissou, Maron and coworkers. Sircoglou, M.; Bontemps, S.; Bouhadir, G.; Saffon, N.; Miqueu, K.; Gu, W.; Mercy, M.; Chen, C.-H.; Foxman, B.; Maron, L.; Ozerov, O. V.; Bourissou, D. *J. Am. Chem. Soc.* **2008**, *130*, 16729.

180. Linsky, J. P.; Pierpont, C. G. *Inorg. Chem.* **1973**, *12*, 2962.

181. Group 11 metallaboratranes were synthesized and characterized by Bourissou and coworkers. Sircoglou, M.; Bontemps, S.; Bouhadir, G.; Saffon, N.; Miqueu, K.; Gu, W.; Mercy, M.; Chen, C.-H.; Foxman, B.; Maron, L.; Ozerov, O. V.; Bourissou, D. *J. Am. Chem. Soc.* **2008**, *130*, 16729.

182. (a) Tsay, C.; Mankad, N. P.; Peters, J. C. *J. Am. Chem. Soc.* **2010**, *132*, 13975. (b) Takaoka, A.; Gerber, L. C. H.; Peters, J. C. *Angew. Chem. Int. Ed.* **2010**, *49*, 4088.

183. (a) Kanzelberger, M.; Zhang, X.; Emge, T. J.; Goldman, A. S.; Zhao, J.; Incarvito, C.; Hartwig, J. F. *J. Am. Chem. Soc.* **2003**, *125*, 13644. (b) Gatard, S.; Çelenligil-Çetin, R.; Guo, C.; Foxman, B. M.; Ozerov, O. V. *J. Am. Chem. Soc*. **2006**, *128*, 2808. (c) Unpublished results from Zhu, Y. and Ozerov, O. V.

184. The Nobel Prize in Chemistry 2005 was awarded jointly to Yves Chauvin, Robert H. Grubbs and Richard R. Schrock *"for the development of the metathesis method in organic synthesis"*.

185. (a) Schrock, R. R. *Chem. Rev.* **2002**, *102*, 145. (b) Grubbs, R. H.; Trnka, T. M.; Sanford, M. S. *Curr. Methods Inorg. Chem.* **2003**, *3*, 187.

186. Olah, J.; De Proft, F.; Veszprémi, T.; Geerlings, P. *J. Phys. Chem. A* **2005**, *109*, 1608.

187. Lauvergnat, D.; Hiberty, P. C.; Danovich, D.; Shaik, S. *J. Phys. Chem.* **1996**, *100*, 5715.

188. Sheldrick, W. S. *In the Chemistry of Organic Silicon Compounds Part I*; Patai, S., Rappoport, Z., Eds.; Wiley-Interscience: New York, 1989.

189. (a) Zybill, C.; Müller, G. *Angew. Chem., Int. Ed. Engl.* **1987**, *26*, 669. (b) Straus, D. A.; Tilley, T. D. *J. Am. Chem. Soc.* **1987**, *109*, 5872.

190. (*a*) Ueno, K.; Tobita, H.; Shimoi, M.; Ogino, H. *J. Am. Chem. Soc.* **1988**, *110*, 4092; (*b*) Tobita, H.; Ueno, K.; Shimoi, M.; Ogino, H. *J. Am. Chem. Soc.* **1990**, *112*, 3415. (c) Ueno, K.; Masuko, A.; Ogino, H. *Organometallics*, **1998**, *18*, 2694. (d) Okazaki, M.; Tobita, H.; Ogino, H. *Chem. Lett.*, **1997**, 437. (e) Koshikawa, H.; Ueno, K.; Tobita, H.; Ogino, H. *Eighty-First Annual Meeting of the Chemical Society of Japan*, Tokyo, **2002**, 3B4-31. (f) Ueno, K.; Ito, S.; Endo, K.; Tobita, H.; Inomata, S.; Ogino, H. *Organometallics*, **1994**, *13*, 3309. (g) Tobita, H.; Sato, T.; Okazaki, M.; Ogino, H. *J. Organomet. Chem.*, **2000**, *611*, 314. (h) Ghadwal, R. S.; Azhakar, R.; Pröpper, K.; Holstein, J. J.; Dittrich, B.; Roesky, H. W. *Inorg. Chem.* **2011**, *50*, 8502.

191. Straus, D. A.; Grumbine, S. D.; Tilley, T. D. *J. Am. Chem. Soc.* **1990**, *112*, 7801.

192. (a) Straus, D. A.; Zhang, C.; Quimbita, G. E.; Grumbine, S. D.; Heyn, R. H.; Tilley, T. D.; Rheingold, A. L.; Geib, S. J. *J. Am. Chem. Soc.* **1990**, *112*, 2673. (b) Grumbine, S. D; Tilley, T. D. *J. Am. Chem. Soc.* **1993**, *115*, 7884. (c) Grumbine, S. D;

Tilley, T. D.; Arnold, F. P.; Rheinglod, A. L. *J. Am. Chem. Soc.* **1994**, *116*, 5495. (d) Mitchell, G. P.; Tilley, T. D. *J. Am. Chem. Soc.* **1998**, *120*, 7635. (e) Mitchell, G. P.; Tilley, T. D. *Angew. Chem. Int. Ed.* **1998**, *37*, 2524.

193. (a) Okazaki, M.; Tobita, H.; Ogino, H. *Dalton Trans.* **2003**, 493.

194. Mitchell, G. P.; Tilley, T. D. *J. Am. Chem. Soc.* **1997**, *119*, 11236.

195. (a) Zhang, C.; Grumbine, S. D.; Tilley, T. D. *Polyhedron*, **1991**, *10*, 1173. (b) Petri, S. H. A.; Eikenberg, D.; Neumann, B.; Stammler D.-G.; Jutzi, P. *Organometallics* **1999**, *18*, 2615.

196 (a) Gilman, H.; Steve, G.; Atwell, W. H. *J. Am. Chem. Soc.* **1964**, *86,* 1596. (b) Halevi, E. A.; West, R. *J. Organomet. Chem.* **1982**, *240*, 129. (c) Tilley, T. D. In *The Chemistry of Organic Silicon Compounds*; Patai, S., Rappoport, Z., Eds.; Wiley: New York, 1989. (d) Ohmura, T.; Masuda, K.; Takase, I.; Suginome, M. *J. Am. Chem. Soc.* **2009**, *131*, 16624. (e) Masuda, K.; Ohmura, T.; Suginome, M. *Organometallics* **2011**, *30*, 1322.

197. (a) Glaser, P. B.; Tilley, T. D. *J. Am. Chem. Soc.* **2003**, *125*, 13640. (b) Brunner, H. *Angew. Chem., Int. Ed.* **2004**, *43*, 2749. (c) Calimano, E.; Tilley, T. D. *J. Am. Chem. Soc.* **2008**, *130*, 9226. (d) Calimano, E.; Tilley, T. D. *J. Am. Chem. Soc.* **2009**, *131*, 11161. (e) Calimano, E.; Tilley, T. D. *Organometallics* **2010**, *29*, 1680. (f) Rankin, M. A.; Maclean, D. F.; Schatte, G.; McDonald, R.; Stradiotto, M. *J. Am. Chem. Soc.* **2007**, *129*, 15855.

198. Gigler, P.; Bechlars, B.; Herrmann, W. A.; Kühn, F. E. *J. Am. Chem. Soc.* **2011**, *133*, 1589.

199. (a) Brown, H. C. *Boranes in Organic Chemistry*; Cornell University Press: Ithaca, NY, 1972. (b) Brown, H. C.; Chandrasekharan, J.; Nelson, D. J. *J. Am. Chem. Soc.* **1984**, *106*, 3768. (c) Jones, P. R. *J. Org. Chem.* **1972**, *37*, 1886. (d) Hommes, N. J. R. E. H.; Schleyer, P. R. *J. Org. Chem.* **1991**, *56*, 4074.

200. Haas, A.; Süllentrup, R.; Krüger, C. *Z. Anorg. allg. Chem.* **1993**, *619*, 819.

201. Pregosin, P. S.; Kunz, R. W. *31P and 13C NMR of Transition Metal Phosphine Complexes* Springer-Verlag, Berlin, **1979**, P97.

202. The solid state structures of **601** and **607** were solved by Dr. David E. Herbert.

203. Latif, L. A. *J. Chem. Res., Synop.* **1995**, *6*, 264.

204. Stahl, S. S.; Labinger, J. A.; Bercaw, J. E. *Inorg. Chem.* **1998**, *37*, 2422.

205. Wanandi, P. W.; Glaser, P. B.; Tilley, T. D. *J. Am. Chem. Soc.* **2000**, *122*, 972.

206. (a) Feldman, J. D.; Mitchell, G. P.; Nolte, J.; Tilley, T. D. *Can. J. Chem*. **2003**, *81*, 1127. (b) Watanabe, C.; Inagawa, Y.; Iwamoto, T.; Kira, M. *Dalton Trans.* **2010**, *39*, 9413.

207. Drew, D.; Doyle, J. R. *Inorg. Synth*. **1990**, *28* 348.

208. (a) Musaev, D. G.; Morokuma, K. *J. Phys. Chem.* **1996**, *100*, 6509. (b) Dickinson, A. A.; Willock, D. J.; Calder, R. J.; Aldridge, S. *Organometallics* **2002**, *21*, 1146. (c) Cundari, T. R.; Zhao, Y. *Inorg. Chim. Acta* **2003**, *345*, 70. (d) Lam, K. C.; Lam, W. H.; Lin, Z.; Marder, T. B.; Norman, N. C. *Inorg. Chem.* **2004**, *43*, 2541.

209. a) Braunschweig, H.; Radacki, K.; Uttinger, K. *Chem. Eur. J.* **2008**, *14*, 7858.

210. (a) Zhu, J.; Lin, Z.; Marder, T. B. *Inorg. Chem.* **2005**, *44*, 9384. (b) Lam, K. C.; Lam, W. H.; Lin, Z.; Marder, T. B.; Norman, N. C. *Inorg. Chem.* **2004**, *43*, 2541.

211. (a) Segawa, Y.; Suzuki, Y.; Yamashita, M.; Nozaki, K. *J. Am. Chem. Soc.* **2008**, *130*, 16069. (b) Yamashita, M.; Suzuki, Y. Segawa, Y.; Nozaki, K. *J. Am. Chem. Soc.* **2007**, *129*, 9570. (c) Segawa, Y.; Yamashita, M.; Nozaki, K. *Science* **2006**, *314*, 113.

212. (a) Baker, R. T.; Ovenall, D. W.; Calabrese, J. C.; Westcott, S. A.; Taylor, N. J.; Williams, I. D.; Marder, T. B. *J. Am. Chem. Soc.* **1990**, *112*, 9399. (c) Knorr, J. R.; Merola, J. S. *Organometallics* **1990**, *9*, 3008.

213. (a) Irvine, G. J.; Lesley, M. J. G.; Marder, T. B.; Norman, N. C.; Rice, C. R.; Robins, E. G.; Roper, W. R.; Whittell, G. R.; Wright, L. J. *Chem. Rev.* **1998**, *98*, 2685. (b) Braunschweig, H. *Angew. Chem., Int. Ed.* **1998**, *37*, 1786. (c) Braunschweig, H.; Colling, M. *Coord. Chem. Rev.* **2001**, *223*, 1. (d) Aldridge, S.; Coombs, D. L. *Coord. Chem. Rev.* **2004**, *248*, 535. (e) Braunschweig, H.; Whittell, G. *Chem.-Eur. J.* **2005**, *11*, 6128.

214. (a) Marder, T. B.; Norman, N. C. *Top. Catal.* **1998**, *5*, 63. (b) Männig, D.; Nöth, H. *Angew. Chem., Int. Ed.* **1985**, *24*, 878.

215. Solid state structures of **701**, **708**, **709** and **710** were solved by Dr. David E. Herbert.

216. Since **706** actually isomerized to make **707** in fluorobenzene, the yield here was calculated based on the weight of the mixtures of **706** and **707**.

217. (a) Dai, C.; Stringer, G.; Marder, T. B.; Scott, A. J.; Clegg, W.; Norman, N. C. *Inorg. Chem.* **1997**, *36*, 272. (b) Hartwig, J. F.; Cook, K. S.; Hapke, M.; Incarvito, C. D.; Fan, Y.; Webster, C. E.; Hall, M. B. *J. Am. Chem. Soc.* **2005**, *127*, 2538. (c) Souza, F. E. S.; Nguyen, P.; Marder, T. B.; Scott, A. J.; Clegg, W. *Inorg. Chim. Acta*. **2005**, *358*, 2001.

218. (a) Van Niekerk, J. N.; Schoening, F. R. L. *Acta. Cryst.* **1953**, *6*, 227. (b) Bratton, W. K.; Cotton, F. A. *J. Am. Chem. Soc.* **1964**, *87*, 921. (c) Bennett, M. J.; Bratton, W. K.; Cotton, F. A.; Robinson, W. R. *Inorg. Chem.* **1968**, *7*, 1570. (d) Cotton, F. A.; DeBoer, B. G.; Laprade, M. D.; Ripal, J. R.; Ucko, D. A. *Acta. Cryst.* **1971**, *B27*, 1664.

219. ESD values were calculated using LINEST function in Microsoft Excel. The reported uncertainty here is two times the results calculated by LINEST function in Microsoft Excel.

220 Maguire, J. A.; Petrillo, A.; Goldman, A. S. *J. Am. Chem. Soc.* **1992**, *114*, 9492.

221. Giordano, G.; Crabtree, R. H. *Inorg. Synth.* **1979**, *19*, 218.

222. Crabtree, R. H.; Morris, G. E. *J. Organomet. Chem.* **1977**, *135*, 395.

VITA

Name: Weixing Gu

Address: Department of Chemistry, Northwestern University
2145 Sheridan Rd.,
Evanston, IL 60208

Email Address: weixinggu1982@gmail.com

Education: B.S., Polymer Science and Engineering, Fudan University, 2004
M.S., Chemistry, Brandeis University, 2008
Ph.D., Chemistry, Texas A&M University, 2011